University of Bari Aldo Moro

Department of Chemistry

PhD in Chemical and Molecular Sciences

Advanced methodologies of valorization of catalytically active automotive waste for remediation of landfill leachates and organic synthesis

PhD: **Mariella MARANGI**

Supervisor:
Prof.ssa Roberta RAGNI
Co-supervisor:
Prof. Pietro COTUGNO
Thesis Supervisors:
Ing. Federico CANGIALOSI
Prof. Gianluca M. FARINOLA
Prof. Francesco NOCITO

2025

Index

List of Abbreviations

AC Activated Carbon
AD Anaerobic Digestion
ANF Anaerobic Filter
AO Anodic Oxidation
AOP Advanced Oxidation Processes
ARL Aerated Lagoon
AST Air Stripping
BAT Best Available Techniques
BAT-AEL Best Available Techniques - Associated Emission Levels
BOD Biological Oxygen Demand
COD Chemical Oxygen Demand
CROL Concentrated Reverse Osmosis Leachate
DMA Dimethylacetamide
DMSO Dimethyl Sulfoxide
DOM Dissolved Organic Matter
EAOPs Electrochemical Advanced Oxidation Processes
EC Electrocoagulation
EF Electro-Fenton
ELV End-of-Life Vehicles
EN European Norms
EO ElectroOxidation
EPA Environmental Protection Agency
E-PS electrochemical persulfate activation
EWC European Waste Code in Italian **CER** (*Codice Europeo dei Rifiuti*)
GPC Gel Permeation Chromatography
HDPE High-Density Polyethylene
HM Heavy Metals
HRT Hydraulic Retention Time
IC Inorganic Carbon
ISO International Organization for Standardization
MBR Membrane Bioreactor
MF Microfiltration
NF Nanofiltration

PAC Powdered Activated Carbon
PCB Polychlorinated Biphenyl
PEF PhotoElectro-Fenton
PGM Platinum Group Metals
PN Particle Number
RBC Rotating Biological Contactors
RO Reverse Osmosis
SBR Sequencing Batch Reactors
SBR-PAC Sequencing Batch Reactors - Powdered Activated Carbon
SCAT Scrap Automotive Catalytic Converters
SEF SonoElectro-Fenton.
SPEF Solar PhotoElectro-Fenton
SSW Steel Scale Waste
TC Total Carbon
TDS Total Dissolved Solids
TN Total Nitrogen
TOC Total Organic Carbon
TSS Total Suspended Solids
TWC Three-Way Catalyst
UASBR Up-flow Anaerobic Sludge Blanket Reactor
UF Ultrafiltration
UV-LEDs Ultraviolet Light-Emitting Diodes
VUV Vacuum Ultraviolet
XOC Xenobiotic Organic Compounds

Synopsis

Waste produced annually worldwide has been increasing in the last decades due to the development of industrialization and the continuous growth of consumption. Within the sole European Union, 2.1 billion tons of waste are ended every year in landfills and such an excessive production increasingly impacts on environmental and human well-being as well as on the economic resources required for waste management. Due to the impossibility to eliminate the production of waste, the most profitable strategy to face issues related to its management consists in the development of sustainable approaches of revalorization in accordance with the principles of Circular Economy.

Hence, reuse and recycling should be prioritized over the commoner option of disposal in landfills. Individual and collective actions to control and differentiate waste have been already adopted but they must be more and more implemented. Landfills remain among the most important facilities in the waste management cycle, but they should always be the last resort. The main concerns associated with landfills are the production of two outputs, i.e. leachate and biogas. Biogas is the final product of anaerobic microbial degradation of organic matter, and it mainly consists of methane (50-70%) and carbon dioxide (30-50%). Leachate is a highly polluted liquid that originates from the infiltration of rainwater through waste and fermentation. Its chemical composition primarily depends on both type and aging of waste in landfills. Both leachate and biogas require appropriate treatments. However, upstream solutions exist to reduce their production, such as a proper execution of separate waste collection, and landfill capping to reduce meteoric infiltration. Currently, biogas is not a significant issue, due to its suitability as a renewable alternative energy source. Conversely, landfill leachate disposal represents a key issue that has not yet received effective solutions worldwide. Indeed, European current regulations impose that to dispose landfill leachates into surface fresh or seawater, it would be necessary to reduce the pollutant load under precise value limits. The most important parameter related to the pollution degree of landfill leachates is the Chemical Oxygen Demand (COD) that is the amount of oxygen required to chemically oxidize organic and inorganic pollutants present in one liter of leachate.

This PhD project aims to develop an innovative and eco-friendly chemical physical methodology to reduce the COD value in landfill leachate concentrate at values next to 160 mg/L, that represents the value limit tolerable by regulations to dispose leachates into marine or freshwater.

The leachate investigated in this thesis was obtained through a reverse osmosis process (CROL, Concentrated Reverse Osmosis Leachate) from a landfill located in the South of Italy (ITALCAVE S.p.A., Taranto-Statte, Apulia Region).

The pristine CROL had 15880 mg/L COD value and pH 8.8. COD.

The research activity was performed in strict collaboration with Tecnologia & Ambiente (T&A, Putignano, Apulia Region) funder of the present PhD position. T&A is a company with extensive experience in chemical processes of remediation of polluted areas, in waste management and treatment, water resource protection, and environmental monitoring of gaseous effluents from industrial activities.

The investigated novel strategy for reduction of COD values of CROLs is based on an oxidation protocol using supported and recyclable catalysts derived from revalorized waste. The focus has been particularly on the reuse of spent scrap automotive catalytic converters (SCATs,) recovered and regenerated from end-of-life vehicles (ELVs). Every year, in the European Union, scrapped vehicles produce 8-9 million tons of waste, ~6000 tons of which are SCATs. SCATs are ceramic materials enriched with noble metals.

Very few examples of SCAT-catalyzed reactions have been reported so far in the literature, being mainly focused on extraction methods of noble metals by hydrometallurgical and pyrometallurgical techniques based on acid leaching treatments of the ceramic material, furnace melting, or ion exchange resin techniques. These processes are energy consuming, environmentally unfriendly and they require the use of chemicals that must be further disposed of.

In this thesis, the SCAT samples used derive from a three-way catalytic converter regenerated by thermal treatment at 450°C to eliminate adsorbed by-products of incomplete fuel combustion without altering the Platinum Group Metals (PGMs) or the porous ceramic support.

In particular, this research work represents the first evidence that SCAT ELV can effectively act as a waste-derived catalyst in simple and eco-friendly Fenton-type oxidation reactions on samples of concentrated landfill leachate, reducing the COD from 15880 mg/L to 579 mg/L, a value that almost meets the threshold for disposal in sewer water.

SCAT was also proven to be an efficient heterogeneous catalyst for Csp2-Csp2 bond forming reactions. Among organic processes, the Suzuki-Miyaura cross-coupling of aryl boronic acids with aryl halides was indeed extensively investigated. After a systematic investigation of the model reaction between phenylboronic acid and 4-iodoanisole to optimize the experimental conditions (SCAT amount, recyclability, base and solvent, reaction temperature, conversion, and selectivity), the study was extended to a wide range of heteroaryl boronic acids and functionalized electrophiles, including aryl and heteroaryl chlorides with reduced reactivity in conventional cross-coupling processes. The good suitability of SCAT for the synthesis of π-conjugated oligomers was also demonstrated using aryl boronic acids and dihalides as the reagents.

As an additional investigation, a COD detection method based on gel permeation chromatography (GPC) was also developed as a possible promising alternative to the conventional EPA 410.4 revised 2.0 protocol. The GPC method, although requiring

further optimization, is expected to be faster and cheaper versus the EPA 410.4 protocol currently used. Since the leachate concentrate is water-soluble, the GPC protocol set up in this study is based on the use of polymethylmethacrylate stationary phase column, requiring only water as the eluent, thus being a highly green detection method.

This further evidence, combined with the proofs of suitability of SCATs as catalysts both for leachate oxidation and organometallic synthesis are in accordance with principles of Green Chemistry and Circular Economy.

Another project carried out during the PhD course deals with the study of valorization of fishing waste as renewable energy source to produce oils suitable as biofuels. An efficient eco-friendly method based on the use of supercritical carbon dioxide (sc-CO_2) as a green solvent was developed starting from fishing waste collected from two trawlers in the southwestern Adriatic Sea.

The extracted lipid oils were then converted into fatty acid methyl esters (FAME), suitable for biofuels production. This output represents another proof of the possibility to avail of green chemical methods of waste treatment to produce added value products in accordance with circular economy.

Chapter 1: Introduction and State of Art

1.1 What is Waste: Scrap or Resource to Manage?

The legal definition of waste in Italy is given by the Article 183 of Legislative Decree 3 April 2006 n. 152: "any substance or object which the holder discards or intends or is required to discard." The *holder is to mean the producer of the waste or the natural or legal person who is in possession of it.* [1]
According to the Article 184, paragraph 1, waste is classified as municipal waste or special waste depending on its origin and, as hazardous or non-hazardous waste on the basis to its danger (see Fig. 1.).
Municipal waste includes household waste, waste of any nature or origin, lying on streets and public areas, and vegetable waste from green areas such as parks, gardens, and cemeteries. Knowing the composition of waste allows for better management of recycling and disposal. If the waste is rich in combustible fractions with high calorific value, it can be burned and converted into heat; conversely, non-recoverable inert materials will end up in landfills.
Special waste derives from industrial processing, commercial and healthcare activities, or from the recovery and disposal of other waste. It can include also sludge from water treatment and wastewater purification, parts of end-of-life motor vehicles, and so on. Hazardous waste, on the other hand, has the dangerous characteristics defined in Annex I, Part IV of Legislative Decree n. 152/2006. Hazardous municipal waste include waste that, although of civil origin, is managed differently, such as drugs and batteries. Hazardous special waste is generated from activities containing high levels of pollutants requiring specific treatments, defined as toxic-harmful, and originating, for example, from chemical processes, such as oils and solvents, or from petroleum refining or leather or textile production, etc. [2-3]
Waste is also classified considering the European Waste Catalogue. Each waste is assigned a code called EWC (European Waste Code), consisting of three pairs of numbers:

1. The first pair indicates the chapter, or the family of activities from which the waste originates.

2. The second pair indicates the subchapter, and identifies, within the activity family of the chapter, a particular productive activity within the family.
3. The third pair of numbers indicates a particular type of waste originating from the specific industrial activity identified with the second pair of numbers.[4]

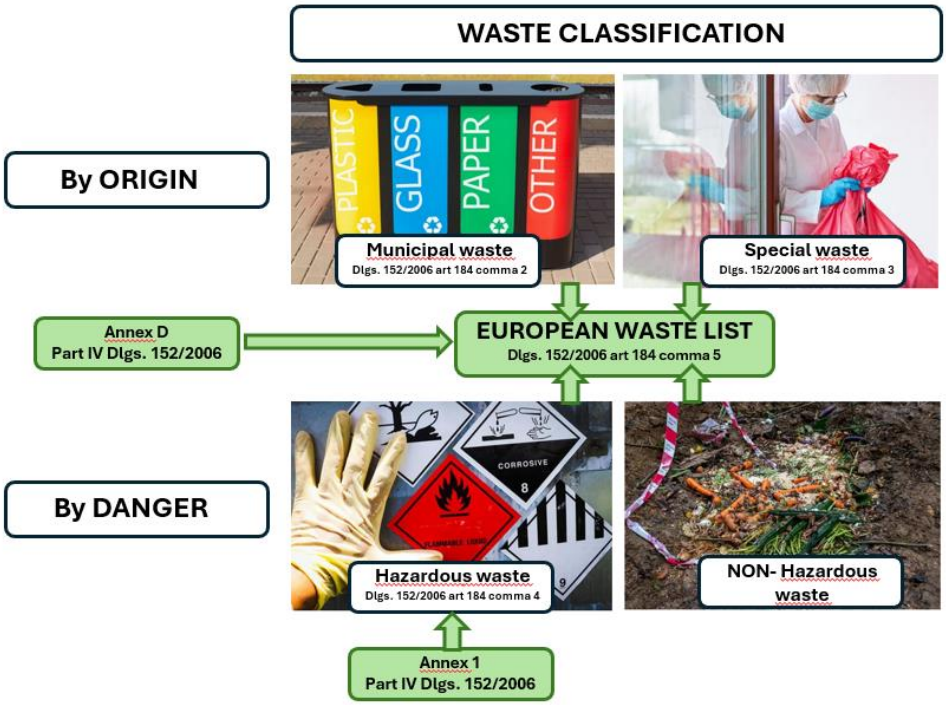

Fig.1. Waste classification

In the 21st century, the consumption of goods increased with industrialization, population growth, and the rising global living standards. Issues related to waste production and disposal increased as a direct consequence. [5-7] Waste is an integral part of human life. According to Eurostat (2020), the total waste generated in the EU by all economic activities and households amounted to 2135 million tons, equal to 4813 kg per capita and per year. Table 1 shows the production of all waste generated in 2020 by the activities of European states. [8]

Table 1 Total waste generated in the EU in 2020 [8]

	Mining and quarrying	Manufacturing	Energy	Waste/water	Construction and demolition	Other economic activities	Households
EU	23.4	10.6	2.3	10.8	37.5	5.9	9.4
Belgium	0.0	20.9	1.5	31.4	30.5	7.9	7.8
Bulgaria	81.6	4.2	5.2	2.9	1.6	2.5	2.0
Czechia	0.3	12.1	1.1	15.5	42.9	12.2	15.9
Denmark	0.1	5.4	3.9	7.5	54.8	10.3	18.0
Germany	1.3	13.7	2.0	12.0	56.3	5.1	9.6
Estonia	15.2	24.6	35.0	4.6	9.8	7.4	3.4
Ireland	9.4	22.4	1.0	12.6	32.6	10.1	12.0
Greece	31.7	11.1	5.3	11.4	19.1	5.5	15.9
Spain	2.3	12.4	0.8	20.8	30.8	11.5	21.3
France	0.1	6.0	0.3	8.1	68.5	6.3	10.8
Croatia	11.6	7.5	1.1	16.3	23.8	19.5	20.2
Italy	0.8	15.2	0.9	24.6	37.8	4.1	16.6
Cyprus	6.9	9.5	0.1	6.6	50.2	9.8	17.0
Latvia	0.0	17.0	4.1	33.7	9.7	12.9	22.6
Lithuania	1.0	32.7	2.3	18.4	8.3	16.3	20.9
Luxembourg	1.1	6.5	0.3	3.5	82.1	4.2	2.2
Hungary	0.8	15.2	11.4	12.1	25.4	7.5	27.6
Malta	1.1	0.9	0.0	2.5	85.3	4.7	5.6
Netherlands	0.1	10.6	0.4	7.4	65.4	8.7	7.4
Austria	0.1	7.5	0.6	3.5	76.5	5.2	6.7
Poland	36.6	16.1	6.6	13.4	13.0	6.6	7.8
Portugal	0.1	17.8	1.3	22.9	10.7	15.4	31.8
Romania	84.3	4.6	3.1	2.0	0.9	2.2	3.0
Slovenia	0.1	17.9	12.1	3.8	6.3	51.4	8.4
Slovakia	1.6	24.0	5.5	8.9	9.0	32.5	18.5
Finland	75.1	8.2	0.8	1.0	11.8	1.0	2.1
Sweden	76.5	3.1	1.2	4.5	9.3	2.3	3.1
Iceland	0.0	24.2	0.0	2.0	3.6	31.0	39.2
Liechtenstein	0.0	1.1	0.0	0.3	92.5	0.1	6.0
Norway	1.3	13.6	1.6	8.0	44.2	12.9	18.4
Montenegro	25.3	2.5	29.0	0.3	13.8	10.5	18.5
North Macedonia	35.1	35.0	0.5	17.9	3.8	7.7	0.0
Serbia	78.0	1.9	13.5	1.1	1.2	0.9	3.5
Türkiye	25.6	19.2	22.6	0.3	0.0	5.8	26.5
Bosnia and Herzegovina	11.3	27.3	46.3	0.0	1.3	0.4	13.4
Kosovo (')	19.9	9.4	52.5	0.3	0.2	3.1	14.6

According to other statistical studies, waste production will increase exponentially and by 2050 it will reach a level 1.7 times higher than in 2017, which was 2.533 billion tons per year. Furthermore, global waste production is expected to triple by 2100. [9-10] The problem associated with an excessive waste production and its unsuitable management, affects environmental pollution through the contamination of soil, air, and water, on citizens welfare, and on the economic resources used for their treatment. [11-13]

In this situation, it is important to look at a "sustainable development." The European Union has been active in this field for years. From the Lisbon Strategy (2000) to the "Europe 2020 strategy", it has set maximum values to be achieved

concerning social inclusion and sustainable development issues. In 2016, the European Commission adopted the United Nations' 2030 Agenda. This establishes 17 main goals.[14] The twelfth goal specifically addresses responsible consumption and production, stating that "currently, global consumption exceeds the capacity of ecosystems to provide resources, and therefore, to develop sustainably, society must revolutionize the production and consumption of goods." The goal is to adopt a virtuous approach toward chemicals and waste. Adopting sustainability principles for waste reduction means that soon, society will need to be in a condition where waste becomes a raw material. Through appropriate processing, it can have a "second life" in the same form or a new form, thus becoming secondary raw materials useful, for example, to industries.[15] *Directive 2008/98/EC of the European Parliament and of the Council of 19 November 2008 on waste and repealing certain Directives* is the legal act that establishes measures aimed at protecting both the environment and human health by preventing or reducing the impacts due to the production and management of waste.[15] Waste can be the raw material of the future, and its proper management, in addition to positive environmental consequences, can also improve socio-economic impacts as it plays a key role in the context of a circular economy.[5][16-20]

In this frame, it is crucial how waste is used. Figure 2 shows the order of waste priority for prevention, processing to reuse, recycling, and energy recovery to landfill disposal. [5,14,17,21,22]

European legislation aims to achieve an intermediate goal of at least 55% recycling by 2025, a target that must be completed by reaching 65% recycling by 2035, accompanied by a gradual reduction in landfill use. [22-24] All remaining waste should primarily be recovered in the form of energy. In this way, both principles of waste hierarchy and of circular economy will be fulfilled and net greenhouse gas emissions should be minimized by 2050. [25-26]

In this regard, the term "Zero Waste" fits within the circular economy framework. It is an ethical, economic, and contemporary concept, initially widespread in the United States and then globally. This means abandoning the waste disposal approach in favor of resource management.[27] Materials, are used as inputs, replacing the need to extract natural resources. [28] "Zero Waste" also means making conscious purchasing choices and ensuring that items last as long as possible.

Considering this new perspective, landfills remain, to this day, the most important facilities in the waste management cycle. Not all waste can be recovered or reused, and for this reason, in the absence of alternatives, it ends up in landfills.[229]

Fig.2. Schemes of the Circular Economy Model and Waste Hierarchy. [30-31]

1.2 The controlled landfill

Although in a circular economy context, recycling, source reduction, biological treatment, and incineration are not enough to stop waste flows, waste production is inevitable, so landfills continue to play a very important role. One of the most important European directives on the location and construction of landfills is 1999/31/EC. This European Directive has been transposed into Italian legislation through Legislative Decree 36/2003, which in Article 2, paragraph 1, letter g, defines a landfill as: "*area dedicated to the disposal of Waste via storage on or in the ground, including the area inside the place of production of the Waste dedicated to disposal of the same by the producer of the same, as well as any area where the Waste is subjected to temporary storage for more than one year*."[32]

Landfills are defined as a waste storage system designed to maintain their structural integrity throughout their lifetime and to minimize any kind of environmental impact.[33] They are the engineering solution for the final disposal

of waste that cannot be recovered in any other way and are designed to serve for a period ranging from 30 to 1000 years (for nuclear waste deposits).[34]

Depending on the type of waste they host, landfills are classified into three different categories: [35]

- Landfills for hazardous waste
- Landfills for non-hazardous waste
- Landfills for inert waste

For each category, based on the type of waste deposited, specific environmental safeguards and technical construction requirements are defined.[36-37]
Landfill ensures the containment and control of the main outputs produced by the disposed waste, which are biogas and leachate.
Once the operational period of a landfill has ended, the control goes on, this being referred to as post-operational management, which lasts for 30 years after the final waste deposition. [38]

1.3 General structure of a landfill

When planning to build a landfill, the first aspect to consider is the choice of the site where it will be constructed. This choice must consider both technical/geological aspects, such as the site's accessibility and soil permeability, and economic/social factors. At the same time, a landfill should not normally be located in areas of karst surface or in areas where surface geological processes such as accelerated erosion, landslides, slope instability, and riverbed migration, could compromise the landfill's integrity; in flood-prone, unstable, and alluvial areas; and in protected natural areas subjected to safeguarding measures. Additionally, for each location site, the local conditions of acceptability of the facility must be examined in relation to the distance from inhabited centers, the location in seismic risk areas, the location in zones of agricultural and food production, or next to significant historical, artistic, archaeological, and landscape assets. [39-40]
To protect soil, subsoil, groundwater, and surface water, barrier systems must be constructed at the bottom and sides of the landfill. These barriers must consist of a composite system of impermeabilization layers. Starting from the basal layer

and moving upward, the first barrier is represented by the geological one, followed by the layer of artificial impermeabilization, and then the drainage layer used to channel leachate.[41] The general structure of a landfill is reported in Fig. 3.

- The geological barrier is placed above the aquifer level and consists of a natural geological formation, usually clay (with a diameter less than 0.002 mm), which meets the requirements of permeability and thickness, both of which influence the residence time. Permeability must be monitored through geological drilling. The requirements in terms of hydraulic conductivity (k) to be met in a landfill for hazardous and non-hazardous waste are $k \leq 10^{-9}$ m/s, while for a landfill for inert waste, k is lower than 10^{-7} m/s. Thickness must be ≥5 m in the first case and ≥1 m in the last two cases.
- If the above requirements are not met, protection is completed with an additional artificial layer characterized by clay material with a thickness of 0.5 m, coupled with HDPE (High-Density Polyethylene) geosynthetic layers with thickness > 2.5 mm. In this case, residence times for landfills with hazardous and non-hazardous waste must be approximately 150 and 25 years, respectively.
- Above the impermeabilization layer, a protection layer made of natural or artificial material must be inserted.
- Finally, a 0.5 m drainage layer for leachate is placed, characterized by draining granular material (gravel, crushed stone with a diameter of 16-64 mm) and permeability $k \geq 10^{-5}$ m/s.
- Two years after the last deposition, a final cover system is necessary, that must be completed within the following 3 years. The cover must isolate waste from the external environment, minimize erosion, infiltration, and service phenomena.

Landfills cover has a multi-layer structure made of the following layers from top to bottom:

  - surface cover layer (thickness: 1m), useful for vegetation growth acting as a barrier against erosion for the underlying layers.
  - draining layer with granular material (thickness ≥0.5m) capable to drain the designed meteoric flow.
  - compact mineral layer (thickness ≥0.5m) integrated with a surface impermeable lining.

- gas drainage and capillary breakage layer (thickness ≥0.5m).
- regularization layer allowing the efficiency of the overlying layers.

Landfills must also be equipped with pumping systems that allow the extraction of biogas and leachate. Obviously, the subsequent management of leachate and biogas must minimize the impact on human health and the environment.

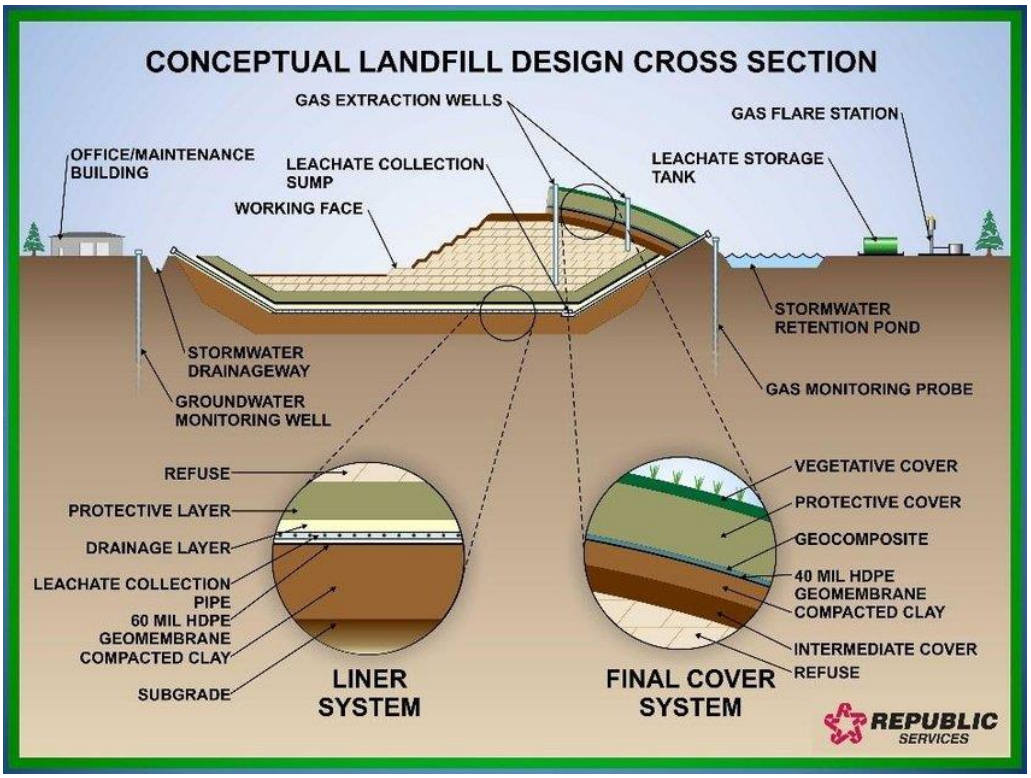

Fig.3. Cross-section view of a modern landfill illustrating the use of geomembranes [42]

1.4 Lifecycle of a landfill

The major inputs in a landfill are solid waste and water, while biogas and leachate are the two main outputs. Materials stored in landfills include both organic and inorganic matter. When waste is deposited, a series of biological, chemical, and physical processes occur that change its form and composition (Fig.4). Physical processes modify its physical characteristics such as volume reduction, precipitation, release, and absorption of substances. Chemical processes mainly

affect leachate quality and include pH variation, redox potential, and solubility. [43]

Five characteristic phases of a landfill's lifecycle can be identified during which the composition of biogas and leachate changes (Fig.4-5), i.e. (1) the aerobic phase, (2) the transition (anaerobic) phase, (3) the anaerobic, methanogenic, unsteady phase, (4) the anaerobic, methanogenic, steady phase and (5) the maturation phase.

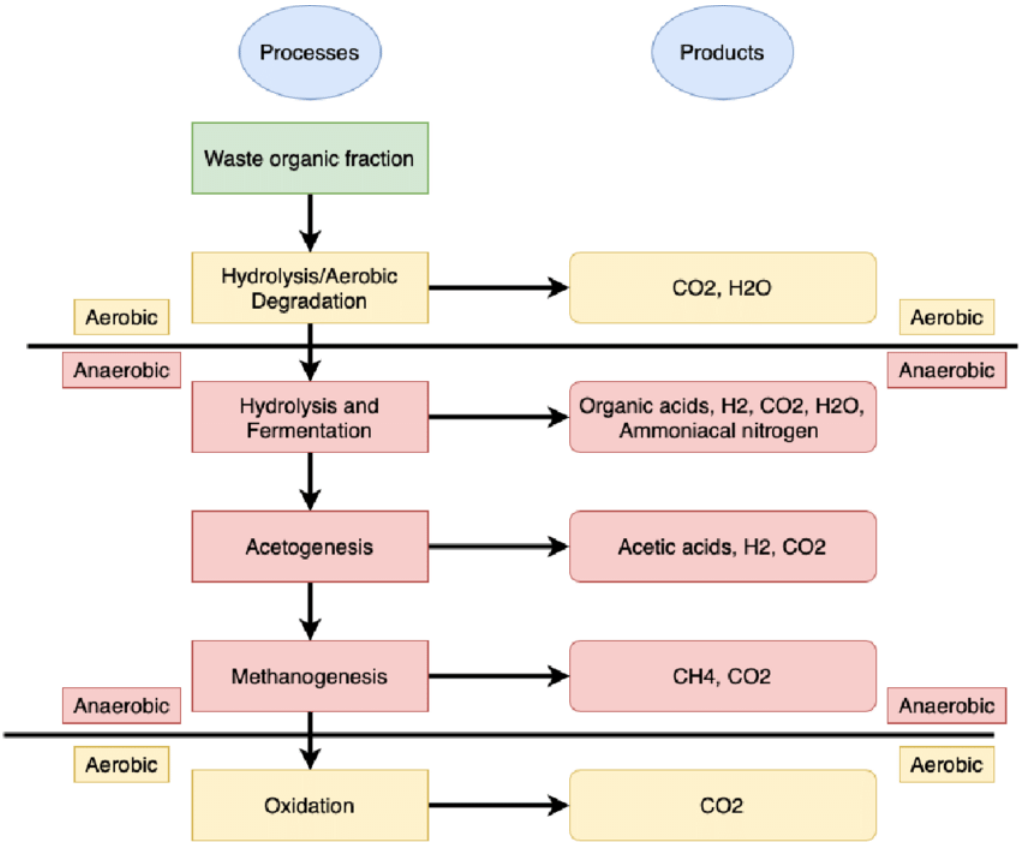

Fig.4. step of waste degradation in landfill [44]

1. **Aerobic Phase:** it is associated with the initial placement of solid waste and accumulation of moisture within landfill. This phase lasts from a few hours to a few days, depending on the initial porosity of the waste and the compaction methods used. During it, complex substrates are degraded. For example, cellulose, which makes up most of the organic fraction of the waste, is degraded to glucose, which is then converted by

bacteria into CO_2 and H_2O. Fats are hydrolyzed to fatty acids and glycerol, and proteins are degraded into amino acids and then into CO_2, H_2O, sulfates, nitrates, and catabolism products.

a. This stage is exothermic, with temperatures reaching 60-70°C. The increase of the partial pressure of carbon dioxide, which dissolves in water to form a weak acid, leads to a decrease in pH. The leachate formed in this initial phase is slightly acidic and it has high COD. During this first phase, the amount of leachate produced is not excessive.

2. **Transition (anaerobic) phase:** Transition from aerobic to anaerobic environment promotes biodegradative processes such as anaerobic respiration, done by acidogenic and acetogenic bacteria. When the oxidation-reduction potential is monitored at 50-100mV, the conditions are ideal for nitrates and sulfates to be reduced to nitrogen and hydrogen sulfides. Methane forms later when the potential rises between 100 and 300 mV. Various products can form from the initial organic substrate, which generally consists of fatty acids, sugars, and amino acids. For example, complex organic material is converted into volatile organic acids. These products and the dissolved carbon dioxide enhance the acidic properties of the leachate. This stage is less exothermic than the previous one and it lasts for several months.

3. **Anaerobic, methanogenic, unsteady phase:** This phase is divided into four sub-phases:

   Hydrolysis: The process occurs through enzymes secreted by fermentative bacteria (hydrolases). High molecular weight compounds (proteins, organic polymers, lipids) are broken down into lower molecular weight compounds (amino acids, mono- and disaccharides, long-chain fatty acids, and glycerol) suitable as energy sources for microorganisms.

   Acidogenesis: Compounds generated are absorbed into the cells of non-methanogenic fermentative bacteria and they subsequently undergo bacterial conversion into simple organic molecules such as volatile fatty acids and alcohols. During this phase, CO_2, H_2, NH_3, H_2S are also produced.

Acetogenesis: Products formed during acidogenesis are converted into acetic acid, hydrogen, and carbon dioxide. In this third phase, due to the acids produced and the high amount of CO_2, there is a decrease in pH values and an increase in the COD, the BOD5 (biochemical oxygen demand. Defined in the 1.6 paragraph, page 18), and the concentration of solubilized heavy metals.

4. **Anaerobic, methanogenic, steady phase:** The progressive development of the methanogenic (strictly anaerobic) population results in the consumption and conversion of the acids produced during phase III into CH_4 and CO_2. This phase lasts since 8 to 40 years. It is associated with higher-quality leachate, as the pH within the landfill increases towards more neutral values, ranging between 6.8 and 8 (controlled by the bicarbonate buffering system). The concentration of BOD5 and COD decreases, whereas metals are subjected to complexation and precipitation.

5. **Maturation phase:** The progressive stabilization of waste results in the gradual availability of less biodegradable organic compounds. The reduction of bacterial activity, and consequently the biogas production, increase diffusion of air into waste, leading to the presence of oxygen and nitrogen in the upper layers. This phase lasts since 10 to 80 years. [44-45]

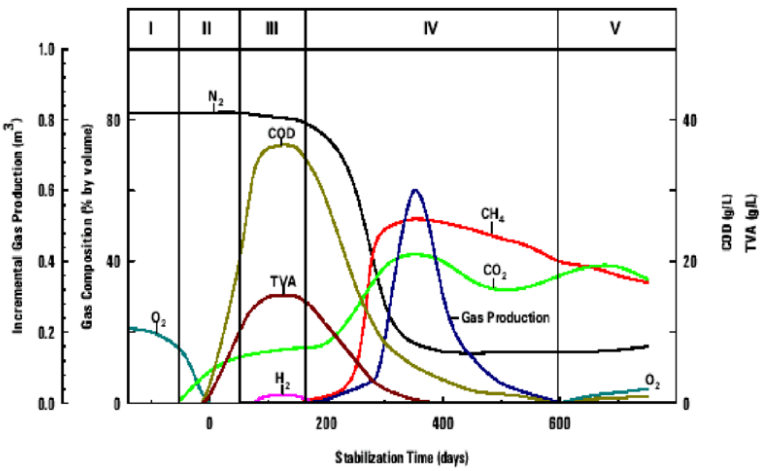

Fig.5. Phases of degradation in a typical landfill [46]

1.5 Leachate production in landfills

Landfill leachate is defined by Legislative Decree 36/2003 (Implementation of Directive 1999/31/EC on the landfill of waste) as a "*liquid that originates predominantly from the infiltration of water into the waste mass or from the decomposition of the same*." [47] It is a liquid rich in undesirable organic and inorganic compounds, characterized by its own unique properties. Approximately 200 hazardous compounds have already been identified in heterogeneous landfill leachates, including aromatic and halogenated compounds, phenols and pesticides. [48] These pollutants represent a significant threat to both the environment and public health. [49-51]

The main factors that characterize leachates are volumetric flow and composition. They are influenced by a series of factors such as the annual precipitation, the surface runoff, the infiltration into the landfill body due to gravitational force, the initial moisture content, the temperature, the waste composition, density, height (as the height of the waste body increases, there is a reduction in the abatement of pollutant concentrations), the landfill age.

Leachate should in principle begin to accumulate at the bottom of the landfill only once waste has reached the field capacity and is saturated with water, reaching a moisture level such that any further water input continues its movement through the waste without quantitative variations. [52-62]

The mechanisms that determine the transfer of pollutants from waste to leachate are divided into three categories:[63] (a) the hydrolysis of waste and biological degradation, (b) the solubilization of salts in waste, (c) the particulate entrainment.

According to Qasim *et al.* [62] in the first phase, lasting few days, the moisture content of the waste increases until it reaches field capacity, and pollutants are generated by desorption from the solid phase to the liquid. In the second phase, lasting several weeks, the increase in the flow rate of produced leachate leads to increased dilution of the infiltration water over desorption, which nonetheless reduces due to the increase in concentration in the adsorbing liquid. In the third and final phase, characterized by degradation and leaching processes, an initial increasing trend is observed followed by a depletion phase.

Therefore, the concentration of organic compounds is influenced by the effect of these processes, while the concentration of inorganic compounds is influenced only by leaching processes.

1.6 The main parameters to define the landfill leachate composition

Landfill leachate requires constant monitoring of contaminants. For this purpose, it is important to detect all carbonaceous compounds and some other elements such as oxygen, hydrogen, and nitrogen in leachate. Two tests are commonly used to measure this presence: the Chemical Oxygen Demand (COD) and the Biological Oxygen Demand (BOD5). Moreover, the Total Organic Carbon (TOC) is another widely used parameter. [64-65]

1.6.1 The Chemical Oxygen Demand (COD)

The Chemical Oxygen Demand (COD) represents the total amount of oxygen required to chemically oxidize the organic matter present in a given volume of water or solution. It is expressed in milligrams of oxygen per liter (mg/L). The COD test quantifies the oxygen-consuming capacity of inorganic and organic matter present in a sample. It is one of the fastest available tests for monitoring water quality during treatments, leading to output values within few hours. [66-67]

The standard method for measuring COD, as described in ISO 6060 and ISO 15705 standards, involves the oxidation of organic matter (for example hydrogen phthalate), in the presence of a strong oxidizing agent (like potassium permanganate or potassium dichromate) in an acidic solution (with sulfuric acid) at a temperature of 150°C for a reflux period of 2 hours. These conditions are essential to convert organic carbon into CO_2 and H_2O. [65][67-68]

Mercury sulfate is used to remove chloride ions, while most of the organic matter can be oxidized by strong oxidizing agents. However, linear chain carboxylic acids require the presence of a catalyst such as silver sulfate for a complete oxidation. During the COD test, silver sulfate is added to facilitate this complete oxidation. [67]

Depending on the type of wastewater considered, different oxidants are used. Potassium permanganate is used for slightly contaminated waters, whereas potassium dichromate is preferred for heavily contaminated wastewaters. Two main procedures are used as the standard process. In the “open reflux” method, the excess of dichromate is determined by titrating the unreduced dichromate with a ferrous ammonium sulfate solution, known as the Mohr’s salt, using ferroin as the indicator. [69-70] According to Li *et al.*, the initial phase involves the reaction of potassium hydrogen phthalate with dichromate. [71]

$$2KC_8H_5O_4 + 10K_2Cr_2O_7 + 41H_2SO_4 \longrightarrow 16CO_2 + 46H_2O + 10Cr_2(SO_4)_3 + 11K_2SO_4$$

Then, $K_2Cr_2O_7$ is replaced by oxygen and, after a digestion process at reflux, the excess unreduced dichromate is titrated with a Fe^{2+} solution, according to the following reaction.

$$Cr_2O_7^{2-} + 6Fe^{2+} + 14H^+ \longrightarrow 2Cr^{3+} + 6Fe^{3+} + 7H_2O$$

In the “closed reflux” method, the excess of dichromate is measured using spectrophotometric techniques or by monitoring Cr^{3+} ions. [72]
These traditional standard methods involve the use of expensive, corrosive, and toxic reagents, which can cause interferences and incomplete oxidation of volatile compounds. For this reason, alternative approaches are also exploited (Table 2).

Table 2 Alternative methods for COD detection [65]

Technique	Kind of modification	Linear range ($mg L^{-1}$)	Detection limit ($mg L^{-1}$)
Standardized method	Standardized method 5220D Closed reflux	NA	> 50
	Scaling and cost reduction	30 – 600	NA
Standardized method: oxidation processes	Advanced oxidation processes: photocatalysis	3.4 – 20	1.2
	Advanced oxidation processes: Fenton-like process	2.0 – 50	2.0
	Oxidation with permanganate	20 – 500	~8
Standardized method: detection methods	Fluorescence	1–100	0.9
	Chemiluminescence	0.16 – 19.24	0.1
	Electrochemical detection: nanon-ickel sensor	10 – 1533	1.1
	Electrochemical sensor based on platinum nanoparticles	NA	1.83
	Photocatalytic and electro photo-catalytic detection	20 – 300	15
	Photochemiresistor sensor based on a Bismuth vanadate type semi-conductor	0.20 – 19.9	0.05
New techniques	Thermal biosensors	5.0 – 3000	1.84

Each approach reported in Table 2 has its own advantages and disadvantages. For instance, using reagents different from the standard techniques can be more eco-friendly. However, a drawback is the need to approximate the concentration of pollutants to set suitable parameters, such as the exposure time to light and the oxidant concentration. [73-74] Changing the detection method, such as using fluorescence and chemiluminescence, may require expensive equipment and it is suitable mainly for lightly polluted waters. [75-76] Chemiluminescence, on the other hand, is more eco-friendly. Other options include the use of electrochemical, photocatalytic, and photo resistive sensors but these methods have limitations such as reduced specific surface area and the limited capacity of UV light to generate wide bands. [77-80]

Among new techniques for COD detection, there are thermal biosensors that can handle interferences but may suffer from incomplete oxidation. [81-82] Methods focused on the detection system are not fully developed yet, as their main goal is to improve the sensitivity of the final response.

In conclusion, none of these techniques can replace the standardized procedure so far. Although they may be cheaper or sensitive, they do not offer the same reliability as the standardized technique, this limiting their use for wastewaters.

1.6.2 Biological Oxygen Demand (BOD)

BOD5 is an indicator used to measure the amount of oxygen required by aerobic microorganisms to decompose the organic matter present in an aqueous solution at 20°C over a period of five days. This value is commonly expressed in milligrams of dissolved oxygen per liter of solution (mg O_2/L). [83-84]

Its origin dates to 1908 when the Royal Commission on River Pollution in the United Kingdom introduced it as a measure of organic pollution in rivers, based on the presumed travel time of water from the source to the estuary in British rivers. [85] In 1936, the American Public Health Association's Standard Methods Committee adopted this parameter as a reference indicator for evaluating the biodegradation of chemical and hazardous substances.

BOD5 has several applications, such as (a) ensuring compliance of wastewater discharges with regulations, (b) assessing the biodegradable fraction of an effluent in treatment plants (indicated by the BOD5/COD ratio), (c) Determining the required size of a treatment plant for a specific area.

During the oxidation process, microorganisms transform the organic matter present into microbial biomass into carbon dioxide and water.

This occurs according to the following reaction:

$$X_i + O_2 + C \longrightarrow X_f + CO_2 + H_2O$$

where X_i and X_f represent the initial and final microbial populations, respectively, and C is the organic matter in the sample.

This technique is affected by issues related to the response time (fixed at five days), the temperature and the amount of available oxygen. Additionally, some compounds in the sample may be toxic, and variations in the concentration and composition of the microbial substrate can cause significant variability in the results, exceeding 20%. [86-89] Due to these issues, various alternatives for BOD analysis have been developed, as shown in Table 3.

Table 3 Alternative techniques for BOD5 detection [65]

Technique	Basis	Advantages	Disadvantages	Response time (media) (h)
Standardized method	The amount of dissolved oxygen is determined after 5 days, which allows calculating the amount of organic matter suitable for oxidization by biological processes	Accurate values are given It can be applied in field	Long analysis time Unknown and variable microbial inoculum Substantial variability in results	120 (5 days)
Biosensors with a redox mediator	Electrochemical species are generated by biological processes, producing a signal that a detector can measure Biosensors use an electrode as a transducer This technique simulates the principle of the standardized method, but it substitutes O_2 with a redox-active synthetic mediator that acts as an electron transfer agent	Shorter analysis time (minutes or hours) The microbial inoculum (species and concentration) is known It needs a smaller work area	Expensive reagents and equipment are needed Microbial inoculum may not be viable for all kinds of wastewater	3.5
Biosensors based on bacterial bioluminescence	Tests are based on redox reactions that induce the formation of reactive oxygen species. When these species react with luminol, they increase the chemiluminescence or bioluminescence signal (if working with bacterial strains with this characteristic)	Low-cost tests It predicts the potential biodegradability of pollutants Automated methods	It requires bioluminescent microbial inoculums It requires reagents that enhance chemiluminescence	1
Biosensors based on immobilized bacterial cells	They consist of a sensitive element (i.e., microorganisms) and a transducer. The microorganisms are immobilized on a membrane with an electrolyte, while the transducer detects changes in the electrolyte solution when organic matter is decomposed	Faster and easier tests Commercial versions of these tests are available High sensitivity Measurement in real-time	Short operational period of the biosensor Lysis of immobilized microorganisms occurs Large, high-cost sensors are needed	0.166

Modifications to the standard method include reducing the response time to obtain faster results and higher sensitivity to biodegradation. However, these modifications entail additional costs due to the use of sophisticated equipment. [90] Some alternative systems have adopted more sensitive techniques, such as fluorescence spectroscopy or the use of optical sensors, to improve the response to biodegradation. Fluorescence spectroscopy can be a suitable alternative, but it is time consuming and it may affect microorganisms.[75,87,91] Optical sensors are still under development and they are reported only in miniaturized systems, but they appear to be more promising. [92]

1.6.3 Total Organic Carbon (TOC)

The Total Organic Carbon (TOC) refers to all the carbon content in organic matter, either dissolved or suspended in water. [93] Its analysis is complementary to that of COD and BOD because it is faster, more accurate, sensitive, and

environmentally friendly. [94] The first step in determining TOC values is the removal of the total inorganic carbon from the sample, by acidification to convert carbonates and bicarbonates into gaseous CO_2. Then, the sample undergoes complete oxidation through heating in the presence of catalysts, converting it into CO_2. After cooling, CO_2 is directed towards an infrared detection cell, generating an electrical signal in millivolts proportional to the amount of CO_2 passing through the cell. What remains in the sample will be only the organic carbon. The completion of the test can take from a few minutes to several hours. [95] Additionally, as highlighted in Tables 4 and 5.

Table 4 Summary of the methods proposed by Federation, W. E., & APH Association to ascertain TOC [65][93]

Technique	Kind of sample	Principle	Minimum detectable concentration (mg TOC / L)
5310 B: Combustion at high temperatures	Samples require a diminishing of the particle size to flow through the hole of the syringes Samples with high levels of organic carbon	A homogenized and diluted sample reacts with an oxidative catalyst (cobalt oxide, platinum, or barium chromate). Organic carbon is oxidized and converted into CO_2, then transported by a carrier gas; it is finally analyzed by titration or non-dispersive infrared (NDIR)	1
5310 C: Oxidation with persulfate (Persulfate/UV and Heated-Persulfate Oxidation Method)	Samples with trace levels of organic carbon	Persulfate oxidizes organic carbon into CO_2; this process needs either heat or UV light. The produced CO_2 can be purged, dried, and transferred by a carrier gas to a non-dispersive infrared analyzer (NDIR). This can be titrated by colorimetry or separated from the liquid stream by a membrane to measure the change in conductivity that it produces	0.01
5310 D: Wet oxidation	Samples with different mixtures of sediments, seawater, brine, and wastewater with less than 0.1 mg TOC	The sample is acidified and purged, the inorganic carbon is removed and oxidized with persulfate in an autoclave at a 116–130 °C The resulting CO_2 is measured by NDIR	0.10

Table 5 Alternative detection systems for the detection of Total Organic Carbon in water[65]

Technique	Kind of sample	Principle	Minimum detectable concentration
Conductivity	Natural saline waters	It is used when oxidation is carried out with UV light. The generated CO_2 dissolves and then interacts with water ions, affecting conductivity	≥ 0.25 mg TOC/L
CO_2 electrode	Synthetic water and natural water Pretreatment required to remove total inorganic carbon	CO_2 diffuses from the sample to the internal solution of the electrode through a selective membrane. Due to its acidic nature, it produces a change in pH that is related to the CO_2 concentration	2×10^{-2} mol L^{-1} CO_2
Reagent free ion chromatography (RF™ -IC) and inductively coupled plasma atomic emission spectrometry (ICP-AES)	Synthetic water and natural water	The sample is introduced directly into the hot plasma without pre-oxidation, and the organic carbon is atomized. Then, carbon is measured by atomic emission spectrophotometry	0.5 mmol L^{-1} (RF™-IC) 0.1 mmol L^{-1} (ICP-AES)
Infrared (TOC-VCSH) coupled to chemiluminescence detector (TNM-1 TN unit)	Environmental waters and purified waters	5310B method (19) is used for infrared, and by chemiluminescence, total nitrogen is determined. Both methods are coupled to generate simultaneous TOC and NT results	0.5–100 mg C/L
Ultraviolet–visible spectroscopy	Saline water and freshwater	Organic matter is determined at a wavelength of 250 – 300 nm. Then absorbance is analyzed with multiple linear regression models to estimate the TOC value and compare it with the traditional method	10–200 mg L^{-1}

Since TOC is a sensitive technique, making significant changes to the methodology is complex. Therefore, modifications focus on various possibilities to detect carbon in the sample. The techniques illustrated in Table 4 have detection limits that become critic when considering the other two parameters (COD and BOD5), requiring special equipment.[93] On the other hand, Table 5 lists more sensitive methods. To ensure complete oxidation of organic matter, preliminary treatments are necessary, and the carbon detection levels are higher than with the standard technique. TOC is the only technique that has been refined over time. [65]

1.7 Qualitative changes in landfill leachate composition

Composition of landfill leachate is generally influenced by various chemical physical parameters such as the pH, the total suspended solids (TSS), the total dissolved solids (TDS), the dissolved organic matter expressed as COD, the biological oxygen demand BOD, or the total organic carbon TOC, the ammoniacal nitrogen (NH_3-N) and total nitrogen (TN), the sulfur compounds, chlorides, phosphorus, heavy metals (HM) bound to the dissolved organic matter (DOM), and recalcitrant organic pollutants.[51,61, 96] These parameters will be discussed in detail in paragraph 1.6.

According to Renou et al. (2008a),[97] the quality of leachate varies from one landfill to another, but also in different sampling points within the same landfill. Although the composition of leachate widely varies during the different phases of a landfill, it is possible to define four types of leachates based on the landfill age (*i. e.* young, intermediate, stabilized, and mature). Typically, young landfills are less than 5 years old; intermediate are 5 - 10 years old; mature landfills include both stabilized and old ones and they are older than 10 years. [61,98] Features of leachate referred to landfill with different ages are shown in Table 6.

Table 6 Leachate characteristics at different landfill ages [99]

Parameters	Landfill age (years)				Reference
	Young (0-5)	Intermediate (5-10)	Stabilized (10-20)	Old (>20)	
pH	<6.5	6.5–7.5	>7.5	-	(Foo and Hameed, 2009)
	3-6	6-7	7-7.5	7.5	(El-Fadel et al., 1997; Scott et al., 2005)
TDS (mg L^{-1})	10,000-25,000	5000-10,000	2000-5000	<1000	(El-Fadel et al., 1997; Scott et al., 2005)
BOD_5 (mg L^{-1})	10,000-25,000	1000-4000	50-1000	<50	(El-Fadel et al., 1997; Scott et al., 2005)
COD (mg L^{-1})	>10,000	4,000–10,000	<4000	-	(Foo and Hameed, 2009)
	15,000-40,000	10,000-20,000	1000-5000	<1000	(El-Fadel et al., 1997; Scott et al., 2005)
BOD_5/COD	0.5–1.0	0.1–0.5	<0.1	-	(Foo and Hameed, 2009)
	0.66-0.625	0.1-0.2	0.05-0.2	<0.05	(El-Fadel et al., 1997; Scott et al., 2005)
Organic compounds	80% volatile fatty acids (VFA)	5–30% VFA+ humic and fulvic acids	Humic and fulvic acids	-	(Foo and Hameed, 2009)
Ammonia nitrogen (mg L^{-1})	<400	N.A	>400	-	(Foo and Hameed, 2009)
	500-1500	300-500	50-200	<30	(El-Fadel et al., 1997; Scott et al., 2005)
TOC/COD	<0.3	0.3–0.5	>0.5	-	(Foo and Hameed, 2009)
Kjeldahl nitrogen (mg L^{-1})	100-200	N.A	N.A	-	(Foo and Hameed, 2009)
	1000-3000	400-600	75-300	<50	(El-Fadel et al., 1997; Scott et al., 2005)
Heavy metals (mg L^{-1})	Low to medium	Low	Low	-	(Foo and Hameed, 2009)
Ca (mg L^{-1})	2000-4000	500-2000	300-500	<300	(El-Fadel et al., 1997; Scott et al., 2005)
Na, K (mg L^{-1})	2000-4000	500-1500	100-500	<100	

In early phases, leachate has high organic content, strong biodegradability, and a relatively low concentration of ammoniacal nitrogen. As landfill ages, the amount of ammoniacal nitrogen in the leachate increases and biodegradability decreases. Intermediate leachate is qualitatively positioned between young and mature leachates. [100] In this case, the organic waste degrades, the concentration of BOD and COD decrease. Typically, non-biodegradable organic substances contributing to COD remain unchanged, while most of biodegradable organic substances assessed by BOD are decomposed during stabilization. Consequently, the BOD/COD ratio (an index of biodegradability) decreases over time.

Thus, in young landfill leachates, COD is high (> 10^4 mg/L) and BOD/COD ratios range from 0.5 and 1. In mature landfill leachates, COD are lower (< $4 \cdot 10^3$ mg/L) and BOD/COD ratio is lower than 0.1. [61]

Moreover, pH of leachate increases with age, whereas heavy metals decrease due to the higher pH of leachate. These conditions increase the difficulty of developing an effective biological treatment for leachate. [100]

Leachate composition depends on the stage of waste evolution. Pollutants present in leachate are divided into four groups. [61]

- The dissolved organic matter includes methane, volatile fatty acids, and refractory compounds such as humic and fulvic acids. The concentration of these compounds and the molecular weight of humic substances increase with the leachate age. Young leachate fractions contain low molecular weight organic compounds with linear chains, while old leachates are rich of oxygenated functional groups such as carboxylic and alcoholic groups. [60][101]
- Inorganic cations and anions are present in concentration depending on pH and on their possible complexation with organic ligands present in solution. Table 7 shows their average concentration in leachates.

Table 7 Average **c**oncentration values of inorganic ions in leachate [61]

	mg/l
COD	140 - 152000
NH_4^+ - N	50 – 2200
Na^+	70 – 7700
K^+	50 – 3700
Ca^{2+}	10 – 7200
Mg^{2+}	30 –15000
Mn^2	0,03 – 1400
Fe^2	3 – 5500
Cl^-	150 – 4500
SO_4^{2-}	8 – 7750
HCO_3^-	610 – 7320

- Heavy metals: Cr^{3+}, Ni^{2+}, Cu^{2+}, Zn^{2+}, Cd^{2+}, Hg^{2+}, and Pb^{2+} whose concentration depends on the landfill and the waste deposited. Humic substances play a crucial role in the complexation of metals. Literature often reports data on leachate with low metal concentrations, which is frequently due to a high presence of colloids that complex metals, masking their presence and influencing their bioavailability and toxicity (Ghosh et al., 1997). [102]
- Xenobiotic organic compounds (XOC) are aromatic hydrocarbons, phenols, chlorinated aliphatic hydrocarbons, pesticides. They originate

from products present in both urban and industrial waste, and their concentration tends to decrease over time.

1.8 Limit values for landfill leachates

1.8.1 European Limit Values for discharge

To minimize the environmental impact, specific maximum threshold values have been established to discharge treated leachate. These values must be met before disposal into surface water bodies, sewer systems, or soil.
The Commission Implementing Decision (EU) 2018/1147, based on the Directive 2010/75/EU of the European Parliament and Council, outlines the conclusions on the Best Available Techniques (BATs) for waste treatment. BATs serve as a reference point to establish conditions to authorize working activities in landfills and they allow to define the maximum emission levels of pollutants in waste. The BAT-associated emission levels (BAT-AEL) for direct and indirect discharges into a water body are detailed in Tables 8 and 9 (Appendix 1 pag.168).
The emission levels in water related to BAT-AEL are measured in µg/L or mg/L as they refer to the amount of substance emitted per volume of water. Regarding water emissions, the BAT-based approach involves monitoring key parameters such as flow, pH, temperature, conductivity, and BOD of the wastewater at critical points such as the inlet and outlet of pretreatment or the inlet and outlet of final treatment. BAT-AEL average values are calculated on water sampled in 24 hours in case of continuous discharge, and on average aliquots of water sampled instantly in case of discontinuous discharge. [103]
BAT requires monitoring water emissions following a specific frequency and complying with EN (European Norms) standards. If these standards are not available, BAT specifies the use of alternative ISO (International Organization for Standardization), national, or international standards that ensure data of equivalent scientific quality (Table 10, Appendix 1, pag.168).
Furthermore, to limit emissions into water, the BAT for wastewater treatment involves the use of an appropriate set of specified techniques as detailed in Table 11 (Appendix 1, pag.168).

1.8.2 Italian Limit Values for Landfill Leachate Discharge

In Italy, the definition of leachate has led to discussions about its status as waste or discharge, as it represents an intermediate case between the two categories. According to Legislative Decree No. 152/2006, leachate can be classified as "waste produced by waste treatment plants" and, therefore, as a special waste (CER code 190702 for leachate from landfills containing hazardous substances and CER code 190703 for leachate from other landfills). Even if leachate is discharged into a water body, it retains this waste nature.

The distinction between waste and discharge becomes relevant when considering the need for treatment plant before discharge. This plant must be authorized according to waste regulations. On the other hand, the discharge of leachate into a surface water body, either directly or after treatment, must comply with the limits established in Legislative Decree No. 152/2006, Table 3 in Annex V of Part III, which concerns discharges (Table 12). [104]

Table 12. Emission Limit Values in Surface Water and Sewer (Legislative Decree 152/06, Part Three, Annex 5 - Table 3) [104]

PARAMETER NUMBER	SUBSTANCES	UNIT OF MEASURE	DISCHARGE INTO SURFACE WATERS	DISCHARGE INTO PUBLIC SEWERS (*)
1	pH		5.5-9.5	5.5-9.5
2	Temperature	°C	(1)	(1)
3	Color		Not perceptible with dilution 1:20	Not perceptible with dilution 1:40
4	Odor		It must not cause disturbances	It must not cause disturbances
5	Coarse materials		Absent	Absent
6	Total suspended solids (TSS) (2)	mg/l	≤ 80	≤ 200
7	BOD: Biochemical Oxygen Demand (asO_2) (2)	mg/l	≤ 40	≤ 250
8	COD: Chemical Oxygen Demand (as O_2) (2)	mg/l	≤ 160	≤ 500
9	Aluminum	mg/l	≤ 1	≤ 2.0
10	Arsenic	mg/l	≤ 0.5	≤ 0.5
11	Barium	mg/l	≤ 20	-
12	Boron	mg/l	≤ 2	≤ 4
13	Cadmium	mg/l	≤ 0.02	≤ 0.02

14	Total chromium	mg/l	≤ 2	≤ 4
15	Chromium VI	mg/l	≤ 0.2	≤ 0.20
16	Iron	mg/l	≤ 2	≤ 4
17	Manganese	mg/l	≤ 2	≤ 4
18	Mercury	mg/l	≤ 0.005	≤ 0.005
19	Nickel	mg/l	≤ 2	≤ 4
20	Lead	mg/l	≤ 0.2	≤ 0.3
21	Copper	mg/l	≤ 0.1	≤ 0.4
22	Selenium	mg/l	≤ 0.03	≤ 0.03
23	Tin	mg/l	≤ 10	
24	Zinc	mg/l	≤ 0.5	≤ 1.0
25	Total cyanides (as CN)	mg/l	≤ 0.5	≤ 1.0
26	Free active chlorine	mg/l	≤ 0.2	≤ 0.3
27	Sulfides (as H_2S)	mg/l	≤ 1	≤ 2
28	Sulfites (as SO_2)	mg/l	≤ 1	≤ 2
29	Sulfates (as SO_3) (3)	mg/l	≤ 1,000	≤ 1,000
30	Chlorides (3)	mg/l	≤ 1,200	≤ 1,200
31	Fluorides	mg/l	≤ 6	≤ 12
32	Total phosphorus (as P) (2)	mg/l	≤ 10	≤ 10
33	Ammoniacal nitrogen (as NH_4)(2)	mg/l	≤ 15	≤ 30
34	Nitrous nitrogen (as N) (2)	mg/l	≤ 0.6	≤ 0.6
35	Nitric nitrogen (as N) (2)	mg/l	≤ 20	≤ 30
36	Fats and oils (Animal/vegetable)	mg/l	≤ 20	≤ 40
37	Total hydrocarbons	mg/l	≤ 5	≤ 10
38	Phenols	mg/l	≤ 0.5	≤ 1
39	Aldehydes	mg/l	≤ 1	≤ 2
40	Aromatic organic solvents	mg/l	≤ 0.2	≤ 0.4
41	Nitrogenous organic solvents (4)	mg/l	≤ 0.1	≤ 0.2
42	Total surfactants	mg/l	≤ 2	≤ 4
43	Phosphorous pesticides	mg/l	≤ 0.10	≤ 0.10
44	Total pesticides (excluding phosphorous) (5)	mg/l	≤ 0.05	≤ 0.05
	Including:			
45	- aldrin	mg/l	≤ 0.01	≤ 0.01
46	- dieldrin	mg/l	≤ 0.01	≤ 0.01

47	- endrin	mg/l	≤0.002	≤ 0.002
48	- isodrin	mg/l	≤ 0.002	≤ 0.002
49	Chlorinated solvents (5)	mg/l	≤ 1	≤ 2
50	Escherichia coli (4)	UFC/100 ml	Note	
51	Acute toxicity test (5)		The sample is not acceptable if, after 24 hours, the number of immobile organisms is equal to or greater than 50% of the total	The sample is not acceptable if, after 24 hours, the number of immobile organisms is equal to or greater than 80% of the total

(*) The limits for discharging into the sewerage indicated are mandatory in the absence of limits set by the competent authority under Article 33, paragraph 1 of this decree or in the absence of a final treatment plant capable of meeting the emission limits of the final discharge. Different limits set by the managing entity must be made comply with indicated in note 2 of table 7 concerning hazardous substances.

1) For watercourses, the maximum variation between average temperatures of any section of the watercourse upstream and downstream of the discharge point must not exceed 3°C. On at least half of any downstream section, this variation must not exceed 1°C. For lakes, the discharge temperature must not exceed 30°C, and the temperature increase in the receiving body must not exceed 3°C at any point beyond 50 meters from the discharge point. For artificial canals, the maximum average water temperature of any section must not exceed 35°C; this condition is subject to the consent of the entity managing the canal. For the sea and estuarine areas of non-significant watercourses, the discharge temperature must not exceed 35°C, and the temperature increase in the receiving body must not exceed 3°C at any point beyond 1000 meters from the discharge point. Environmental compatibility of the discharge with the receiving body must also be ensured, and the formation of thermal barriers at river mouths must be avoided.

2) Regarding urban wastewater discharges, the limits in table 1 apply, and for sensitive areas, those in table 2 also apply. Regarding industrial wastewater discharges into sensitive areas, the concentration of total phosphorus and total nitrogen must be 1 and 10 mg/l, respectively.

3) These limits do not apply to discharge into the sea; in this regard, estuarine areas are equated with coastal marine waters, provided that natural variations in sulfate or chloride concentrations are not disturbed on at least half of any downstream section of the discharge.

4) In the authorization for the discharge of urban wastewater treatment plants by the competent authority, the most appropriate limit should be set considering the environmental and health conditions of the receiving water body and existing uses. A limit not exceeding 5,000 CFU/100 ml is recommended.

5) The toxicity test is mandatory. In addition to the Daphnia magna test, acute toxicity tests may be conducted on Ceriodaphnia dubia, Selenastrum capricornutum, bioluminescent bacteria, or organisms such as Artemia salina for saltwater discharges or other organisms as indicated under point 4 of this annex. In the case of multiple toxicity tests, consider the worst result. A positive result in the toxicity test does not directly lead to the application of sanctions under Title V; it also requires further analytical investigations, the search for toxicity causes, and their removal.

1.9 Landfill Leachate Treatment Techniques

Waste is the cause of the presence of various types of toxic contaminants in leachate. [105] The main difficulties in treating leachate stem from its possible concentration of different toxic metals, heavy metals, humic/fulvic acid, ammonia, COD/BOD, and other emerging pollutants. [97] Few technologies, when used alone, are capable of fully treating landfill leachate. Most technologies employ an integrated system that combines biological, chemical, and physical processes. This integrated and hybrid approach has proven to be more effective. [106-110] The following sections will provide an analysis of current leachate treatment techniques, considering their operating principles, efficiency, advantages, and disadvantages.

1.9.1 Biological Treatments

The biological treatment of leachate is mainly divided into two types of processes: aerobic and anaerobic. The aerobic method uses oxygen and aerobic microorganisms to break down organic compounds into CO_2. The anaerobic method employs anaerobic microorganisms to convert organic substances into CO_2, CH_4, NH_3, volatile fatty acids, and simpler organic compounds. [97][111-112] Both techniques are effective in removing contaminants such as polycyclic aromatic hydrocarbons, organic halogens, and polychlorinated biphenyls (PCBs). [113] Aerobic treatment is convenient and effective for young leachate that contains dissolved and suspended organic compounds with a very high BOD5/COD ratio (>0.5). [114] Additionally, the aerobic process ensures the removal of nitrogen from old leachate through nitrification and denitrification. [115]

1.9.1.1 Aerobic Processes

Typical aerobic treatments can occur by different processes, the most important being: aerated lagoons, sequencing batch reactors, rotating biological contactors, membrane bioreactors, and trickling filters. [116]

- **Aerated Lagoon (ARL)**

An aerated treatment basin is an area where oxygen is mechanically introduced to facilitate the aerobic decomposition of organic materials and contaminants present in the leachate. These basins are equipped with surface devices that agitate water to improve the contact between water and air, and submerged devices that release air bubbles at the bottom, thus increasing the amount of dissolved oxygen in water. [117] Solid residues and sediments resulting from biological decomposition accumulate at the bottom, forming a layer of sediments that can be periodically removed. Easy and quick to install, they require low operational and maintenance costs. [118] A study conducted using the ARL technique demonstrated removal rates of 80% and 75% of N and COD, with initial concentrations of 1.241 mg/L and 1.740 mg/L, respectively. These high removal rates are partly due to evaporation actions and the longer retention time. [117] The main drawbacks are related to the dependency of bacterial activity on the basin temperature, with the optimal temperature range being between 20 and 40°C. [119] Other disadvantages include high energy consumption, prolonged aeration times, and the management of produced sediments.

- **Sequencing Batch Reactors (SBR)**

SBR is based on the operational principles of the fill-and-draw procedure. [120] This method aims to reduce aeration costs by up to 25% combining aerobic and anaerobic treatments for nitrification and denitrification. [120-121] An SBR is designed to handle leachate through four phases: filling, reaction, stabilization, and sedimentation.[122] In the filling phase, leachate and potential nutrients are added. During aeration, oxygen supports aerobic microorganisms in decomposing organic matter, while mixing keeps solids in suspension. [123-124] After 18-20 hours of aeration, sludge settles. Studies show that SBR with coagulation by alumina Al_2O_3 achieves removal rates of COD, ammoniacal nitrogen (NH_3-N), and total suspended solids (TSS) by 85%, 94%, and 92%, respectively. SBR effectively reduces heavy metals like Cd (95%) and Pb (95%). [125] When integrated with a membrane bioreactor, the powdered activated carbon (SBR-PAC) achieves maximum removals of COD (66.1%), NH_3-N (99.66%), and leachate color

(82.3%), with a low sludge volume of 130.1 mL/g. [126] Advantages include effective removal of BOD, COD, and nutrients, with reduced odor issues. Disadvantages involve high energy costs, the need for precise control, and management of excess sludge. [127-128]

- **Rotating Biological Contactors (RBC)**

A rotating biological contactor (RBC) consists of discs mounted on a horizontal shaft that rotates slowly, promoting the growth of microorganisms on discs surface. Rotating at 1-2 rpm, discs alternate between leachate and air, facilitating biomass aeration and contaminants degradation. [129-130] RBCs are effective in treating leachate with high organic matter and NH_3-N contents, thanks to their low energy consumption and ease of management. [131] However, they require periodic biomass treatments and are sensitive to high temperatures. Their effectiveness in reducing BOD, COD, phenols, and nitrates varies based on factors such as rotation speed and temperature. [130] One study reported reductions of 74% for COD and 43% for NH_3-N in leachate with initial COD of 1.154 mg/L and NH_3-N of 834 mg/L, but performance declined above 20°C, with a maximum BOD5 removal of 40%. [132-133]

- **Membrane Bioreactor (MBR)**

A MBR reactor combines a biological treatment with a membrane filtration system. Leachate is introduced into an aeration tank where microorganisms degrade the organic matter through the aerobic decomposition of contaminants. In this phase, microorganisms grow and reproduce, forming a biomass (activated sludge) that degrades the organic and inorganic compounds in leachate. After the biological treatment, an effluent passes through ultrafiltration or microfiltration membrane modules, which retain suspended solids and microorganisms, allowing only clean water to pass through. Pressure or vacuum applied pushes water through the membranes, while solids and microorganisms are retained and concentrated in the return sludge, which is periodically removed for further treatment or disposal. [107,134] There are two types of MBRs depending on the orientation of the membrane module: the submerged

MBR, where the membrane module is immersed in the aeration tank, and the external side-stream MBR, where the membrane module is positioned outside the aeration tank. MBR offers numerous advantages versus other biological treatments of leachates, including limited space requirements, reduced production of excess sludge with consequently lower disposal costs, flexibility in managing various pollutant loads and leachate volumes by adjusting sludge concentration and flow through the membranes, and the production of high-quality final effluents. [135] However, MBR disadvantages include the high cost of membranes, difficulties in cleaning and replacement, complicated maintenance due to clogging, and high energy consumption.[107][136-137] According to a study, the maximum concentration of BOD, volatile suspended solids, NH_3-N, and total nitrogen (TN) that an MBR can remove are 6000, 500, 4000, and 6000 mg/L, respectively. This means that MBR can remove 95–99% of BOD5. [138] By pretreating with air stripping, MBR can efficiently remove 44% of the COD. A high contaminant removal efficiency from leachate can be obtained by integrating MBR with other treatment technologies, such as ultrafiltration and nanofiltration, reaching approximately 88% removal yield. [139]

- **Trickling Filters**

A trickling filter is an aerobic biological reactor consisting of a bed support made of gravel, rocks, plastic, or other materials with a high specific surface area, through which the leachate is distributed. Microorganisms grow on the surface of the support, forming a biofilm that degrades the organic matter and other contaminants. However, the trickling filter is not recommended for leachate produced from young landfills, due to the high concentration of total suspended solids (TSS) and fungal growth, which reduce its removal efficiency. [140-141] An experimental-scale study compared the treatment performance of trickling filters and SBR, using leachate from the same source. The trickling filter showed significantly high removal efficiency for TSS (73%), BOD5 (77%), and NH_3-N (60%), while the SBR showed removal efficiencies of 63% for TSS, 84% for BOD5, and 65% for NH_3-N, respectively. [123] Therefore, trickling filters proved to be economically advantageous for treating leachate, especially from mature landfills. [61]

1.9.1.2 Anaerobic Processes

Leachate treatment can be also accomplished through a variety of anaerobic procedures, including anaerobic digestions, up-flow anaerobic sludge blanket reactors and anaerobic filters.

- **Anaerobic Digestion (AD)**

An anaerobic digester treats leachate through biological decomposition of the organic matter in the absence of oxygen. Decomposition occurs in a sealed tank equipped with mixing systems for uniform contact with anaerobic microorganisms. The tank is typically heated to optimal temperatures of 30°C to 40°C to allow the mesophilic microorgaism activity or 50°C to 60°C for thermophilic microorganisms. [142]
The AD process converts organic compounds into biogas (CH_4 and CO_2) and effectively removes trace metals up to 50%. [143-144] While AD can recover renewable energy and reduce organic load, its drawbacks are due to the high AD installation costs, sensitivity to temperature, pH, and organic load. [145]

- **Up-Flow Anaerobic Sludge Blanket Reactor (UASBR)**

UASBR is effective for treating leachate, particularly from industrial wastewater with high organic loads. Leachate flows upward through a sludge bed of anaerobic microorganisms, converting the organic matter into biogas (mainly methane and carbon dioxide) by several biochemical processes. The produced biogas is collected, while a clarified effluent exits for further treatment. A study varying hydraulic retention time (HRT) has shown that UASBR removed 87% COD after 13 hours, while another UASBR achieved 91% COD removal after 20 hours, thus demonstrating the benefits of increased HRT. [146]
UASBR has low operational costs and effectively removes recalcitrant organic compounds. However, it faces challenges like long process times and sensitivity to temperatures. [147-148]

- **Anaerobic Filters (ANF)**

ANFs are reactors with fixed or fluid beds containing materials for packing like gravel, plastic, or woodchips, which support the growth of anaerobic microorganisms. Leachate enters from the bottom and flows upward through the filter bed, typically with a hydraulic retention time (HRT) of 12 to 36 hours, in either continuous or intermittent modes. The wastewater treated is collected at the top and may undergo further treatments.[107] ANF efficiently decomposes the organic matter and suspended solids, effectively treating NH_3-N. [149] Low-cost materials such as biochar and activated carbon can reduce COD and TOC by up to 95% and 80%, while significantly eliminating *E. coli*. [150] ANF also removes heavy metals, but is affected by volatile fatty acid levels, which can decrease methane production. [151] Disadvantages include sensitivity to changes in organic load, the need for regular maintenance to prevent clogging, and long stabilization periods for microbial populations.

1.9.2 Chemical/Physical Treatments

Chemical physical treatments are employed either as a pretreatment or final purification step, as well as to target specific pollutants (Renou et al., 2008). [97] They are commonly used to eliminate suspended solids, colloidal particles, color, and specific classes of pollutants such as heavy metals, polychlorinated biphenyls, and persistent organic compounds like humic and fulvic acids. These techniques include coagulation-flocculation, adsorption, chemical precipitation, membrane filtration, ion exchange, air stripping, electrochemical methods, and advanced oxidation processes (AOP). [97][152]

1.9.2.1 Coagulation/Flocculation

Flocculation and coagulation are two processes often used in combination. Coagulation involves the addition of chemicals into solutions, that destabilize particles eliminating their surface charge and favoring agglomeration. [116,153] Flocculation combines small aggregates into larger ones that are separated by precipitation and filtration. [154-155] Commonly used coagulants are aluminum oxide (Al_2O_3) and ferric chloride ($FeCl_3$). They reduce pollutants by up to 70%, 68%, and 44% respectively at pH 8, 7, and 4. Additionally, $FeCl_3$ can reduce COD by 66%, 79%, and 43%, respectively, and has proven to be effective in removing humic acids. [156] Coagulation and flocculation are relatively simple methods that can be successfully used in the treatment of leachate from old landfills. However, this treatment leads to moderate reductions in COD and TOC and it produces sludge. In some cases, the use of traditional chemical coagulants can increase the concentration of aluminum or iron in the liquid phase. [157] Although the method is easy to use, in the leachate treatment industry, coagulation/flocculation techniques are mainly used as a pretreatment before other more robust processes, such as adsorption and advanced oxidation processes (AOP). [158]

1.9.2.2 Adsorption

Adsorption is the most used technique to remove persistent organic compounds present in landfill leachate. This technique is based on physico-chemical processes where fluids, whether gas or liquid, are attracted to the surfaces of

solid adsorbent materials through physical or chemical bonds. [159-160] Proper preparation of adsorbent materials, such as activated carbon, natural clay minerals, and biochar, is essential to ensure effective adsorption of contaminants through electrostatic attraction, hydrogen bonding, complexation, hydrophobic interaction, and physical adsorption. [161] Table 13 lists various types of food waste that have proven to be effective adsorbent materials for leachate treatment. [162]

Table 13 Efficiencies of different food waste adsorbents for LFL treatment. [116]

Raw material	Leachate initial characteristics	Preparation conditions	Treatment conditions	Adsorption capacity	Removal Efficiency (%)
Banana frond	COD 2336 mg/L, NH_3-N 2550 mg/L, boron 7.50 mg/L, iron 9.31 mg/L	Act. Time 4 min, IR. 1.75 KOH, act. power 600 W, microwave heating	Shaking speed 120 rpm	Boron, 11.09 mg/gIron, 26.15 mg/g	Boron 97.45% and Total Iron 95.14%
Coffee ground	COD 1478 mg/L, NH_3-N 3796.75 mg/L, pH 7.5, iron 4.57 mg/L, PO_4-P 260 mg/L	Act. Temp 600 °C, IR. 0.50 H_2SO_4, act. time 60 min, chemical activation	Shaking speed 300 rpm, contact time 150 mints	N.A	Iron 77% PO_4-P 84%
Durian Peel Palm	COD 3100 mg/L	Act. Temp 800 oC, Act. time 2.1 h, conventional heating	Shaking speed 320 rpm, contact time 180	COD 61.72 mg/g	COD 41.98%
Tamarind fruit seed	COD 2336 mg/L, NH_3-N 2550 mg/L, pH 8.2,	Act. Power 600 W, IR 1:1.50 KOH, act. time 8 min, microwave heating	Shaking speed 120 rpm	COD 64.93 mg/g	COD 79.93%
Sugarcane bagasse	COD 2700 mg/L, NH_3-N2550, PO_4-P 285 mg/L	Act. Power 600 W, IR 1:1.25 KOH, act. time 5 min, microwave heating	Shaking speed 120 rpm	NH_3-N and PO_4-P, 138.46 mg/g,	NH3-N 79.63%, PO_4-P 85.06%
Rice husk carbon composite	COD 9530 to 7330 mg/L and NH_3-N 685–735 mg/L	Composite adsorbent prepared from rice husk carbon waste (75%, w/w), commercial AC (8.22%, w/w), and ordinary Portland cement (16.78%, w/w)	Shaking speed 200 rpm; contact time 120 mints	COD 3.11 mg/g, NH_3-N 12.9 mg/g	COD 27.61%, NH_3-N 51.0%

*I.R. (impregnation ratio) = mass of activating agent / mass of organic material (Converted into AC).

Despite their effectiveness, activated carbon (AC) is the most used adsorbent. Thanks to its intrinsic physical properties, such as a large surface area, microporous structure, high adsorption capacity, and surface reactivity, activated carbon can remove contaminants like heavy metals. [160][163-164] Activated carbon is amorphous and it contains numerous pores and pockets which, based on their size, allow it to be classified as either powdered (<0.074mm) or granular (>0.1mm). Powdered activated carbon is particularly useful for treating old leachate, while granular activated carbon is more suitable when leachate contains aromatic compounds and condensed structures. [116] The rate of contaminant removal depends on the depth of the bed and the contact time of the adsorbent. Therefore, it is essential to develop integrated and hybrid treatment processes for the effective removal of heavy metals. [163] For example, stabilized leachates with a COD of 4500–8000 mg/L, resulting from coagulation pretreatment (which removes 50% of the COD), showed greater COD removal

(80%) when using activated carbon adsorption. [165] Additionally, adsorption using activated carbon combined with biological treatment has allowed effective treatment of landfill leachate in terms of nonbiodegradable organic substances, COD, and color. [97] One disadvantage of this technique is the need for frequent regeneration of the columns or a high consumption of powdered activated carbon (PAC). [116] For this reason, clay minerals like palygorskite are gaining attention due to their global availability as a natural mineral, excellent cost-effectiveness, and ability to rapidly remove high levels of NH_3-N. [166]

1.9.2.3 Chemical Precipitation

Chemical precipitation is generally used as a pretreatment to remove non-biodegradable and recalcitrant pollutants, such as sulfur, heavy metals, and ammoniacal compounds, from leachate. [97, 160, 167, 168] This technique is simple, effective, and economical, converting dissolved ionic contaminants into insoluble precipitates through chemical reactions. These precipitates are then removed by settling or filtration. [61][169-170] Struvite precipitation, (magnesium ammonium phosphate), has been used to study the removal of ammoniacal nitrogen from anaerobically pretreated leachate at the Odayeri landfill in Turkey. Using this process, ammonia is transformed into urea, a nitrogen fertilizer. Approximately 50% of COD and 90% of NH_3-N, with initial concentrations of COD at 4024 mg/L and NH_3-N at 2240 mg/L, were removed. [160] Ozturk *et al.* used Struvite to precipitate NH_3-N from anaerobically pretreated leachate, achieving a removal efficiency of 90% for NH_3-N and 50% for COD. [167] Another study demonstrated the effectiveness of Struvite precipitation for removing ammonium from stabilized leachate at the WENT landfill in Hong Kong, achieving approximately 98% NH_3-N removal at pH 9 within just 15 minutes. [171]

Struvite precipitation forms an insoluble compound that can be easily separated from the liquid, and the resulting sludge can be used as nitrogen fertilizer if the leachate does not contain heavy metals. However, since COD is not significantly reduced during treatment, it is necessary to combine this method with biological phases. [172]

Hence, despite the effectiveness of precipitation techniques, additional treatment processes are required to make the leachate safe according to environmental regulations. [173] Moreover, this technique may have disadvantages, such as the need for large amounts of precipitants, sensitivity to

pH, and the issue to dispose of the resulting sludge if it cannot be used as fertilizer. [160]

1.9.2.4 Membrane Filtration

Membrane filtration avails of selective permeability of molecules, allowing ions and molecules to pass through a barrier with varying porosity. This barrier selectively resists to the flow of components, facilitating their separation. [174-175] In landfill leachate treatment, membrane technology is generally used at the beginning or at the end of the process. Based on the membrane pores size filtration can be classified as microfiltration (MF), ultrafiltration (UF), nanofiltration (NF), and reverse osmosis (RO). [176]

-Microfiltration

Microfiltration, with pores ranging from 0.05 to 10 µm, is used to capture microbial cells, various sized colloidal particles, and suspended solids. This method cannot be used alone and it is recommended as a pretreatment in combination with other membrane processes (ultrafiltration, nanofiltration, or reverse osmosis) or to support chemical treatments. [177] For instance, Piatkiewicz *et al.* used microfiltration as a pretreatment stage, achieving a COD reduction of ~35%. [178]

-Ultrafiltration

Ultrafiltration, with pore sizes between 1 and 100 nm, operates under pressures up to 10 bar. This process is suitable to remove macromolecules and particles from landfill leachate, enabling the separation of organic substances and the analysis of the molecular weight of organic pollutants. It was used in large-scale membrane bioreactors and can serve as a pretreatment for reverse osmosis or as a post-biological treatment. [179-181] For instance, Kulikowska *et al.* and Bohdziewicz *et al.* achieved COD reductions of 46.7% and 50%, respectively, using ultrafiltration alone. [179,182]

-Nanofiltration

Nanofiltration has a molecular weight cut-off ranging from 200 to 1000 Dalton, corresponding to porosities between 0.5 and 2 nm. Due to its properties, which are intermediate between ultrafiltration and reverse osmosis, it repels charged solutes smaller than the membrane pores, as well as larger neutral solutes and salts. It removes recalcitrant organic compounds, inorganic substances, heavy metals, and sulfate ions, but has low rejection rates for chloride and sodium. [153,160,167,183,184] Nanofiltration can remove about 60-70% of COD and 50% of ammonia in landfill leachate, and when combined with other methods, it can remove 70-80% of COD. In the treatment of anaerobically pretreated landfill leachate from Odayeri, Turkey, COD removal of 89% and NH_3-N removal of 72% were achieved. [167] Additionally, nanofiltration effectively removes heavy metals, with over 88% of metallic cations (Pb^{2+}, Zn^{2+}, and Cd^{2+}) removed in stabilized leachate with initial concentrations below 0.70 mg/L. [184] Despite these advantages, nanofiltration membranes can be contaminated by various substances during treatment, including dissolved organic and inorganic compounds, colloids, and suspended particles. [176]

-**Reverse Osmosis**

Reverse osmosis is one of the most effective technologies used in the last decade for leachate treatment due to its flexibility under various temperature and pH conditions. This process uses applied pressure across a semipermeable membrane, creating two solutions at high (concentrate) and a very low (permeate) salt concentration. [153] Reverse osmosis significantly reduces the concentrations of metallic cations in the solvent. Its efficiency is measured by the rejection rate, which can exceed 98% for COD and 99% for heavy metals. [185-186] For example, complete elimination of dioxins from the Yachiyo landfill in Japan was achieved using this technique. [187]

Table 14 Removal of organic and inorganic compounds using UF, NF or RO [160]

Location of landfill	Kind of process	Type of membrane	Species	Pressure (bar)	Initial concentration (mg/L)				BOD/COD	pH	Rejection rates (%)		
					COD	NH_3–N	Metal	BOD			COD	NH_3–N	Metal
NA	NF	NTR-7250	Cr(III) Cu(II) Pb(II)	3	NA	NA	0.69 0.23 0.03	NA	NA	NA	NA	NA	100 99 93
Odayeri (Turkey)	NF	SW	NA	25	3000	950	NA	NA	NA	NA	89	72	NA
Mustankorkea (Finland)	NF	Desal 5-DL	NA	6–8	920	220	NA	84	0.40	7.6	66	50	NA
Spillepeng (Sweden)	NF	AFC-30	Pb(II) Zn(II) Cd(II)	20	2000	NA	0.61 0.50 0.03	NA	NA	NA	NA	NA	97 88 94
Chung Nam (South Korea)	RO	SW-4040	NA	NA	1500	1400	NA	450	0.30	NA	97	96	NA
Yachiyo (Japan)	RO	DT	Mn(II)	9–11	97.4	33.7	4.77	5	0.05	6.0	100	98	100
Pietramelina (Italy)	RO	SW30-2521	Cd(II) Zn(II) Cu(II)	52	3840	NA	0.50	1200	0.31	6.0	98	NA	100 97 99
Hedeskoga (Sweden)	RO	AFC99	Cr(III)	40	1254	541	0.02	125	0.10	7	95	82	NA
Spillepeng (Sweden)	RO	NA	NA	30	925	280	NA	NA	NA	6.5	98	98	NA
Wijster (Holland)		NA	NA	40	335	140	NA	NA	NA	6.5	98	98	NA
Ihlenberg (Germany)	RO	NA	NA	36–60	1797	366	0.25	54	0.03	7.7	99	100	98
	NF			NA	17000	3350	NA	510	0.03	6.4	96	58	NA
Lipówka (Poland)	RO	SS	NA	27.6	1780	743	NA	331	0.28	7–8	97	NA	NA
	UF	PVC	NA	3							52	NA	NA

NA: not available.

In Table 14, the reduction efficiencies of COD, NH_3-N, and heavy metals by the previously analyzed membrane techniques are compared. All reduction percentages are very high, but reverse osmosis stands out as the most effective technique. However, reverse osmosis often fails in the effective separation of ammonia. To improve ammonia reduction in the permeate, reverse osmosis can be used in two or more stages or integrated with a pre-treatment of stripping or a biological nitrification and denitrification phase. [153] Despite its advantages, reverse osmosis has some disadvantages, including the generation of large volumes of concentrate (about 20% of the leachate, which requires disposal or further treatment), low retention of small molecules, membrane fouling (which can reduce its durability and productivity), and high energy consumption. [153,176,188] The passage of water through the membranes depends on porosity, hydrophilicity, material, roughness, thickness, and membrane charge. [189] Polyamide or cellulose acetate membranes offer better removal of organic compounds and NH_3-N and they can operate over a wide temperature range (5-35°C) versus polyvinyl chloride. This is due to the higher porosity and hydrophilicity of polyamide. [189] The choice of appropriate membranes for leachate treatment depends on various factors, including the characteristics of the wastewater, the nature and

concentration of materials present in the leachate, pH, and temperature. [190]

1.9.2.5 Ion Exchange based treatment

Ion exchange technology utilizes resins made of polymeric matrices or synthetic organic materials containing functional ionic groups with exchangeable ions. [191] This process, reversible between solid and liquid phases, is widely used in drinking water treatment, nitrate removal, water softening, and in landfill leachate treatment to remove ammonia, organic compounds, and trace metals. [61,134,153,191] Solid ion exchange particles can be natural-inorganic (such as zeolites) or organic-synthetic resins developed from high molecular weight polyelectrolytes. [192] Both ion exchange resins and natural ion exchange materials have demonstrated a wide range of applications in water and wastewater treatment. [193] Zeolites, natural ion exchangers, are composed of hydrated aluminosilicates with a molecular structure including silica and aluminum tetrahedra linked by covalent bonds with common oxygen atoms. [194] One study showed that zeolite-based resins are effective in removing Cd (75%), Mn (23%), and NH_3-N (86%) from treated leachate. [195]

Another study used zeolites to treat leachate effluent with NH_3-N (211–505 mg/L), nitrates (0.5–8.4 mg/L), and COD (1048–2574 mg/L), achieving removal efficiencies of 90% for NH_3-N, 98% for nitrates, and 74% for COD. [196] For nitrate removal, water passes through a synthetic resin that exchanges anions, including nitrates, with chloride. [191] When the exchange capacity is saturated, the resin is regenerated with a suitable solution, such as sodium chloride, potassium chloride, caustic soda, or acidic solution. The highly concentrated ion exchange residues require careful disposal.[191] The use of ion exchange in landfill leachate treatment is limited by the high concentrations of anions (such as chloride and NH_3-N, over 2000 mg/L) and cations (such as sodium and calcium, over 1000 mg/L) in raw or biologically pretreated leachates. Zeolites and silicates, despite being inexpensive and sustainable natural materials, have limitations in leachate treatment. The complexity and variability of leachate composition, with multiple contaminants, make natural ion exchange materials unlikely to be suitable for this purpose. Although zeolites have been used to remove ammonia, their regeneration has not proven economically advantageous, making the

technology more suitable for sites with reduced ammonia flow rates and concentrations. [191]

1.9.2.6 Air Stripping (Ast)

AST is effective to remove volatile organic compounds from leachates, such as CH_4, NH_3, and H_2S. [97] It is a physical separation process in which pollutants are removed from leachates by injecting air. In some cases, hot air or steam is used to facilitate stripping, or water is heated conductively or resistively. [197] The continuous air injection into the water increases the dissolved oxygen content, allowing aerobic degradation processes. [198] This treatment, although simple and less expensive suffers from atmospheric pollution and odor emissions due to the release of NH_3 and H_2S. [199] For this reason, it is always necessary to combine it with a gas recovery treatment, such as an activated carbon unit that purifies the gaseous effluent. [200]

1.9.2.7 Electrochemical methods

In recent years, electrochemical methods have been employed to treat highly toxic and biologically non-degradable organic materials. They offer advantages such as reduced sludge production, operational simplicity, short operation times, and high efficiency. [201] They are used in the treatment of leachate since they have been shown to effectively remove COD, ammoniacal nitrogen, and heavy metal pollutants. [202] The most common methods include electrocoagulation (EC) and electrooxidation (EO). [153,203]

- Electrocoagulation (EC)

EC is effective to remove large colloids and suspended particles. [204-205] The working principle is electrolysis in which, applying a bias between electrodes, a sacrificial anode is dissolved and the generated cations act as coagulants in the form of metallic hydroxides that favor precipitation of pollutants. Meanwhile water is reduced to H_2 at the cathode (Figure 6) [206-208]

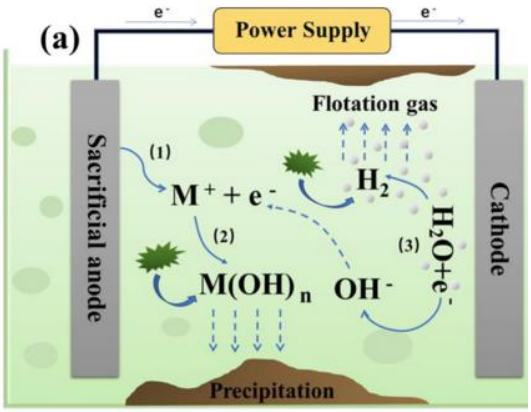

Fig.6. EC mechanism[204]

EC efficiency depends on various factors, including the material, shape, and spacing of electrodes, as well as the current density.

The most used **electrode materials** are iron and aluminum. During the treatment of leachate, a low current density with aluminum electrodes leads to a significant removal of total nitrogen, while iron electrodes are more efficient working at high current density and for long times. [209] For example, COD removal can reach 70% in 20 minutes at a current density of 10 mA/cm² using an Al electrode, while COD removal is 65% at the same time, with 8 mA/cm² current density, using an Fe electrode.

In general, the applied current density is directly proportional to the degree of anode dissolution and determines the amount of coagulant generated during the process, influencing the mass transfer of the anode and the removal of pollutants. If the current density is too high, the system's energy consumption increases, and toxic disinfection by-products are produced. Despite the effectiveness of electrocoagulation in treating landfill leachates, this technique has still some limitations. The main disadvantage is the continuous dissolution of the "sacrificial anode" that must be constantly replaced. Moreover, metal ions may be released into the effluent, causing secondary pollution and a large amount of sludge containing metal ions is produced, and it requires further treatment. [204]

- Electrooxidation (EO)

EO promotes the removal of pollutants through direct and indirect oxidation. The degradation of organic matter by direct oxidation involves

two phases: first, pollutants are adsorbed onto the surface of the anode; subsequently, direct electron transfer oxidizes the organic matter.

Indirect oxidation, on the other hand, occurs by oxidation of water at the anode that generates hydroxyl radicals that oxidize the organic matter. The nature of the electrode is crucial in this case. [208] "Active" metallic anodes with high oxidation state form metal oxides that contribute to the removal of organic matter, while "inactive" anodes promote the formation of hydroxyl radicals to mineralize pollutants. In addition to hydroxyl radicals, electrochemically generated oxidants such as hypochlorite and hypochlorous acid can destroy the organic matter as well. [204] The most common oxidants produced are hypochlorite ClO^- and hypochlorous acid HClO. For landfill leachate, the indirect oxidation process by active chlorine is useful for the removal of ammoniacal nitrogen and COD reduction.

The efficiency of EO in treating landfill leachate depends on many factors, such as the anode material, the current density, and pH. Higher electrocatalytic activity of the anode material leads to faster electron transfer and less fouling. Anodes like BDD, titanium-based, ruthenium, iridium, tin oxide, and lead dioxide (PbO_2) are commonly used in leachate treatment for their high stability and ability to release active chlorine. [210] Current density influences the oxidation of chloride ions in the leachate: higher current densities improve oxidation capacity and pollutant removal. [50]

Compared to EC, EO produces less sludge but has high energy consumption and operational costs. However, combining EO with other processes can effectively reduce energy consumption. EO can be used as a to improve the biodegradability of wastewater or as a post-treatment to eliminate refractory organic matter. A further limitation of EO is the formation of toxic chlorinated by-products during indirect oxidation mediated by chlorine.

1.9.2.8 Advanced Oxidation Processes (AOP)

AOPs are nowadays one the processes of election to purify leachates from organic matter. [211-213] AOPs rely on the *in situ* generation of oxidants, such as hydroxyl radicals and sulfate radicals, that oxidize pollutants like organic compounds, salts, and inorganic acids, transforming them into H_2O and CO_2. [214]

AOPs include various techniques, such as ozone oxidation, ultraviolet radiation, ultrasonication, Fenton oxidation, and electrochemical oxidation. The combination of these techniques can enhance their efficiency.

- Ozone Oxidation Process

Ozone is a powerful oxidant capable to react with organic molecules both directly and indirectly through hydroxyl radicals (·OH) it generates in water. Direct ozone reactions can occur by redox mechanism, cycloaddition, electrophilic substitution or nucleophilic substitution mechanism. Predominance of direct or indirect reactions depends on factors such as temperature, pH, and chemical composition of leachate. Hydroxyl radicals, formed since direct oxidation, have a short lifespan but oxidizing power higher than ozone, making them effective against organic and inorganic substances. [215-216]

However, the degradation of some organic contaminants is relatively low and this can lead to the formation of toxic gases and intermediate by-products, such as aldehydes and carboxylic acids, which do not react with ozone, resulting in incomplete mineralization. To overcome these limitations, ozonation can be combined with other AOP techniques, such as treatment with H_2O_2, UV radiation, or ultrasounds.[217] This combination increases the production of hydroxyl radicals, thereby improving the treatment efficiency. [216]

The combination of ozone (O_3) and hydrogen peroxide (H_2O_2) is also known as the peroxone process. Literature shows that leachate, with high COD (5230 mg/L) low biodegradability (BOD5/COD = 0.1), and intense dark color, was significantly improved using the combined use of ozone and hydrogen peroxide, [218] thus leading to COD reductions of up to 48%, 0.7 biodegradability, and 94% color removal (Table 15). [219]

Table 15 Example of application of O_3/H_2O_2 in landfill leachate treatment. [219]

No.	COD (mg/L)	BOD (mg/L)	pH	R_{COD}[a] %	H_2O_2/O_3 (g/g)	BOD/COD[b]	O_3/COD (g/g)
1	2000	na	na	95	0.4	na	3.5[c]
2	600	na	na	92	0.4	na	3.3[c]
3	na	na	8	97	1.0[d]	na	2.5 g/L[e]
4	na	na	8	70	0.5[d]	na	na
5	895	43	8.2	28	na	0.14	0.76
6	2000	160	8.4	92[f]	0.3	0.13	1.5
7	1360	<5	8.4	93[f]	0.3	0.32	1.5

Note: na, not available.

[a] COD removal efficiency.

[b] BOD/COD after oxidation treatment.

[c] Transferred ozone mass to mass of initial COD.

[d] It is unknown if this ratio is mass ratio or molar ratio.

[e] Ozone dose.

[f] Heterogeneous catalytic ozonation with H_2O_2.

- Combined O_3/UV method

Combining O_3 with UV treatment involves the photochemical decomposition of ozone (at $\lambda < 310$ nm) to promote the formation of H_2O_2 and ·OH radicals. UV radiation causes the breakdown of dissolved ozone, facilitating subsequent reactions between atomic oxygen and water that produce thermally excited H_2O_2. The generated H_2O_2 then decomposes into ·OH radicals.

For example, using such hybrid O_3/UV process, Chen *et al.* successfully achieved highly effective mineralization of total organic carbon (TOC) using 96 W of UV radiation and 3.8 g/h ozone amount. This approach enables the degradation of dinitrotoluene and trinitrotoluene. [220] Examples of application of O_3/UV process for treatment of landfill leachate are reported in Table 16.

Table 16 Example of application of O_3/UV in landfill leachate treatment [219]

No.	COD (mg/L)	BOD (mg/L)	pH[a]	R_{COD}[b] (%)	BOD/COD[c]	UV (W)	O_3/COD (g/g)
1	1280	100	2.0	54	na	100	na
2	1280	100	2.0	47	na	500	na
3	26 000	2920	7.8	63[d]	0.32	1500	3.5[e]
4	26 000	2920	7.8	61[d]	0.35	1500	4.7[e]
5	2300	210	8.0	50	na	15	1.0

Note: na, not available.

[a] Reaction pH.

[b] COD removal efficiency.

[c] BOD/COD after oxidation treatment.

[d] Removal efficiency of TOC, the TOC concentration of raw leachate was 14 616 mg/L.

[e] Ratio of TOC removed to O_3.

- Combined O_3/catalysts method

Ozonation can be also catalyzed by Cu(II), Mn(II), Cr(III), Co(II), Fe(II), Fe(III), and Zn(II) ions under homogeneous conditions or by use of metal oxides (such as MnO_2, TiO_2, Al_2O_3, CeO_2) on supports (such as metal-modified zeolites, activated carbon, SiO_2) as heterogeneous catalysts. The effectiveness of the process depends on operational parameters such as the pH of the solution and the type of catalyst used. [216]

- The Fenton Oxidation method

The Fenton process, extensively studied in recent years, is one of the most cost-effective options among potential physicochemical technologies for leachate treatment. [221] The Fenton reagent consists in a mixture of Fe (II) salt, used as the catalyst, and the oxidant H_2O_2.

Due to its oxidation potential (1.80 V), H_2O_2 is theoretically effective as an oxidizing agent for leachate treatment. However, its slow reaction rates with organics and slow self-decomposition rate, H_2O_2 alone is not effective to degrade recalcitrant compounds present in a high strength of stabilized leachate. For this reason, H_2O_2 is activated with Fe(II) based catalysts to oxidize most recalcitrant pollutants. The Fenton system relies on an electron transfer between H_2O_2 and Fe^{2+} leading to ·OH radicals. Radicals

produced in this way degrade organic compounds, according to the following mechanisms: [222]

Initial reactions:

$$H_2O_2 + Fe^{2+} \longrightarrow Fe^{3+} + OH^- + {}^{\bullet}OH \quad K_1 = 70M^{-1}s^{-1} \quad \textbf{(1)}$$

$$H_2O_2 + Fe^{3+} \longrightarrow Fe(OOH)^{2+} + H^+ \longleftrightarrow Fe^{2+} + HO_2^{\bullet} + H^+ \quad \textbf{(2)}$$

$$OH^- + Fe^{3+} \longrightarrow Fe(OH)^{2+} \longleftrightarrow Fe^{2+} + {}^{\bullet}OH \quad \textbf{(3)}$$

Propagation:

$${}^{\bullet}OH + H_2O_2 \longrightarrow HO_2^{\bullet} + H_2O \quad K_2 = 3.3 \times 10^7 M^{-1}s^{-1} \quad \textbf{(4)}$$

$$HO_2^{\bullet} + H_2O_2 \longrightarrow {}^{\bullet}OH + H_2O + O_2 \quad \textbf{(5)}$$

$$HO_2^{\bullet} + HO_2^- \longrightarrow {}^{\bullet}OH + OH^- + O_2 \quad \textbf{(6)}$$

Termination:

$$Fe^{2+} + {}^{\bullet}OH \longrightarrow Fe^{3+} + OH^- \quad K_2 = 3.2 \times 10^8\, M^{-1}s^{-1} \quad \textbf{(7)}$$

$$HO_2^{\bullet} + Fe^{3+} \longrightarrow Fe^{2+} + H^+ + O_2 \quad \textbf{(8)}$$

$${}^{\bullet}OH + HO_2^{\bullet} \longrightarrow H_2O + O_2 \quad \textbf{(9)}$$

$${}^{\bullet}OH + {}^{\bullet}OH \longrightarrow H_2O_2 \quad \textbf{(10)}$$

Radicals interact with organic compounds, extracting an electron from Fe(II) and converting it into Fe(III). The formation rate of ·OH radicals is increased through the reaction between Fe(II) and H_2O_2. When Fe(II) is added into the system, the initiation of the chain reactions by ·OH leads to a degradation of the organic pollutants, and, as consequence, to a decrease of COD. [223] When recalcitrant compounds in the leachate are oxidized by Fenton reagents, they can undergo a primary degradation, structural changes that improve biodegradability, or degradation that reduces toxicity, eventually producing CO_2 and H_2O. [224]

The Fenton oxidation process is affected by several factors, including the concentrations of Fe(II) and H_2O_2, the pH, reaction by-products, the ratio of organic materials to Fenton reagents and temperature. [225]

For example, Zhang *et al.* reported that increasing the temperature from 13 to 37°C slightly improved COD removal from 90 to 94% at an initial concentration of 1000 mg/L. [226] This suggests that higher temperatures enhance the degradation rate of organic pollutants in leachate, likely because higher temperatures accelerate the reaction between H_2O_2 and Fe^{2+}, thus increasing the production rate of oxidizing species such as ·OH radicals. [227-228] Although the increase of H_2O_2 improves organic degradation, its optimal concentration must be chosen carefully, as excess of H_2O_2 can act as a scavenger for ·OH radicals, reducing the Fenton oxidation rate. [229]

With regard to Fe(II) concentration, although high values accelerate the Fenton reaction, only a small amount of Fe(II) is necessary to catalyze H_2O_2 decomposition. An ideal mass molar ratio of ~3.0 for H_2O_2 /Fe(II) achieves rapid oxidation and effective degradation of recalcitrant compounds in leachate.

pH is also crucial to optimize the Fenton oxidation. Indeed, low pH (2.5 to 3) increases the reaction's oxidation efficiency. [175,226] while, when pH exceeds 4, the H_2O_2 decomposition rate decreases due to Fe(II) complex formation with the buffer, inhibiting ·OH radical formation. [230] At pH levels below 3.0, $Fe(OOH)^{2+}$ forms and reacts slowly with H_2O_2, producing fewer ·OH radicals. [231]

In summary, the Fenton oxidation can completely degrade recalcitrant pollutants and convert toxic materials into less harmful compounds, reducing toxicity and enhancing leachate biodegradation. Its homogeneous catalytic nature makes the Fenton process simple and energy-efficient, as it requires no additional energy input. [224] However, the process has drawbacks, such as high operational costs due to the chemicals needed and sludge disposal expenses. [232] H_2O_2 is highly aggressive and can cause corrosion issues. The homogeneous catalyst added as Fe(II) salts cannot be retained during degradation, as the oxidation process produces iron hydroxide sludge that must be disposed of, adding to the cost. Additionally, a continuous supply of chemicals is required to prevent the process from stagnating. [233-234]

Heterogeneous processes are favored to overcome some of these issues. For the treatment of organic materials in wastewater, the heterogeneous Fenton method (also known as Fenton-like) is an important alternative

since it enables catalyst recycling and reduces the production of solid sludge, thereby decreasing the process's environmental impact and enhancing its cost-effectiveness. There is still a significant need to find catalysts with improved selectivity, higher efficiency, and greater recyclability. Several articles in the literature discuss efforts to enhance this method.

The use of transition metals other than iron as catalytic sources is the subject of numerous investigations. For instance, Hussain *et al.* utilized copper supported on zirconia as a catalyst. Unlike iron, copper does not form stable compounds with intermediate products. According to the results, depending on the initial organic load in the wastewater stream, the proposed catalyst may achieve nearly complete removal of organic compounds through various simultaneous oxidation processes. Additionally, even after four cycles, the catalyst continued to function effectively. [235] Hussain *et al.* also proposed using steel scale waste (SSW). SSW, a byproduct of steel production, contains high amounts of iron and oxides. It effectively removed about 75% of the recalcitrant organic load from landfill leachate. [236]

- Ultraviolet light assisted Oxidation

UV radiation (100-380 nm) has been recognized as the best disinfection method against microbes, viruses, pathogens and other chemical contaminants in drinking water. Primarily, UV sources with low pressure (partial pressure = 1 Pa) are mercury lamps with monochromatic emission. Typically, 254 nm wavelength is used for disinfection, closely matching DNA maximum absorption wavelength. However, UV lamps have several drawbacks, such as high energy consumption, relatively short lifespan (10.000 hours), and the presence of toxic mercury that requires proper disposal. [216] The extensive use of UV-LEDs /ultraviolet light emitting diodes), which contain non-toxic materials like gallium and aluminum nitride or just aluminum nitride, has mitigated many of the limitations associated with conventional UV rays. [237] Hamamoto et al. (2007) used a 365 nm UV(A)-LED source to remove *Escherichia coli* from aqueous solutions, achieving better results than conventional 254 nm UV. [238] A distinctive feature of UV-LEDs is their adjustable pulsed illumination during

disinfection. Wengraitis *et al.* (2013) used a 272 nm pulsed UV(C)-LED source at a frequency of 1 Hz to inactivate *Escherichia coli*, finding its inactivation capacity superior to continuous illumination at the same UV dose. [239] Additionally, various studies have explored vacuum UV (VUV) irradiation for degrading natural organic matter in water. Thomson et al. (2004) demonstrated that using VUV irradiation at 185 nm significantly increased the mineralization efficiency and biodegradability of natural organic matter compared to conventional 254 nm UV radiation. [240] Furthermore, UV oxidation processes can be combined with other AOPs) such as H_2O_2, ozone, and Fenton, to further enhance disinfection performance.

- Combined UV/H_2O_2 method

UV irradiation and H_2O_2 oxidation can be also combined to improve performances. The UV/H_2O_2 process involves the use of UV light to enhance the oxidation power of hydrogen peroxide on organic compounds through the generation of hydroxyl radicals (·OH). [241] Firstly, many organic contaminants that absorb UV light undergo molecular changes, making them more reactive with oxidants. Secondly, UV light catalyzes the decomposition of H_2O_2 into two ·OH radicals by breaking the O-O bonds of H_2O_2. [242] Ince, studied the treatment of leachate from the Stuttgart landfill in Germany using the UV/H_2O_2 process and found a 59% reduction in COD with an initial concentration of 1280 mg/L. [243] This result was lower than Steensen's study at the Braunschweig landfill, which achieved a 90% COD reduction with an initial concentration of 1200 mg/L. The discrepancy may be due to Steensen using more UV lamps, increasing the activation of organic molecules and making them more susceptible to oxidation. [244]
The effectiveness of the UV/H_2O_2 process for COD removal depends on various reaction conditions, including the total organic load in the leachate, the type and concentration of organic contaminants, light transmittance (affected by turbidity or color), the H_2O_2 amount, the kind and concentration of dissolved inorganic substances (such as carbonates and iron), and pH levels. [245] For optimal COD removal, a pH between 3 and 4 is ideal for the UV/H_2O_2 process. Overall, the UV/H_2O_2 process outperforms the UV/O_3 counterpart in COD removal. With COD concentrations between

1200 and 1280 mg/L, the UV/H_2O_2 system can achieve up to 90% COD removal at a pH of 3 to 4, whereas the UV/O_3 system achieves less than 55% removal at the same COD concentrations and a pH of 2.0. This is because H_2O_2 readily splits into two ·OH radicals under UV light, enhancing the degradation of organic contaminants or transforming them into harmless substances. [243] However, the UV/H_2O_2 process has some drawbacks. Due to the low molar absorption of H_2O_2 in the 200–300 nm range, a high dose of H_2O_2 and prolonged UV exposure with strong, broad-spectrum UV output are necessary, leading to higher energy consumption compared to the UV/O_3 process. [246] Additionally, the UV/H_2O_2 process is sensitive to the scavenging effects of carbonates in basic conditions (pH 8–9). High concentrations of H_2O_2 can act as radical scavengers, slowing the oxidation rate, while low concentrations of H_2O_2 generate insufficient ·OH radicals, resulting in a slower oxidation rate. [245-246]

- Combined UV/H_2O_2/O_3 method

Despite being a powerful oxidizing agent, ozone alone is not so efficient to degrade the persistent compounds found in leachate. [247] When combined with UV light and hydrogen peroxide, it can effectively oxidize more resistant substances. Adding H_2O_2 to the UV/O_3 system accelerates ozone decomposition, which in turn increases the generation rate of hydroxyl radicals. [248] In a study on leachate treatment at the Stuttgart landfill in Germany, Ince reported that the O_3/H_2O_2/UV process outperformed both the UV/O_3 and UV/H_2O_2 methods. At an initial COD concentration of 1280 mg/L, the O_3/H_2O_2/UV system achieved 89% COD removal, compared to 54% for UV/O_3 and 59% for UV/H_2O_2. This improvement is likely due to the synergistic effect of H_2O_2 and ozone in generating ·OH radicals, which effectively degrade the persistent compounds in the leachate. Additionally, the treated effluent's COD was reduced to below 140 mg/L, meeting local discharge standards. [243] Regarding energy consumption, the O_3/H_2O_2/UV system is a viable option, especially if ozone generation costs are low. [253] The recommended optimal pH for the process is 2–3 when using H_2O_2 and 8–9 when using ozone. [175,226] A significant advantage of the O_3/H_2O_2/UV system is the absence of pollution from the photoreactor, ensuring uninterrupted oxidation processes. [250]

- UV/H_2O_2/Fe^{2+} (photo-Fenton oxidation)

Irradiating with UV light during the Fenton process can enhance COD removal. UV light causes the photolysis of Fe(III) oxalate complexes, generating Fe^{2+} ions. that further drive the Fenton process. Additionally, Fe^{2+} ions are generated from the interaction of UV light with $Fe(OH)^{2+}$, which then react with H_2O_2 to produce more ·OH radicals. These radicals are highly reactive and initiate the oxidation of pollutants in the leachate, leading to the mineralization of organic pollutants. The organic radicals (R·) generated in the reaction react quickly with dissolved oxygen, forming peroxyl radicals (RO_2·), which initiate further oxidation reactions. [251] The pH value is crucial for the photo-Fenton oxidation process, with most studies using acidic conditions between pH 2 and 4. Besides pH, the intensity of radiation and the concentration of H_2O_2 and Fe^{2+} significantly influence ·OH formation. With initial COD concentrations ranging from 1150 to 5200 mg/L, the photo-Fenton process can achieve 70% COD removal, which is slightly higher than that achievable by UV/H_2O_2 systems at similar COD levels. The biodegradability of the leachate improves significantly, indicating that the photo-Fenton process can transform the organic molecules into more degradable forms. [252] The photo-Fenton process is cost-effective, particularly since sunlight can be used instead of UV light, reducing treatment costs. [243] However, its performance in acidic conditions is not as good as that of UV/H_2O_2 for COD removal. Like the Fenton process, it produces sludge from iron hydroxide precipitation, which requires further disposal. [253] Additionally, carbonate and bicarbonate ions can interfere by acting as radical scavengers, forming a solid layer on UV lamps, hindering UV penetration and reducing its effectiveness in the leachate. [253] Full-scale application of UV lamps requires high energy consumption, increasing the operational cost of the photo-Fenton process. [244]

- Combined UV/TiO_2 method

TiO_2 is the most widely used catalyst due to its stability and non-toxicity. As a semiconductor, it absorbs light with a wavelength below 385 nm, requiring 1 W/m^2 of light. [254] When combined with UV irradiation, TiO_2

initiates the generation of hydroxyl radicals. Its wide band gap energy (E = 3.2 eV) facilitates reduction-oxidation reactions under UV light at 400 nm. [255-256] However, this method is less explored for leachate treatment due to its high operational costs stemming from significant energy consumption.

- Ultrasound-Based Oxidation Process (US)

Ultrasonic treatment modifies the particle size distribution of wastewater, breaking down larger particles and making microorganisms more accessible for disinfection. In this process, operational parameters such as power density and intensity, frequency, energy dosage, and treatment duration are crucial.

High-power, low-frequency ultrasound generates cavitation, creating intense shear forces in liquids. The extreme conditions of cavitational bubble collapse and particle collisions grind the material into very fine particles. When ultrasound propagates through a liquid, the waves produce alternating cycles of compression and rarefaction (high and low pressure). During the low-pressure cycles, small cavitation bubbles form and grow until they reach a critical size and collapse violently, having absorbed the maximum energy. Cavitation can be of two types: acoustic and hydrodynamic. Acoustic cavitation is generated by high-power ultrasonic waves with frequencies ranging from tens of kHz to tens of MHz, while hydrodynamic cavitation results from the reduction in static pressure caused by compression during flow through asymmetric geometries. [257]

Cavitation can increase the biodegradability of recalcitrant compounds present in wastewater or leachate, causing their complete mineralization due to the action of ·OH radicals. Most studies indicate that increasing the inlet pressure improves the biodegradability of wastewater. [258] This method is also widely used for bacterial inactivation and various biological and chemical applications. [259] The process performance can be further optimized when combined with other advanced oxidation processes (AOPs).

- Combined US/O_3 method

When ozone is used in combination with cavitation, it produces a higher number of hydroxyl radicals through the dissociation of ozone and the subsequent reaction of atomic oxygen with water. [260] According to a study by Tizaoui et al., a cavitation-assisted method can accomplish comparable results with significantly less ozone consumption. The study focused on leachate treatment using only ozone at a concentration of 80 g/m³ and showed a 27% COD removal in 1 hour. [218] Another study by Rajoriya et al. reported that the combination of ozone with cavitation results in higher COD removal compared to using only ozone. [261]

- Combined US/H_2O_2 method

The use of H_2O_2 with ultrasound increases the generation rate of hydroxyl radicals due to the efficient dissociation of added H_2O_2, leading to higher COD removal.
As hydroperoxyl radicals are less reactive than hydroxyl radicals and can also have the scavenging effect of undissociated hydrogen peroxide, continuously increasing the H_2O_2 loading does not lead to higher COD removal. [262]

- Combined US/Fenton method

The combination of ultrasound with Fenton treatment resulted in the highest COD removal, attributed to the intensified production of hydroxyl radicals, making this combination the most efficient approach compared to H_2O_2 or ozone with ultrasound. [110] Using Fenton chemistry produces hydroxyl radicals more quickly than using just H_2O_2

1.9.2.9 Electrochemical Advanced Oxidation Processes (EAOPs)

EAOPs have gained significant recognition for their clean and efficient approach in generating ·OH radicals without the addition of chemicals. These techniques are capable of decomposing organic pollutants to their fully mineralized state. [263] Various technologies included in EAOPs are anodic oxidation (AO), electro-

Fenton (EF), photoelectro-Fenton (PEF), and sonoelectro-Fenton (SEF) oxidations. [204][264-268] The key reactions that occur in different types of EAOPs are summarized in Fig. 7. Other EAOP technologies, such as electroperoxone and electrochemical persulfate activation (E-PS), have proven successful in treatment of leachate wastewater and in soil remediation.

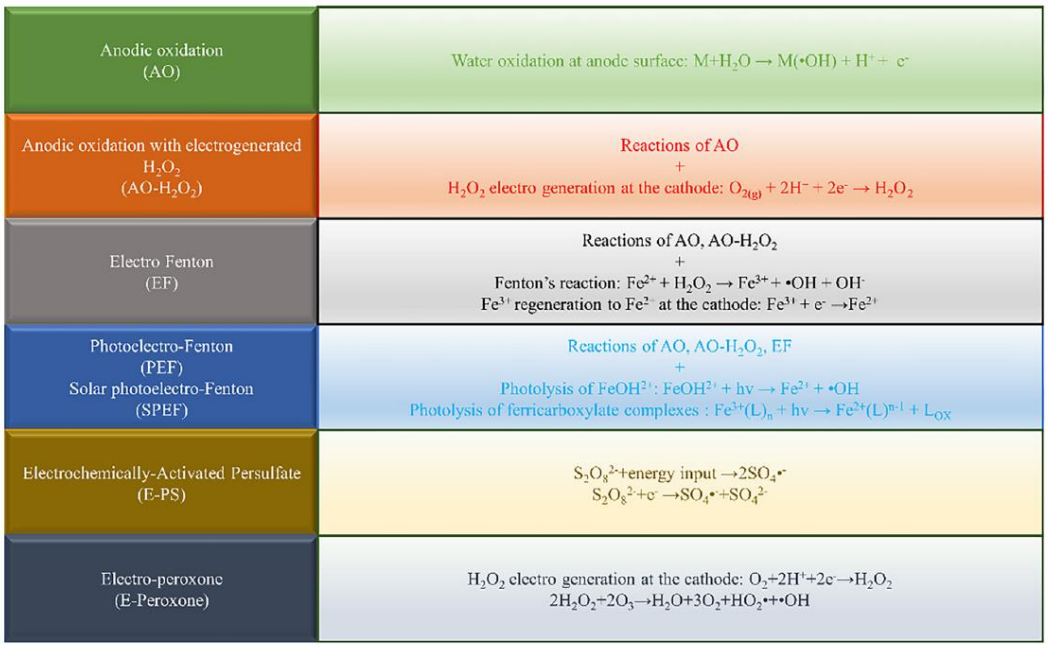

Fig. 7. EAOPs and their main reactions.[269]

Anodic oxidation (AO), can occur by two main processes, the first one based on direct electron transfer between the metal and the pollutant at the anode surface and the second one oxidation of water at the anodic surface with generation of hydroxy radicals that react with contaminants leading to their degradation.

The Electro-Fenton (EF) approach is based on the generation of H_2O_2 by two-electron reduction of O_2 on a suitable electrode material (usually a carbon-based electrode material). [270] Moreover, H_2O_2 leads to the formation of ·OH through the Fenton reaction and Fe^{2+} can be generated on the cathode surface. [270-271] Compared to the typical Fenton process, EF offers various benefits, such as the possibility to generate Fenton's reagent *in situ* reducing costs and risks related to the H_2O_2 storage and handling or the prevention of parasitic reactions that lead to ·OH waste due to the low concentration of Fenton's reagent.

EF efficiencies can be also enhanced combining this process with artificial UV or natural solar light irradiation (Photoelectro-Fenton PEF and Solar Photoelectro-Fenton SPEF). [263]

Moreover, EF can be improved by ultrasounds (Sonoelectro-Fenton) capable to promote the decomposition of H_2O_2 into additional hydroxyl radicals and the continuous ultrasonic cleaning increases the regeneration of Fe^{2+} and reduces electrodes passivation. [272-273]

Other EAOPs used for wastewater and leachate treatment include electrochemically activated persulfate technology and electro-peroxone technologies. The generation of sulfate radicals ($SO_4^{-}\cdot$) through the electrochemical activation of persulfate has gained popularity in recent years, particularly for degradation of persistent organic contaminants. [274-275] Energy transfer to persulfate ion generates two $SO_4^{-}\cdot$ radicals. that can oxidize non selectively organic matter, having redox potentials comparable to hydroxyl radicals. [276]

The electro-peroxone process is an innovative EAOP that starts with the generation of H_2O_2 at the cathode. H_2O_2 facilitates the transformation of ozone produced by a generator into hydroxyl radicals and [277] this method considerably enhances the efficiency and lowers the energy consumption with respect to traditional ozone treatment methods.

The effectiveness of reducing organic contaminants in aqueous solutions using the mentioned EAOPs relies on various operational parameters, such as the initial concentration of organic compounds, properties of the supporting electrolyte, electrode potential, applied current density, liquid flow rate, agitation speed, temperature, and pH. [278] EAOP techniques are advantageous due to their high efficiency in degrading stubborn organic pollutants, minimal auxiliary chemical needs, mild reaction conditions, lack of secondary treatment, and wide applicability [279-280]

- Hybrid biological EAOP processes

In response to the significant operational costs associated with implementing EAOPs, there has been a trend towards adopting combined treatment strategies that incorporate biological processes. This approach aims to optimize the efficiency of both wastewater and soil treatment [279] [281-283] Figure 8 shows a summary diagram of the suitable techniques to be

adopted based on the initial characteristics of the wastewater to be treated. The choice of treatment technology depends on the specific characteristics of wastewater and the desired quality of the treated effluent. Preliminary tests and analyses are necessary before selecting an appropriate treatment method. Wastewater with high toxicity, low biodegradability, and high TOC should first be pretreated with EAOPs to convert non-biodegradable pollutants into a more biodegradable form and partially or completely remove toxic compounds that could hinder the effectiveness of subsequent biological treatment. For more biodegradable wastewater with high COD values, EAOPs can be used as a pretreatment stage to break down complex organic compounds, simplifying the biological treatment process. It is crucial to recognize that EAOPs generally demand more energy and resources compared to biological treatments. Consequently, for wastewater with low toxicity or low biodegradability, it is more efficient to start with biological treatment to eliminate many organic pollutants. Then, EAOPs can be adopted to target specific and persistent pollutants. Furthermore, EAOPs can be used as a final step to enhance the quality of the treated effluent.

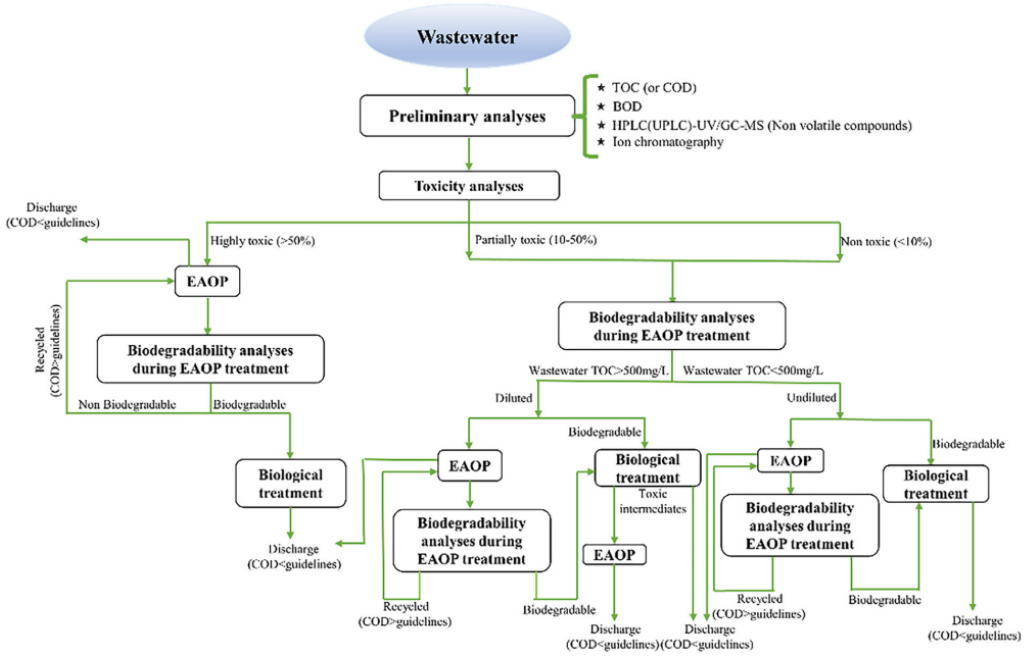

Fig.8. Treatment option for a specific toxic and/or non-biodegradable wastewater [269,284]

Upon combination of EAOPs with a biological treatment, various key factors must be considered. Indeed, after EAOP, adjustments of some parameters are necessary (*e.g.* EF process requires a pH of around 3, while biotreatment requires a neutral pH). [285] Transition to neutral pH causes Fe to precipitate as sludge, this requiring an additional intermediate step to extract the iron hydroxide sludge. Moreover, to minimize chemical and energy consumption and reduce operational costs, it is advisable to limit mineralization levels during the pretreatment phase. Intermediates produced during the electrochemical oxidation (EO) can be also toxic for biological systems.

Other factors that must be considered when EAOPs are integrated with biological treatment systems are the reactors operating modes, the effluent biodegradability, the ideal conditions for both methods, and reactors efficiency. These elements are vital for designing a robust and effective combined system. [286]

Proper concentration of oxidant chemical species is also essential because excessive amounts of oxidizing agents can lead to over-mineralization of the effluents, resulting in a lack of carbon sources for microbial growth during subsequent biotreatment stages.

In summary, and more in general, integration of biological processes with physicochemical methods has proven to be highly effective. Tables 17, 18 and 19 summarize the main adopted hybrid techniques and their effectiveness in reducing COD in landfill leachate.

Table 17 Combined Physicochemical and Biological Treatments for Landfill Leachate Treatment [287]

Combined treatment methods	pH	Initial COD (mg/L)	COD removal efficiency (%)
Photo Fenton/activated sludge	–	12,797	98
Oxidation/coagulation-flocculation	8.15	985	> 90
Aerobic biological oxidation/Fenton	7.6	6790	> 90
Electrocoagulation/anaerobic activated sludge	9	6400	92
Ozonation/aerobic oxidation	6.2	850	73
UASB/SBR/MF/RO	6.5-9	8000-20,000	99.8
Coagulation/hydrolysis acidification–SBR/electro-Fenton	7.1	9765	97.8
Electro-ozonation/SBR	7.34	3018	88.2
SBR/aeration cell-Fenton/adsorption	6.7	41,800	97.2
Coagulation/Fenton/biological aerated filtering	5-8	600-700	88
SBR/coagulation/Fenton/upflow biological aerated filter	8.75	3000	97.3
Air stripping/aerobic and anaerobic processes	7.9	30,000	80
Coagulation-flocculation/SBR	7.11	53,199	98
Submerged anaerobic membrane bioreactor/MBR	7.5	570	96.1
SBR/electro-oxidation	8.6	3973	98
SBR/RO	7.84	2180	96.7
Fenton/aerated biomass	8.5	3909	83
SBR/Fenton-like/SBR	8.2	22,300	95
Electro-Fenton/MBR	8.1	23,200	94.5
Aerobic SBR/adsorption	9.66	3200	43
Constructed wetland/adsorption	7.95	2301	86.7
Photo Fenton/MBR	8.1	24,000	96.2
MBR/UF/electro-oxidation	–	2122	94
Trickling filters/electrocoagulation	8.21	765	80
Activated sludge/coagulation/photo Fenton	7.5	4084	96
Coagulation-flocculation/constructed wetland	5.82	902.5	92.6

Table 18 Combined physicochemical treatments for landfill leachate treatment [287]

Combined treatment methods	pH	Initial COD (mg/L)	COD removal efficiency (%)
Electrocoagulation/filtration	–	–	94
Filtration/adsorption	8.5	1101	94.6
Ozonation/oxidation	–	–	92
Fenton/UF	7.7	1750	80
Fenton/adsorption	8.31	10,193	> 90
Fenton/adsorption	–	–	> 90
Electrocoagulation/electro-oxidation/AOP	6.4	8580 ± 200	95.6
Electrocoagulation/flotation	–	13,600	96
Coagulation-flocculation/EAOP	8.37	1585	> 90
Filtration/adsorption/photo Fenton + ozone	8.9	11,950	95.1
Photo electro-oxidation/adsorption	7.73	1113	67.2
Coagulation-flocculation/solar photo Fenton	8.3	6200	73
Coagulation-flocculation/adsorption	8	6730	86
NF/coagulation/photo Fenton	8.5	1330	91.5
Coagulation/ozonation	8.2	4000	87
Ultrasonic/Fenton	7.8	14,000	92
Coagulation-flocculation/adsorption	–	–	43.24
Coagulation/sand filtration/MF/RO	8.44	2700	99.4
Fenton/adsorption	8.4	3135	82
Coagulation-flocculation/adsorption	8.03	8951	82
Fenton/filtration/adsorption	8.3	5346	99.9
Fenton/coagulation-flocculation	8.3	704	85
Coagulation-flocculation/photo Fenton	8.0	2800	68
RO/electro-oxidation	7.94	2589	> 86
Coagulation-flocculation/adsorption	7.61	22,000	59

Table 19 multistage treatment strategies for the remediation of urban landfill leachates. [288]

Multistage treatment strategy	Operational conditions	Efficiency
Coagulation + Powdered activated carbon (PAC) adsorption + Air stripping	Coagulation: $[FeCl_3]$ = 838 mg Fe L^{-1}, pH = 5.6; PAC adsorption: [PAC] = 1.5 g L^{-1}; Air stripping: air flow rate = 3.5 mL min^{-1}, pH = 11.5, duration = 24 h	COD removal: ~71% Ammonium removal: 95%
Air stripping + Fenton process + Biological treatment in an aerobic sequencing batch reactor (SBR) + Coagulation	Air stripping: air flow rate = 15 L min^{-1}, pH = 11.0, duration = 18 h; Fenton process: pH = 3.0, [Fe] = 4.0 g L^{-1}, $[H_2O_2]$ = 6.0 g L^{-1}; Biological treatment: cycle time = 24 h, pH = 7, hydraulic retention time = 5 d, sludge retention time = 15 d, [dissolved oxygen] = 2.5–4 mg L^{-1}; Coagulation: $[Fe_2(SO_4)_3]$ = 223 mg Fe L^{-1}, pH 5.0	COD removal: 93% Ammonium removal: 98%
Biological treatment by anaerobic ammonium oxidation (anammox) + Photo-Fenton process with UVC light (PF-UVC)	Anammox: cycle time = 24 h, pH = ~7.4, hydraulic retention time = 2 d, sludge retention time = 8 d; PF-UVC process: pH = 3.0, [Fe] = 150 mg L^{-1}, $[H_2O_2]$ = 1.0 g L^{-1}	COD removal: 98% Ammonium removal: >88%
First biological treatment in an aerobic/anoxic reactor + Solar photo-Fenton process (SPF) + Second biological treatment in an aerobic reactor	First biological treatment: cycle time = 58 d, pH = 7.5–9.0, [dissolved oxygen] = >0.5 mg L^{-1} for nitrification and < 0.5 mg L^{-1} for denitrification; SPF process: pH = 2.8, [Fe] = 80 mg L^{-1}, $[H_2O_2]$ = 100–500 mg L^{-1}; Second biological treatment: cycle time = 29 d, pH = 7.5–9.0, dissolved oxygen = >0.5 mg L^{-1}	COD removal: 98% Ammonium removal: 99%
Fenton process + Biological treatment in an aerobic submerged membrane bioreactor + Reverse osmosis	Fenton process: pH = 3.0, [Fe] = 1.1 g L^{-1}, $[H_2O_2]$ = 2.0 g L^{-1}; Biological treatment: polyvinylidene fluoride (PVDF) hollow fiber membrane, air flow rate = 0.1–0.15 m^3 h^{-1}, liquid flux = 2 L $m^{-2}h^{-1}$, hydraulic retention time = 4 d, sludge retention time = 45 d; Reverse osmosis: total effective filtrating area = 66 cm^2, pressure = 2.8 MPa, BW aromatic polyamide composite membrane (Bows, USA)	COD removal: 99% Ammonium removal: 95%
Coagulation + Solar photo-Fenton process (SPF) + Biological treatment in an aerobic reactor	Coagulation: $[FeCl_3]$ = 112 mg Fe L^{-1}, pH = 2.8 (consecutively repeated coagulations); SPF process: pH = 2.8, [Fe] = 56 mg L^{-1}, $[H_2O_2]$ = 0.7–1.0 g L^{-1}; Biological treatment: Zhan-Wellens test	COD removal: >30%
First biological treatment in an aerobic reactor + Coagulation + Solar photoelectro-Fenton process (SPEF) + Second biological treatment in an anoxic reactor	First biological treatment: cycle time = 138–164 h, pH 6.5–9.0, [dissolved oxygen] = 2–4 mg L^{-1}; Coagulation: $[FeCl_3]$ = 240 mg Fe L^{-1}, pH = 3.3; SPEF process: pH = 2.8, [Fe] = 60 mg L^{-1}, current density = 200 mA cm^{-2}; Second biological treatment: Zhan-Wellens test	COD removal: 97% Ammonium removal: ~99%

1.10 Noble Metals

Transition metals such as Ru, Rh, Pd, Ag, Os, Ir, Pt, and Au are defined as "noble" due to their low chemical reactivity, allowing them to be used predominantly in pure form or in metal alloys. [289] These noble metals rank among the ten most valuable and expensive elements, and they are also some of the rarest on Earth, with extremely limited availability. [290] Since noble metals are limited natural resources, it is foreseeable that they will be eventually depleted, making it necessary to reduce their use, find alternatives, and/or fully recycle them. [291-292] Moreover, since not all nations possess noble metal deposits, conflicts may arise over their control. The main producers of noble metals are distributed across different regions of the world, with some nations emerging as leaders in their production, such as China, Russia, and South Africa. Russia is among the major producers, especially for palladium, rhodium, osmium, ruthenium, and iridium. (Fig. 9) South Africa is known for having some of the largest reserves of these metals, particularly platinum. North America (USA and Canada) also plays a significant role in the production of these metals, frequently appearing among the top producers of palladium, rhodium, iridium, and platinum. Regarding gold, besides China, other major producers include Australia and the United States, both of which have a long-standing tradition of gold production. Mexico and Peru, on the other hand, stand out in silver production, where they hold a leading position globally. [293-300]

The price scale of the various noble metals is Ir > Rh > Au > Pd > Pt > Ru > Os > Ag. [301]

Despite their countless applications, transition metals global demand is dominated by industrial catalysis, particularly for the production of catalytic converters. [302-303]

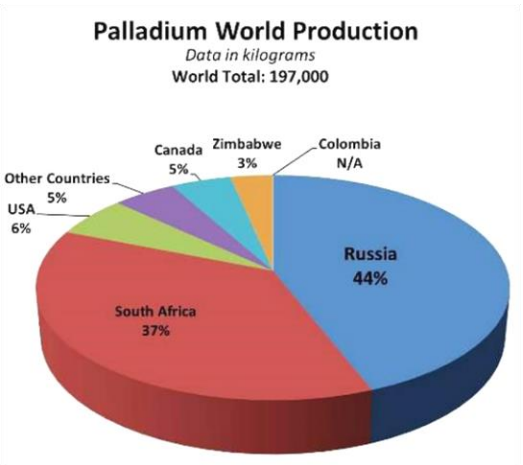

Fig.9. Palladium world production [304]

1.11 Scrap Automotive Catalytic Converters (SCATs)

End-of-life vehicles (ELVs) are now recognized as a significant source of diverse recyclable materials, attracting the interest of both industrial and academic sectors. The primary goal is to establish new sustainable production methods in accordance with the Circular Economy model, that aims to tackle the critical issue of resource depletion by reusing waste and minimizing its disposal. In the sole European Union, ELVs generate over 8 million tons of waste annually, including 6000 tons of scrap automotive catalytic converters (SCATs). [305]

Catalytic converters (SCATs) were firstly introduced in the late 1970s as devices aimed at reducing exhaust emissions from internal combustion engines by converting harmful gases such as carbon monoxide (CO), hydrocarbons, and nitrogen oxides (NOx) resulting from incomplete combustion into less harmful substances like carbon dioxide, water vapor, and nitrogen gas. [306]

Since 1994, following the introduction of the European Directive 94/12/EC on air quality, all engines manufactured or imported into the European Union were required to incorporate catalytic converters that ensure emissions within legal limits. These converters were mandatory in gasoline-powered vehicles since 1993 and diesel-powered vehicles since 1997. [307]

Initially, two-way catalytic converters were used to reduce emissions of hydrocarbons and carbon monoxide. However, advancements in technology and increasingly stringent emission standards have led to the development of more efficient systems. By the late 1970s, it was discovered that specific combinations of precious metals, particularly Pt and Rh, could oxidize CO and hydrocarbons while simultaneously reducing nitrogen oxides NOx. [308] This discovery enabled the transition from the old two-way catalysts to the more advanced "three-way catalysts" (TWC), (fig.10), so called for their ability to simultaneously remove all the three major pollutants. [309]

$$C_xH_{x+2}\ [(3x+1)/2]\ O_2 \longrightarrow xCO_2 + (x+1)\ H_2O$$

$$2CO + O_2 \longrightarrow 2CO_2$$

$$2NOx \longrightarrow xO_2 + N_2$$

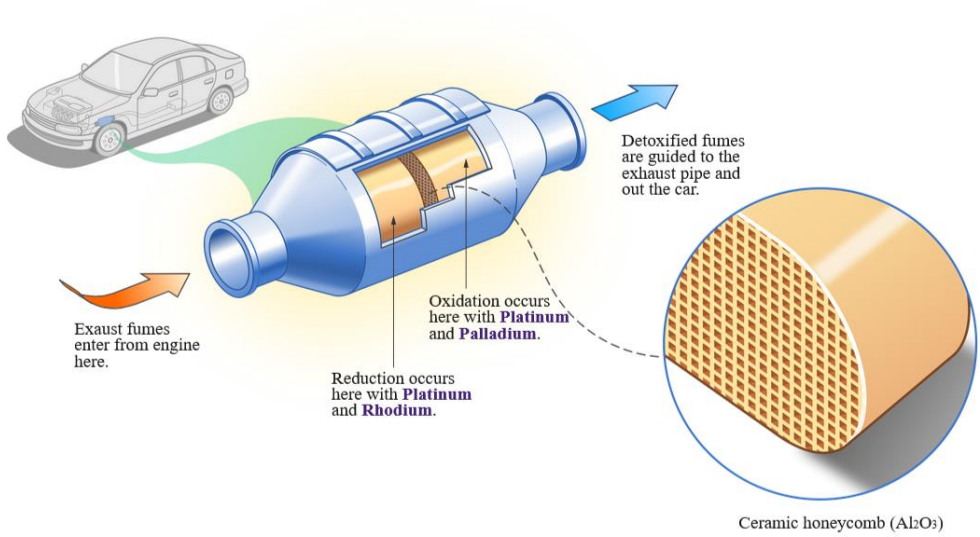

Fig.10. three-way automotive catalytic converters (TWCs) [310]

1.11.1 Design and Composition of SCATs

The core component of a catalytic converter is its structure. It mainly consists of a metal casing that contains a monolithic ceramic substrate onto which the catalytically active material is deposited. This monolith is a single block with a honeycomb design, featuring numerous parallel channels that run lengthwise and are open at both ends, fig. 11. This configuration allows for minimal pressure loss while maximizing the internal surface area. Cordierite is the primary material used for fabrication of monoliths. It is a mixed oxide consisting of $2MgO{\cdot}2Al_2O_3{\cdot}5SiO_2$, along with smaller amounts of Fe and Ca oxides, along with small amounts of iron and calcium oxides. Cordierite offers several key advantages, including a high melting point (1300°C), strong mechanical durability, and most importantly, a very low coefficient of thermal expansion, which is essential for withstanding thermal shocks. [305][311-314]

Fig.11. Ceramic honeycomb

To further increase the specific surface area, the monolith is coated with a thin layer of material with high surface area, known as the washcoat. The washcoat

also aids in distributing the active phase more uniformly [307] The material used for the washcoat is γ-alumina, a highly porous compound composed primarily of Al_2O_3, TiO_2, and SiO_2. It is well-suited because it has high thermal stability and excellent pore distribution. γ-Alumina can be used on its own, or it can be enhanced with additives like ceria (CeO_2), which helps regulating the oxygen levels in the gas mixture passing through the catalyst via the following reaction. [315-316]

$$2CeO_2 \rightleftharpoons Ce_2O_3 + 1/2\ O_2$$

Additionally, ceria is a good catalyst for "steam reforming" and hydrogen generated in this process acts as a reducing agent.

$$CO/CH + H_2O \longrightarrow CO_2 + H_2$$

The "washcoat" is generally deposited onto the monolith by impregnation with a slurry in H_2O of γ-alumina, additives, and the metal phase, all suspended in water. This slurry adheres as a thin film to the monolith surface, which is then dried and calcined to solidify the coating. [307]

The active catalytic phase consists of noble metal nanoparticles from the platinum group metals (PGMs), including Pt, Pd, and Rh. These metals are highly resistant to volatilization under typical operating conditions, which prevents their loss. [289] They stably adhere to the host substrate and act as highly efficient catalysts for the redox reactions of the gaseous combustion products.

The treatment of automotive exhaust gases hinges on the use of these precious metals, each of which plays a distinct role. Rhodium (Rh) is particularly effective for NOx reduction and is the key component for NOx control in three-way catalysts. Pd and Pt are instead used to promote the oxidation reactions of CO and HC. The exhaust gases pass through these honeycomb cells at temperatures above 300-350 degrees; gases activate the catalyst and trigger oxidation and reduction reactions. Various PGMs content in catalytic converters has been reported in the literature so far. For example, Hagelüken *et al.* (2012) estimate that the total PGM content can reach up to 2.000 ppm in the ceramic substrate, or roughly 0.1% by weight. [315] Other sources suggest a typical composition of 0.08% Pt, 0.04% Pd, and 0.005-0.007% Rh in automotive catalytic converters. [289] According to Barefoot *et al.* (1997), the PGM content includes Pt in concentration ranging from 300 to 1.000 µg/g, Pd from 200 to 800 µg/g, and Rh from 50 to 100 µg/g. [317] Jimenez de Aberasturi *et al.* (2011) reported that the total PGM

amount does not exceed 1.000 ppm, while Yakoumis *et al.* showed average PGM levels of 601-885 ppm for Pt, 1302-1884 ppm for Pd, and 248-343 ppm for Rh. [307,318] Three-way catalysts typically have a Pt/Rh ratio of 5-20:1, resulting in a total metal content of 0.9-2.2 g L^{-1}, and a Pd/Pt ratio of 2:5, with an overall precious metal content of around 1.5 g L^{-1}. For optimal performance, these metals must be precisely deposited in specific locations and at different layers of the washcoat to prevent the agglomeration of metal nanoparticles, which would reduce their catalytic efficiency. [318]

1.11.2 Revaluation of Spent Catalytic Converters (SCAT)

The technological evolution of internal combustion engines in recent years has seen a clear acceleration due to the growing awareness of energy savings and the reduction of pollutant emissions. The composition of the TWC has undergone continuous modifications over years, driven by the need to comply with legislative limits imposed by regulations. In 1985, emission limits were introduced in Europe, known as Euro standards, which have become increasingly stringent with the improvement of abatement technologies. The Euro classes range from Euro 0 to Euro 6: the lower the number, the greater the environmental impact of vehicles.[319] The imposed limits are expressed in g/km. Euro 1 and 2 standards from the 1990s only concerned carbon monoxide, the total amount of hydrocarbons, nitrogen oxides, and particulate matter in the case of diesel vehicles.

The limit on PN (particle number per distance traveled) was only introduced starting with the Euro 6 limits. [320]

In Europe, the regulation addressing the disposal of waste from vehicle dismantling is the 2000 regulation called "End of Life Vehicles." It emphasizes the importance of recycling, particularly stressing that all European Union member states are required to adopt and encourage all forms of recovery, making producers responsible for adopting low environmental impact techniques. As a result, spent catalytic converters and the metals they contain are among the materials to be recovered. [321]

The revaluation of spent SCATs has been mainly reported in scientific literature so far, with the goal of recovering PGMs through pyro- and hydrometallurgical processes under difficult experimental conditions, working at extremely high

temperatures (1500-1900 °C) to melt the ceramic substrate and leaching the PGMs with strong acidic and oxidizing reagents. [322]

- The **pyrometallurgical process** described by Rumpold *et al.* for the recovery of PGMs from automotive catalysts involves several stages. The spent catalyst, which contains ceramic materials like cordierite (a compound of silicon, aluminum, and magnesium oxide), is melted at extremely high temperatures ranging from 1500°C to 1900°C. These temperatures can be achieved using techniques such as plasma torches or electric arc heating. During this process, the ceramic portion of the catalyst turns into a liquid slag, while the denser precious metals (PGMs) separate and accumulate in an underlying molten metal bath, which is typically composed of copper but may also include iron, lead, or nickel. A key mechanism to enhance the recovery efficiency of PGMs is the collection through collector metal drop. [323]

  Droplets form in the metal bath, and when they come in contact with the slag, they create a larger interface area between the slag and the metal. Due to turbulence, droplets capture small PGM particles that might otherwise not settle in the metal bath. This phenomenon significantly contributes to improve the PGM recovery rate. Once the metal bath is enriched with PGMs, it undergoes further treatment via electrowinning or electrorefining. In these processes, PGMs concentrate in a sludge residue, which is subsequently purified to separate individual metals. Purification techniques include methods such as solvent extraction, precipitation, and ion exchange. [324]
- **Hydrometallurgical processes**, although less commonly used compared to pyrometallurgical methods, employ chemical agents such as strong acids and oxidizers, including HCl combined with H_2O_2 or aqua regia (a mixture of HCl and HNO_3), that are the main leaching agents. [325-326] PGMs, known for their resistance to corrosion and acids, require aggressive conditions to dissolve and form soluble complexes that can be further processed. However, not all PGMs can be completely dissolved using aqua regia.

  As an alternative, the "pregnant" solution (rich in dissolved precious metals) can be separated from the remaining ceramic material and treated with sulfuric acid or sodium hydroxide under pressure. In this way, PGMs remain solid and can be separated through simple filtration. A drawback of this approach is the high volume of wastewater that needs to be managed and disposed of. The previously separated "pregnant" solution can then be processed using various techniques to concentrate and recover the PGMs. Techniques include cementation, where a

less noble metal (such as zinc or iron) is added to the solution to precipitate the more noble metals like PGMs; solvent extraction, which effectively concentrates the solution and separates platinum, palladium, and rhodium; and ion exchange, where PGMs are retained on columns and subsequently recovered. [327]

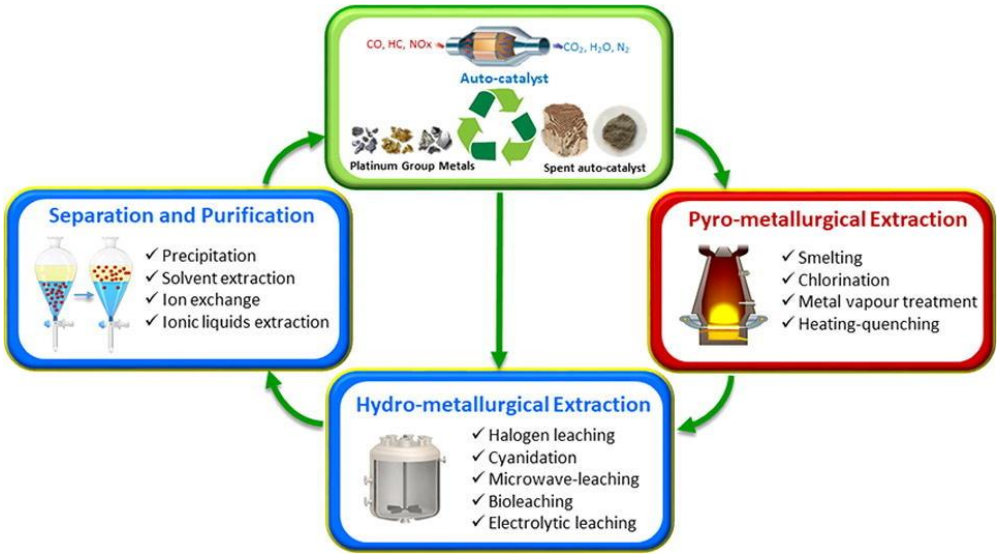

Fig.12. Pyro- and hydrometallurgical processes to recover PGMs [328]

Both processes, summarized in fig.12, feature advantages and disadvantages. The pyrometallurgical process is highly efficient, with recovery rates exceeding 95% for metals such as platinum and palladium, and about 85% for rhodium. [323,329]

Conversely, the hydrometallurgical process consumes less energy compared to the pyrometallurgical one, as it does not require high temperatures to melt the waste material. Although efficient in extracting and recovering precious noble metal nanoparticles, these processes are not environmentally friendly, as they produce additional toxic waste for disposal, require long processing times, and consume large amounts of energy. [330]

An alternative and eco-friendly strategy for the revaluation of SCATs could involve their direct use as supported catalysts. A prior regeneration step would be necessary, involving thermal treatment at temperatures of ~450°C (lower than those used in pyrometallurgical processes to melt cordierite), to remove the impurities adsorbed on the surface of SCAT without altering either the PGM

nanoparticles or the porous ceramic substrate. This approach would not generate additional waste and is expected to give new life to ELV-SCAT as supported catalytic materials for a variety of chemical reactions.

Scientific literature shows very limited examples of investigations into the catalytic efficiency of revaluated SCAT in organic reactions, mainly focusing on reduction or oxidation processes. For example, Zengin *et al.* reported the hydrogenation reaction of carbon-carbon double bonds in a series of alkenes at room temperature (Scheme 1) under a hydrogen atmosphere in the presence of tetrahydrofuran solvent and a SCAT catalyst extracted from a Fiat Siena, which covered 140.000 km and was previously regenerated through a thermal treatment at 120 °C for 12 hours. After regeneration, an analysis was conducted using X-Ray Fluorescence, which revealed the presence of Pd at 0.47% concentration and Rh at 0.04%. Subsequently, the catalytic activity of this material was tested. Results showed that the catalyst could be easily reused after simple filtration, maintaining its activity over 1-4 reaction cycles. Additionally, alumina and ceramic were tested separately to evaluate their catalytic capabilities in the hydrogenation of carbon-carbon double bonds, but no significant reactions were recorded. [331]

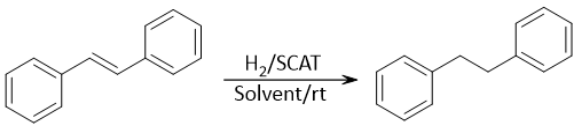

Scheme 1. Reagents and condition: trans-stilbene (1.00 mmol), solvent (15 ml), rt, 1 atm, H_2.

A similar procedure was reported by the same group for the hydrogenation of sunflower oil into saturated fats, using a SCAT catalyst. Hydrogenation is a fundamental process that allows for the saturation of unsaturated bonds present in oils, thereby improving their physical and chemical properties, as well as increasing oxidative stability, which is crucial for extending the shelf life of food products and for industrial applications. Traditionally, hydrogenation of vegetable oils is carried out using noble metal-based catalysts, such as Pd and Pt. In particular, the authors examined the effectiveness of the SCAT previously examined by Zengin *et al.* This catalyst underwent a regeneration and characterization process prior to use. The regeneration was carried out through a pre-wash with chromic acid and distilled water to remove dust and carbonaceous particles, followed by a thermal treatment at 120 °C to enhance

the catalytic activity and restore the desired properties. The hydrogenation of vegetable oils was performed in the presence of hydrogen, in a controlled atmosphere, using the SCAT catalyst. Results demonstrated that the regenerated catalyst was effective in promoting the saturation of unsaturated bonds in vegetable oils. During the trials, several parameters, such as temperature, pressure, and reaction time, were monitored to optimize the hydrogenation conditions. The final analysis showed that the quality of the vegetable oils treated with the recovered catalyst was comparable to that obtained using traditional catalysts. [332]

Cova *et al.* also reported good catalytic activity of SCAT in continuous hydrogenation reactions of unsaturated alcohols (*e.g.* isopulegol to menthol, Scheme 2) and aromatic aldehydes (*e.g.* vanillin to vanillyl alcohol) using a SCAT catalyst previously purified by ultrasound in a series of solvents (hot water, ethanol, acetone) and dried at 500°C in an oven under a flow of N_2 and H_2. [305]

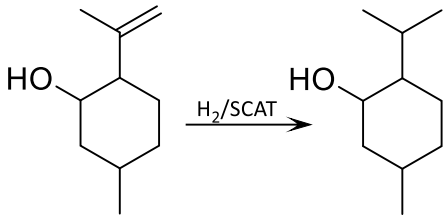

***Scheme 2**. hydrogenation of (−)-isopulegol (1) to (−)-menthol (2)*

The catalytic efficiency of SCAT in reduction processes has also been investigated after additional deposition of transition metal nanoparticles. [333-335] For example, the continuous selective hydrogenation of α,β-unsaturated aldehydes to unsaturated alcohols (e.g. cinnamaldehyde to cinnamyl alcohol see (figure 13) was reported using a SCAT catalyst enhanced by mechanochemical incorporation of ruthenium nanoparticles into the cordierite without solvent. [334]

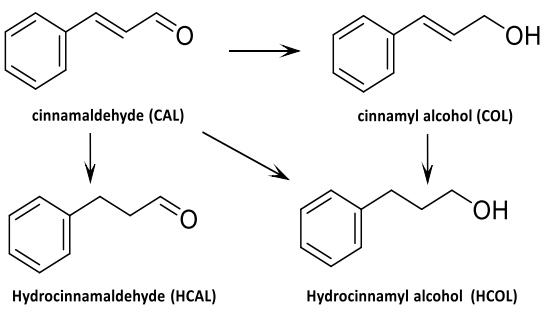

Fig.13. Reaction pathways in the hydrogenation of cinnamaldehyde [334]

Ruthenium-based catalysts were successfully synthesized using a mechanochemical method, followed by chemical reduction. The interaction between ruthenium and the recycled catalytic converter had a significant impact

on ruthenium's performance. Both studies highlighted the effectiveness of SCATs, showing that they can not only be used directly as catalysts but also as supports, as demonstrated in the specific case of ruthenium.

A Fe/SCAT tandem cyclization-hydrogenation process in continuous mode of (+)-citronellal to (-)-menthol was also achieved (Figure 14). [335]

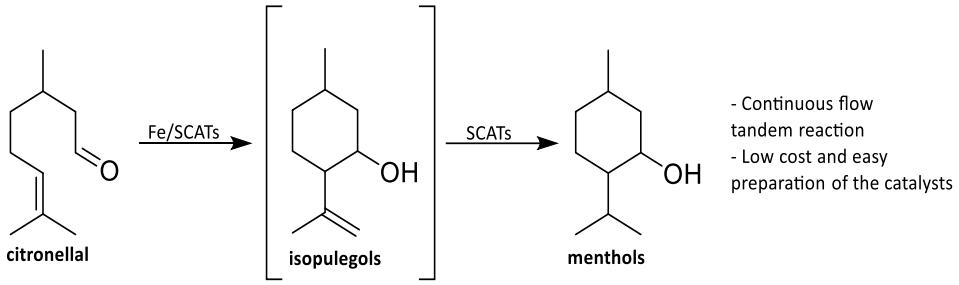

Fig. 14. cyclization-hydrogenation process in continuous mode of (+)-citronellal to (-)-menthol

Before use, the recycled SCATs underwent a washing and drying process to remove carbonaceous residues and other surface pollutants. Specifically, 50 g of SCAT were dissolved in a solution of distilled water and ethanol (in a 1:1 ratio) and subjected to ultrasound treatment for 2 hours, reaching a temperature of approximately 323 K. After treatment, the SCAT was filtered, repeatedly washed with water, acetone, and ethanol, and then dried in an oven at 373 K for 12 hours. Subsequently, several Fe/SCAT and Fe/SiO_2 catalysts were prepared by varying the weight percentage of iron (wt%). The comparison of catalytic activities revealed that the Fe/SCAT catalysts were particularly efficient. Besides demonstrating the catalytic activity, SCATs themselves showed a certain degree of activity in the cyclization of citronellal to isopulegol, thereby contributing to an increase in the final yield of menthols. Furthermore, the catalytic system displayed excellent robustness, as highlighted by long-term stability tests, with no metal loss and no changes in the morphology or oxidation state of the metal. Under optimized conditions, it was possible to produce (−)-menthol with a yield of approximately 77% starting from enantiomerically pure (+)-citronellal.
In another study, Zuliani *et al.* developed Ni-based catalysts and co-catalysts through a solvent-free mechanochemical approach, using SiO_2 (Ni/SiO_2) and the

ceramic cores of catalytic converters (Ni/SCATs) as supports. These catalysts and co-catalysts were employed in the hydrodeoxygenation of anisole. Under standard batch reaction conditions, at 200 °C and 4 MPa of H_2, the combined use of Ni/SiO_2 and Ni/SCATs resulted in an anisole conversion exceeding 97% in just 40 minutes, with a reaction rate over 50% faster than that obtained with pure Ni/SiO_2. [336]

Among the rare studies on non-reductive reactions catalyzed by SCAT, Isgoren *et al.* recently reported the suitability of revaluated automotive catalytic converters for the oxidative degradation of the pesticide malathion in aqueous phase, as a potential strategy for wastewater treatment (figure 15).

The used SCAT underwent a series of preliminary treatments, including the washing of monolithic substrate drying at 105 °C, grounding, and passing through a fine mesh sieve. The recovered material showed high catalytic efficiency in both the removal of malathion and the elimination of its toxicity. The maximum malathion removal efficiency of 88% was achieved under optimal conditions. Furthermore, toxicity tests based on bacterial bioluminescent response confirmed that malathion was converted in compounds non-toxic for bacteria. [337]

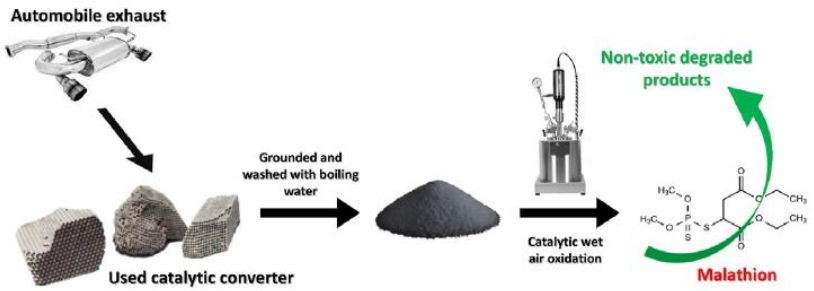

Fig. 15 oxidative degradation of the pesticide using SCATs [337]

In this context, the use of SCAT-based catalysts in carbon-carbon bond formation reactions has been almost completely unexplored, with the only exception being a proof of concept by Trzeciak *et al.* on their possible suitability in the hydroformylation of 1-hexene and in cross-coupling reactions of phenyl iodide with butyl acrylate or phenylboronic acid, respectively. (Scheme 3-4) [338]

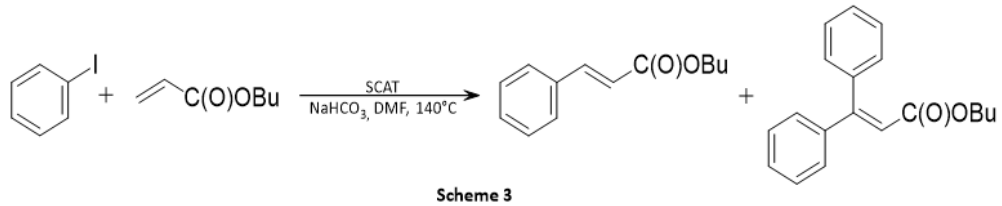

Scheme 3

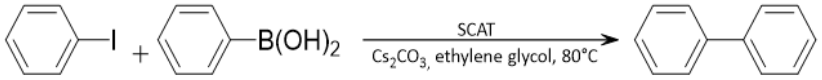

Scheme 4

These results confirmed the high catalytic potential of the waste materials, although the reactions have not yet been systematically explored and studied in depth.

1.12 Suzuki Miyaura Cross Coupling Reactions

Carbon-carbon coupling reactions are essential to produce many products in sectors such as pharmaceuticals, agriculture, and detergents. Initially studied in the 19th century, these processes were inefficient and produced low yields due to the formation of by-products. However, since the 1960s, the introduction of transition metal catalysts significantly enhanced reaction efficiencies and yields. These reactions are generally classified into two kinds: the homocoupling and the cross-coupling processes. Homocoupling reactions include the Wurtz, Glaser, Ullmann, and Pinacol reactions, while cross-coupling reactions include the Heck, Suzuki, Sonogashira, Stille, Hiyama, Kumada, and Negishi reactions. [339]
Cross-coupling reactions use metal catalysts such as Pd(II) and Pd(0) [340-342] Ni(II), [343-345] Cu(II), [346-354] Fe (II) and Fe(III), [348-350] that are often supported on materials like carbon nanotubes and graphene oxide and can be employed in forms such as nanoparticles, nanocomposites, or complexes to achieve high yields and product purity degree. [351-356]
Specifically, the Suzuki cross-coupling reaction is particularly important to the availability of common organometallic reagents such as boronic acids, mild reaction conditions, environmental compatibility, and the use of safe reagents. This reaction requires fewer catalysts and generates easily separable by-products.

Suzuki and Miyaura published the first paper on the Suzuki-Miyaura coupling reaction in 1995 highlighting its importance for various industrial applications due to its ability to produce functional compounds. First discovered in 1981, the Suzuki reaction gained significant recognition, culminating in the 2010 Nobel Prize in Chemistry awarded to Akira Suzuki, Richard F. Heck, and Ei-ichi Negishi. Cross-coupling reactions are known for their broad tolerance of functional groups and high selectivity. The Suzuki reaction involves using aryl halides as electrophiles and organoboranes as nucleophiles, along with a metal catalyst, a base, aqueous and organic solvents, and reaction temperatures between 60 and 100°C. Generally, such reactions proceed between an organic electrophile R1-X and an organoboron nucleophile R^2-BY_2 in the presence of a metal catalyst, usually palladium complexes like LnPd0, ideed by an organic or inorganic base MA (Fig. 12.). According to Scheme 5, the mechanism is based on a catalytic cycle that includes three steps: a) the oxidative addition of an organic halide or pseudohalide to the palladium complex, which represents the slow stage of the reaction; b) the transmetallation between the adduct and the boronate R^2-BY_2 in the presence of the base MA, and finally, c) the reductive elimination which produces the R^1-R^2 compound with a new C–C bond and regenerates the catalyst, (Fig.16) [357]

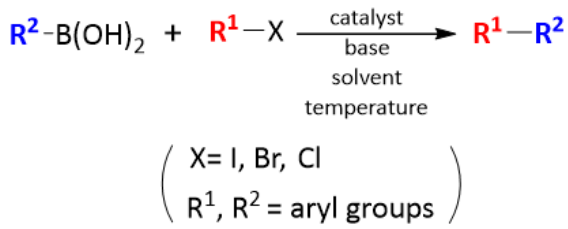

Scheme 5

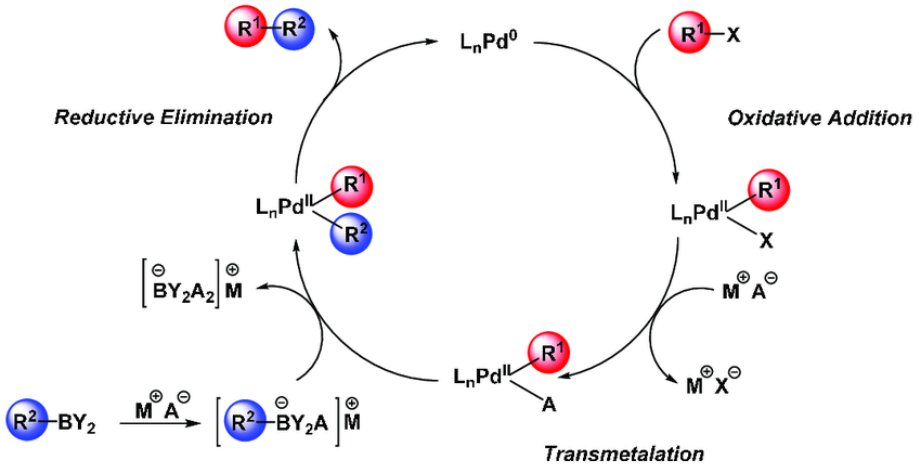

Fig.16. catalytic cycle of Suzuki-Miyaura cross-coupling reactions[357]

1.12.1 Catalysts and solvents suitable for the Suzuki cross-coupling

The catalyst plays a crucial role in the Suzuki coupling reaction, as it accelerates the reaction rate without being consumed. Approximately 85% of Suzuki reactions depend on a catalyst, which can be classified into three main classes: homogeneous, heterogeneous, or biocatalysts. Homogeneous catalysts offer high activity but they are difficult to recover, while heterogeneous catalysts are more easily recyclable. Nanocatalysts, due to their large surface area relative to their volume, combine the benefits of both, offering high efficiency, stability, and selectivity. Although biocatalysts are environmentally friendly, they still have to achieve widespread industrial use. Consequently, nanocatalysts are favored in industrial applications for their effectiveness and sustainability. [339]

Among PGMs, Pd is especially valued for its excellent catalytic activity and wider application in cross-coupling processes.

Solvents also play an important role in Suzuki coupling reactions, affecting both the reaction's efficiency and its environmental footprint. A variety of polar and polar or non-polar solvents can be employed, including DMF, THF, DMSO, 1,4-dioxane, water, methanol, ethanol, and toluene. [359-360] In line with the principles of green chemistry, the focus is on using cost-effective and non-toxic materials, aiming to minimize the generation of contaminants.

Chapter 2: Results

2.1 Chemical Composition of SCAT

The catalyst examined in this study is a "three-way catalytic" automotive converter. As reported in the literature, this kind of automotive converter catalyzes both the oxidation of fuel hydrocarbons into carbon dioxide and the reduction of nitrogen oxide exhaust gases from vehicles into nitrogen gas.[307][361-362] The SCAT sample used herein was sourced from an Italian end-of-life vehicle (Fiat Bravo) that was registered in 1995 and scrapped in 2018 after covering 235.000 kilometers. It was regenerated through a simple process involving calcination in a muffle furnace at 450 °C for 3 hours to eliminate aged combustion residues. Afterwards, the catalyst was ground into a fine powder using a mortar and was it directly used in oxidation reactions and in Suzuki-Miyaura cross-coupling processes as a heterogeneous transition metal catalyst supported on porous ceramic. An ICP-MS analysis was performed to determine the presence and amount of catalytic metals on the ceramic material of the regenerated SCAT. As shown in Table 20, the most abundant elements are aluminum (32.5%) and silicon (35.1%), which compose the ceramic support, followed by cerium (3.3%), magnesium (3.1%), and iron (1.8%). Chromium, zinc, titanium, and zirconium were also detected with weight percentages of 0.2%, 0.42%, 0.4%, and 0.25%, respectively. The percentages of transition metals are even lower (0.15% for Pd, 0.07% for Pt, and 0.008% for Rh).

Tab.20. Chemical composition of the catalytic converter by ICP-MS

Element	Al	Si	Ce	Mg	Fe	Cr	Zn	Ti	Zr	**Pd**	**Pt**	**Rh**
% wt	32.5	35.1	3.3	3.1	1.8	0.2	0.42	0.4	0.25	**0.15**	**0.07**	**0.008**

To confirm the ICP analysis, a TEM analysis was carried out.
TEM analyses performed on the three samples show the formation of nanoparticles on the order of a few tens of nm, with the presence of Rh, Pd, and Pt. (fig. 17)

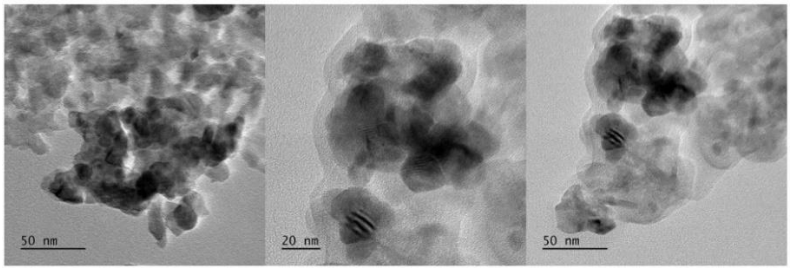

Fig.17. Metal nanoparticles observed in untreated spent catalytic converters

2.2 Landfill Leachate composition

Leachate samples were collected at the ITALCAVE S.p.A landfill, an Italian company located in Statte, in the province of Taranto (Figure 18, coordinates: latitude 40° 31'24'' N, longitude 17° 12'58'' E, at an altitude of 45 meters above sea level, in the Apulia region of southern Italy). The landfill is located in a limestone quarry equipped with high-density polyethylene pipes that direct the leachate to impermeable collection wells, from where it is pumped and transferred to silos. Founded in 1973, the company specializes in environmental services, focusing on waste management. ITALCAVE's main activities include the treatment, recovery, and disposal of both hazardous and non-hazardous waste from various industrial and urban sources. The leachate sample under investigation was obtained concentrating the landfill leachate via reverse osmosis (CROL, concentrated reverse osmosis leachate). CROL was then stored into polyethylene bottles and kept at 4 °C to avoid potential thermal degradation.

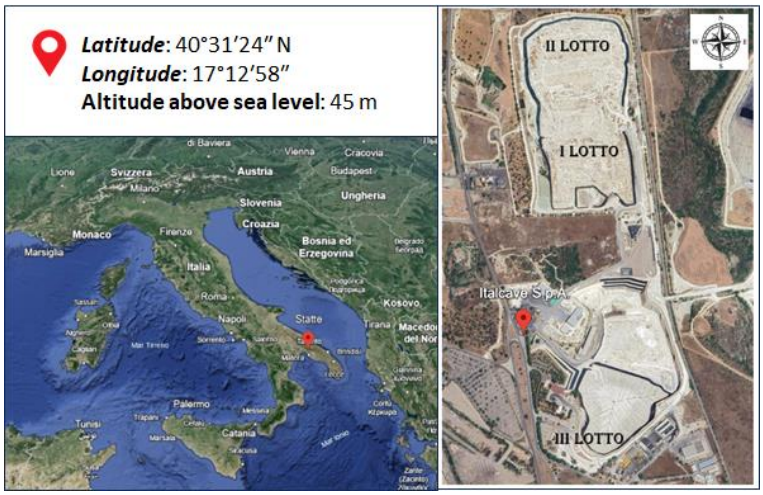

Fig. 18. ITALCAVE landfill panoramic picture

The average characteristics of the CROL are shown in Table 21. Data clearly show the presence of high amounts of chloride and sulfate anions (9648 and 25573 mg/L), ammonia nitrogen (8150 mg/L). The key parameter which this research work has been focused on is the Chemical Oxygen Demand value that, as expected for a concentrated reverse osmosis leachate, was high (15880 mg/L). Hence, the main target of this PhD thesis, has been to research effective eco-friendly methods to reduce the CROL COD to values below the tolerated threshold levels. Indeed, according to the 2010/75/UE Parliament regulation the highest tolerated COD for aqueous waste samples range between 30 and 300 mg/L to discharge them into water bodies. These values are also variable depending on each country, with 160 mg/L and 500 mg/L being the tolerated thresholds by Italian laws to discharge landfill leachate into shallow waters or sewerages, respectively.[104]

Table 21 General characteristics of concentrate from reverse osmosis produced by the Italcave's landfill leachate treatment (CROL)

Parameter	Results
Alkalinity (meq/L)	300
Fluoride (mg/L)	12,2
Sulfate (mg/L)	25573
Chloride (mg/L)	9648
Phosphate (mg/L)	301,2
Total phosphorus (%)	0,008
Ammonia nitrogen (mg/L)	8150
COD (mg/L)	**15880**
Conductivity at 20 ºC (µS/cm)	409000
Density (g/cm^3)	1,04
Boro (mg/kg)	66,8
Calcium (mg/kg)	37,3
Magnesium (mg/kg)	159
Potassium (mg/kg)	2692
Silicon (mg/kg)	75,5
Sodium (mg/kg)	4509
pH	7,34
Dry residue at 105 ºC (%)	5,00
Dry residue at 600 ºC (%)	3,07
Total suspended solids (mg/L)	175
Kinematic viscosity 20°C (cSt)	0,848

2.2.1 Calculation of Dry Residue as a Percentage of CROL

To begin the study on the treatment of CROL, a preliminary determination of the percentage of fixed residue was conducted. CROL was subjected to heating in a muffle furnace at three different temperatures: 105°C, 600°C, and 900°C. The study aimed to obtain information on the kind of solids present in the leachate. At 105°C, water evaporation and the removal of volatile components such as residual organic solvents, dissolved gases, and moisture occurred. The corresponding residue was primarily composed of inorganic and organic substances that do not decompose at this temperature. At 600°C, the residue underwent complete combustion of hydrocarbons and other volatile organic compounds. The resulting solid product mainly included inorganic minerals and ash. This process allowed quantification of the volatile organic matter fraction in the residue. At 900°C, complete oxidation of the organic and inorganic compounds in the ash occurred, allowing measurement of the amount of persistent inorganic compounds such as mineral salts, metal oxides, and other refractory species. The residue obtained after heating at 900°C was made of the inorganic fraction of the leachate that did not volatilize or burn (Figure 19). The percentage of dry residue was calculated by relating the dry weight to the wet weight. By treating 13 g of leachate and heating it for 2 hours at various temperatures in the muffle furnace, fixed residue values of 3.7% at 105°C, 2.35% at 600°C, and 2.16% at 900°C were obtained.

Fig.19 solid residue

2.2.2 CROL oxidation reactions

Experiments were performed to compare the effectiveness of SCAT in different advanced oxidation processes. Specifically, the effect of traditional oxidation of leachate on COD using the Fenton protocol was compared to the oxidation catalyzed by SCAT.

The CROL (15 mL) was initially acidified to pH 3 by adding H_2SO_4 (110 µL) to remove carbonates in the form of carbon dioxide. The acidification induced the precipitation of a dark product, which was separated from the aqueous phase by centrifugation. The supernatant was then divided into three 5 mL aliquots (L1, L2, and L3).

The L1 sample was used to determine the COD value (13.750 mg/L) following CROL acidification, according to the EPA 410.4 protocol (Revision 2.0 "Determination of Chemical Oxygen Demand by Semi-Automated Colorimetry").[363]

Samples L2 and L3 were treated with H_2O_2 (35%, 350 µL) in the presence of two different catalysts: $FeCl_2$ (100 mg) for L2 and SCAT (100 mg) for L3. The choice to use 350 µL of H_2O_2 was based on an estimate that 13 g of O_2 would be needed to completely oxidize one liter of leachate (COD=0). The reactions were conducted at 70°C for 150 minutes, and after cooling to room temperature and centrifugation (3500 rpm for 3 min), the COD of the supernatant was determined (1880 mg/L for L2, 1716 mg/L for L3).

These results indicate not only the efficiency of SCAT but also the same effectiveness compared to $FeCl_2$, given the same volume of oxidizing agent. This is particularly significant considering that, with the same weight of the two catalysts, the amount of active metals present in SCAT is significantly lower than that in $FeCl_2$. Furthermore, SCAT is recoverable and does not generate the sludge typical of the traditional Fenton process, reducing environmental impact.

After demonstrating the catalyst's effectiveness, oxidation reactions were conducted following the same experimental procedure applied to sample L3. In this phase, the CROL was initially acidified with sulfuric acid and then divided into 5 mL aliquots to perform oxidation reactions with H_2O_2 and the SCAT catalyst. The experimental conditions of the oxidation were adjusted in terms of the amount of H_2O_2 (from 130 to 530 µL), SCAT (from 50 to 300 mg), pH (from 3 to 12), reaction temperature (from 25°C to 70°C), and reaction time (from 60 to 240

minutes), with the aim of minimizing the COD through acidic oxidative treatment.

Tab. 22. Effect of varying H_2O_2, temperature, and catalyst parameters

SAMPLE	H_2O_2 (µL)	SCAT (mg)	$FeCl_2$ (mg)	TEMPERATURE (°C)	TIME (h)	COD (mgO_2/L)
1	530	/	/	70	1	3446
2	/	50	/	70	1	5176
3	350	/	100	70	1	1880
4	350	100	/	70	1	1716
5	530	100	/	70	1	1304
6	265	100	/	70	1	1834
7	130	100	/	70	1	2124
8	530	50	/	70	1	2816
9	530	150	/	70	1	**980**
10	530	200	/	70	1	1156
11	530	300	/	70	1	1306
12	530	150	/	60	1	1280
13	530	100	/	60	1	2362
14	530	50	/	60	1	3548
15	530	150	/	50	1	1970
16	530	100	/	50	1	2564
17	530	50	/	50	1	3610
18	530	150	/	25	4	3542
19	530	200	/	25	4	3432

As shown in Table 22, the COD value can be reduced to 3446 mg/L using 530 µL of H_2O_2 without a catalyst (test 1) and to 5176 mg/L using 50 mg of SCAT without an oxidant (test 2). In a series of experiments conducted at 70°C (tests 1-11), the amount of H_2O_2 was varied with respect to the calculated stoichiometric value of 350 µL, while keeping the amount of catalyst constant at 100 mg. In these tests, hydrogen peroxide was used in quantities lower than the stoichiometric value (265 µL and 130 µL) or in excess (530 µL). The best result in terms of COD reduction was obtained using an excess of hydrogen peroxide (530 µL), with a reduction in COD to 1304 mg/L (test 5). COD values of 1834 mg/L and 2124 mg/L were determined when operating with less oxidant (respectively 265 µL in test 6 and 130 µL in test 7).

Subsequently, with the same amount of hydrogen peroxide (530 µL), the effect of SCAT quantity was studied. Starting with 100 mg, the amount of catalyst was halved and doubled. The best COD reduction was obtained with 150 mg of catalyst, lowering the COD to 980 mg/L (test 9). Using larger or smaller amounts of catalyst compared to this condition, less significant COD reductions were

observed. A good compromise was reached using 200 mg of SCAT, corresponding to a final COD value of 1156 mg/L (test 10). When the temperature was reduced to 50°C and 60°C, the COD values obtained were generally higher than those recorded at 70°C, except for test 12 (COD 1156 mg/L), conducted at 60°C using the same conditions as test 9 (530 µL of H_2O_2 and 150 mg of catalyst). However, further temperature reductions, such as 50°C, resulted in a worsening of COD reduction, regardless of the amount of catalyst and hydrogen peroxide used.
Finally, in the tests conducted at room temperature with 530 µL of H_2O_2 and 150 mg of catalyst, the COD was reduced to 3542 mg/L after 4 hours of reaction (test 18). Increasing the amount of catalyst did not lead to significant improvements under these conditions (test 19).
The best operating conditions were thus found to be at 70°C, with amounts of hydrogen peroxide and catalyst of 530 µL and 150 mg, respectively: under these conditions, the minimum COD value observed was 980 mg/L.

2.2.3 Determination of COD by Gel Permeation Chromatography (GPC)

In parallel with the COD determination using the EPA method, a preliminary study was also performed to demonstrate the possibility to develop an innovative COD detection technique based on gel permeation chromatography (GPC). This approach offers potential advantages in terms of speed and cost, making COD determination more efficient. The chromatographic peaks obtained from the GPC analysis (Figures 20 and 21) were considered indicative of COD. The preliminary results, although qualitative, were very promising as they show a significant reduction in the chromatographic peak related to the organic eluate. This reduction is evident when comparing the response of the L1 sample treated only with H_2SO_4, to the L2 sample subjected to oxidation with H_2O_2 and $FeCl_2$, and to the L3 sample, subjected to oxidation with H_2O_2 and SCAT (Figure 20).
A similar trend was observed in Figure 21 for the samples subjected to different treatments: the leachate acidified to pH 3, the sample treated only with hydrogen peroxide, the sample treated only with the SCAT catalyst, and the CROL at pH 3 subjected to oxidation with 530 µL of H_2O_2 and 150 mg of SCAT. The relative intensity of the peaks was coherent with the reduction in COD values detected using the EPA method, which were respectively 13.750 mg/L, 3446 mg/L, 5176 mg/L, and 980 mg/L.

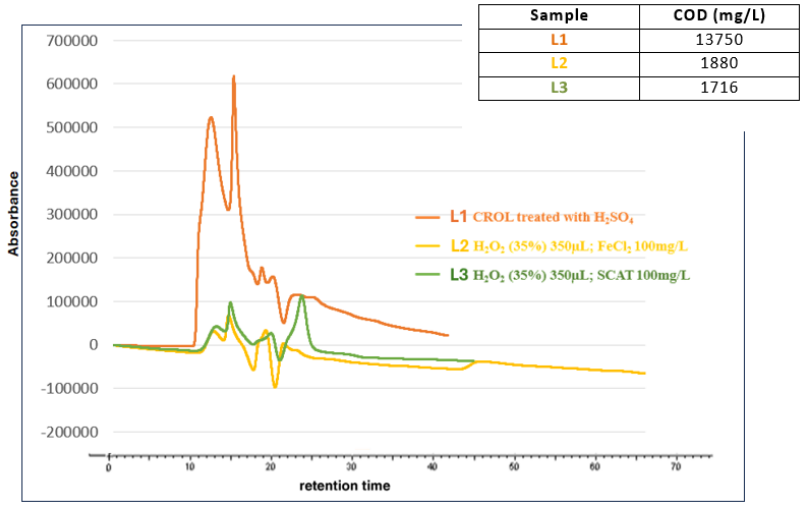

Sample	COD (mg/L)
L1	13750
L2	1880
L3	1716

Fig.20. GPC chromatographic profiles for samples L1, L2 and L3

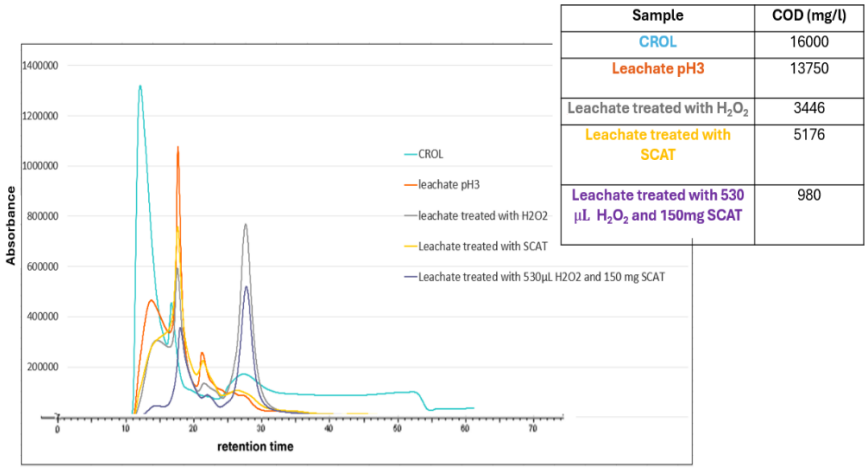

Sample	COD (mg/l)
CROL	16000
Leachate pH3	13750
Leachate treated with H_2O_2	3446
Leachate treated with SCAT	5176
Leachate treated with 530 µL H_2O_2 and 150mg SCAT	980

Fig.21. Chromatographic profiles obtained from GPC analysis

2.2.4 Effect of pH on the different phases of CROL treatment

To confirm the importance of acidification as the preliminary phase in the treatment of CROL, experiments were performed to study the variation in the final COD value with respect to pH. The raw leachate (CROL) was acidified with H_2SO_4 aliquots, reaching final pH values of 3, 4, and 5. Tests were also carried out following the addition of NaOH, bringing the pH values to 10 and 12. After adjusting the initial pH, samples were subjected to the oxidation process using the best experimental conditions previously identified (Tab. 22, test 9).
At a purely qualitative level, after the oxidation reactions, a bleaching of the previously acidified samples was observed versus those treated under alkaline conditions (Figure 22).

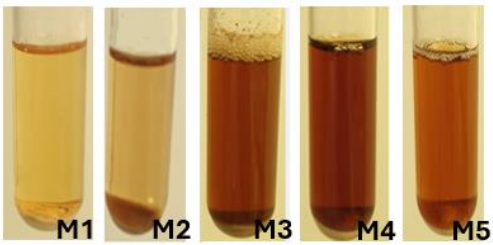

Fig.22. Color change of samples brought to: M1(pH3); M2(pH4); M3(pH5); M4(pH10); M5(pH12)

Spectrophotometric analyses to determine the final COD values confirmed the qualitative evaluation, showing COD values of 1031, 1570, and 2372 mg/L for samples acidified to pH 3, 4, and 5, respectively. Conversely, the COD values were significantly higher (7014 and 7098 mg/L, respectively, Table 23) for samples treated at pH 10 and 12.

Tab.23 Influence of pH directly tuned for CROL

Sample	pH	H_2SO_4 (µL) Add to 5mL of CROL	NaOH (mg)	H_2O_2 (µL)	SCAT (mg)	Temperature (°C)	Time (h)	COD mgO_2/L
M1	3	26	-	530	150	70	1	**1031**
M2	4	23	-	530	150	70	1	1570
M3	5	21	-	530	150	70	1	2372
M4	10	-	79	530	150	70	1	7014
M5	12	-	136	530	150	70	1	7098

This result highlights the importance of starting the leachate treatment at pH 3 by adding sulfuric acid, which removes carbonates in the form of carbon dioxide and improves the effectiveness of hydrogen peroxide.

Then, to analyze the effect of pH on the oxidation process, the leachate acidified to pH 3 was divided into five aliquots, and by addition of sodium hydroxide, pH was set to values between 4 and 12. Under the same model operating conditions, samples at pH 8, 10, and 12 showed COD values between 1100 and 1650 mg/L, while the best results (579 and 668 mg/L) were obtained at pH 5 and 6, respectively (Table 24).

Tab.24 Influence of pH on COD following initial precipitation at pH 3 and subsequent addition of NaOH

Sample	pH	H_2SO_4 (µL) Add in 5mL of CROL	NaOH (mg)	H_2O_2 (µL)	SCAT (mg)	Temperature (°C)	Time (h)	COD (mg O_2/L)
M1	3	26	-	530	150	70	1	1031
M6	4	26	3,5	530	150	70	1	**668**
M7	5	26	4,4	530	150	70	1	**579**
M8	8	26	10	530	150	70	1	1639
M9	10	26	57,1	530	150	70	1	1006
M10	12	26	82,1	530	150	70	1	1116

After identifying pH 5 as the optimal value for oxidation, a study was conducted to evaluate the importance of the sequence of operational phases. Two distinct

approaches were tested. In the first, the pH of leachate was initially set to 3, then increased to pH 5 by adding NaOH immediately before oxidation.
In the second approach, the pH was directly set to 5 by adding H_2SO_4, and after oxidation, further acid was added to remove carbonates and reach pH 3. The results showed that the first approach was significantly more effective than the second, leading to a COD reduction to 579 mg/L, compared to 1856 mg/L with the second approach. Therefore, the importance of initially acidifying the leachate to pH 3 and subsequently raising it to pH 5 with the addition of sodium hydroxide was validated as a good approach to improve the effectiveness of the treatment.

2.2.4.1 H_2O_2 amount necessary for CROL oxidation

Once pH 5 was identified as the optimal value for oxidation, the second parameter investigated was the concentration of hydrogen peroxide to be used under these working conditions. Starting from the stoichiometric amount of 350 µL of 35% hydrogen peroxide required to ideally eliminate the COD of the initial leachate concentrate (CROL), oxidation experiments were conducted using both an excess (480 and 530 µL) and a deficit (120 and 240 µL) of the oxidant, while keeping other experimental conditions constant.

The COD value decreased as the amount of hydrogen peroxide used increased: the maximum reduction (96%) in COD to a final value of 580 mg/L was achieved using 530 µL of H_2O_2 (Table 25)

Tab.25 Optimization of the amount of H_2O_2

Sample	pH	H_2O_2 (µL)	SCAT (mg)	Temperature (°C)	Time (h)	COD (mg O_2/L)
M12	5	530	150	70	1	**680**
M13	5	480	150	70	1	1228
M14	5	350	150	70	1	1714
M15	5	240	150	70	1	2202
M16	5	120	150	70	1	3700

2.2.4.2 CROL titration curves

To evaluate the amounts of acid and base needed to set the pH of CROL, titration curves were plotted as shown in Figures 23 and 24. This assessment was useful to estimate the amounts of H_2SO_4 and NaOH that would be required in a potential scale-up of the process. I was estimated that in a hypothetical plant treating 1 m^3 of CROL, 4.7 L of sulfuric acid would be necessary to acidify the leachate from an initial pH of 9 to a final pH of 3 (Figure 23). On the other hand, to reach a pH of 5, 1.7 L of 1M NaOH solution would be required (Figure 24).

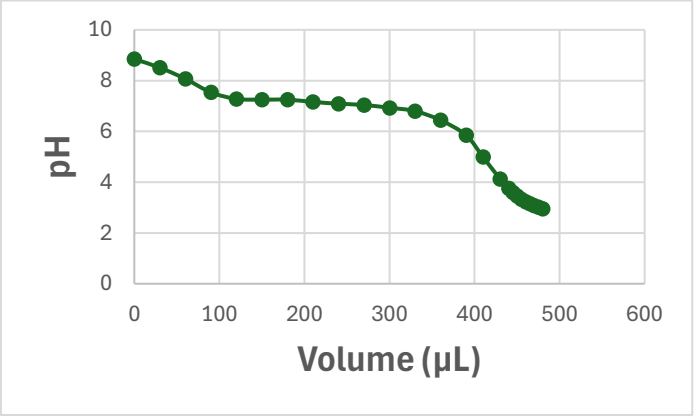

Fig.23. Titration curve: amount of H_2SO_4 required to acidify leachate from pH9 to pH3

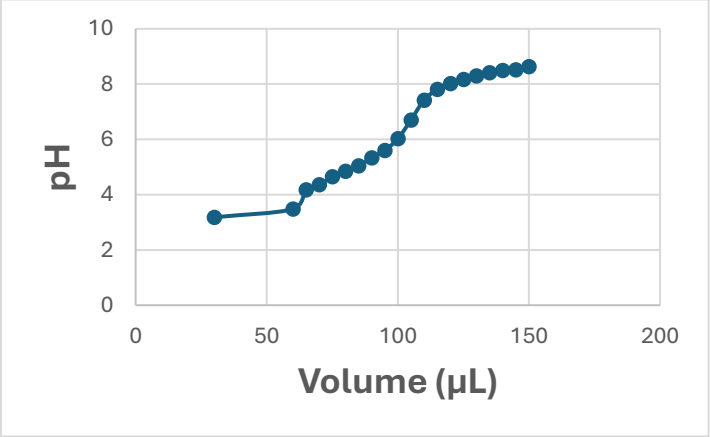

Fig.24. Titration curve: amount of NaOH needed to reach pH 5 values starting from pH3

2.2.4.3 Analysis of Cations and Anions in CROL after each treatment step

Monitoring changes in the ionic balance at each stage is useful to assess the effectiveness of leachate treatment process. For this purpose, anions and cations were analyzed in the initial CROL, in the acidified leachate (pH 3) before and after oxidation, and in the leachate subsequently alkalized (pH 5) before and after oxidation. In all cases, the oxidation process was carried out on 5 mL of the initial sample with the addition of 530 µL of H_2O_2 and 150 mg of SCAT, with the sole difference being the starting value of pH. The results of cations and anions analysis are reported in tables 26 and 27. All values are expressed in mg/L, and next to each element, the corresponding standard deviation is indicated in brackets.

Tab.26 cation analysis

CATIONS	CROL (mg/L)	CROL at pH 3 (mg/L)	CROL acidified at pH 3 after oxidation (mg/L)	CROL at pH 5 (mg/L)	CROL basified at pH 5 after oxidation (mg/L)
Al (0.1)	1.42	0.482	36.2	0.521	14.7
As (0.04)	0.459	0.417	1.7	0.459	1.3
B (0.04)	24.9	24.8	16.4	25.8	22.6
Ba (0.04)	0.291	0.312	0.339	0.289	0.375
Be (0.004)	0	0	0	0	0
Ca (0.1)	34.8	35.5	47	36.8	42.2
Cd (0.001)	0.002	0.001	0.001	0.001	0.002
Co (0.04)	0.155	0.106	0.065	0.109	0.099
Cr (0.04)	6	2.38	1.56	2.48	2.02
Cu (0.04)	0.056	0	0.283	0	0.208
Fe (0.1)	10.7	4.68	1.82	4.56	2.48
Hg (0.001)	0	0	0	0	0
K (0.4)	2248	2207	1434	2332	2047
Mg (0.1)	89.5	92.4	60.7	95.6	83.9
Mn (0.04)	0.134	0.138	0.197	0.14	0.181
Mo (0.04)	0.049	0.024	0.023	0.019	0.033
Na (0.1)	3906	3865	3596	4565	4537
Ni (0.04)	0.97	0.652	0.539	0.673	0.596

Pb (0.04)	0.022	0	0.066	0.004	0.036
Sb (0.02)	0.154	0.093	0.092	0.1	0.097
Se (0.004)	0	0	0	0	0
Si (0.02)	57.6	42.8	35.7	44	43.5
Sn (0.001)	0.694	0.06	0.009	0.057	0.014
Te (0.04)	0.018	0.068	0.572	0.049	0.429
Ti (0.04)	2.77	0.522	0.079	0.539	0.055
Tl (0.001)	0	0	0	0	0
V (0.04)	0.906	0.59	0.423	0.606	0.572
Zn (0.04)	0.393	0.316	6.82	0.342	5.6
P tot (1.6)	0.007	0.006	0.013	0.006	0.004

Tab.27 anion analysis

ANIONS	**CROL (mg/L)**	**CROL at (pH3) (mg/L)**	**CROL acidified at pH 3 after oxidation (mg/L)**	**CROL at pH5 (mg/L)**	**CROL basified at pH 5 after oxidation (mg/L)**
F^-	< 200	< 20	< 30	< 20	< 30
Cl^-	7291	7548	4367	8480	6847
NO_2^-	< 200	< 20	< 30	< 20	< 30
Br^-	< 2000	< 200	< 300	< 200	< 300
NO_3^-	< 2000	< 200	< 300	< 200	< 300
SO_4^{2-}	11862	26496	15276	29508	24117
PO_4^{3-}	< 2000	< 200	< 300	< 200	< 300

From the cation analysis in Table 26, considering a percentage of instrumental error, the amount of most cations is almost constant after acidification, alkalization, and throughout the oxidation process. However, a significant increase in aluminum and zinc levels was observed. Specifically, the concentration of aluminum rose from 1.42 mg/L in the CROL to 36.2 mg/L after oxidation at pH 3 and to 14.7 mg/L after oxidation at pH 5. As for zinc, values increased from 0.393 mg/L in the CROL to 6.82 mg/L after oxidation at pH 3 and 5.6 mg/L after oxidation at pH 5. These increases suggest that, after the treatment, metals may dissolve into the leachate. The SCAT composition, including 35.5% w/w of Al and 0.42% w/w of Zn, may support this hypothesis.

Oxidation may facilitate the dissolution of these metals, leading to an increase in their concentration in the sample analyzed.
Conversely, a decrease in iron and chromium levels was observed. Iron, starting from a value of 10.7 mg/L in the CROL, decreases to 4.86 mg/L after acidification at pH 3 and to 4.56 mg/L after alkalization at pH 5. Similarly, chromium drops from 6 mg/L to 2.38 mg/L and 2.48 mg/L in the respective acidification and alkalization processes. These reductions can be attributed to pH conditions: at acidic values, chromium and iron may precipitate as insoluble compounds contributing to the reduction of their concentration in the leachate.
Finally, a further minimal decrease in iron and chromium levels is observed after the oxidation process. After oxidation at pH 3, iron concentration drops to 1.82 mg/L and 2.48 mg/L after oxidation at pH 5, while chromium decreases to 0.283 mg/L and 2.02 mg/L, respectively. This further decrease may be due to the involvement of these metals in the oxidation process.
The analysis of anions, shown in Table 27 reveals a decrease in all anions at the various stages up to oxidation except for sulfates. This increase was expected, as the addition of sulfuric acid to a solution naturally leads to an increase in sulfate concentration.

2.2.5 Catalyst Recovery

The recyclability of the catalyst in subsequent oxidation reactions was also evaluated. Using the same operational conditions as the oxidation model, after each cycle, the catalyst was washed three times with ultrapure water and subsequently reused in the next oxidation. The results shown in Figure 25, indicate that the catalytic activity of SCAT remains almost unchanged for at least four consecutive cycles. However, starting from the fifth cycle, a gradual decrease in activity is observed. This decline can be attributed to various factors, including possible desorption and leaching of transition metals during washing or contact with the reaction mixture. Additionally, the high temperatures and aggressive operating conditions might cause physical or chemical degradation of SCAT. Residues and reaction products from the leachate could accumulate on the catalyst's surface, inhibiting its activity and decreasing performance over time. Contaminants present in the leachate may also poison the catalyst, compromising its effectiveness.

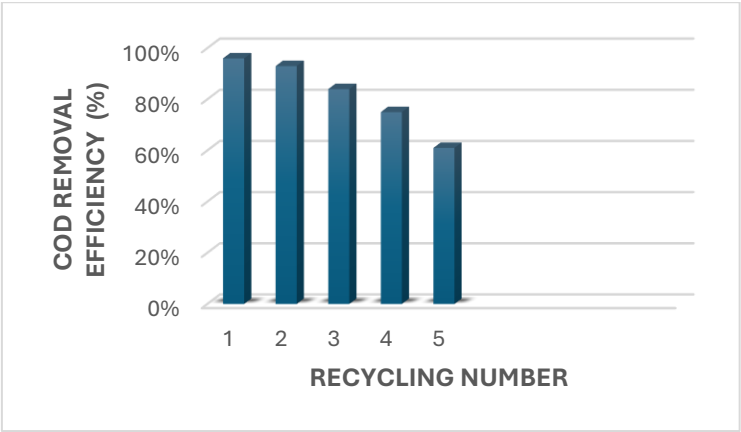

Fig.25. Number of catalyst recycling in the oxidative treatment of CROL

2.2.6 TOC detection

Besides evaluating the reduction of the COD, the Total Organic Carbon (TOC) was also examined. It was calculated subtracting the concentration of inorganic carbon (IC) from the total carbon (TC) concentration. This parameter provides a measure of the presence of organic compounds in the leachate, which may arise from the decomposition of waste or the introduction of external materials. Measuring TOC is useful to identify contamination levels and determine whether specific treatments are necessary before disposal. Treatment processes for leachate, such as chemical or biological oxidation, aim to reduce the organic content. Monitoring TOC, along with COD, allows for the assessment of the effectiveness of these processes, highlighting their efficiency when TOC values decrease.

In this regard, as with the study of anions and cations, TOC values were also analyzed for the pristine CROL, the acidified leachate (pH 3) before and after oxidation, and the subsequently basified leachate (pH 5) before and after oxidation. The results are reported in Table 28.

Tab.28 TOC detection

	TOC (Total organic carbon) (mg/L)	**TC (Total carbon) (mg/L)**	**TIC (Total inorganic carbon) (mg/L)**
RAW LEACHATE (CROL)	3202	5117	1915
CROL ACIDIFIED (pH3)	2077	2119	42.34
BASIFICATION (pH5)	2025	2078	53.12
CROL ACIDIFIED (pH3) post oxidation	1890	1904	13.79
BASIFICATION ph5 (post oxidation)	1325	1339	14.07

A reduction of TOC values was observed, consistent with the findings related to COD and previously reported. Starting from the CROL, an initial decrease of TOC values was detected. Then, a further reduction was observed after the oxidation process by addition of 530 µL of H_2O_2 and 150 mg of SCAT, whether the process was conducted at an initial pH of 3 or at pH 5. In the latter case, as predicted by the observed improvement in COD reduction, the best result was achieved also for TOC, highlighting the effectiveness of the oxidative treatment under less acidic pH conditions.

On the other hand, when analyzing the behavior of total inorganic carbon, a significant reduction was noted even during the acidification phase at pH 3. This result was consistent with expectations since the acidification phase aims to eliminate the present carbonates. Subsequently, inorganic carbon is almost completely removed through the oxidation process, confirming the overall effectiveness of the treatment in reducing both the organic and inorganic components of leachate.

2.2.7 Comparison of SCAT and $FeSO_4 \cdot 7H_2O$ efficiency at equal amounts of catalytically active iron

As part of the study on landfill leachate treatment, a comparison was made between the efficiency of the classic Fenton reaction, conducted using $FeSO_4 \cdot 7H_2O$, and the use of regenerated SCAT waste as alternative catalyst. The goal was to evaluate the behavior of these two different catalysts to compare their effectiveness by employing amounts with the same content of catalytically active iron.

To define the necessary quantities, data available in literature were used. Sanem *et al.* performed a classic Fenton oxidation using 41.5 g/L of $FeSO_4 \cdot 7H_2O$, known to contain 20% active iron ($FeSO_4 \cdot 7H_2O$ molecular weight: 278 g/mol, Fe atomic weight: 55.8 g/mol). This ratio leads to a content of approximately 8.4 g of iron per 41.5 g of $FeSO_4 \cdot 7H_2O$.

The same approach was applied to the SCAT catalyst, which is a composite containing various elements, as determined by the ICP analysis described in section 3.1.1. In this case, iron represents about 3% of the total content. Therefore, to obtain 8.4 g of iron, 264 g of SCAT were required.

Once the reference quantities were established, a systematic study was conducted on both catalysts, progressively varying the iron content. Specifically, the amount of iron was reduced in successive tests, using 4, 2, and 1 g of iron, as shown in table 29. The goal of this reduction was to evaluate whether effective results could be achieved using lower quantities of catalyst, thus improving the process efficiency. The monitored parameter in this study was TOC (total organic carbon). For each fixed amount of iron, experiments were conducted by varying the quantity of hydrogen peroxide, using exactly 530, 250, and 50 µL. All reactions were carried out at an initial acidic pH 3, maintained at room temperature for a duration of 84 minutes under constant stirring, following the conditions described in ref.[364]

Tab. 29 Amount of SCAT and $FeSO_4 \cdot 7H_2O$ used at equal iron content

Volume (L)	$FeSO_4 \cdot 7H_2O$ (g/L)	Catalytically active Iron in $FeSO_4 \cdot 7H_2O$ (g/L)	Catalytically active Iron in SCAT (g/L)
1	41,5	**8.4**	264
1	20	**4**	132
1	10	**2**	66
1	5	**1**	34

The TC content of the untreated landfill leachate (CROL) was found to be 3743 mg/L. Subsequently, the sample was acidified to a pH of 3 before proceeding with the various oxidation stages. After acidification, the TOC decreased to 2626 mg/L, corresponding to a 30% reduction, only attributed to the lowered pH. Then, the effect of different oxidation processes was studied. The results, presented in Figure 26, show a significant reduction in both TOC and color using the classic Fenton process, with $FeSO_4 \cdot 7H_2O$ as the catalyst. Specifically, using 2 g of iron and 50 µL of H_2O_2,

TOC dropped to 792.4 mg/L, reflecting a 78% reduction from the initial value of 3743 mg/L. It was hypothesized that TOC reduction is more efficient with lower amounts of hydrogen peroxide and catalyst, likely due to factors related to the kinetics and chemical equilibrium of the reaction. An excess of H_2O_2 could lead to its rapid decomposition into water and oxygen, without contributing to the oxidative process of the leachate. This phenomenon is particularly pronounced in the presence of ferrous catalyst excess, which accelerates the unwanted decomposition of H_2O_2, so reducing the amount of oxidant available for actual oxidation.

Another determining factor is the generation of hydroxyl radicals (·OH), which are the main agents of oxidation. Excessive amounts of catalyst or H_2O_2 can promote uncontrolled production of ·OH radicals, which may react with other radicals or with hydrogen peroxide itself, forming less reactive byproducts. Additionally, catalyst saturation could limit the activity of active sites, decreasing the effectiveness of the process and generating undesirable by-products. An excess of H_2O_2 could also lead to the formation of large amounts of Fe^{3+}, which

is less efficient in generating hydroxyl radicals with respect to Fe^{2+}. Therefore, a lower concentration of H_2O_2 and catalyst ensures a better balance between the production of hydroxyl radicals and the efficient consumption of the oxidant, preventing decomposition and the formation of by-products.

Conversely, the results obtained using the SCAT as a catalyst showed the opposite behavior. In this case, the best reduction of TOC and color was achieved with a higher amount of iron (8.4 g) and a lower amount of H_2O_2 (50 µL), resulting in a final TOC of 988 mg/L, equivalent to 74% reduction. Decreases in catalytic efficiency were observed with lower amounts of iron at various H_2O_2 concentrations, with a corresponding increase in residual color. The efficiency observed with the catalytic composite can be attributed to its composition, which includes, besides iron, noble metals such as platinum, palladium, and rhodium. The higher catalytic activity could therefore be due not only to the presence of iron but also of noble metals. Using higher amounts of SCAT increases the available active surface area and the noble metals load, thus promoting interactions between leachate molecules and H_2O_2 on the catalytic surface, enhancing the effectiveness of the oxidative process.

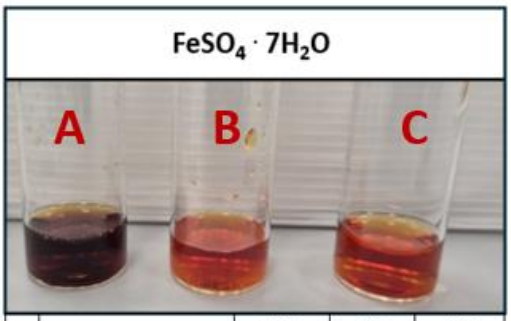

		TOC (mg/L)	TC (mg/L)	TIC (mg/L)
A	8.4 g Catalytically active Iron in $FeSO_4 \cdot 7H_2O$; 50µL H_2O_2 (1%)	1094	1079	<5
B	8.4 g Catalytically active Iron in $FeSO_4 \cdot 7H_2O$; 250µL H_2O_2 (5%)	1622	1613	<5
C	8.4 g Catalytically active Iron in $FeSO_4 \cdot 7H_2O$; 530µL H_2O_2 (10%)	1379	1512	132.9

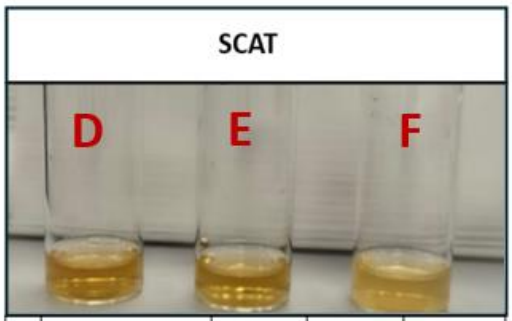

		TOC (mg/L)	TC (mg/L)	TIC (mg/L)
D	8.4 g Catalytically active Iron in SCAT; 50µL H_2O_2 (1%)	988	977	<5
E	8.4 g Catalytically active Iron in SCAT; 250µL H_2O_2 (5%)	1340	1326	<5
F	8.4 g Catalytically active Iron in SCAT; 530µL H_2O_2 (10%)	1118	1107	<5

$FeSO_4 \cdot 7H_2O$

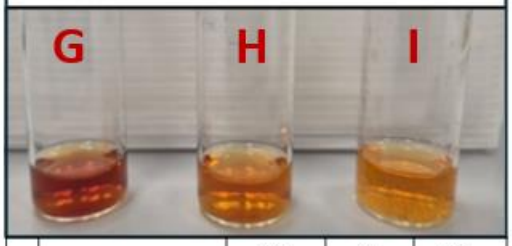

		TOC (mg/L)	TC (mg/L)	TIC (mg/L)
G	4 g Catalytically active Iron in $FeSO_4 \cdot 7H_2O$; 50µL H_2O_2 (1%)	1291	1239	1.214
H	4 g Catalytically active Iron in $FeSO_4 \cdot 7H_2O$; 250µL H_2O_2 (5%)	1194	1186	<5
I	4 g Catalytically active Iron in $FeSO_4 \cdot 7H_2O$; 530µL H_2O_2 (10%)	1513	1502	<5

SCAT

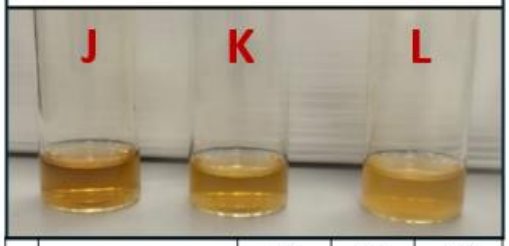

		TOC (mg/L)	TC (mg/L)	TIC (mg/L)
J	4 g Catalytically active Iron in SCAT; 50µL H_2O_2 (1%)	1835	1839	3,875
K	4 g Catalytically active Iron in SCAT; 250µL H_2O_2 (5%)	1944	1942	<5
L	4 g Catalytically active Iron in SCAT; 530µL H_2O_2 (10%)	1975	1967	<5

$FeSO_4 \cdot 7H_2O$

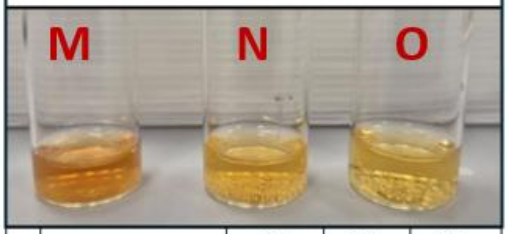

		TOC (mg/L)	TC (mg/L)	TIC (mg/L)
M	2 g Catalytically active Iron in $FeSO_4 \cdot 7H_2O$; 50µL H_2O_2 (1%)	792.4	872.0	79.64
N	2 g Catalytically active Iron in $FeSO_4 \cdot 7H_2O$; 250µL H_2O_2 (5%)	965.0	1047	82.04
O	2 g Catalytically active Iron in $FeSO_4 \cdot 7H_2O$; 530µL H_2O_2 (10%)	1310	1316	5.569

SCAT

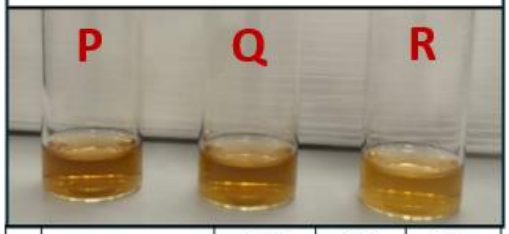

		TOC (mg/L)	TC (mg/L)	TIC (mg/L)
P	2 g Catalytically active Iron in SCAT; 50µL H_2O_2 (1%)	1925	1927	2.303
Q	2 g Catalytically active Iron in SCAT; 250µL H_2O_2 (5%)	2164	2162	<5
R	2 g Catalytically active Iron in SCAT; 530µL H_2O_2 (10%)	2101	2102	0.499

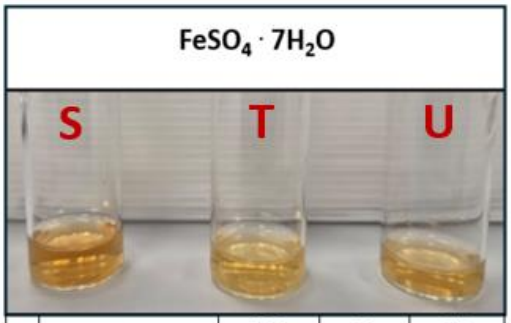

		TOC (mg/L)	TC (mg/L)	TIC (mg/L)
S	1 g Catalytically active Iron in $FeSO_4 \cdot 7H_2O$; 50µL H_2O_2 (1%)	811.2	1099	287.3
T	1 g Catalytically active Iron in $FeSO_4 \cdot 7H_2O$; 250µL H_2O_2 (5%)	999.5	1240	240.2
U	1 g Catalytically active Iron in $FeSO_4 \cdot 7H_2O$; 530µL H_2O_2 (10%)	1261	1386	124.6

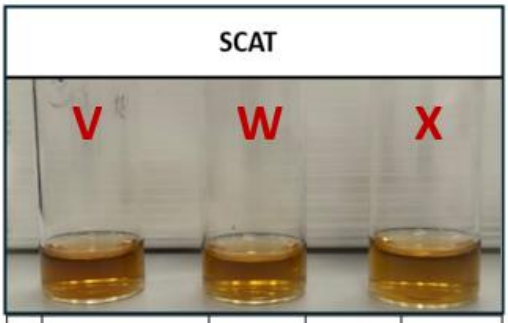

		TOC (mg/L)	TC (mg/L)	TIC (mg/L)
V	1 g Catalytically active Iron in SCAT; 50µL H_2O_2 (1%)	2067	2053	<5
W	1 g Catalytically active Iron in SCAT; 250µL H_2O_2 (5%)	2260	2247	<5
X	1 g Catalytically active Iron in SCAT; 530µL H_2O_2 (10%)	2261	2245	<5

Fig. 26. $FeSO_4 \cdot 7H_2O$ and SCAT comparison

2.3 SCAT catalyzed Suzuki-Miyaura Cross-Coupling Reactions

2.3.1 Optimization of the experimental conditions

To evaluate the suitability of SCAT as heterogeneous catalyst in Csp^2-Csp^2 bond forming reactions, the Suzuki-Miyaura cross-coupling process of aryl halides with aryl boronic acids was selected as the model case study, due to the possibility to work under eco-friendly conditions, in air and aqueous non-toxic solvents. The suitability of the SCAT catalyst was firstly tested through a model reaction between phenylboronic acid and 4-iodoanisole (Scheme 6). Various tests were made to evaluate the effects of different bases, solvents, and catalyst amounts on the reaction conversion and selectivity.

The solvent effect was analyzed performing the reaction in 1 hour under reflux using potassium carbonate as the base. As reported in Table 30, no reaction was observed with ethanol, water, tetrahydrofuran, or toluene, likely due to the poor solubility of the reagents and the base in these solvents (tests 1-4). Conversely, using only dimethylacetamide (DMA) at 100 °C, good selectivity (96%) but low conversion (35%) to the expected product was observed (test 5).

Increasing the temperature at 120 °C improved the efficiency of the reaction in DMA (conversion 47% and selectivity 99%, test 6). However, rather than further heating the mixture to the boiling point of DMA (160 °C), more eco-sustainable solvents were explored, such as mixtures of water and ethanol in various proportions (Table 30, tests 7-11). An excess of water improved both conversion and selectivity, with the best results obtained at 80 °C in a 4:1 volume ratio of H_2O to EtOH, achieving complete conversion (>99%) (test 11).

At the same temperature of 80 °C, lower amounts of water reduced the conversion from 75% to 60%, with varying H_2O:EtOH ratios from 3:1 to 1:2 (tests 10-7), but the selectivity remained nearly unchanged (from 99% to 90%). Finally, to verify the possibility of conducting the reaction at lower temperatures, the reaction was carried out at 70 °C (test 12), observing a reduction in conversion to 75%, which confirms a better efficiency upon working at 80 °C reaction temperature (entry 11).

Scheme 6: (*i*) **1** (0.16 mmol; 19.51mg), **2** (0.11 mmol; 25.74mg), SCAT 200 mg, base (0.16 mmol; 22.11mg), reaction time: 1 h. Conversion and selectivity detected *via* GC-MS

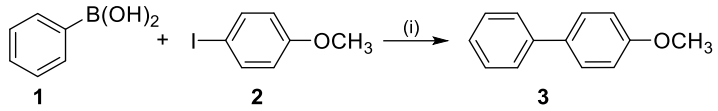

Tab. 30 Solvent screening for the model reaction of Scheme 6

Entry	Solvent	Base	Temperature (°C)	Conversion (%)	Selectivity (%)
1	EtOH	K_2CO_3	60	-	-
2	H_2O	K_2CO_3	100	-	-
3	THF	K_2CO_3	66	-	-
4	Toluene	K_2CO_3	120	-	-
5	DMA	K_2CO_3	100	35	96
6	DMA	K_2CO_3	120	47	>99
7	H_2O/EtOH (1:2)	K_2CO_3	80	60	90
8	H_2O/EtOH (1:1)	K_2CO_3	80	70	>99
9	H_2O/EtOH (2:1)	K_2CO_3	80	70	>99
10	H_2O/EtOH (3:1)	K_2CO_3	80	75	>99
11	**H_2O/EtOH (4:1)**	**K_2CO_3**	**80**	**>99**	**>99**
12	H_2O/EtOH (4:1)	K_2CO_3	70	75	>99

Subsequently, the effectiveness of alternative bases to K_2CO_3 was evaluated. As shown in Table 31, the use of $CaCO_3$, Cs_2CO_3, and $NaHCO_3$ led to a reduction in conversion (tests 1-3). Conversely, when using tributylamine or NaOH the base, no cross-coupling product and low conversion to the homocoupling product were observed (10% and 60%, tests 4 and 5). The use of tetrabutylammonium acetate (TBAA) also resulted in poor conversions and selectivity (test 6). Additional experiments were carried out to test the suitability of these bases as

ionic liquid solvents, but in the presence of TBAA at 100 °C, conversion and selectivity were low (10% and 20%, respectively, in test 7, Table 31).

Tab. 31 Screening of bases for the model reaction of Scheme 6 at 80 °C in a mixture of water and ethanol 4:1 vol

Entry	Base	Conversion (%)	Selectivity (%)
1	$CaCO_3$	85	30
2	Cs_2CO_3	50	80
3	$NaHCO_3$	20	70
4	$(Bu)_3N$	10	0
5	NaOH	60	0
6	TBAA	30	50
7	TBAA*	10	20

* Solvent-free, reaction temperature 100 °C

Table 32 also reports the amounts of SCAT used in the model reaction at 80 °C, in the presence of a water-ethanol mixture (4:1 volume ratio) and potassium carbonate as the base. As shown in Table 32, the maximum conversion and selectivity for the reaction described in Scheme 6 were achieved using 200 mg of SCAT with respect to 0.11 mmol (22.4 mg) of iodobenzene. According to ICP-MS analysis, this amount of SCAT corresponds to approximately 0.3 mg of catalytically active palladium nanoparticles (equivalent to 0.15 wt% of Pd in SCAT, as reported in Table 20). Consequently, the weight percentage of Pd relative to iodobenzene is estimated to be 1.3% (*i.e.* 0.3 mg out of 22.4 mg). Reducing the SCAT amount to 100 mg significantly lowered the conversion to 30%, with 80% selectivity for the cross-coupling product (test 2, Table 32). An improvement was observed when using 150 mg of catalyst, resulting in nearly complete selectivity and 80% conversion (test 3). However, the use of 200 mg of SCAT was considered the optimal condition to achieve maximum conversion and selectivity (test 1, Table 32).

Tab. 32: Screening of the amount of SCAT in the model reaction of Scheme 6 (80 °C in a 4:1 vol. mixture of water and ethanol)

Entry	SCAT	Conversion (%)	Selectivity (%)
1	**200**	**>99**	**>99**
2	100	30	80
3	150	80	>99

2.3.2 Substrates scope in the Suzuki-Miyaura cross-coupling

After optimizing the reaction conditions, the Suzuki-Miyaura cross-coupling was performed on a series of arylboronic acids and aryl halides. The results, shown in Table 33, indicate high yields (80-99%) and good selectivity in almost all processes investigated. These reactions were successful not only for a wide variety of aryl iodides and bromides functionalized with electron-donating or electron-withdrawing groups but also for aryl chlorides, which are known to be less reactive.

Considering the ideal reaction conditions, which involved a limiting reagent of 0.11 mmol and 200 mg of catalyst (containing only 0.15% palladium), the Turnover Number (TON) and Turnover Frequency (TOF) were calculated, yielding values of 274 for both TON and TOF. Compared to the TON of 980 reported by Senemoglu et al., who used a microwave-assisted aqueous system catalyzed by an unsymmetrical sulfonated water-soluble Pd(II)-pyridylimine, the SCAT catalyst may appear less efficient in terms of TON. Nevertheless, the robustness and versatility of the SCAT catalyst remain important, especially considering that SCAT is originally a waste material that does not require any complex treatment for its use. [365][366]

Tab.33 Reaction of cross-coupling Suzuki Miyaura

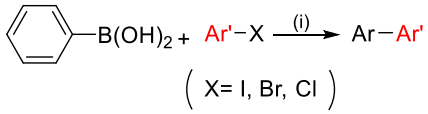

Cross coupling products: Ar–Ar'

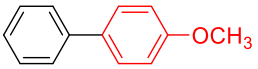

3 (80%, X=I, t=2h; 92%, X=Br, t=3h)

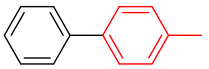

4 (92%, X=I, t=1.30h; 82%, X=Br, t=3h)

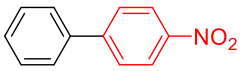

5 (75%, X=I, t=15 min; 91%, X=Br, t=1h)

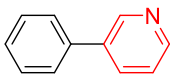

6 (87%, X=I, t=3h)

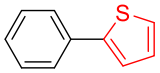

7 (95%, X=I, t=1h)

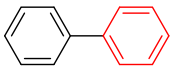

8 (95%, X=I, t=1h; 81%, X=Br, t=3h; 99%, X=Cl, t=3h)

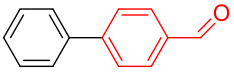

9 (93%, X=I, t=2h; 97%, X=Br, t=1h)

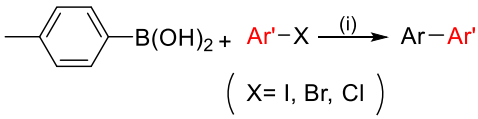

Cross coupling products: Ar–Ar'

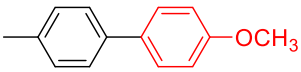

10 (92%, X=I, t=3h; 90%, X=Br, t=3h)

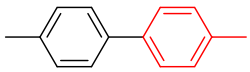

11 (93%, X=I, t=2h; 91%, X=Br, t=5h)

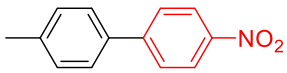

12 (88%, X=I, t=2h; 88%, X=Br, t=2h)

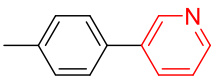

13 (83%, X=I, t=3h)

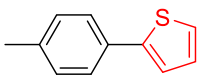

14 (91%, X=I, t=3h; 30%, X=Br, t=18h)

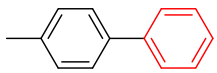

15 (90%, X=I, t=3h; 93%, X=Br, t=8h)

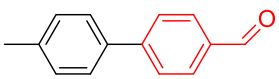

16 (94%, X=I, t=3h; 92%, X=Br, t=3h)

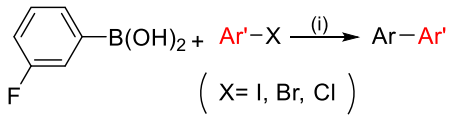

Cross coupling products: Ar−Ar'

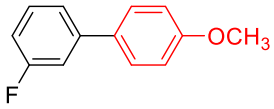

17 (93%, X=I, t=2h; 80%, X=Br, t=3h)

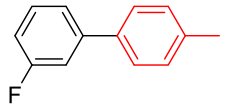

18 (96%, X=I, t=3h; 55%, X=Br, t=5h)

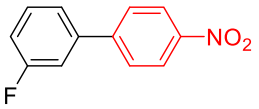

19 (93%, X=I, t=1h; 93%, X=Br, t=2h)

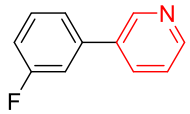

20 (89%, X=I, t=3h)

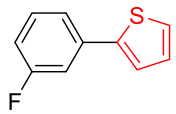

21 (92%, X=I, t=1h; 80%, X=Cl, t=20h)

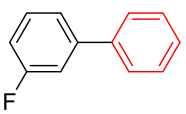

22 (89%, X=I, t=1h; 72%, X=Br, t=6h; 92%, X=Cl, t=3h)

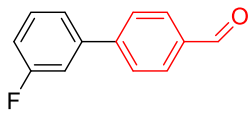

23 (91%, X=I, t=3h; 92%, X=Br, t=3h)

As indirect evidence that the catalytic effect of SCAT in cross-coupling reactions is attributable to the traces of transition metals present, reactions were also carried out using a sample of SCAT subjected to an acid leaching treatment, which removes the transition metals. As expected, no cross-coupling product was obtained under these conditions.

The effectiveness of SCAT was further examined in reactions involving variously functionalized arylboronic acids and aryl iodides (Table 34). These reactions, performed at 80°C in a mixture of H_2O and EtOH as the solvent, led to fair and high isolated yields (60% to 90%) of the cross-coupling product, with relatively short reaction times, usually on the order of a few hours. The effect of the position of functional groups on the aryl iodide was also evaluated to extend the generality of the method and complete the systematic study (Table 35).

Tab.34 Results of Suzuki-Miyaura cross-coupling reactions tested on different boronic acids

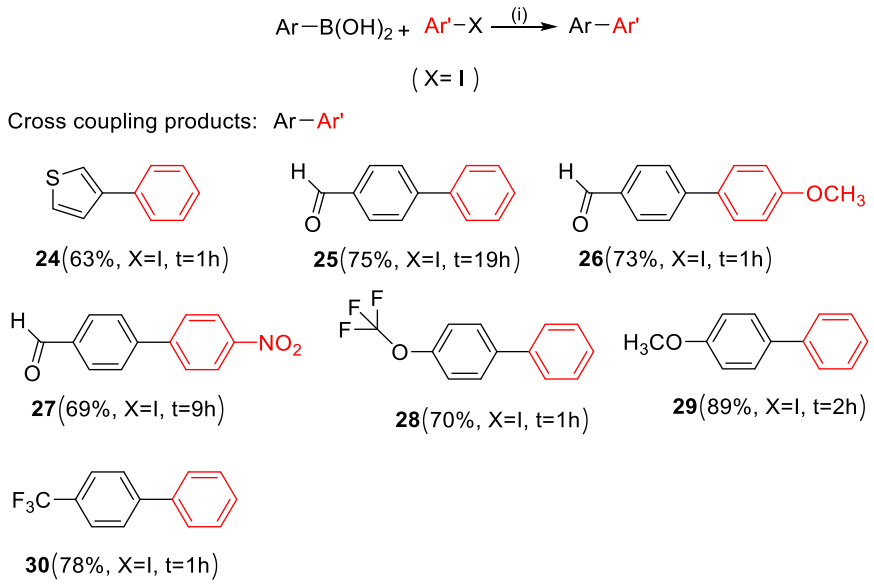

Tab.35 Results of Suzuki-Miyaura cross-coupling reactions tested on aryl halides with substituents in ortho and meta

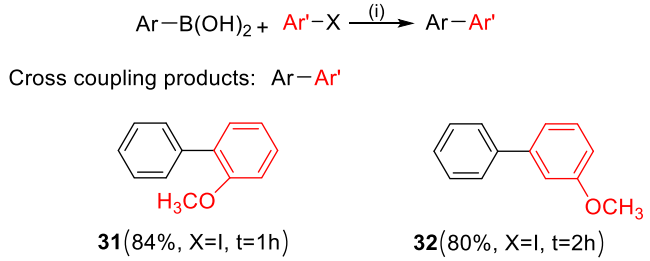

SCAT were also effective for reactions involving arylboronic acids and aryl dihalides (Table 36), with the aim to extend the application to π-conjugated oligomers that represent model systems with defined molecular weights, and model precursor products in order to extend the investigation to the synthesis of SCAT catalyzed polymerization protocols. As shown in Scheme 7, the regenerated SCAT efficiently catalyzes the reaction between phenyl boronic acid and 2,7-diiodo-9,9-dihexylfluorene, leading to an example of arylene small oligomer. In

this case, besides SCAT, the presence of tetrabutylammonium bromide as phase transfer catalyst was important to favor the reaction.
This experiment represents the first example of use of SCAT waste as catalysts for the synthesis of polyconjugated oligomers that will be extended to the synthesis of polymers in the future.

Tab.36 synthesis of π-conjugated oligomers

Scheme 7: (*i*) 1 (0.16 mmol; 19.51mg), **2** (0.055 mmol; 32mg), SCAT 200 mg, K_2CO_3 (0.16 mmol; 22.11mg), TBAB 125mg, H_2O 2mL, EtOH 0.5mL, reaction time: 1 h, temperature: 80°C

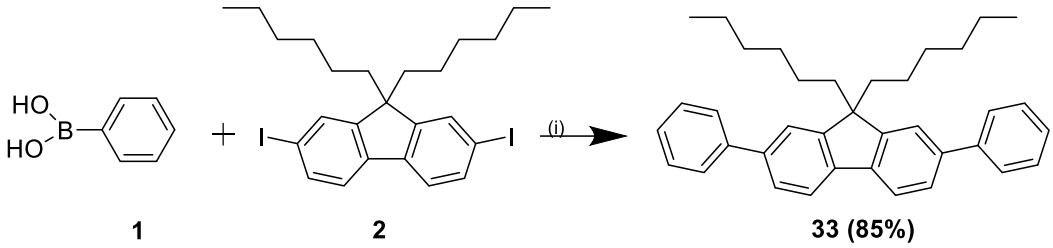

1 **2** **33 (85%)**

2.3.3 Catalyst recovery

Finally, the recyclability of the catalyst was evaluated. For this study, the cross-coupling reaction between phenylboronic acid and 2-iodothiophene was used (Scheme 8). The catalyst was recovered by centrifugation (4000 rpm for 2 minutes), washing with water and ethanol, and calcination in a muffle furnace at 450°C for 1 hour after each reaction. Calcination was necessary because when only washing was performed, the catalyst's efficiency was completely lost at the fifth cycle. In contrast, with calcination, the catalytic activity could be extended up to nine cycles, though it was lower than during the first five cycles (Figure 27). To investigate the cause of the transition metal loss, ICP-MS analysis of the reaction mixture was performed, which excluded the presence of these metals in solution. This ruled out the desorption of catalytic species into the solution.
The loss of metals during calcination was also studied by placing a quartz filter, commonly used for atmospheric metal sampling, on top of the SCAT inside the muffle furnace. ICP-MS analysis of the filter's mineralization extract confirmed the presence of Pd (0.045%), highlighting that calcination can alter the composition of SCAT over time. This observation is further supported by a

recorded reduction in palladium content, which decreased from an initial 0.15% to 0.07% after nine recycling. It is hypothesized that the undetected fraction of palladium may have been lost due to insufficient retention on the filter, adhesion to the walls of the vials and the loss of part of the SCAT during processing steps.

Scheme 8: (*i*) 1 (0.16 mmol; 19.51mg), **2** (0.11 mmol; 12µL), SCAT 200 mg, K_2CO_3 (0.16 mmol; 22.11mg), H_2O 2mL, EtOH 0.5mL, reaction time: 1 h, temperature: 80°C

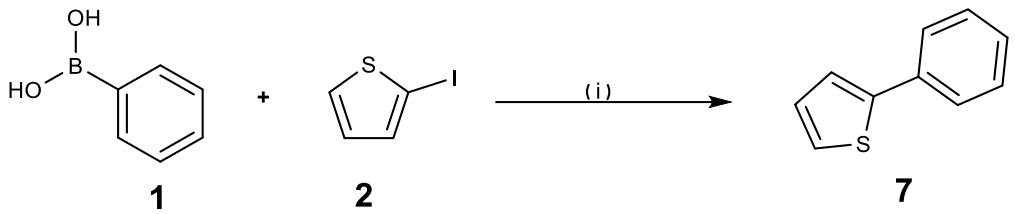

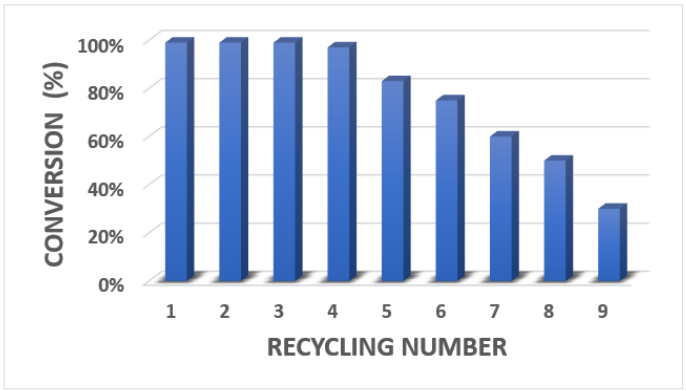

Fig. 27 Recyclability of the catalyst

Chapter 3: Materials and Methods

All reagents and solvents were purchased from Sigma-Aldrich and used without further purification.

3.1 SCAT Regeneration and Characterization

Exhausted SCAT was obtained from a Fiat Bravo car registered in Italy on 1995 and scrapped in 2018 after travelling 235000 km. The exhaust SCAT sample was firstly regenerated by calcination in a muffle at 450 °C for ~3 hours to remove adsorbed organic and inorganic residues of uncompleted automotive fuel combustion. ICP-MS analysis was then carried out to determine the presence and weight percentage of catalytically active metals supported onto the regenerated SCAT ceramic material.

For this aim, SCAT powder (5 g) crushed in a mortar was subjected to microwave-assisted mineralization with HCl (16 ml), H_2O_2 (1 ml) and H_2SO_4 (1 ml). [326] The resulting solution was diluted with deionized water (32 ml) and used for ICP-MS analysis. Mineralization of the sample was performed in a Microsynth Milestone FKV Advanced Microwave Synthesis Labstation and ICP-MS was carried out by Thermo Scientific iCAP Q spectrometer after a microwave-assisted.

TEM micrographs of a sample of SCAT powder after thermal regeneration were acquired by a JEOL JEM 2100Plus Transmission Electron Microscope (JEOL, Japan) operating with 200kV acceleration voltage, and equipped with 8-megapixel Gatan (Gatan, USA) Rio Complementary Metal-Oxide-Superconductor (CMOS) camera.

3.2 Experimental procedure for leachate oxidation reactions

Leachate (1 L) was placed in a beaker under magnetic stirring at room temperature and acidified with 1.7 mL of concentrated H_2SO_4 until reaching pH 3. Subsequently, the sample was centrifuged at 4000 rpm for 3 minutes to separate the residue from the supernatant. The supernatant was then divided into 5 mL aliquots and transferred into screw cap round bottom tubes for

subsequent oxidation treatments. Oxidation was performed in most cases over one-hour, varying parameters such as temperature, amount of oxidant (35% H_2O_2), and quantity of SCAT, to determine the optimal conditions. Additionally, comparative oxidation tests were conducted under the same conditions using $FeSO_4 \cdot 7H_2O$ as a catalyst instead of SCAT to compare catalyst efficiency. At the end of the oxidation process, the samples were cooled and centrifuged again at 3500 rpm for 2 minutes. Finally, an aliquot of the supernatant was taken for COD or TOC determination as described in the following analytical methods.

3.3 COD-TOC-TC-TIC Detection

The protocol used for COD determination is the EPA Method 410.4 (Revision 2.0: "Determination of Chemical Oxygen Demand by Semi-Automated Colorimetry"). COD determination was carried out using a cuvette test and it involves a digestion phase at 150°C for 2 hours followed by spectrophotometric measurement. All oxidation tests were conducted using 5 mL of the initial sample. After the oxidation, 2.5 mL of the sample were mixed with 3.5 mL of catalytic solution and 1.5 mL of digestion solution.

The d**igestion solution** was prepared dissolving $K_2Cr_2O_7$ (0.00867mol, 2.55 g), 42 mL of concentrated H_2SO_4, and $HgSO_4$ (0.0281mol, 8.35 g) to 250 mL of distilled water.

The **Catalytic solution** was obtained dissolving Ag_2SO_4 (0.00705mol, 2.2 g) and concentrated H_2SO_4 (4.17mol, 409 g).

The oxidation of organic matter occurs through digestion, which involves the use of an excess of potassium dichromate ($K_2Cr_2O_7$) in an acidic environment at high temperature. Any chlorides present are eliminated using mercury sulfate ($HgSO_4$), while silver sulfate (Ag_2SO_4) acts as a catalyst. After the digestion phase, the test tubes need to cool down before the spectrophotometric reading can be performed. The standard used at different concentrations for the calibration curve was potassium hydrogen phthalate (KHP), and the specific wavelength used by the spectrophotometer is 660 nm.

- The **Spectrophotometer** used is a Perkin Elmer UV/Vis/NIR Lambda 950. This instrument operates in the ultraviolet, visible, and near-infrared regions. It features a double beam, a double monochromator, and covers the entire

spectrum from 175 to 3300 nm. The two light sources are tungsten and deuterium, and the source change is computer-controlled. The instrument is also equipped with two detectors: a gridless type for the UV/Vis range and a Peltier-cooled PbS detector for the near-infrared range. Additionally, the instrument includes a 150 mm integrating sphere with a spectral range from 200 to 2500 nm. This sphere is equipped with a photomultiplier and a Peltier-cooled PbS detector. Polystyrene cuvettes with a single transparent window and a capacity of 4 mL were used for the spectrophotometric reading.

- **Gel Permeation Chromatography (GPC) Detention:** parallel to the determination of COD using the EPA method, a study was initiated to develop a COD determination method based on gel permeation chromatography (GPC). Since the concentrate is water-soluble, a polymethylmethacrylate stationary phase column was used, as opposed to the traditional polystyrene columns commonly employed for organic substances insoluble in aqueous environments. Due to the good water solubility, the concentrated samples were directly diluted (1:1 vol) with an aqueous solution of sodium azide and potassium nitrate used as the eluent mixture. The samples were then filtered with a 0.45 µm nylon filter and injected into a GPC (Knauer, Germany). The GPC was performed using an eluent flow rate of 1 mL/min.
- **Total organic carbon** was evaluated using a Shimadzu TOC-L analyzer. The TOC-L series employs the catalytic oxidation method, with a detection limit of 5%. The instrument is initially conditioned with an airflow of 0.6 L/min at a pressure of 200 kPa. This method effectively oxidizes not only low molecular weight organic compounds that are easily decomposable but also insoluble and macromolecular organic compounds that are difficult to decompose. The total carbon (TC) concentration in the sample was determined comparing it with a calibration curve constructed with points at 5 mg/L, 50 mg/L, and 100 mg/L. By subjecting the oxidized sample to the sparging process, the inorganic carbon (IC) in the sample was converted into carbon dioxide, and the IC concentration was measured using NDIR detection. The TOC concentration was calculated by subtracting the IC concentration from the obtained TC concentration. The carrier gas used in this instrument is air. All analyzed samples were prepared by taking an aliquot of the sample under examination and bringing it to a volume of 40 mL with ultrapure water using various dilutions. Subsequently, they were analyzed. For liquid samples determination, the TC standard is prepared using a

solution of ultrapure water and potassium hydrogen phthalate. For the TIC standard, a solution of ultrapure water containing $NaHCO_3$ and Na_2CO_3 is prepared.

3.4 Cations and Anions Determination

The variation of cations and anions at each single step was evaluated respectively using: ICP-OES (by Thermo Scientific iCAP 7000 Series and Dionex ICS-6000 Ion Chromatography System by Thermo Scientific.

- The **ICP-OES** (Inductively Coupled Plasma Optical Emission Spectroscopy) of the Thermo Scientific iCAP 7000 series offers high spectral resolution, enabling accurate separation of emission lines. This instrument covers a wide range of wavelengths, including most of the UV-visible spectrum. Thanks to its high sensitivity, it can detect very low concentrations of elements, down to parts per billion (ppb). For the analysis, 10 mL were taken, and in some cases, where necessary, when the sample was turbid, a digestion process was performed. The digestion consists of adding 2 mL of nitric acid and 6 mL of hydrochloric acid. The sample was digested using an automated digestion system, DigiPrep Jr from SCP Science, for 2 hours at 95°C. Afterwards, it is filtered with a 0.45 µm Teflon filter and brought to the desired volume, specifically 20 mL. In other cases, when the sample was less turbid and thus did not require digestion, the reading was taken directly from the sample as is. Ultrapure water was used to bring the digested solution to volume (20 mL), while acidified water with nitric and hydrochloric acid was used to bring the undigested samples to volume.
- The Thermo Scientific Dionex ICS-6000 **Ion Chromatography** system was equipped with a series of specific columns for different types of analytes, including cations and amines. This instrument can handle a high number of samples with precision and automation, including automatic sample preparation such as dilution. Additionally, it can detect and quantify ions at very low concentration levels, ensuring high reproducibility of results thanks to the precision of the system. The calibration curve involves the use of standards of analytes such as fluorides, chlorides, nitrites, nitrates, sulfates, and bromides. The calibration curve points range from 0.1 mg/L to 5 mg/L for fluorides

and nitrites, while for the other analytes, the calibration curve ranges from 1 mg/L to 100 mg/L. The sample must be previously filtered with a 0.45 µm nylon filter, transferred into 1.5 ml vials, and analyzed, with possible dilutions in case of out-of-range values. For sludge samples, a leaching test was performed. The sample was mixed with ultrapure water in a 1:9 ratio and left to rotate for 24 hours. Subsequently, the sample was filtered with a 0.45 micrometer nylon filter, transferred into 1.5 ml vials, and analyzed. Also, in this case, different dilutions were carried out in the presence of out-of-range values.

3.5 General Procedure of Suzuki Miyaura Cross-Coupling Reactions

Reactions were performed suspending the aryl boronic acid, the aryl halide, the SCAT grounded powder and the base in 2.5 mL of the solvent inside a 10 mL screw cap round bottom tube. The reaction mixture was stirred at the selected reaction temperature heating it inside a dry-bath metal block for tubes in contact with a heating magnetic stirrer plate. The reaction course was monitored over time *via* GM-MS analysis and, after observing its maximum conversion, it was cooled at room temperature and subjected to centrifugation at 4000 rpm for 2 min to separate the SCAT catalyst that was recovered and regenerated by thermal treatment. The organic mixture in the supernant was then subjected to extraction with ethyl acetate (3x 10mL) in the presence of water and the collected organic phase was dried with anhydrous sodium sulphate. After filtration and evaporation of the solvent at reduced pressure, the crude cross-coupling product was purified via column chromatography. Spectroscopic characterization of all products and experimental details of each reaction are reported in the results chapters.
To evaluate the efficiency of the reaction, parameters such as conversion, selectivity, and isolated yield were considered.

- The conversion was calculated as the percentage of the starting reagent that is transformed into the product during the reaction, but it does not provide direct information about the quality of the products formed. It is calculated as it follows:

$$\text{Conversion (\%)} = \frac{\text{Quantity of initial reagent consumed}}{\text{Initial quantity of reagent}} \times 100$$

- The selectivity allows assessing how effectively the cross-coupling product was obtained compared to other side reactions, such as homo-coupling products. High selectivity indicates that the reaction primarily produced the desired compound.

$$\text{Selectivity (\%)} = \frac{\text{Quantity of product desired}}{\text{Quantity of reagents transformed in total}} \times 100$$

-The yield represents the amount of the desired product obtained at the end of the reaction, in relation to the theoretically expected amount based on the reaction stoichiometry. A high yield indicates that most of the reagents were successfully transformed into the desired product and that the separation and purification were efficient.

$$\textbf{Yield (\%)} = \frac{\text{Quantity of isolated product}}{\text{Theoretical quantity of product}} \times 100$$

3.6 GC-MS Characterization

Reaction conversions were detected observing reagents consumption and cross-coupling product formation *via* GC-MS spectrometry by a Thermo Scientific Trace 1310-TSQ 8000 gas chromatograph coupled with triple quadrupole mass spectrometer.

3.7 SCAT Recovery Procedure After the Cross-Coupling Reaction

After centrifugation, the catalyst sample used for the reaction was collected in a porcelain crucible and kept at 450 °C in a muffle furnace for 60 min. During the thermal treatment, a sintered glass filter was used to cover the crucible containing the catalyst powder, with the aim to estimate the eventual

sublimation of PGM nanoparticles from SCAT and their incorporation in the filter. After cooling to room temperature, the catalyst powder was reused in the same reaction, to evaluate its catalytic efficiency in subsequent cycles. ICP-MS analysis of both SCAT and sintered filter was carried out after the whole series of cross coupling reactions performed using the same recycled catalyst, to estimate the overall effect of its thermal regeneration on PGM reduction in recycled sample.

Chapter 4: Experimental Section

4.1 ^{1}H and ^{13}C NMR Characterization of cross-coupling products

Reaction products were characterized via ^{1}H and ^{13}C NMR spectroscopy with a Agilent 500 spectrometer. Both ^{1}H and ^{13}C NMR spectra were acquired using an 11.7 Tesla magnetic field, with resonance frequencies of 500 MHz for ^{1}H and 125 MHz for ^{13}C. The typical recording parameters included a spectral width of 31250 Hz for ^{13}C and 9000 Hz for ^{1}H, using a 90° observing pulse at room temperature. "The ^{1}H and ^{13}C NMR spectra were obtained using 99.80% deuterated chloroform purchased from Eurisotop."

4-methoxy-1,1'-biphenyl

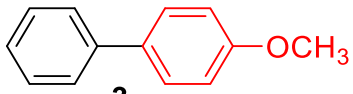

3

The reaction was performed according to the general procedure reported in the thesis (Section 2.3.2).The product was isolated as a white solid by column chromatography on silica gel with hexane as eluent; m.p 86 – 87 °C; ^{1}H NMR (500 MHz, $CDCl_3$) δ (ppm): 7.54 – 7.59 (m, 4H), 7.41 – 7.46 (m, 2H), 7.30 – 7.35 (m, 1H), 6.98 – 7.02 (m, 2H), 3.87 (s, 3H); ^{13}C NMR (125 MHz, $CDCl_3$) δ (ppm): 159.3, 141.0, 133.9, 128.9, 128.4, 126.9, 126.8, 114.4, 55.5. The spectroscopic data are in agreement with the literature. [367] GC-MS, m/z: 184.1 $[M]^+$.

4-methyl-1,1'-biphenyl

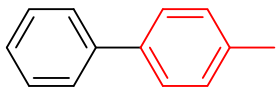

4

The reaction was performed according to the general procedure reported in the thesis (Section 2.3.2). The product was isolated as a white solid by column

chromatography on silica gel with hexane as eluent; m.p 49–50 °C; ^{1}H NMR (500 MHz, $CDCl_3$) δ (ppm): δ 7.50 (d, *J*=7.8 Hz, 2H), 7.36 (d, *J*=7.9 Hz, 2H), 7.27-7.31 (m, 1H), 7.24 (t, *J*=7.4 Hz, 2H), 7.04 (d, *J*=7.9 Hz, 2H), 2.29 (s, 3H); ^{13}C NMR (125 MHz, $CDCl_3$) δ (ppm): 136.86, 131.64, 131.33, 130.92, 130.15, 126.99, 122.6, 119.14, 21.03. The spectroscopic data are in agreement with the literature. [368] GC-MS, m/z: 3ea: 168.1 $[M]^+$.

4-nitro-1,1'-biphenyl

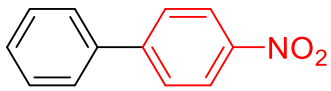

5

The reaction was performed according to the general procedure reported in the thesis (Section 2.3.2).The product was isolated as a yellow solid by column chromatography on silica gel with hexane/ethyl acetate (9:1) as eluent; m.p 112-113 °C; ^{1}H NMR (500 MHz, $CDCl_3$) δ (ppm): 8.30 (d, J = 8.0 Hz, 2H), 7.74 (d, J = 8.0 Hz, 2H), 7.62 (d, J = 8.0 Hz, 2H), 7.52-7.43 (m, 3H);^{13}C NMR (125 MHz, $CDCl_3$): δ (ppm)= 147.7, 147.2, 138.9, 129.2, 129.0, 127.9, 127.5, 124.2. The spectroscopic data are in agreement with the literature. [369] GC-MS, m/z: 199.1 $[M]^+$.

3-phenylpyridine

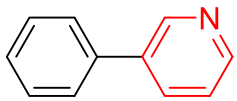

6

The reaction was performed according to the general procedure reported in the thesis (Section 2.3.2).The product was isolated as a withe solid by column chromatography on silica gel with hexane/ ethyl acetate (7:3) as eluent; m.p 49–50 °C; ^{1}H NMR (500 MHz, $CDCl_3$) δ (ppm): 8.77 (s, 1H), 8.52 (d, J = 4.0 Hz, 1H), 7.80 (d, J = 8.0 Hz, 1H), 7.51 (d, J = 8.0 Hz, 2H), 7.41 (t, J = 8.0 Hz, 2H), 7.34 (d, J= 8.0 Hz, 1H), 7.30 (dd, J = 4.0 Hz, 8.0 Hz, 1H); ^{13}C NMR (125 MHz, $CDCl_3$) δ (ppm): 147.5, 147.3, 136.9, 135.7, 133.3, 128.1, 127.1, 126.2, 122.5. The spectroscopic data are in agreement with the literature. [370] GC-MS, m/z: 155.1 $[M]^+$.

2-phenylthiophene

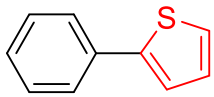

7

The reaction was performed according to the general procedure reported in the thesis (Section 2.3.2).The product was isolated as a light yellow solid by column chromatography on silica gel with hexane/DCM, (9.5:0.5) as eluent; m.p 33–35 °C; ^{1}H NMR (400 MHz, $CDCl_3$) δ (ppm): H NMR (500 MHz, $CDCl_3$) δ ppm: 7.54 (d,J = 7.9 Hz, 2H), 7.30 (t, J = 7.6 Hz, 2H), 7.17-7.24 (m, 3H), 7.00 (dd, J = 3.6, 4.8 Hz, 1H); ^{13}C NMR (125 MHz, $CDCl_3$) δ (ppm): 144.6, 134.5, 129.0, 128.1, 127.6, 126.2, 124.9, 123.2. The spectroscopic data are in agreement with the literature. [371] GC-MS, m/z: 160.0 $[M]^+$.

Biphenyl

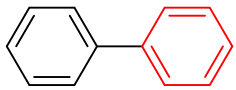

8

The reaction was performed according to the general procedure reported in the thesis (Section 2.3.2).The product was isolated as a colorless solid by column chromatography on silica gel with hexane as eluent; m.p 86 – 87 °C; ^{1}H NMR (500 MHz, $CDCl_3$) δ (ppm): 7.59 (d, 4H), 7.43-7.39 (t, 4H),7.33-7.30 (d, 2H); ^{13}C NMR (125 MHz, $CDCl_3$) δ (ppm): 141.3, 128.8, 128.6, 127.3, 127.2. The spectroscopic data are in agreement with the literature. [372] GC-MS, m/z: 154.1 $[M]^+$.

4-Phenylbenzaldehyde

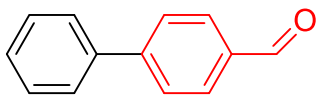

9

The reaction was performed according to the general procedure reported in the thesis (Section 2.3.2).The product was isolated as a white solid by column chromatography on silica gel with hexane/ethyl acetate (9:1) as eluent; m.p 57 – 59 °C; ^{1}H NMR (500 MHz, $CDCl_3$) δ (ppm): 10.06 (s, 1H), 7.96 (d, 2H, J = 8.4 Hz),

7.76 (d, 2H, J = 8.2 Hz), 7.64 (d, 2H, J = 7.1 Hz), 7.49 (t, 2H, J = 7.2 Hz), 7.42 (t, 1H, J = 7.2 Hz); ^{13}C NMR (125 MHz, $CDCl_3$) δ (ppm): 192.1, 147.4, 140.0, 135.4, 130.5, 129.3, 128.7, 127.9, 127.6. The spectroscopic data are in agreement with the literature. [373] GC-MS, m/z: 182.0 $[M]^+$.

4-Methoxy-4'-methyl-1,1'biphenyl

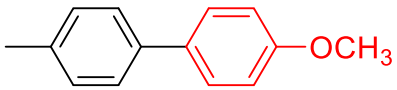

10

The reaction was performed according to the general procedure reported in the thesis (Section 2.3.2).The product was isolated as a white solid by column chromatography on silica gel with hexane/ethyl acetate (9:1) as eluent; m.p 108-109 °C; ^{1}H NMR (500 MHz, $CDCl_3$) δ (ppm): 7.52 (md, J = 8.8 Hz, 2H), 7.46 (md, J = 8.0 Hz, 2H), 7.22 (md, J = 7.9 Hz, 2H), 7.00 (md, J = 8.8 Hz, 2H), 3.85 (s, 3H), 2.39 (s, 3H); ^{13}C-NMR (125 MHz, $CDCl_3$) δ(ppm): 158.9, 137.9, 136.3, 133.7, 129.4, 127.9, 126.6, 114.1, 55.3, 21.0. The spectroscopic data are in agreement with the literature. [374] GC-MS, m/z: 198.1 $[M]^+$.

4,4'-dimethyl-1,1'- biphenyl

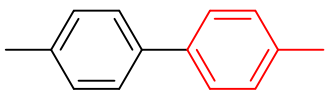

11

The reaction was performed according to the general procedure reported in the thesis (Section 2.3.2).The product was isolated as a white solid by column chromatography on silica gel with hexane as eluent; m.p 124-126 °C; ^{1}H NMR (500 MHz, $CDCl_3$) δ (ppm): 7.48-7.46 (d, 4H), 7.23- 7.21 (d, 4H), 2.40 (s, 6H); ^{13}C NMR (125 MHz, $CDCl_3$) δ(ppm): 138.4, 136.8, 129.6, 126.9, 21.2 ppm. The spectroscopic data are in agreement with the literature. [375] GC-MS, m/z: 182.1 $[M]^+$.

4-methyl-4'-nitro-1,1'-biphenyl

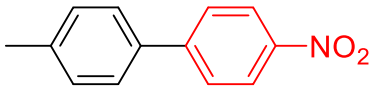

12

The reaction was performed according to the general procedure reported in the thesis (Section 2.3.2).The product was isolated as a yellow solid by column chromatography on silica gel with hexane/ethyl acetate (9:1) as eluent; m.p 154-155 °C; ^{1}H NMR (500 MHz, $CDCl_3$) δ (ppm): 7.49 – 7.51 (m, 2H), 7.33 – 7.37 (m, 2H), 7.27 (s, 2H), 7.00 (s, 2H), 2.50 (s, 3H); ^{13}C NMR (125 MHz, $CDCl_3$) δ 147.64, 139.20, 135.90, 129.99, 127.55, 127.31, 124.18, 21.31. The spectroscopic data are in agreement with the literature. [376] GC-MS, m/z: 213.1 $[M]^+$.

3-(p-Tolyl)pyridine

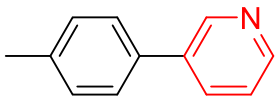

13

The reaction was performed according to the general procedure reported in the thesis (Section 2.3.2).The product was isolated as a white solid by column chromatography on silica gel with hexane/ethyl acetate (7:3) as eluent; m.p 58-60 °C; ^{1}H NMR (500 MHz, $CDCl_3$) δ (ppm): 8.77 (s, 1H), 8.50 (s, 1H), 7.78 (d, J = 8.0 Hz, 1H), 7.41 (d, J = 8.0 Hz, 2H), 7.28 (dd, J = 4.0 Hz, 8.0 Hz, 1H), 7.20 (d, J = 8.0 Hz, 2H), 2.34 (s, 3H); ^{13}C NMR ($CDCl_3$, 125 MHz) δ(ppm): 148.2, 138.1, 136.5, 135.0, 134.2, 129.8, 127.0, 123.6, 21.2. The spectroscopic data are in agreement with the literature. [375] GC-MS, m/z: 169.1 $[M]^+$.

2-(p-tolyl)thiophene

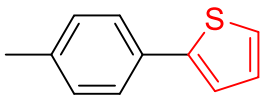

14

The reaction was performed according to the general procedure reported in the thesis (Section 2.3.2).The product was isolated as a white solid by column chromatography on silica gel with hexane/ethyl acetate (9:1) as eluent; m.p

104.7-106.3 °C; ^{1}H NMR (500 MHz, $CDCl_3$) δ (ppm): 7.51- 7.26 (dd, J = 8.3 Hz, 2H), 7.24 (dd, J = 2.5 Hz, 2H), 7.18 (d, J = 8.3 Hz, 2H), 7.06 (t, J = 3.5 Hz, 1H), 2.38 (s, 3H); ^{13}C NMR ($CDCl_3$, 125 MHz) δ(ppm): 144.51, 138.22, 137.22, 136.60, 131.60, 129.50, 129.39, 127.86, 127.74, 125.80, 124.19, 122.51, 21.09. The spectroscopic data are in agreement with the literature. [377] GC-MS, m/z: 174.0 $[M]^+$.

4-Methyl-1,1'-biphenyl

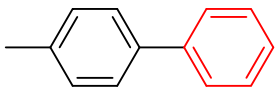

15

The reaction was performed according to the general procedure reported in the thesis (Section 2.3.2).The product was isolated as a white solid by column chromatography on silica gel with hexane as eluent; m.p 46-48 °C; ^{1}H NMR (500 MHz, $CDCl_3$) δ (ppm): 2.48 (s, 3H), 7.33 (d, J= 7.6 Hz, 2H), 7.40 (t, J= 7.6 Hz, 1H), 7.50 (t, J= 7.6 Hz, 2H), 7.58 (d, J= 8.0 Hz, 2H), 7.66 (d, J= 7.2 Hz, 2H); ^{13}C NMR (125 MHz, $CDCl_3$) δ(ppm): 21.1, 126.9, 127.0, 128.7, 129.4, 137.0, 138.3, 141.1. The spectroscopic data are in agreement with the literature. [368] GC-MS, m/z: 168.1 $[M]^+$.

4'-methyl-[1,1'-biphenyl]-4-carbaldehyde

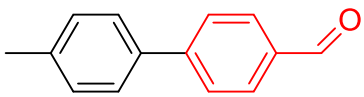

16

The reaction was performed according to the general procedure reported in the thesis (Section 2.3.2).The product was isolated as a white solid by column chromatography on silica gel with hexane/ethyl acetate (9,5:0.5) as eluent; m.p 76-78 °C; ^{1}H NMR (500 MHz, $CDCl_3$) δ (ppm): 10.05 (s, 1H), 7.94 (d, J = 8.1 Hz, 2H), 7.74 (d, J =8.0 Hz, 2H), 7.55 (d, J = 7.9 Hz, 2H), 7.29 (d, J = 7.8 Hz, 2H), 2.42 (s, 3H); ^{13}C NMR (125 MHz, $CDCl_3$) δ(ppm): 192.1, 147.3, 138.7, 136.9, 135.1, 130.4,129.9, 127.5, 127.3, 21.3. The spectroscopic data are in agreement with the literature. [378] GC-MS, m/z: 196.0 $[M]^+$.

3-fluoro-4'-methoxy-1,1'-biphenyl

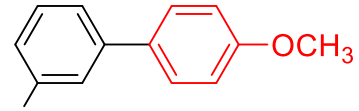

17

The reaction was performed according to the general procedure reported in the thesis (Section 2.3.2).The product was isolated as a white solid by column chromatography on silica gel with hexane/ethyl acetate (9,5:0,5) as eluent; m.p 65-67 °C; ^{1}H NMR (500 MHz, $CDCl_3$) δ (ppm): 7.50 (d, J = 7.0 Hz, 2H), 7.42 (td, J = 7.9, 1.8 Hz, 1H), 7.31 – 7.26 (m, 1H), 7.19 (td, J = 7.5, 1.3 Hz, 1H), 7.17 – 7.11 (m, 1H), 6.99 (d, J = 8.8 Hz, 2H), 3.86 (s, 3H); ^{13}C NMR (125 MHz, $CDCl_3$) δ(ppm): 159.9, 159.4, 130.64, 130.3, 128.9, 128.5, 128.3, 124.4, 116.2, 114.1, 55.5. The spectroscopic data are in agreement with the literature. [379] GC-MS, m/z: 202.1 $[M]^+$.

3-fluoro-4'-methyl-1,1'-biphenyl

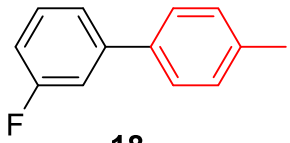

18

The reaction was performed according to the general procedure reported in the thesis (Section 2.3.2).The product was isolated as a white solid by column chromatography on silica gel with hexane as eluent; m.p 46-48 °C; ^{1}H NMR (500 MHz, $CDCl_3$) δ (ppm): 7.48 (d, J = 8.0 Hz, 2H), 7.41-7.34 (m, 2H), 7.29-7.25 (m, 3H), 7.06-6.97 (m, 1H), 2.40 (s, 3H); ^{13}C NMR (125 MHz, $CDCl_3$) δ(ppm): 21.13, 113.67, 113.85, 122.55, 126.93, 129.60, 130.15, 137.09, 137.74, 143.47, 164.22. The spectroscopic data are in agreement with the literature. [380] GC-MS, m/z: 186.1 $[M]^+$.

3-fluoro-4'-nitro-1,1'-biphenyl

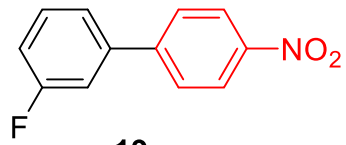

19

The reaction was performed according to the general procedure reported in the thesis (Section 2.3.2).The product was isolated as a yellow solid by column chromatography on silica gel with hexane/ethyl acetate (9,5:0,5) as eluent; m.p 98-100 °C; ^{1}H NMR (500 MHz, $CDCl_3$) δ (ppm): 8.21 (d, J = 8.8 Hz, 2H), 7.62 (d, J = 8.8 Hz, 2H), 7.43 – 7.35 (m, 1H), 7.31 (d, J = 7.9 Hz, 1H), 7.21 (dt, J = 9.8, 2.1 Hz, 1H), 7.04 (td, J = 8.4, 1.9 Hz, 1H); ^{13}C NMR (125 MHz, $CDCl_3$) δ(ppm):163.2, 147.6, 146.3, 141.0, 130.7, 127.3, 124.2, 123.3, 115.4, 114.1. The spectroscopic data are in agreement with the literature. [381] GC-MS, m/z: 217.0 $[M]^+$.

3-(3-fluorophenyl)pyridine

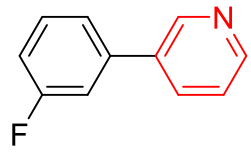

20

The reaction was performed according to the general procedure reported in the thesis (Section 2.3.2).The product was isolated as a white solid by column chromatography on silica gel with hexane/ethyl acetate (7:3) as eluent; m.p 56-58 °C; ^{1}H NMR (500 MHz, $CDCl_3$) δ (ppm): 8.84 (s, 1H), 8.62 (s, 1H), 7.90 – 7.82 (m, 1H), 7.48 – 7.41 (m, 1H), 7.41 – 7.34 (m, 2H), 7.28 (dd, J = 12.1, 2.0 Hz,1H), 7.10 (td, J = 8.3, 2.0 Hz, 1H); ^{13}C NMR (125 MHz, $CDCl_3$) δ(ppm): 163.22, 148.97, 148.14, 140.03, 135.41, 134.38, 130.64,123.63, 122.78, 114.97, 114.01. The spectroscopic data are in agreement with the literature. [382] GC-MS, m/z: 173.1 $[M]^+$.

2-(3-fluorophenyl)thiophene

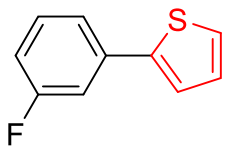

21

The reaction was performed according to the general procedure reported in the thesis (Section 2.3.2).The product was isolated as a colorless oil by column chromatography on silica gel with hexane as eluent; m.p 44-48 °C; ^{1}H NMR (500 MHz, $CDCl_3$) δ (ppm): 7.42 (s, 1H), 7.40 (t, J = 7.9 Hz, 1H), 7.28 (d, J = 3.4 Hz, 3H), 7.27 (d, J = 3 Hz, 1H), 6.94 (t, J = 6.8 Hz, 1H); ^{13}C NMR (125 MHz, $CDCl_3$) δ(ppm): 164.36, 161.91, 142.95, 136.52, 130.37, 128.05, 125.413, 124.29, 122.68, 114.71, 114.093. The spectroscopic data are in agreement with the literature [383] GC-MS, m/z: 178.0 $[M]^+$.

3-fluoro-1,1'-biphenyl

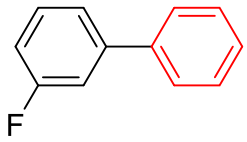

22

The reaction was performed according to the general procedure reported in the thesis (Section 2.3.2).The product was isolated as a colorless liquid by column chromatography on silica gel with hexane as eluent; m.p 42-44 °C; ^{1}H NMR (500 MHz, $CDCl_3$) δ (ppm): 7.62-7.59 (m, 2H), 7.50-7.46 (m, 2H), 7.43-7.38 (m, 3H), 7.34-7.31 (m, 1H), 7.09-7.04 (m, 1H). ^{13}C NMR (125 MHz, $CDCl_3$) δ(ppm): 163.4, 161.0,143.5, 140.0, 130.3, 128.9, 127.9, 127.1, 122.8, 114.2, 113.5. The spectroscopic data are in agreement with the literature [384] GC-MS, m/z: 172.1 $[M]^+$.

3'-Fluoro-[1,1'-biphenyl]-4-carbaldehyde

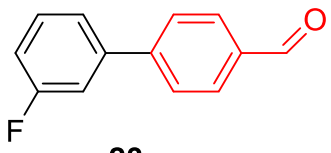

23

The reaction was performed according to the general procedure reported in the thesis (Section 2.3.2).The product was isolated as a colorless needles by column chromatography on silica gel with hexane/ethyl acetate (9,5:0,5) as eluent; m.p 54-57 °C; ^{1}H NMR (500 MHz, $CDCl_3$) δ (ppm): 10.07 (s, 1H), 8.01 - 7.88 (m, 4H), 7.67 - 7.46 (m, 3H), 7.28 - 7.13 (m, 1H); ^{13}C NMR (125 MHz, $CDCl_3$) δ(ppm):193.0, 163.1, 144.8, 141.6, 135.9, 131.4, 130.5, 127.9, 123.6, 115.7, 114.3. The spectroscopic data are in agreement with the literature. [385] GC-MS, m/z: 200.1 $[M]^+$.

3-phenylthiophene

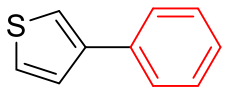

24

The reaction was performed according to the general procedure reported in the thesis (Section 2.3.2).The product was isolated as a white solid by column chromatography on silica gel with hexane as eluent; m.p 90-91 °C; ^{1}H NMR (500 MHz, $CDCl_3$) δ (ppm): 7.60 (d, J= 8.4, 2H), 7.44-7.42 (m, 1H), 7.40-7.34 (m,4H), 7.32-7.31 (m, 1H); ^{13}C NMR (125 MHz, $CDCl_3$) δ(ppm): 142.3, 135.8, 128.7, 127.1, 126.4, 126.3, 126.2, 120.2. The spectroscopic data are in agreement with the literature. [386] GC-MS, m/z: 160.0 $[M]^+$.

[1,1'-biphenyl]-4-carbaldehyde

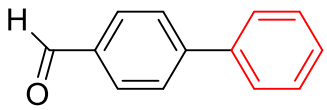

25

The reaction was performed according to the general procedure reported in the thesis (Section 2.3.2).The product was isolated as a white solid by column

chromatography on silica gel with hexane/ethyl acetate (9:1) as eluent; m.p 58-61 °C; ^{1}H NMR (500 MHz, $CDCl_3$) δ (ppm): 10.03 (s, 1H), 7.91 (d, J = 8.2 Hz, 2H), 7.78 (d, J = 8.2 Hz, 2H), 7.68 – 7.61 (m, 2H), 7.46 (t, J = 7.3 Hz, 2H), 7.39 (t, J = 7.3 Hz, 1H); ^{13}C NMR (125 MHz, $CDCl_3$) δ(ppm): 191.83, 147.8, 139.60, 135.11, 130.18, 128.98, 128.40, 127.58, 127.27. The spectroscopic data are in agreement with the literature. [387] GC-MS, m/z: 182.1 $[M]^+$.

4'-methoxy-[1,1'-biphenyl]-4-carbaldehyde

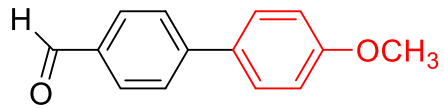

26

The reaction was performed according to the general procedure reported in the thesis (Section 2.3.2).The product was isolated as a white solid by column chromatography on silica gel with hexane/ethyl acetate (9:1) as eluent; m.p 105-111 °C; ^{1}H NMR (500 MHz, $CDCl_3$) δ (ppm): 10.03 (s, 1H), 7.93 (d, J = 8.2 Hz, 2H), 7.72 (d, J = 8.1 Hz, 2H), 7.60 (d, J = 8.7 Hz, 2H), 7.01 (d, J = 8.7 Hz, 2H), 3.87 (s, 3H); ^{13}C NMR (125 MHz, $CDCl_3$) δ(ppm): 192.0, 160.1, 146.8, 134.7, 132.1, 130.3, 128.5, 127.1, 114.5, 55.4. The spectroscopic data are in agreement with the literature. [388] GC-MS, m/z: 212.1 $[M]^+$.

4'-nitro-[1,1'-biphenyl]-4-carbaldehyde

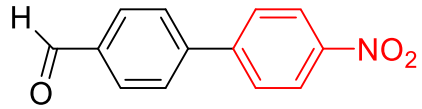

27

The reaction was performed according to the general procedure reported in the thesis (Section 2.3.2).The product was isolated as a white solid by column chromatography on silica gel with hexane/ethyl acetate (7,5:2,5) as eluent; m.p 124-128 °C; ^{1}H NMR (500 MHz, $CDCl_3$) δ (ppm): 10.10 (s, 1H), 8.34 (dd, J = 8.7, 1.8 Hz, 2H), 8.01 (dd, J = 8.2, 1.6 Hz, 2H), 7.77 (dd, J = 8.5, 1.5 Hz, 4H); ^{13}C NMR (125 MHz, $CDCl_3$) δ(ppm): 191.6, 147.8, 146.0, 144.5, 136.3, 130.4, 128.2, 128.1, 124.3. The spectroscopic data are in agreement with the literature. [381] GC-MS, m/z: 227.1 $[M]^+$.

4-(trifluoromethoxy)-1,1'-biphenyl

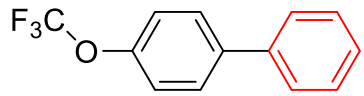

28

The reaction was performed according to the general procedure reported in the thesis (Section 2.3.2).The product was isolated as a white solid by column chromatography on silica gel with hexane/ethyl acetate (8:2) as eluent; m.p 52-54 °C; ^{1}H NMR (500 MHz, $CDCl_3$) δ (ppm): 7.55 (m, 4H), 7.46 (t, J = 7.5 Hz, 2H), 7.35 (t, J= 7.3 Hz, 1H), 7.28 (d, J = 8.1 Hz, 2H); ^{13}C NMR (125 MHz, $CDCl_3$) δ(ppm): 148.7, 140.0, 139.9, 128.9, 128.4, 127.6, 127.1, 121.8, 121.2, 119.3. The spectroscopic data are in agreement with the literature. [389] GC-MS, m/z: 238.1 $[M]^+$.

4-methoxy-1,1'-biphenyl

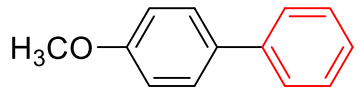

29

The reaction was performed according to the general procedure reported in the thesis (Section 2.3.2).The product was isolated as a white solid by column chromatography on silica gel with hexane/ethyl acetate (9:1) as eluent; m.p 86 – 87 °C; ^{1}H NMR (500 MHz, $CDCl_3$) δ (ppm): 7.56 – 7.59 (m, 4H), 7.41 – 7.46 (m, 2H), 7.30 – 7.36 (m, 1H), 6.98 – 7.04 (m, 2H), 3.88 (s, 3H); ^{13}C NMR (125 MHz, $CDCl_3$) δ (ppm): 159.3, 141.0, 133.9, 128.9, 128.3, 126.7, 126.8, 114.4, 55.5. The spectroscopic data are in agreement with the literature. The spectroscopic data are in agreement with the literature. [374] GC-MS, m/z: 184.1 $[M]^+$.

1-phenyl-4-(trifluoromethyl)benzene

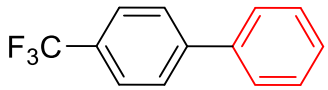

30

The reaction was performed according to the general procedure reported in the thesis (Section 2.3.2).The product was isolated as a white solid by column chromatography on silica gel with hexane/DCM (9:1) as eluent; m.p 51 – 55 °C; ^{1}H NMR (500 MHz, $CDCl_3$) δ (ppm): 7.73 (s, 4H), 7.68 (d, J = 7.4 Hz, 2H), 7.52 (t, J = 7.5 Hz, 2H), 7.49 (t, J = 7.4 Hz, 1H);^{13}C NMR (125 MHz, $CDCl_3$) δ (ppm): 144.7, 139.8, 129.1, 129.3, 128.1, 127.2, 127.3, 125.9, 124.1. The spectroscopic data are in agreement with the literature. [374] GC-MS, m/z: 222.1 $[M]^+$.

2-methoxy-1,1'-biphenyl

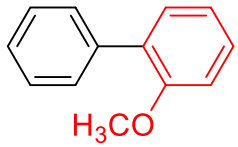

31

The reaction was performed according to the general procedure reported in the thesis (Section 2.3.2).The product was isolated as a white solid by column chromatography on silica gel with hexan as eluent; m.p 38 - 41 °C; ^{1}H NMR (500 MHz, $CDCl_3$) δ (ppm): 7.48 (d, J = 9.5 Hz, 2H), 7.39 (t, J = 7.3 Hz, 2H), 7.36 - 7.33 (m, 3H), 7.02 (t, J = 7.4 Hz, 1H), 7.01 (d, J = 8.7 Hz, 1H), 3.81 (s, 3H); ^{13}C NMR (125 MHz, $CDCl_3$) δ (ppm): 156.7, 138.3, 130.2, 130.1, 129.2, 128.5, 128.0, 127.1, 120.8, 111.1, 55.8. The spectroscopic data are in agreement with the literature. [390] GC-MS, m/z: 184.1 $[M]^+$.

3-methoxy-1,1'-biphenyl

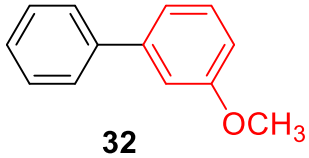

32

The reaction was performed according to the general procedure reported in the thesis (Section 2.3.2).The product was isolated as a white solid by column chromatography on silica gel with hexan as eluent; m.p 43 – 48 °C; ^{1}H NMR (500 MHz, $CDCl_3$) δ (ppm): 3.81 (s, 3H), 6.88 (d, J = 8.0 Hz, 1H), 7.11 (d, J = 1.6 Hz, 1H), 7.13 (d, J = 7.6 Hz, 1H), 7.29-7.31 (m, 2H), 7.40 (t, J = 7.6 Hz, 2H), 7.55 (d, J = 7.6 Hz, 2H). ^{13}C NMR (125 MHz, $CDCl_3$) δ (ppm):) 55.8, 112.3, 112.4, 119.1, 127.2, 127.4, 128.5, 129.3, 141.0, 142.9, 159.7. The spectroscopic data are in agreement with the literature. [391] GC-MS, m/z: 184.1 $[M]^+$.

9,9-dihexyl-2,7-diphenyl-9H-fluorene

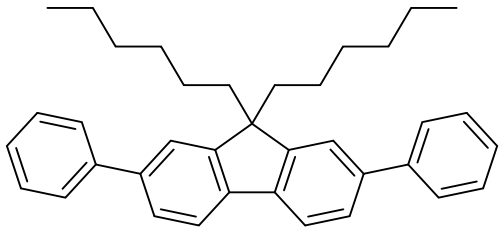

33

The reaction was performed according to the general procedure reported in the thesis (Section 2.3.2; Scheme 7). The product was isolated as a white solid by column chromatography on silica gel with hexane/DCM (8:2) as eluent; m.p. 80 – 150 °C; ^{1}H NMR (500 MHz, $CDCl_3$) δ (ppm): δ 7.79 (d, J = 7.8 Hz, 2H), 7.70 (m, 4H), 7.61 (m, 4H), 7.50 (m, 4H), 7.38 (m, 2H), 2.06 (m, 4H), 1.15 (m, 12H), 0.7 (m, 10H); ^{13}C NMR (125 MHz, $CDCl_3$, ppm): δ 151.84, 145.23, 142.44, 139.87, 133.51, 128.05, 125.07, 124.45, 122.41, 119.68, 55.24, 40.43, 31.79, 30.01, 29.18, 23.73, 22.59, 14.05. GC-MS, m/z: 486.3 $[M]^+$.

Conclusions

In summary, the activities carried out during the PhD project have been focused on the development of innovative and eco-friendly protocols to reduce the Chemical Oxygen Demand (COD) of landfill leachate concentrate samples, to values next to the limits set by current regulations (160 mg/L). The COD is an important parameter to estimate the presence of undesirable oxidizable organic and inorganic substance, thus allowing to assess the environmental risk related to leachate concentrate disposal. Reducing COD is a critical target at both national and international levels, as it can contribute to solve the issue of leachate disposal, which accumulates in large amounts in landfills. The research was carried out in deep collaboration with the Tecnologia & Ambiente environmental service company (T&A, Putignano, Apulia Region, Italy), funder of the PhD position.

Recyclable waste materials derived from spent automotive converters (SCATs) were used as heterogeneous catalysts for both the oxidative treatment of leachate concentrates with hydrogen peroxide and for Csp2-Csp2 bond forming reactions such as the Suzuki-Miyaura cross-coupling of aryl boronic acids with aryl halides. The regenerated SCAT was found to be highly efficient in both processes, ensuring up to five and nine recovery cycles for leachate oxidation and Suzuki cross coupling respectively.

Moreover, Gel Permeation Chromatography was demonstrated to be a promising technique for COD detection, with the possibility to avail of polymethylmethacrylate and water as the green stationary phase and the solvent, respectively. Despite the need for further optimization, this method has been proven to be very straightforward, fast and eco sustainable with respect to the well-known EPA 410.4 revised 2.0 protocol.

A further project investigated during the PhD course dealt with the study of supercritical fluid-based extraction of biofuel from fishing waste collected from two trawlers in the southwestern Adriatic Sea. Supercritical carbon dioxide (sc-CO_2) was used as a green solvent for this aim and the extracted lipid oils, were then converted into fatty acid methyl esters (FAME) suitable as biodiesel. This

work led to the publication of the article “Green production of biofuels from fish discards using supercritical Carbon Dioxide as the extraction solvent.” authored by Sini V., Carluccio A., Marangi M., Ragni R., D’Onghia G., Cotugno P. in 2022 IEEE International Workshop on Metrology for the Sea; Learning to Measure Sea Health Parameters (MetroSea) (pp. 91-95).

Main outputs of the research activity

1. **Oxidative treatments of landfill leachate to reduce COD**
   The effectiveness of regenerated SCAT as heterogeneous catalyst was studied in the oxidation reaction of landfill leachate concentrate with hydrogen peroxide. Leachate COD was reduced from 16.000 mg/L to 579 mg/L. Considering that the limit for disposal in the sewage system is 500 mg/L, this result is highly significant. The best results of 96% COD reduction were achieved by firstly working at pH 3 to remove carbonates and then at pH 5 to perform the oxidation reaction with hydrogen peroxide (530 µL) and SCAT (150 mg),. Furthermore, the recyclability of the catalyst was demonstrated for at least five consecutive cycles.
2. **SCAT catalyzed Suzuki Miyaura cross coupling reactions**
   SCAT efficacy was demonstrated in Suzuki-Miyaura cross-coupling reactions of a wide variety of heteroaryl boronic acids with heteroaryl halides. The experimental protocol was optimized by the model reaction between phenylboronic acid and 4-iodoanisole and then extended to a wide variety of substrates, investigating the electronic effects and positions of various functional groups in reagents. The results showed fair to high yields (80-99%) and good selectivity not only when using iodides and bromides but also for some aryl chlorides, known to be less reactive. The SCAT catalyst was also effective in reactions between arylboronic acids and aryl dihalides, useful for the synthesis of π-conjugated oligomers. Moreover, the recyclability of the catalyst up to nine consecutive reactions was also demonstrated by calcination at 450°C for one hour and washing with water and ethanol. This output demonstrates the promising suitability of SCATs as catalytic waste materials for Csp2-Csp2 bond forming reactions. Future studies could explore the application of SCAT in other types of catalytic reactions, increasing its potential in synthetic chemistry. In particular, this study could serve as a

foundation for testing the efficiency of other metals beyond palladium, such as platinum for the reduction of alkenes or rhodium for the hydroformylation of olefins. These investigations could further expand the scope of SCAT as a versatile catalyst derived from recycled materials, reinforcing its role in the development of sustainable and innovative methodologies in organometallic synthesis.

3. **Biofuel production by supercritical carbon dioxide based extraction of lipid oils from fishing waste**

   The effectiveness of supercritical carbon dioxide (sc-CO_2) as eco-friendly solvent for the extraction of lipid oils from fishing waste was demonstrated in collaboration with other researchers of the group where the PhD work was carried out. Experiments were firstly made to find the experimental parameters (s-CO2 pressure, flow, and temperature) to optimize the extraction yield. A 10% (w/w) yield of fish oil extract (i.e. 10 g of oil vs 100 g of dry fish waste) was observed working at 30 MPa, 50 °C, and 1 l/min sc-CO_2 flow rate. The transesterification reaction on the extracted oil led to a mixture of saturated and unsaturated fatty acid methyl esters (FAME) with C14-C25 alkyl chains, with higher abundance for methyl hexadecanoate, (Z,Z)-methyl octadeca-9,12-dienoate, and trans-methyl-13-octadecenoate, all suitable for use as biodiesel oils.

In conclusion, the three years PhD overall research work can be regarded as a fruitful activity to prove the concept that waste regeneration is more profitable than disposal and that “waste for waste” treatment strategies can be extremely useful to face the environmental impact of goods consumption, in accordance with the Green Deal and Circular Economy.

Bibliography

[1] https://www.mase.gov.it/pagina/recycling-and-waste-management
[2] Available online: https://www.arpalombardia.it/temi-ambientali/rifiuti/classificazione-rifiuti/
[9] Available online: https://www.mase.gov.it/pagina/la-classificazione-dei-rifiuti
[4] Galanti, A., (2018). La classificazione dei rifiuti con" codice specchio". 177–216
[5] Stoeva, K., Alriksson, S., (2017). Influence of recycling programmes on waste separation behaviour. Waste Manag. 68, 732–741
[6] D'Amato, A., Mancinelli, S., Zoli, M., (2016). Complementarity vs substitutability in waste management behaviors. Ecol. Econ. 123, 84–94
[7] Feo, G., Ferrara, C., Iannone, V., Parente, P., (2019). Improving the efficacy of municipal solid waste collection with a communicative approach based on easily understandable indicators. Sci. Total Environ. 651, 2380–2390.
[8] Statistics, E. E. P. (2020). Available online: https://ec. europa. eu/eurostat/statistics-explained/index. php. *Renewable_energy_statistics (accessed on 22 November 2018)*.
[9] Pfaltzgraff, L.A.; De Bruyn, M.; Cooper, E.C.; Budarin, V.; Clark, J.H. (2013). Green Chemistry Food waste biomass: A resource for high-value chemicals. Green Chem., 15, 307–314.
[10] World Bank, (2013). Global Waste on Pace to Triple by 2100. October 30. Available online:
http://www.worldbank.org/en/news/feature/2013/10/30/global-waste-on-pace-to-triple.
[11] OECD. Environment at a Glance (2015). OECD Indicators; OECD Publishing: Paris, France; p. 48.
[12] Zaman, A.U.; Lehmann, S., (2013). The zero waste index: A performance measurement tool for waste management systems in a “zero waste city”. J. Clean. Prod. 50, 123–132.
[13] Mesjasz-Lech, A., (2021). Municipal UrbanWaste Management—Challenges for Polish Cities in an Era of Circular Resource Management. Resources 2021, 10, 55.

[14] EU Approach to Sustainable Development. Available online: https://ec.europa.eu/info/strategy/international-strategies/sustainable-development-goals/eu-approach-sustainable-development_pl.
[15] Kozłowski, K. Ogromne Korzys´ci Płyna¸ce z Segregacji Odpadów. Available online: https://www.prawo.pl/biznes/ogromnekorzysci- plynace-z-segregacji-odpadow,160018.html.
[16] Razminiené, K.; Vinogradova, I.; Tvaronavi˘ciené, M., (2021). Clusters in Transition to Circular Economy: Evaluation of Relation. Acta Montan. Slovaca, 26, 455–465.
[17] Pandey, R.U., Surjan, A., Kapshe, M., (2018). Exploring linkages between sustainable consumption and prevailing green practices in reuse and recycling of household waste: case of Bhopal city in India. J. Clean. Prod. 173, 49–59.
[18] Awasthi, A.K., Cucchiella, F., D'Adamo, I., Li, J., Rosa, P., Terzi, S., Wei, S., Zeng, X., (2018). Modelling the correlations of e-waste quantity with economic increase. Sci. Total Environ. 613–614, 46–53.
[19] Pietzsch, N., Ribeiro, J.D.L., Medeiros, J.F., (2017). Benefits, challenges and critical factors of success for zero waste: a systematic literature review. Waste Manag. 67, 324–353
[20] Millward-Hopkins, J., Busch, J., Purnell, P., Zwirner, O., Velis, C.A., Brown, A., Iacovidou, E., (2018). Fully integrated modelling for sustainability assessment of resource recovery from waste. Sci. Total Environ. 612, 613–624.
[21] Ma, J., Hipel, K.W., Hanson, M.L., Cai, X., Liu, Y., (2018). An analysis of influencing factors on municipal solid waste source-separated collection behavior in Guilin, China by using the theory of planned behavior. Sustain. Cities Soc. 37, 336–343. https://doi.org/ 10.1016/j.scs.2017.11.037
[22] Matsuda, T., Hirai, Y., Asari, M., Yano, J., Miura, T., Ii, R., Sakai, S., (2018). Monitoring environmental burden reduction from household waste prevention. Waste Manag. 71, 2–9.
[23] Nový Ak˘cný Plán Pre Obehové Hospodárstvo. Available online: https://eur-lex.europa.eu/legal-content/SK/TXT/HTML/?uri=CELEX:52020DC0098&from=SK
[34] Odpady a Obaly. Available online: https://www.minzp.sk/eu/oblasti/odpady-obaly/
[25] Europe 2050 Strategy. Available online: https://climate.ec.europa.eu/eu-action/climate-strategies-targets/2050-long-termstrategy_sk

[26] Polishchuk, V.; Kelemen, M.; Włoch, I.; Tymoshenko, O.; Mlavets, Y., (2022). The hybrid mathematical model for the evaluation and selection of iron ore raw materials in the context of the European Green Deal. Acta Montan. Slovaca, 27, 569–580.
[27] ZeroWaste International Alliance. Available online: https://zwia.org
[28] Cole, C.; Osmani, M.; Quddus, M.; Wheatley, A.; Kay, K., (2014) Towards a ZeroWaste Strategy for an English Local Authority. Resour.Conserv. Recycl. 89, 64–75.
[29] Bruno, M.; Abis, M.; Kuchta, K.; Simon, F.G.; Grönholm, R.; Hoppe, M.; Fiore, S., (2021). Material flow, economic and environmental assessment of municipal solid waste incineration bottom ash recycling potential in Europe. J. Clean. Prod. 317, 128511.
[30]https://www.europarl.europa.eu/topics/en/article/20151201STO05603/circular-economy definition-importance-and-benefits
[31]https://environment.ec.europa.eu/topics/waste-and-recycling/waste-framework-directive_en
[32] Legislative Decree n. 36 of January 13, 2003. Implementation of Directive 1999/31/EC on the landfill of waste. Available online: file:///C:/Download/Firefox%20Download/DLGS%2036_2003-1.pdf
[33] Holzlöhner, U., Meggyes, T., & Seeger, S. (1999). Landfill technology in Germany. *Land Contamination & Reclamation*, *7*(2), 109-119.
[34]Available online: https://www.isprambiente.gov.it/it/attivita/formeducambiente/stage-e-tirocini/ricerca-stage/raccomandazioni-tecniche-per-la-progettazione thesis of D. Di Bartolo, (2007), Raccomandazioni tecniche per la progettazione geotecnica e strutturale delle discariche
[35] Osazee, I. T. (2021). Landfill in a sustainable waste disposal. *European Journal of Environment and Earth Sciences*, *2*(4), 67-74
[36] Wysocka, M. E. (2015). Influence of location of landfills on groundwater quality. Rocznik Ochrony Środowiska, 17, 1074-1093. (in Polish).
[37] Wysocka, M. E. (2018). Contamination of land under an unsealed municipal municipal waste landfill. Scientific Review of Environmental Engineering and Management, 27(2), 132-141. (in Polish).
[38] Laner, D., Crest, M., Scharff, H., Morris, J. W., & Barlaz, M. A. (2012). A review of approaches for the long-term management of municipal solid waste landfills. *Waste management*, *32*(3), 498-512.

[39] Obwieszczenie Ministra Klimatu i Środowiska z dnia 6 sierpnia (2022) r. w sprawie ogłoszenia jednolitego tekstu rozporządzenia Ministra Środowiska w sprawie składowisk odpadów. (Dz. U. z 2022 r., poz. 1902). https://isap.sejm.gov.pl/isap.nsf/DocDetails. xsp?id=WDU20220001902 (in Polish).
[40] Wysocka, M. (2023). Location of waste landfills in the aspect of hydrogeological conditions. *Economics and Environment*, *87*(4), 729-18.
[41] Available online: https://www.ambientesicurezzaweb.it/discariche-il-nuovo-decreto-cambia-la-disciplina-di-settore/
[42] Alzahrani, S. K. (2017). *Effect of time on soil-geomembrane interface shear strength* (Master's thesis, University of Dayton)
[43] Abdel-Shafy, H. I., Ibrahim, A. M., Al-Sulaiman, A. M., & Okasha, R. A. (2023). Landfill leachate: Sources, nature, organic composition, and treatment: An environmental overview. *Ain Shams Engineering Journal*, 102293.
[44] Tang, Y. Y., Tang, K. H. D., Maharjan, A. K., Aziz, A. A., & Bunrith, S. (2021). Malaysia moving towards a sustainability municipal waste management. *Industrial and Domestic Waste Management*, *1*(1), 26-40.
[45] Karthikeyan, O. P., & Joseph, K. (2006). Bioreactor landfills for sustainable solid waste management. *Kavazanjian Jr, E., Matasovic, N., & Stokoe, KH (1996). II, and Bray, JD (1996). Insitu shear wave velocity of solid waste from surface wave measurements. Environmental Geotechnics, Edited by M. Kamon, AA Balkema, Rotterdam, the Netherlands*, *1*, 97-102.
[46] Vaidya, R. D. (2002). *Solid waste degradation, compaction and water holding capacity* (Doctoral dissertation, Virginia Tech).
[47] Decreto legislativo 13 gennaio 2003, n. 36 Attuazione della direttiva 1999/31/CE relativa alle discariche di rifiuti (G.U. n. 59 del 12 marzo 2003). https://www.bosettiegatti.eu/info/norme/statali/2003_0036.htm
[48] Jensen, D. L., Ledin, A., and Christensen, T. H. (1999). Speciation of heavy metals in landfill-leachate polluted groundwater. *Water Research* 33, 2642–2650.
[49] Park, J. Y., and Batchelor, B. (2002). A multi-component numerical leach model coupled with a general chemical speciation code. *Water Research* 36, 156–166.
[50] Moraes, P. B., and Bertazzoli, R. (2005). Electrodegradation of landfill leachate in a flow electrochemical reactor. *Chemosphere* 58, 41–46.

[51] Gajski, G., Oreˇsˇcanin, V., and Garaj-Vrhovac, V. (2012). Chemical composition and genotoxicity assessment of sanitary landfill leachate from Rovinj, Croatia. *Ecotoxicology and Environmental Safety* 78, 253–259.
[52] Foo, K. Y., and Hameed, B. H. (2009). An overview of landfill leachate treatment via activated carbon adsorption process. *Journal of Hazardous Materials* 171, 54–60.
[53] Harmsen, K. (1983). Theories of cation adsorption by soil constitutes: discrete-site models. In G. H. Bolt (Ed.), *Soil chemistry, B, physico-chemical models* (pp.77–139). Amsterdam: Elsevier.
[54] Stegman, R., and Ehrisg, H. J. (1989). Leachate production and quality: Results of landfill processes and operation. In *International Landfill Symposium* (October 9–13, 1989), Cagliari, Italy.
[55] Baig, S., Coulomb, I., Courant, P., and Liechti, P. (1999). Treatment of landfill leachates: Lapeyrouse and Satrod case studies. *Ozone: Science & Engineering* 21, 1–22.
[56] Christensen, T. H., Kjeldsen, P., Bjerg, P. L., Jensen, D. L., Christensen, J. B., Baun, A., Albrechtsen, H.-J., and Heron, G. (2001). Biogeochemistry of landfill leachate plumes. *Applied Geochemistry* 16, 659–718.
[57] El-Fadel, M., Bou-Zeid, E., Chahine, W., and Alayli, B. (2002). Temporal variation of leachate quality from pre-sorted and baled MSW with high organic and moisture content. *Waste Management* 22, 269–282.
[58] Nanny, M. A., and Ratasuk, N. (2002). Characterization and comparison of hydrophobic neutral and hydrophobic acid dissolved organic carbon isolated from three municipal landfill leachates. *Water Research* 36, 1572–1584.
[59] Rapti-Caputo, D., and Vaccaro, C. (2006). Geochemical evidences of landfill leachate in groundwater. *Engineering Geology* 85, 111–121.
[60] Kulikowska, D., and Klimiuk, E. (2008). The effect of landfill age on municipal leachate composition. *Bioresource Technology* 99, 5891–5895.
[61] Luo, H., Zeng, Y., Cheng, Y., He, D., & Pan, X. (2020). Recent advances in municipal landfill leachate: A review focusing on its characteristics, treatment, and toxicity assessment. *Science of the Total Environment*, *703*, 135468.
[62] Qasim, R., Burchinal, J.C., (1970). Leaching from simulated landfills". J. Water Pollut. Control Fed. 42 (3), 371–379.
[63] Andreottola, G., & Cannas, P. (1992). Chemical and biological characteristics of landfill leachate. *Landfilling of waste: leachate.*, 65-88.

[64] Zaher K, Hammam G (2014) Correlation between biochemical oxygen demand and chemical oxygen demand for various wastewater treatment plants in Egypt to obtain the biodegradability indices. Int J Sci Basic Appl Res IJSBAR 13(1):42–48
[65] Aguilar-Torrejón, J. A., Balderas-Hernández, P., Roa-Morales, G., Barrera-Díaz, C. E., Rodríguez-Torres, I., & Torres-Blancas, T. (2023). Relationship, importance, and development of analytical techniques: COD, BOD, and, TOC in water—An overview through time. *SN Applied Sciences*, *5*(4), 118.
[66] Dedkov Y, Elizarova O, Kel´ina S (2000) Dicromate method for the determination of chemical oxygen demand. J Anal Chem 55(8):777–781
[67] Hu, Z., Grasso, D., 2005. WATER ANALYSIS | chemical oxygen demand. In: Encyclopedian of Analytical Science. Elsevier, pp. 325–330.
[68] International Standard ISO 5815. (1983) Water quality determination of biochemical oxygen demand after n day (BODn) Dilution and seeding method.
[69] Geerdink R, van den Hurk R, Epema O (2017) Chemical Oxygen Demand: Historical perspectives and future challenges. Anal Chim Acta 961:1–11
[70] Li S, Zheng F, Cai S, Liang W, Li Y (2013) A visible light assisted photocatalytic system for determination of chemical oxygen demand using 5-sulfosalicylic acid in situ surface modified titanium dioxide. Sens Actuators B Chem 188:280–285
[71] Li J, Luo G, He L, Xu J, Lyu J (2018) Analytical approaches for determining chemical oxygen demand in water bodies: a review. Crit Rev Anal Chem 48(1):47–65
[72] Ma J (2017) Determination of chemical oxygen demand in aqueous samples with non-electrochemical methods. Trends Environ Anal Chem 14:37–43
[73] Le G, Yang H, Yu X (2018) Improved UV/O3 method for measuring the chemical oxygen demand. Water Sci Technol 77(5):1271–1279
[74] Moreira F, Boaventura R, Brillas E, Vilar V (2017) Electrochemical advanced oxidation processes: a review on their application to synthetic and real wastewaters. Appl Catal B 202:217–261
[75] Bridgeman J, Baker J, Carliell-Marquet C, Carstea E (2013) Determination of changes in wastewater quality through a treatment works using fluorescence spectroscopy. Environ Technol 34(23):3069–3077
[76] Li C, Song G (2009) Photocatalytic degradation of organic pollutants and detection of chemical oxygen demand by fluorescence methods. Sens Actuators B Chem 137(2):432–436

[77] Nurdin M, Zaeni A, Rammang E, Maulidiyah M, Wibowo D (2017) Reactor design development of chemical oxygen demand flow system and its application. Anal Bioanal Electrochem 9(3):480–494
[78] Si H, Pan N, Zhang X, Liao J, Rumyantseva M, Gaskov A, Lin S (2019) A real-time on-line photoelectrochemical sensor toward chemical oxygen demand determination based on field-effect transitor using an extended gate with 3D TiO2
nanotubes arrays. Sens Actuators B Chem 289:106–113
[79] Wang X, Zhang S, Wang H, Yu H, Wang H, Zhang S, Peng F (2015) Visible light photoelectrochemical properties of hydrogenated TiO2 nanorod film and its application in the detection of chemical oxygen demand. RSC Adv 5(93):76315–76320
[80] Wibowo D, Ruslan M, Nurdin M (2017) Determination of COD based on photoelectrocatalysis of FeTiO3.
TiO2/Ti electrode. In: IOP conference series: materials science and engineering. Surabaya, East Java: Institute of Physics Publishing.
[81] Yao N, Liu Z, Chen Y, Zhou Y, Xie B (2015) A novel thermal sensor for the sensitive measurement of chemical oxygen demand. Sensors 15(8):20501–20510
[82] Yao N, Wang J, Zhou Y (2014) Rapid determination of the chemical oxygen demand of water using a thermal biosensor. Sensors 14(6):9949–9960
[83] Nagel B, Dellweg H, Gierasch L (1992) Glossary for chemists of terms used in biotechnology (IUPAC recommendations 1992). Pure Appl Chem 64(1):143–168
[84] Jouanneau, S., Recoules, L., Durand, M. J., Boukabache, A., Picot, V., Primault, Y., ... & Thouand, G. (2014). Methods for assessing biochemical oxygen demand (BOD): A review. Water research, 49, 62-82
[85] Great Britain, 1908. Royal Commission on Sewage Disposal. Cornell University Library. ed. Final report of the commissioners appointed to inquire and report what methods of treating and disposing of sewage (including any liquid from any factory or manufacturing process) may properly be adopted. General summary of conclusions and recommendations.
[86] Chang IS, Jang JK, Gil GC, Kim M, Kim HJ, Cho BW, Kim BH (2004) Continuous determination of biochemical oxygen
demand using microbial fuel cell type biosensor. Biosens Bioelectron 19(6):607–613

[87] Jouanneau S, Recoules L, Durand M, Boukabache A, Picot V, Primault Y, Thouand G (2014) Methods for assessing biochemical oxygen demand (BOD): a review. Water Res 49:62–82
[88] Kim B, Chang I, Gil G, Park H (2003) Novel BOD (biological oxygen demand) sensor using mediator-less microbial fuel cell. Biotech Lett 25(7):541–545
[89] Pasco N, Baronian K, Jeffries K, Hay J (2000) Biochemical mediator demand–a novel rapid alternative for measuring biochemical oxygen demand. Appl Microbiol Biotechnol 53(5):613–618
[90] Costa SP, Cunha E, Azevedo AM, Pereira SA, Neves AF, Vilaranda AG, Saraiva ML (2018) Microfluidic chemiluminescence system with yeast *Saccharomyces cerevisiae* for rapid biochemical oxygen demand measurement. ACS Sustain Chem Eng 6(5):6094–6101
[91] Carstea E, Bridgeman J, Baker A, Reynolds D (2016) Fluorescence spectroscopy for wastewater monitoring: a review.
Water Res 95:205–219
[92] Recoules L, Jouanneau S, Thouand G, Gue AM, Boukabache A (2019) Towards a miniaturized device to evaluate the BOD parameter of wastwater. Int J Environ Sci Develop 10(6):178–182
[93] Federation WE, Association APH (2005) Standard methods for the examination of water and wastewater. American Public Health Association (APHA), Washington
[94] Dubber D, Gray N (2010) Replacement of Chemical Oxygen Demand (COD) with Total Organic Carbon (TOC) for monitoring wastewater treatment performance to minimize disposal of toxic analytical waste. J Environ Sci Health Part A 45:1595–1600
[95] Boyles, W. (1997). Chemical oxygen demand. *Technical information series, Booklet,(9)*, *24*.
[96] Lou, Z. Y., Zhao, Y. C., Yuan, T., Song, Y., Chen, H. L., and Zhu, N. W. (2009). Natural attenuation and characterization of contaminants composition in landfill leachate under different disposing ages. *Science of the Total Environment* 407, 3385–3391.
[97] Renou, S., Givaudan, J.G., Poulain, S., Dirassouyan, F. and Moulin, P. (2008) Landfill Leachate Treatment: Review and Opportunity. Journal of Hazardous Materials, 150, 468-493.

[98] Gomez, M., Corona, F., & Hidalgo, M. D. (2019). Variations in the properties of leachate according to landfill age. *Desalination and Water Treatment*, *159*, 24-31.
[99] Contemporary Environmental Issues of Landfill Leachate: Assessment and Remedies - Scientific Figure on ResearchGate. Available from: https://www.researchgate.net/figure/Physicochemical-parameters-of-leachate-of-different-age_tbl1_275523716]
[100] Wang, K., Li, L., Tan, F., & Wu, D. (2018). Treatment of landfill leachate using activated sludge technology: A review. *Archaea*, *2018*
[101] Calace, N., Liberatori, A., Petronio, B. M., and Pietroletti, M. (2001). Characteristics of different molecular weight fractions of organic matter in landfill leachate and their role in soil sorption of heavy metals. *Environmental Pollution* 113,331–339.
[102] https://www.amapspa.it/wp-content/uploads/2020/07/DS-02-RELAZIONE-CALCOLI-IDRAULICI.pdf
[103] Commission Implementing Decision (EU) 2018/1147 of 10 August 2018 establishing best available techniques (BAT) conclusions for waste treatment, under Directive 2010/75/EU of the European Parliament and of the Council (notified under document C(2018) 5070) (Text with EEA relevance. http://data.europa.eu/eli/dec_impl/2018/1147/oj
[104] http://www.edizionieuropee.it/law/html/6/Zn1_04_019_all5.pdf
[105] Fernandes, A., Pacheco, M. J., Ciríaco, L., & Lopes, A. J. A. C. B. E. (2015). Review on the electrochemical processes for the treatment of sanitary landfill leachates: present and future. *Applied Catalysis B: Environmental*, *176*, 183-200.
[106] Boonyaroj, V., Chiemchaisri, C., Chiemchaisri, W., & Yamamoto, K. (2017). Enhanced biodegradation of phenolic compounds in landfill leachate by enriched nitrifying membrane bioreactor sludge. *Journal of hazardous materials*, *323*, 311-318.
[107] Ahmed, F. N., & Lan, C. Q. (2012). Treatment of landfill leachate using membrane bioreactors: A review. *Desalination*, *287*, 41-54.
[108] Jafary, T., Daud, W. R. W., Aljlil, S. A., Ismail, A. F., Al-Mamun, A., Baawain, M. S., & Ghasemi, M. (2018). Simultaneous organics, sulphate and salt removal in a microbial desalination cell with an insight into microbial communities. *Desalination*, *445*, 204-212.
[109] Jamil, F., Ala'a, H., Naushad, M., Baawain, M., Al-Mamun, A., Saxena, S. K., & Viswanadham, N. (2020). Evaluation of synthesized green carbon catalyst from

waste date pits for tertiary butylation of phenol. *Arabian journal of chemistry*, *13*(1), 298-307
[110] Umar, M., Aziz, H. A., & Yusoff, M. S. (2010). Trends in the use of Fenton, electro-Fenton and photo-Fenton for the treatment of landfill leachate. *Waste management*, *30*(11), 2113-2121.
[111] Jafary, T., Al-Mamun, A., Alhimali, H., Baawain, M. S., Rahman, M. S., Rahman, S., ... & Tabatabaei, M. (2020). Enhanced power generation and desalination rate in a novel quadruple microbial desalination cell with a single desalination chamber. *Renewable and Sustainable Energy Reviews*, *127*, 109855.
[112] Rahman, S., Jafary, T., Al-Mamun, A., Baawain, M. S., Choudhury, M. R., Alhaimali, H., ... & Tabatabaei, M. (2021). Towards upscaling microbial desalination cell technology: a comprehensive review on current challenges and future prospects. *Journal of Cleaner Production*, *288*, 125597.
[113] Wiszniowski, J., Robert, D., Surmacz-Gorska, J., Miksch, K., & Weber, J. V. (2006). Landfill leachate treatment methods: A review. *Environmental chemistry letters*, *4*, 51-61.
[114] Li, W., Zhou, Q., & Hua, T. (2010). Removal of organic matter from landfill leachate by advanced oxidation processes: a review. *International Journal of Chemical Engineering*, *2010*(1), 270532.
[115] Mandal, P., Dubey, B. K., & Gupta, A. K. (2017). Review on landfill leachate treatment by electrochemical oxidation: Drawbacks, challenges and future scope. Waste Management, 69, 250-273.
[116] Siddiqi, S. A., Al-Mamun, A., Baawain, M. S., & Sana, A. (2022). A critical review of the recently developed laboratory-scale municipal solid waste landfill leachate treatment technologies. *Sustainable Energy Technologies and Assessments*, *52*, 102011.
[117] Mehmood, M.K., Adetutu, E., Nedwell, D.B. and Ball, A.S. (2009) In Situ Microbial Treatment of Landfill Leachate Using Aerated Lagoons. Bioresource Technology, 100, 2741-2744. https://doi.org/10.1016/j.biortech.2008.11.031
[118] Sawaittayothin, V., & Polprasert, C. (2007). Nitrogen mass balance and microbial analysis of constructed wetlands treating municipal landfill leachate. *Bioresource technology*, *98*(3), 565-570.
[119] Schmidt, T., Harris, P., Lee, S., & McCabe, B. K. (2019). Investigating the impact of seasonal temperature variation on biogas production from covered anaerobic lagoons treating slaughterhouse wastewater using lab scale studies. *Journal of Environmental Chemical Engineering*, *7*(3), 103077.

[120] Singh, M., & Srivastava, R. K. (2011). Sequencing batch reactor technology for biological wastewater treatment: a review. *Asia-pacific journal of chemical engineering*, *6*(1), 3-13.
[121] Kennedy, K. J., & Lentz, E. M. (2000). Treatment of landfill leachate using sequencing batch and continuous flow upflow anaerobic sludge blanket (UASB) reactors. *Water Research*, *34*(14), 3640-3656.
[122] Dutta, A., & Sarkar, S. (2015). Sequencing batch reactor for wastewater treatment: recent advances. *Current Pollution Reports*, *1*, 177-190..
[123] Aluko, O. O., & Sridhar, M. K. (2013). Evaluation of leachate treatment by trickling filter and sequencing batch reactor processes in Ibadan, Nigeria. *Waste management & research*, *31*(7), 700-705.
[124] Yan, J., & Hu, Y. Y. (2009). Comparison of partial nitrification to nitrite for ammonium-rich organic wastewater in sequencing batch reactors and continuous stirred-tank reactor at laboratory-scale. *Water Science and Technology*, *60*(11), 2861-2868.
[125] Yong, Z. J., Bashir, M. J., Ng, C. A., Sethupathi, S., & Lim, J. W. (2018). A sequential treatment of intermediate tropical landfill leachate using a sequencing batch reactor (SBR) and coagulation. *Journal of environmental management*, *205*, 244-252.
[126] Aziz, S. Q., Aziz, H. A., & Yusoff, M. S. (2011). Powdered activated carbon augmented double react-settle sequencing batch reactor process for treatment of landfill leachate. *Desalination*, *277*(1-3), 313-320.
[127] Kurniawan, T. A., Lo, W., Chan, G., & Sillanpää, M. E. (2010). Biological processes for treatment of landfill leachate. *Journal of Environmental Monitoring*, *12*(11), 2032-2047.
[128] H. Yan, I.T. Cousins, C. Zhang, Q. Zhou, Perfluoroalkyl acids in municipal landfill leachates from China: occurrence, fate during leachate treatment and potential impact on groundwater, Sci. Total Environ. 524 (2015) 23–31.
[129] Castillo, E., Vergara, M., & Moreno, Y. (2007). Landfill leachate treatment using a rotating biological contactor and an upward-flow anaerobic sludge bed reactor. *Waste management*, *27*(5), 720-726.
[130] Patwardhan, A. W. (2003). Rotating biological contactors: a review. *Industrial & engineering chemistry research*, *42*(10), 2035-2051.
[131] Hippen, A., Helmer, C., Kunst, S., Rosenwinkel, K. H., & Seyfried, C. F. (2001). Six years' practical experience with aerobic/anoxic deammonification in biofilm systems. *Water science and technology*, *44*(2-3), 39-48.

[132] Kulikowska, D., Jóźwiak, T., Kuczajowska-Zadrożna, M., Pokój, T., & Gusiatin, Z. (2011). Efficiency of nitrification and organics removal from municipal landfill leachate in the rotating biological contactor (RBC). *Desalination and Water Treatment*, *33*(1-3), 125-131.
[133] Henderson, J. P., Besler, D. A., Atwater, J. A., & Mavinic, D. S. (1997). Treatment of methanogenic landfill leachate to remove ammonia using a rotating biological contactor (RBC) and a sequencing batch reactor (SBR). *Environmental technology*, *18*(7), 687-698.
[134] Hashisho, J., & El-Fadel, M. (2016). Membrane bioreactor technology for leachate treatment at solid waste landfills. *Reviews in Environmental Science and Bio/Technology*, *15*, 441-463.
[135] Nath, A., & Debnath, A. (2022). A short review on landfill leachate treatment technologies. Materials Today: Proceedings, 67, 1290-1297
[136] Hashisho, J., El-Fadel, M., Al-Hindi, M., Salam, D., & Alameddine, I. (2016). Hollow fiber vs. flat sheet MBR for the treatment of high strength stabilized landfill leachate. *Waste management*, *55*, 249-256.
[137] Xue, Y., Zhao, H., Ge, L., Chen, Z., Dang, Y., & Sun, D. (2015). Comparison of the performance of waste leachate treatment in submerged and recirculated membrane bioreactors. *International Biodeterioration & Biodegradation*, *102*, 73-80.
[138] Rizkallah, M., El-Fadel, M., Saikaly, P. E., Ayoub, G. M., Darwiche, N., & Hashisho, J. (2013). Hollow-fiber membrane bioreactor for the treatment of high-strength landfill leachate. *Waste management & research*, *31*(10), 1041-1051.
[139] Amaral, M. C., Moravia, W. G., Lange, L. C., Zico, M. R., Magalhães, N. C., Ricci, B. C., & Reis, B. G. (2016). Pilot aerobic membrane bioreactor and nanofiltration for municipal landfill leachate treatment. *Journal of Environmental Science and Health, Part A*, *51*(8), 640-649.
[140] Mondal, B., & Warith, M. A. (2008). Use of shredded tire chips and tire crumbs as packing media in trickling filter systems for landfill leachate treatment. *Environmental technology*, *29*(8), 827-836.
[141] Torretta, V., Ferronato, N., Katsoyiannis, I. A., Tolkou, A. K., & Airoldi, M. (2016). Novel and conventional technologies for landfill leachates treatment: A review. *Sustainability*, *9*(1), 9.
[142] Chelliapan, S., Arumugam, N., Din, M. F. M., Kamyab, H., & Ebrahimi, S. S. (2020). Anaerobic treatment of municipal solid waste landfill leachate. In *Bioreactors* (pp. 175-193). Elsevier.

[143] Kheradmand, S., Karimi-Jashni, A., & Sartaj, M. (2010). Treatment of municipal landfill leachate using a combined anaerobic digester and activated sludge system. *Waste management*, *30*(6), 1025-1031.
[144] Hombach, S. T., Oleszkiewicz, J. A., Lagasse, P., Amy, L. B., Zaleski, A. A., & Smyrski, K. (2003). Impact of landfill leachate on anaerobic digestion of sewage sludge. *Environmental technology*, *24*(5), 553-560.
[145] Berenjkar, P., Islam, M., & Yuan, Q. (2019). Co-treatment of sewage sludge and mature landfill leachate by anaerobic digestion. *International Journal of Environmental Science and Technology*, *16*, 2465-2474.
[146] Singh A, Saini J, Lohchab R. (2016) Landfill Leachate Treatment by Upflow Anaerobic Sludge Blanket Reactor.
[147] Müller, G. T., Giacobbo, A., dos Santos Chiaramonte, E. A., Rodrigues, M. A. S., Meneguzzi, A., & Bernardes, A. M. (2015). The effect of sanitary landfill leachate aging on the biological treatment and assessment of photoelectrooxidation as a pre-treatment process. *Waste management*, *36*, 177-183.
[148] Mainardis, M., Buttazzoni, M., & Goi, D. (2020). Up-flow anaerobic sludge blanket (UASB) technology for energy recovery: a review on state-of-the-art and recent technological advances. *Bioengineering*, *7*(2), 43.
[149] Inanc, B., Calli, B. A. R. I. Ş., & Saatci, A. (2000). Characterization and anaerobic treatment of the sanitary landfill leachate in Istanbul. *Water Science and Technology*, *41*(3), 223-230.
[150] Kaetzl, K., Lübken, M., Gehring, T., & Wichern, M. (2018). Efficient low-cost anaerobic treatment of wastewater using biochar and woodchip filters. *Water*, *10*(7), 818.
[151] Wu, Y. C., Hao, O. J., Ou, K. C., & Scholze, R. J. (1988). Treatment of leachate from a solid waste landfill site using a two-stage anaerobic filter. *Biotechnology and bioengineering*, *31*(3), 257-266.
[152] Naveen, B. P., Mahapatra, D. M., Sitharam, T. G., Sivapullaiah, P. V., & Ramachandra, T. V. (2017). Physico-chemical and biological characterization of urban municipal landfill leachate. *Environmental Pollution*, *220*, 1-12.
[153] Mojiri, A., Aziz, H. A., & Aziz, S. Q. (2013). Trends in physical-chemical methods for landfill leachate treatment. *International journal of scientific research in environmental sciences*, *1*(2), 16-25
[154] E. Baruth, American Water Works Association, 'Water treatment plant design', New York: McGraw- Hill, 2005, ISBN: 0071418725.

[155] Costa, A. M., Alfaia, R. G. D. S. M., & Campos, J. C. (2019). Landfill leachate treatment in Brazil–An overview. *Journal of environmental management*, *232*, 110-116.
[156] Tejera, J., Miranda, R., Hermosilla, D., Urra, I., Negro, C., & Blanco, Á. (2019). Treatment of a mature landfill leachate: comparison between homogeneous and heterogeneous photo-Fenton with different pretreatments. *Water*, *11*(9), 1849.
[157] Silva AC, Dezotti M, Sant'Anna GL (2004). Treatment and detoxification of a sanitary landfill leachate. Chemosphere, 55: 207–214.
[158] Verma, M., & Kumar, R. N. (2016). Can coagulation–flocculation be an effective pre-treatment option for landfill leachate and municipal wastewater co-treatment?. *Perspectives in Science*, *8*, 492-494.
[159] Reshadi, M. A. M., Bazargan, A., & McKay, G. (2020). A review of the application of adsorbents for landfill leachate treatment: Focus on magnetic adsorption. *Science of the total environment*, *731*, 138863.
[160] Kurniawan, T. A., Lo, W. H., & Chan, G. Y. (2006). Physico-chemical treatments for removal of recalcitrant contaminants from landfill leachate. *Journal of hazardous materials*, *129*(1-3), 80-100.
[161] Arif, M., Liu, G., Yousaf, B., Ahmed, R., Irshad, S., Ashraf, A., ... & Rashid, M. S. (2021). Synthesis, characteristics and mechanistic insight into the clays and clay minerals-biochar surface interactions for contaminants removal-A review. *Journal of Cleaner Production*, *310*, 127548.
[162] Zhang, Z. H., Zhu, H. J., Zhou, C. H., & Wang, H. (2016). Geopolymer from kaolin in China: An overview. *Applied Clay Science*, *119*, 31-41.
[163] Erabee, I. K., Ahsan, A., Jose, B., Aziz, M. M. A., Ng, A. W. M., Idrus, S., & Daud, N. N. N. (2018). Adsorptive treatment of landfill leachate using activated carbon modified with three different methods. *KSCE Journal of Civil Engineering*, *22*, 1083-1095.
[164] Foo, K. Y., Lee, L. K., & Hameed, B. H. (2013). Preparation of activated carbon from sugarcane bagasse by microwave assisted activation for the remediation of semi-aerobic landfill leachate. *Bioresource technology*, *134*, 166-172.
[165] Papastavrou, C., Mantzavinos, D., & Diamadopoulos, E. (2009). A comparative treatment of stabilized landfill leachate: Coagulation and activated carbon adsorption vs. electrochemical oxidation. *Environmental technology*, *30*(14), 1547-1553.

[166] Cheng, Y., Huang, T., Shi, X., Wen, G., & Sun, Y. (2017). Removal of ammonium ion from water by Na-rich birnessite: performance and mechanisms. *Journal of Environmental Sciences*, *57*, 402-410.
[167] Ozturk, I., Altinbas, M., Koyuncu, I., Arikan, O., & Gomec-Yangin, C. (2003). Advanced physico-chemical treatment experiences on young municipal landfill leachates. *Waste management*, *23*(5), 441-446.
[168] Çeçen, F., & Gürsoy, G. (2000). Characterization of landfill leachates and studies on heavy metal removal. *Journal of Environmental Monitoring*, *2*(5), 436-442.
[169] Kabdaslı, I., Tünay, O., Öztürk, I., Yılmaz, S., & Arıkan, O. (2000). Ammonia removal from young landfill leachate by magnesium ammonium phosphate precipitation and air stripping. *Water science and technology*, *41*(1), 237-240.
[170] Tengrui, L., Al-Harbawi, A. F., Qiang, H., & Jun, Z. (2007). Comparison between biological treatment and chemical precipitation for nitrogen removal from old landfill leachate. *American Journal of Environmental Sciences*, *3*(4), 183-187.
[171] Li, X. Z., Zhao, Q. L., & Hao, X. D. (1999). Ammonium removal from landfill leachate by chemical precipitation. *Waste management*, *19*(6), 409-415.
[172] Li, X. Z., & Zhao, Q. L. (2001). Efficiency of biological treatment affected by high strength of ammonium-nitrogen in leachate and chemical precipitation of ammonium-nitrogen as pretreatment. *Chemosphere*, *44*(1), 37-43.
[173] Lee, S. D., Mallampati, S. R., & Lee, B. H. (2017). Hybrid zero valent iron (ZVI)/H2O2 oxidation process for landfill leachate treatment with novel nanosize metallic calcium/iron composite. *Journal of the Air & Waste Management Association*, *67*(4), 475-487.
[174] Visvanathan, C., Aim, R. B., & Parameshwaran, K. (2000). Membrane separation bioreactors for wastewater treatment. *Critical reviews in environmental science and technology*, *30*(1), 1-48.
[175] Calli, B., Mertoglu, B., & Inanc, B. (2005). Landfill leachate management in Istanbul: applications and alternatives. *Chemosphere*, *59*(6), 819-829.
[176] Anqi, T., Zhang, Z., Suhua, H., & Xia, L. (2020, September). Review on landfill leachate treatment methods. In *IOP Conference Series: Earth and Environmental Science* (Vol. 565, No. 1, p. 012038). IOP Publishing.
[177] Peng, Y. (2017). Perspectives on technology for landfill leachate treatment. *Arabian Journal of Chemistry*, *10*, S2567-S2574.

[178] Piatkiewicz, W., Biemacka, E., & Suchecka, T. (2001). A polish study: treating landfill leachate with membranes. *Filtration & separation*, *38*(6), 22-26.
[179] Bohdziewicz, J., Bodzek, M., & Górska, J. (2001). Application of pressure-driven membrane techniques to biological treatment of landfill leachate. *Process Biochemistry*, *36*(7), 641-646.
[180] Syzdek, A. C., & Ahlert, R. C. (1984). Separation of landfill leachate with polymeric ultrafiltration membranes. *Journal of Hazardous materials*, *9*(2), 209-220.
[181] Tabet, K., Moulin, P., Vilomet, J. D., Amberto, A., & Charbit, F. (2002). Purification of landfill leachate with membrane processes: preliminary studies for an industrial plant. *Separation Science and Technology*, *37*(5), 1041-1063.
[182] Kulikowska, D., Zielińska, M., & Konopka, K. (2019). Treatment of stabilized landfill leachate in an integrated adsorption–fine-ultrafiltration system. *International Journal of Environmental Science and Technology*, *16*, 423-430.
[183] Urase, T., Salequzzaman, M., Kobayashi, S., Matsuo, T., Yamamoto, K., & Suzuki, N. (1997). Effect of high concentration of organic and inorganic matters in landfill leachate on the treatment of heavy metals in very low concentration level. *Water science and technology*, *36*(12), 349-356.
[184] Linde, K., & Jönsson, A. S. (1995). Nanofiltration of salt solutions and landfill leachate. *Desalination*, *103*(3), 223-232.
[185] Hasar, H., Unsal, S. A., Ipek, U., Karatas, S., Cınar, O., Yaman, C., & Kınacı, C. (2009). Stripping/flocculation/membrane bioreactor/reverse osmosis treatment of municipal landfill leachate. *Journal of Hazardous Materials*, *171*(1-3), 309-317.
[186] Abdel-Shafy HI, Hegemann W, Guindi KA, Tawfik NS, Teschner K. (2005). Membrane Bioreactor for the Treatment of Wastewater in an Egyptian Plant. Central European J of Occupational & Environ Medicine. 11(33):217–23.
[187] Ushikoshi, K., Kobayashi, T., Uematsu, K., Toji, A., Kojima, D., & Matsumoto, K. (2002). Leachate treatment by the reverse osmosis system. *Desalination*, *150*(2), 121-129.
[188] Choo, K. H., & Lee, C. H. (1996). Membrane fouling mechanisms in the membrane-coupled anaerobic bioreactor. *Water research*, *30*(8), 1771-1780.
[189] Madaeni, S. S., & Mansourpanah, Y. C. O. D. (2003). COD removal from concentrated wastewater using membranes. *Filtration & separation*, *40*(6), 40-46.
[190] Alvarez-Vazquez, H., Jefferson, B., & Judd, S. J. (2004). Membrane bioreactors vs conventional biological treatment of landfill leachate: a brief

review. *Journal of Chemical Technology & Biotechnology: International Research in Process, Environmental & Clean Technology*, *79*(10), 1043-1049.
[191] https://www.sepa.org.uk/media/61145/ippc-s503-guidance-for-the-treatment-of-landfill-leachate-part-1.pdf
[192] Bashir, M. J., Aziz, H. A., Yusoff, M. S., & Adlan, M. N. (2010). Application of response surface methodology (RSM) for optimization of ammoniacal nitrogen removal from semi-aerobic landfill leachate using ion exchange resin. *Desalination*, *254*(1-3), 154-161.
[193] Wang, S., & Peng, Y. (2010). Natural zeolites as effective adsorbents in water and wastewater treatment. *Chemical engineering journal*, *156*(1), 11-24.
[194] Mojiri, A., & Branch, I. K. (2011). Review on membrane bioreactor, ion exchange and adsorption methods for landfill leachate treatment. *Aust. J. Basic Appl. Sci*, *5*(12), 1365-1370.
[195] Kasmuri, N., Sabri, S. N. M., Wahid, M. A., Rahman, Z. A., Abdullah, M. M., & Anur, M. Z. K. (2018, November). Using zeolite in the ion exchange treatment to remove ammonia-nitrogen, manganese and cadmium. In *AIP Conference Proceedings* (Vol. 2031, No. 1). AIP Publishing.
[196] Scandelai, A. P. J., Zotesso, J. P., Jegatheesan, V., Cardozo-Filho, L., & Tavares, C. R. G. (2020). Intensification of supercritical water oxidation (ScWO) process for landfill leachate treatment through ion exchange with zeolite. *Waste Management*, *101*, 259-267.
[197] Hansen, B. R., & Davies, S. R. (1994). Review of potential technologies for the removal of dissolved components from produced water. *Chemical Engineering Research and Design;(United Kingdom)*, *72*(A2).
[198] Chuang, K.T. (1993). U.S. Patent No. 5,190,668. Washington, DC: U.S. Patent and Trademark Office.
[199] Ferraz, F. M., Povinelli, J., & Vieira, E. M. (2013). Ammonia removal from landfill leachate by air stripping and absorption. *Environmental technology*, *34*(15), 2317-2326.
[200] Cheung, K. C., Chu, L. M., & Wong, M. H. (1997). Ammonia stripping as a pretreatment for landfill leachate. *Water, air, and soil pollution*, *94*, 209-221.
[201] Zhang, M., Shi, Q., Song, X., Wang, H., & Bian, Z. (2019). Recent electrochemical methods in electrochemical degradation of halogenated organics: a review. *Environmental Science and Pollution Research*, *26*, 10457-10486.

[202] Pirsaheb, M., Azizi, E., Almasi, A., Soltanian, M., Khosravi, T., Ghayebzadeh, M., et al., 2016. Evaluating the efficiency of electrochemical process in removing COD and NH4-N from landfill leachate. Desalin. Water Treat. 57, 6644–6651.
[203] Al Lawati, M. J., Jafary, T., Baawain, M. S., & Al-Mamun, A. (2019). A mini review on biofouling on air cathode of single chamber microbial fuel cell; prevention and mitigation strategies. *Biocatalysis and Agricultural Biotechnology*, *22*, 101370.
[204] Guo, Z., Zhang, Y., Jia, H., Guo, J., Meng, X., & Wang, J. (2022). Electrochemical methods for landfill leachate treatment: A review on electrocoagulation and electrooxidation. *Science of the total environment*, *806*, 150529.
[205] Deng, Y., Zhu, X., Chen, N., Feng, C., Wang, H., Kuang, P., & Hu, W. (2020). Review on electrochemical system for landfill leachate treatment: Performance, mechanism, application, shortcoming, and improvement scheme. *Science of the total environment*, *745*, 140768.
[206] Bayramoglu, M., Kobya, M., Can, O. T., & Sozbir, M. (2004). Operating cost analysis of electrocoagulation of textile dye wastewater. *Separation and Purification Technology*, *37*(2), 117-125.
[207] Deng, Y., & Englehardt, J. D. (2007). Electrochemical oxidation for landfill leachate treatment. *Waste management*, *27*(3), 380-388.
[208] Panizza, M., & Cerisola, G. (2009). Direct and mediated anodic oxidation of organic pollutants. *Chemical reviews*, *109*(12), 6541-6569.
[209] Malinovic, B. N., Djuricic, T., & Zoric, D. (2019, February). The impact of electrode material in the treatment of landfill leachate by electrocoagulation process. In *IOP Conference Series: Materials Science and Engineering* (Vol. 477, No. 1, p. 012040). IOP Publishing.
[210] Turro, E., Giannis, A., Cossu, R., Gidarakos, E., Mantzavinos, D., & Katsaounis, A. (2012). Reprint of: electrochemical oxidation of stabilized landfill leachate on DSA electrodes. *Journal of hazardous materials*, *207*, 73-78.
[211] Krishnan, S., Rawindran, H., Sinnathambi, C. M., & Lim, J. W. (2017, June). Comparison of various advanced oxidation processes used in remediation of industrial wastewater laden with recalcitrant pollutants. In *IOP Conference Series: Materials Science and Engineering* (Vol. 206, No. 1, p. 012089). IOP Publishing.
[212] Ganiyu, S. O., Martínez-Huitle, C. A., & Oturan, M. A. (2021). Electrochemical advanced oxidation processes for wastewater treatment:

Advances in formation and detection of reactive species and mechanisms. *Current Opinion in Electrochemistry*, *27*, 100678.
[213] Chin, Y. T., Bashir, M. J., Amr, S. S. A., & Alazaiza, M. Y. (2022). Factorial design and optimization of thermal activation of persulfate for stabilized leachate treatment. *Desalination and Water Treatment*, *250*, 211-220.
[214] Liotta, L. F., Gruttadauria, M., Di Carlo, G., Perrini, G., & Librando, V. (2009). Heterogeneous catalytic degradation of phenolic substrates: catalysts activity. *Journal of hazardous materials*, *162*(2-3), 588-606.
[215] Jamali, G. A., Devrajani, S. K., Memon, S. A., Qureshi, S. S., Anbuchezhiyan, G., Mubarak, N. M., ... & Siddiqui, M. T. H. (2024). Holistic insight Mechanism of ozone-based oxidation process for wastewater treatment. *Chemosphere*, 142303.
[216] Shah, M. P., Bera, S. P., & Tore, G. Y. (Eds.). (2022). *Advanced Oxidation Processes for Wastewater Treatment: An Innovative Approach*. CRC Press.
[217] Miklos, D. B., Remy, C., Jekel, M., Linden, K. G., Drewes, J. E., & Hübner, U. (2018). Evaluation of advanced oxidation processes for water and wastewater treatment–A critical review. *Water research*, *139*, 118-131.
[218] Tizaoui, C., Bouselmi, L., Mansouri, L., & Ghrabi, A. (2007). Landfill leachate treatment with ozone and ozone/hydrogen peroxide systems. *Journal of hazardous materials*, *140*(1-2), 316-324.
[219] Wang, F., Smith, D. W., & El-Din, M. G. (2003). Application of advanced oxidation methods for landfill leachate treatment–A review. *Journal of Environmental Engineering and Science*, *2*(6), 413-427.
[220] Chen, W. S., Juan, C. N., & Wei, K. M. (2007). Decomposition of dinitrotoluene isomers and 2, 4, 6-trinitrotoluene in spent acid from toluene nitration process by ozonation and photo-ozonation. *Journal of Hazardous Materials*, *147*(1-2), 97-104.
[221] Deng, Y. (2007). Physical and oxidative removal of organics during Fenton treatment of mature municipal landfill leachate. *Journal of Hazardous Materials*, *146*(1-2), 334-340.
[222] Pera-Titus, M., García-Molina, V., Baños, M. A., Giménez, J., & Esplugas, S. (2004). Degradation of chlorophenols by means of advanced oxidation processes: a general review. *Applied Catalysis B: Environmental*, *47*(4), 219-256.
[223] Venkatadri, R., & Peters, R. W. (1993). Chemical oxidation technologies: ultraviolet light/hydrogen peroxide, Fenton's reagent, and titanium dioxide-

assisted photocatalysis. *Hazardous waste and hazardous materials*, *10*(2), 107-149.
[224] Lopez, A., Pagano, M., Volpe, A., & Di Pinto, A. C. (2004). Fenton's pre-treatment of mature landfill leachate. *Chemosphere*, *54*(7), 1005-1010.
[225] Choi, H. J. (1998). *Evaluation of fenton's process for the treatment of landfill leachate*. university of Delaware.
[226] Zhang, H., Choi, H. J., & Huang, C. P. (2006). Treatment of landfill leachate by Fenton's reagent in a continuous stirred tank reactor. *Journal of Hazardous Materials*, *136*(3), 618-623.
[227] Tang, W. Z. (2003). *Physicochemical treatment of hazardous wastes*. CRC Press.
[228] Sun, J. H., Sun, S. P., Wang, G. L., & Qiao, L. P. (2007). Degradation of azo dye Amido black 10B in aqueous solution by Fenton oxidation process. *Dyes and pigments*, *74*(3), 647-652.
[229] Kim, J. S., Kim, H. Y., Won, C. H., & Kim, J. G. (2001). Treatment of leachate produced in stabilized landfills by coagulation and Fenton oxidation process. *Journal of the Chinese Institute of Chemical Engineers*, *32*(5), 425-429.
[230] Lindsey, M. E., & Tarr, M. A. (2000). Quantitation of hydroxyl radical during Fenton oxidation following a single addition of iron and peroxide. *Chemosphere*, *41*(3), 409-417.
[231] Pignatello, J. J., Liu, D., & Huston, P. (1999). Evidence for an additional oxidant in the photoassisted Fenton reaction. *Environmental Science & Technology*, *33*(11), 1832-1839.
[232] Kiwi, J., Lopez, A., & Nadtochenko, V. (2000). Mechanism and kinetics of the OH-radical intervention during Fenton oxidation in the presence of a significant amount of radical scavenger (Cl-). *Environmental Science & Technology*, *34*(11), 2162-2168.
[233] Zhang, H., Choi, H. J., & Huang, C. P. (2005). Optimization of Fenton process for the treatment of landfill leachate. *Journal of hazardous materials*, *125*(1-3), 166-174.
[234] Szpyrkowicz, L., Juzzolino, C., & Kaul, S. N. (2001). A comparative study on oxidation of disperse dyes by electrochemical process, ozone, hypochlorite and Fenton reagent. *Water research*, *35*(9), 2129-2136.
[235] Hussain, S., Aneggi, E., Trovarelli, A., & Goi, D. (2022). Removal of organics from landfill leachate by heterogeneous fenton-like oxidation over copper-based catalyst. *Catalysts*, *12*(3), 338.

[236] Hussain, S., Aneggi, E., Maschio, S., Contin, M., & Goi, D. (2021). Steel scale waste as a heterogeneous Fenton-like catalyst for the treatment of landfill leachate. *Industrial & Engineering Chemistry Research*, *60*(31), 11715-11724.
[237] Chatterley, C., & Linden, K. (2010). Demonstration and evaluation of germicidal UV-LEDs for point-of-use water disinfection. *Journal of water and health*, *8*(3), 479-486.
[238] Hamamoto, A., Mori, M., Takahashi, A., Nakano, M., Wakikawa, N., Akutagawa, M., ... & Kinouchi, Y. (2007). New water disinfection system using UVA light-emitting diodes. *Journal of applied microbiology*, *103*(6), 2291-2298.
[239] Wengraitis, S., McCubbin, P., Wade, M. M., Biggs, T. D., Hall, S., Williams, L. I., & Zulich, A. W. (2013). Pulsed UV-C disinfection of Escherichia coli with light-emitting diodes, emitted at various repetition rates and duty cycles. *Photochemistry and photobiology*, *89*(1), 127-131.
[240] Thomson, J., Roddick, F. A., & Drikas, M. (2004). Vacuum ultraviolet irradiation for natural organic matter removal. *Journal of Water Supply: Research and Technology—AQUA*, *53*(4), 193-206.
[241] Benitez, F. J., Beltran-Heredia, J., Acero, J. L., & Pinilla, M. L. (1997). Simultaneous photodegradation and ozonation plus UV radiation of phenolic acids—major pollutants in agro-industrial wastewaters. *Journal of Chemical Technology & Biotechnology: International Research in Process, Environmental AND Clean Technology*, *70*(3), 253-260.
[242] Bolton, J. R. (1999). Ultraviolet applications handbook. Bolton Photosciences Inc., Ayr, Ont. *also published in Europ. Photchem. Assoc. Newsl*, (66-9), 36.
[243] Ince, N. H. (1998). Light-enhanced chemical oxidation for tertiary treatment of municipal landfill leachate. *Water environment research*, *70*(6), 1161-1169.
[244] Steensen, M. (1997). Chemical oxidation for the treatment of leachate-process comparison and results from full-scale plants. *Water Science and Technology*, *35*(4), 249-256.
[245] Müller, J. P., Gottschalk, C., & Jekel, M. (2001). Comparison of advanced oxidation processes in flow-through pilot plants (Part II). *Water science and technology*, *44*(5), 311-315.
[246] Benitez, F. J., Beltran-Heredia, J., Acero, J. L., & Rubio, F. J. (2001). Oxidation of several chlorophenolic derivatives by UV irradiation and hydroxyl radicals. *Journal of Chemical Technology & Biotechnology*, *76*(3), 312-320.

[247] Höfl, C., Sigl, G., Specht, O., Wurdack, I., & Wabner, D. (1997). Oxidative degradation of AOX and COD by different advanced oxidation processes: a comparative study with two samples of a pharmaceutical wastewater. *Water Science and Technology*, *35*(4), 257-264.
[248] Kusakabe, K., Aso, S., Wada, T., Hayashi, J. I., Morooka, S., & Isomura, K. (1991). Destruction rate of volatile organochlorine compounds in water by ozonation with ultraviolet radiation. *Water Research*, *25*(10), 1199-1203.
[249] Wenzel, A., Gahr, A., & Niessner, R. (1999). TOC-removal and degradation of pollutants in leachate using a thin-film photoreactor. *Water research*, *33*(4), 937-946.
[250] Wang, Z. P., Zhang, Z., Lin, Y. J., Deng, N. S., Tao, T., & Zhuo, K. (2002). Landfill leachate treatment by a coagulation–photooxidation process. *Journal of hazardous materials*, *95*(1-2), 153-159.
[251] Kim, S. M., Geissen, S. U., & Vogelpohl, A. (1997). Landfill leachate treatment by a photoassisted Fenton reaction. *Water Science and Technology*, *35*(4), 239-248.
[252] De Morais, J. L., & Zamora, P. P. (2005). Use of advanced oxidation processes to improve the biodegradability of mature landfill leachates. *Journal of hazardous materials*, *123*(1-3), 181-186
[253] Geenens, D., Bixio, B., & Thoeye, C. (1999, October). Advanced oxidation treatment of landfill leachate. In *Proceedings of the Seventh International Waste Management and Landfill Symposium, Sardinia, Italy* (pp. 261-268).
[254] Navarro, P., Sarasa, J., Sierra, D., Esteban, S., & Ovelleiro, J. L. (2005). Degradation of wine industry wastewaters by photocatalytic advanced oxidation. *Water Science and technology*, *51*(1), 113-120.
[255] Bekbölet, M., Lindner, M., Weichgrebe, D., & Bahnemann, D. W. (1996). Photocatalytic detoxification with the thin-film fixed-bed reactor (TFFBR): clean-up of highly polluted landfill effluents using a novel TiO2-photocatalyst. *Solar Energy*, *56*(5), 455-469.
[256] Chiron, S., Fernandez-Alba, A., Rodriguez, A., & Garcia-Calvo, E. (2000). Pesticide chemical oxidation: state-of-the-art. *Water Research*, *34*(2), 366-377.
[257] Sun, X., Liu, J., Ji, L., Wang, G., Zhao, S., Yoon, J. Y., & Chen, S. (2020). A review on hydrodynamic cavitation disinfection: The current state of knowledge. *Science of the Total Environment*, *737*, 139606.

[258] Padoley, K. V., Saharan, V. K., Mudliar, S. N., Pandey, R. A., & Pandit, A. B. (2012). Cavitationally induced biodegradability enhancement of a distillery wastewater. *Journal of hazardous materials*, *219*, 69-74.
[259] Mezule, L., Tsyfansky, S., Yakushevich, V., & Juhna, T. (2009). A simple technique for water disinfection with hydrodynamic cavitation: Effect on survival of Escherichia coli. *Desalination*, *248*(1-3), 152-159.
[260] Raut-Jadhav, S., Badve, M. P., Pinjari, D. V., Saini, D. R., Sonawane, S. H., & Pandit, A. B. (2016). Treatment of the pesticide industry effluent using hydrodynamic cavitation and its combination with process intensifying additives (H2O2 and ozone). *Chemical Engineering Journal*, *295*, 326-335.
[261] Rajoriya, S., Bargole, S., George, S., & Saharan, V. K. (2018). Treatment of textile dyeing industry effluent using hydrodynamic cavitation in combination with advanced oxidation reagents. *Journal of Hazardous Materials*, *344*, 1109-1115.
[262] Eljaiek-Urzola, M., Guardiola-Meza, L., Ghafoori, S., & Mehrvar, M. (2018). Treatment of mature landfill leachate using hybrid processes of hydrogen peroxide and adsorption in an activated carbon fixed bed column. *Journal of Environmental Science and Health, Part A*, *53*(3), 238-243.
[263] Sirés, I., Brillas, E., Oturan, M. A., Rodrigo, M. A., & Panizza, M. (2014). Electrochemical advanced oxidation processes: today and tomorrow. A review. *Environmental Science and Pollution Research*, *21*, 8336-8367.
[264] Mohajeri, S., Hamidi, A. A., Isa, M. H., & Zahed, M. A. (2019). Landfill leachate treatment through electro-Fenton oxidation. *Pollution*, *5*(1), 199-209.
[265] Brillas, E. (2020). A review on the photoelectro-Fenton process as efficient electrochemical advanced oxidation for wastewater remediation. Treatment with UV light, sunlight, and coupling with conventional and other photo-assisted advanced technologies. *Chemosphere*, *250*, 126198.
[266] Theerthagiri, J., Madhavan, J., Lee, S. J., Choi, M. Y., Ashokkumar, M., & Pollet, B. G. (2020). Sonoelectrochemistry for energy and environmental applications. *Ultrasonics Sonochemistry*, *63*, 104960.
[267] Chen, C. X., Aris, A., Yong, E. L., & Noor, Z. Z. (2022). A review of antibiotic removal from domestic wastewater using the activated sludge process: removal routes, kinetics and operational parameters. *Environmental Science and Pollution Research*, 1-16.

[268] Chen, S., & He, Z. (2022). Sonoelectrochemical activation of peroxymonosulfate: Influencing factors and mechanism of FA degradation, and application on landfill leachate treatment. *Chemosphere*, *296*, 133365.
[269] Zeng, W., Yao, B., Zhou, Y., Yang, J., & Zhi, D. (2024). Combination of electrochemical advanced oxidation and biotreatment for wastewater treatment and soil remediation. *Journal of Environmental Sciences*.
[270] Zhou, W., Xie, L., Gao, J., Nazari, R., Zhao, H., Meng, X., ... & Ma, J. (2021). Selective H2O2 electrosynthesis by O-doped and transition-metal-O-doped carbon cathodes via O2 electroreduction: a critical review. *Chemical Engineering Journal*, *410*, 128368.
[271] Martínez-Huitle, C. A., & Panizza, M. (2018). Electrochemical oxidation of organic pollutants for wastewater treatment. *Current Opinion in Electrochemistry*, *11*, 62-71.
[272] Ghjair, A. Y., & Abbar, A. H. (2023). Applications of advanced oxidation processes (Electro-Fenton and sono-electro-Fenton) for COD removal from hospital wastewater: Optimization using response surface methodology. *Process Safety and Environmental Protection*, *169*, 481-492.
[273] Nidheesh, P. V., Zhou, M., & Oturan, M. A. (2018). An overview on the removal of synthetic dyes from water by electrochemical advanced oxidation processes. *Chemosphere*, *197*, 210-227.
[274] Liu, W., Lv, G., Sun, X., He, L., Zhang, C., & Li, Z. (2019). Theoretical study on the reaction of anthracene with sulfate radical and hydroxyl radical in aqueous solution. *Ecotoxicology and Environmental Safety*, *183*, 109551.
[275] Wang, J., Zhi, D., Zhou, H., He, X., & Zhang, D. (2018). Evaluating tetracycline degradation pathway and intermediate toxicity during the electrochemical oxidation over a Ti/Ti4O7 anode. *Water research*, *137*, 324-334.
[276] Zhi, D., Lin, Y., Jiang, L., Zhou, Y., Huang, A., Yang, J., & Luo, L. (2020). Remediation of persistent organic pollutants in aqueous systems by electrochemical activation of persulfates: A review. *Journal of Environmental Management*, *260*, 110125.
[277] Wang, Y., Yu, G., Deng, S., Huang, J., & Wang, B. (2018). The electro-peroxone process for the abatement of emerging contaminants: Mechanisms, recent advances, and prospects. *Chemosphere*, *208*, 640-654.
[278] Moreira, F. C., Boaventura, R. A., Brillas, E., & Vilar, V. J. (2017). Electrochemical advanced oxidation processes: a review on their application to

synthetic and real wastewaters. *Applied Catalysis B: Environmental*, *202*, 217-261.
[279] Moreira, F. C., Soler, J., Fonseca, A., Saraiva, I., Boaventura, R. A., Brillas, E., & Vilar, V. J. (2015). Incorporation of electrochemical advanced oxidation processes in a multistage treatment system for sanitary landfill leachate. *Water research*, *81*, 375-387.
[280] Oturan, M. A., & Aaron, J. J. (2014). Advanced oxidation processes in water/wastewater treatment: principles and applications. A review. *Critical reviews in environmental science and technology*, *44*(23), 2577-2641.
[281] Ganzenko, O., Huguenot, D., Van Hullebusch, E. D., Esposito, G., & Oturan, M. A. (2014). Electrochemical advanced oxidation and biological processes for wastewater treatment: a review of the combined approaches. *Environmental Science and Pollution Research*, *21*, 8493-8524.
[282] Thiam, A., Zhou, M., Brillas, E., & Sirés, I. (2014). Two-step mineralization of Tartrazine solutions: study of parameters and by-products during the coupling of electrocoagulation with electrochemical advanced oxidation processes. *Applied Catalysis B: Environmental*, *150*, 116-125.
[283] Urtiaga, A. M., Pérez, G., Ibáñez, R., & Ortiz, I. (2013). Removal of pharmaceuticals from a WWTP secondary effluent by ultrafiltration/reverse osmosis followed by electrochemical oxidation of the RO concentrate. *Desalination*, *331*, 26-34.
[284] Oller, I., Malato, S., & Sánchez-Pérez, J. A. (2011). Combination of advanced oxidation processes and biological treatments for wastewater decontamination—a review. *Science of the total environment*, *409*(20), 4141-4166.
[285] Brillas, E., Sirés, I., & Oturan, M. A. (2009). Electro-Fenton process and related electrochemical technologies based on Fenton's reaction chemistry. *Chemical reviews*, *109*(12), 6570-6631
[286] Parra, S., Malato, S., & Pulgarin, C. (2002). New integrated photocatalytic-biological flow system using supported TiO2 and fixed bacteria for the mineralization of isoproturon. *Applied Catalysis B: Environmental*, *36*(2), 131-144.
[287] Babaei, S., Sabour, M. R., & Moftakhari Anasori Movahed, S. (2021). Combined landfill leachate treatment methods: an overview. *Environmental Science and Pollution Research*, *28*(42), 59594-59607.

[288] Webler, A. D., Moreira, F. C., Dezotti, M. W., Mahler, C. F., Segundo, I. D. B., Boaventura, R. A., & Vilar, V. J. (2019). Development of an integrated treatment strategy for a leather tannery landfill leachate. *Waste Management*, *89*, 114-128.
[289] Rao, C. R. M., & Reddi, G. S. (2000). Platinum group metals (PGM); occurrence, use and recent trends in their determination. *TrAC Trends in Analytical Chemistry*, *19*(9), 565-586.
[290] Bao, D. (2020). Dynamics and correlation of platinum-group metals spot prices. *Resources Policy*, *68*, 101772.
[291] Karim, S., & Ting, Y. P. (2020). Ultrasound-assisted nitric acid pretreatment for enhanced biorecovery of platinum group metals from spent automotive catalyst. *Journal of Cleaner Production*, *255*, 120199.
[292] Trinh, H. B., Lee, J. C., Suh, Y. J., & Lee, J. (2020). A review on the recycling processes of spent auto-catalysts: Towards the development of sustainable metallurgy. *Waste Management*, *114*, 148-165.
[293] Wilburn, D. R., & Bleiwas, D. I. (2004). Platinum-group metals—world supply and demand. *US geological survey open-file report*, *1224*, 2004-1224.
[294]https://matthey.com/documents/161599/509431/2002+full+review+en.pdf/6c4a84c7-a7af-5cca-4327-7c42d984579b?t=1655877255051
[295] Saguru, C., Ndlovu, S., & Moropeng, D. (2018). A review of recent studies into hydrometallurgical methods for recovering PGMs from used catalytic converters. *Hydrometallurgy*, *182*, 44-56.
[296]https://matthey.com/documents/161599/164195/AR-2003.pdf/0a2ff31c-169a-8853-8ed6-108144a61536
[297] Gunn, G. (2014). Platinum-group metals. *Critical metals handbook*, 284-311.
[298] Hughes, A. E., Haque, N., Northey, S. A., & Giddey, S. (2021). Platinum group metals: A review of resources, production and usage with a focus on catalysts. *Resources*, *10*(9), 93.
[299]https://technology.matthey.com/content/journals/10.1595/205651316X692121
[300] O'Connor, C., & Alexandrova, T. (2021). The geological occurrence, mineralogy, and processing by flotation of platinum group minerals (PGMs) in South Africa and Russia. *Minerals*, *11*(1), 54.
[301] Chen, D., & Mu, S. (2023). Revitalizing osmium-based catalysts for energy conversion. *Energy Reviews*, 100053.

[302] Pianowska, K., Kluczka, J., Benke, G., Goc, K., Malarz, J., Ochmański, M., & Leszczyńska-Sejda, K. (2023). Solvent extraction as a method of recovery and separation of platinum group metals. *Materials*, *16*(13), 4681.
[303] Bossi, T., & Gediga, J. (2017). The environmental profile of platinum group metals. *Johnson Matthey Technology Review*, *61*(2), 111-121.
[304] Chemical Elements for South Africa's Future NSTF National Science & Technology Forum, "Rare Metals in New Technologies", Annelize Botes, 18 March 2019.
[305] Cova, C. M., Zuliani, A., Manno, R., Sebastian, V., & Luque, R. (2020). Scrap waste automotive converters as efficient catalysts for the continuous-flow hydrogenations of biomass derived chemicals. *Green Chemistry*, *22*(4), 1414-1423.
[306] Rood, S., Eslava, S., Manigrasso, A., & Bannister, C. (2020). Recent advances in gasoline three-way catalyst formulation: A review. *Proceedings of the Institution of Mechanical Engineers, Part D: Journal of Automobile Engineering*, *234*(4), 936-949.
[307] Yakoumis, I., Moschovi, A. M., Giannopoulou, I., & Panias, D. (2018, March). Real life experimental determination of platinum group metals content in automotive catalytic converters. In *IOP Conference Series: Materials Science and Engineering* (Vol. 329, p. 012009). IOP Publishing.
[308] Farrauto, R. J., & Heck, R. M. (1999). Catalytic converters: state of the art and perspectives. *Catalysis Today*, *51*(3-4), 351-360.
[309] Twigg MV. Catalytic control of emissions from cars. Catal Today 2011; 163: 33–41.
[310] CC BY 4.0; Ümit Kaya via LibreTexts
[311] Faber, J., & Brodzik, K. (2018, September). Influence of preparation and analysis methods on determination of Rh, Pd and Pt content in automotive catalysts samples. In *IOP Conference Series: Materials Science and Engineering* (Vol. 421, No. 4, p. 042018). IOP Publishing.
[312] Kašpar, J., Fornasiero, P., & Hickey, N. (2003). Automotive catalytic converters: current status and some perspectives. *Catalysis today*, *77*(4), 419-449.
[313] Heck, R. M., & Farrauto, R. J. (2001). Automobile exhaust catalysts. *Applied Catalysis A: General*, *221*(1-2), 443-457.

[314] Pietrelli, L., & Fontana, D. (2013). Automotive spent catalysts treatment and platinum recovery. *International Journal of Environment and Waste Management*, *11*(2), 222-232.
[315] Hagelüken, B. C. (2012). Recycling the platinum group metals: A European perspective. *Platinum Metals Review*, *56*(1), 29-35.
[316] Saternus, M., & Fornalczyk, A. (2013). Possible ways of refining precious group metals (PGM) obtained from recycling of the used auto catalytic converters. *Metalurgija*, *52*(2), 267-270.
[317] Barefoot, R. R. (1997). Determination of platinum at trace levels in environmental and biological materials. *Environmental Science & Technology*, *31*(2), 309-314.
[318] De Aberasturi, D. J., Pinedo, R., De Larramendi, I. R., De Larramendi, J. R., & Rojo, T. (2011). Recovery by hydrometallurgical extraction of the platinum-group metals from car catalytic converters. *Minerals engineering*, *24*(6), 505-513.
[319] https://www.bmcatalysts.co.uk/app/uploads/2020/01/Importance-Euro-Emissions-03-2019.pdf
[320] https://www.transportpolicy.net/standard/eu-light-duty-emissions/
[321] Directive 2000/53/EC of the European Parliament and of the Council of 18 September 2000, Official Journal of the European Communities, L269/34. Published: 21st October, 2000
[322] Rumpold, R., & Antrekowitsch, J. (2012). Recycling of platinum group metals from automotive catalysts by an acidic leaching process. *The Southern African Institute of mining and metallurgy platinum*, *2012*, 695-714
[323] Benson, M., Bennett, C.R., Harry, J.E., Patel, M.K., and Cross, M. The recovery mechanism of platinum group metals from catalytic converters in spent automotive exhaust systems Resources. Conservation and Recycling, vol. 31, 2000. pp. 1-7
[324] Hagelüken, C. Autoabgaskatalysatoren: Grundlagen, Herstellung, Entwicklung, Recycling, Ökologie. 2. aktualisierte und erweiterte Auflage. Expert Verlag Renningen, 2005]
[325] Barakat, M. A., & Mahmoud, M. H. H. (2004). Recovery of platinum from spent catalyst. *Hydrometallurgy*, *72*(3-4), 179-184.
[326] De Aberasturi, D. J., Pinedo, R., De Larramendi, I. R., De Larramendi, J. R., & Rojo, T. (2011). Recovery by hydrometallurgical extraction of the platinum-group metals from car catalytic converters. *Minerals engineering*, *24*(6), 505-513.

[327] Kononova, O. N., Melnikov, A. M., Borisova, T. V., & Krylov, A. S. (2011). Simultaneous ion exchange recovery of platinum and rhodium from chloride solutions. *Hydrometallurgy*, *105*(3-4), 341-349.
[328] Trinh, H. B., Lee, J. C., Suh, Y. J., & Lee, J. (2020). A review on the recycling processes of spent auto-catalysts: Towards the development of sustainable metallurgy. *Waste Management*, *114*, 148-165
[329] Hagelüken, C. Recycling von Autoabgaskatalysatoren. Schriftenreihe der GDMB, vol. 115, 2008.pp. 69-85.
[330] Peng, Z., Li, Z., Lin, X., Tang, H., Ye, L., Ma, Y., ... & Jiang, T. (2017). Pyrometallurgical recovery of platinum group metals from spent catalysts. *Jom*, *69*, 1553-1562.
[331] Zengin, M., Genc, H., Demirci, T., Arslan, M., & Kucukislamoglu, M. (2011). An efficient hydrogenation of various alkenes using scrap automobile catalyst. *Tetrahedron Letters*, *52*(18), 2333-2335.
[332] Sonmez, F., Ercan, H., Genc, H., Arslan, M., Zengin, M., & Kucukislamoglu, M. (2013). Hydrogenation of some vegetable oils by scrap automobile catalyst. *Journal of Chemistry*, *2013*(1), 169109.
[333] Boldrini, D. E., Sánchez M, J. F., Tonetto, G. M., & Damiani, D. E. (2012). Monolithic stirrer reactor: performance in the partial hydrogenation of sunflower oil. *Industrial & engineering chemistry research*, *51*(38), 12222-12232.
[334] Cova, C. M., Zuliani, A., Muñoz-Batista, M. J., & Luque, R. (2019). Efficient Ru-based scrap waste automotive converter catalysts for the continuous-flow selective hydrogenation of cinnamaldehyde. *Green Chemistry*, *21*(17), 4712-4722.
[335] Zuliani, A., Cova, C. M., Manno, R., Sebastian, V., Romero, A. A., & Luque, R. (2020). Continuous flow synthesis of menthol via tandem cyclisation–hydrogenation of citronellal catalysed by scrap catalytic converters. *Green Chemistry*, *22*(2), 379-387.
[336] Zuliani, A., Kikhtyanin, O., Cova, C. M., Rodriguez-Padron, D., Kubička, D., & Luque, R. (2022). Boosting the Ni-Catalyzed Hydrodeoxygenation (HDO) of Anisole Using Scrap Catalytic Converters. *Advanced Sustainable Systems*, *6*(4), 2100394
[337] Isgoren, M., Gengec, E., Veli, S., Hassandoost, R., & Khataee, A. (2023). The used automobile catalytic converter as an efficient catalyst for removal of malathion through wet air oxidation process. *International Journal of Hydrogen Energy*, *48*(17), 6499-6509.

[338] Mieczyńska, E., Gniewek, A., & Trzeciak, A. M. (2012). Spent automotive three-way catalysts towards CC bond forming reactions. *Applied Catalysis A: General*, *421*, 148-153.
[339] Farhang, M., Akbarzadeh, A. R., Rabbani, M., & Ghadiri, A. M. (2022). A retrospective-prospective review of Suzuki–Miyaura reaction: From cross-coupling reaction to pharmaceutical industry applications. *Polyhedron*, *227*, 116124.
[340] Kiani, M., Rabiee, N., Bagherzadeh, M., Ghadiri, A. M., Fatahi, Y., Dinarvand, R., & Webster, T. J. (2020). High-gravity-assisted green synthesis of palladium nanoparticles: The flowering of nanomedicine. *Nanomedicine: Nanotechnology, Biology and Medicine*, *30*, 102297.
[341] Tang, W., Li, J., Jin, X., Sun, J., Huang, J., & Li, R. (2014). Magnetically recyclable Fe@ Pd/C as a highly active catalyst for Suzuki coupling reaction in aqueous solution. *Catalysis Communications*, *43*, 75-78.
[342] Jasim, S. A., Ansari, M. J., Majdi, H. S., Opulencia, M. J. C., & Uktamov, K. F. (2022). RETRACTED: Nanomagnetic Salamo-based-Pd (0) Complex: an efficient heterogeneous catalyst for Suzuki–Miyaura and Heck cross-coupling reactions in aqueous medium.
[343] Soliev, S. B., Astakhov, A. V., Pasyukov, D. V., & Chernyshev, V. M. (2020). Nickel (II) N-heterocyclic carbene complexes as efficient catalysts for the Suzuki—Miyaura reaction. Russian Chemical Bulletin, 69, 683-690.
[344] Tamizh, M. M., & Karvembu, R. (2012). Synthesis of triethylphosphite complexes of nickel (II) and palladium (II) with tridentate Schiff base ligand for catalytic application in carbon–carbon coupling reactions. *Inorganic Chemistry Communications*, *25*, 30-34.
[345] Xiang, J., Li, P., Chong, H., Feng, L., Fu, F., Wang, Z., ... & Zhu, M. (2014). Bimetallic Pd-Ni core-shell nanoparticles as effective catalysts for the Suzuki reaction. *Nano Research*, *7*, 1337-1343.
[346] Pratihar, J. L., Mandal, P., Lai, C. K., & Chattopadhyay, S. (2019). Tetradentate amido azo Schiff base Cu (II), Ni (II) and Pd (II) complexes: Synthesis, characterization, spectral properties, and applications to catalysis in C–C coupling and oxidation reaction. *Polyhedron*, *161*, 317-324.
[347] Rabiee, N., Bagherzadeh, M., Kiani, M., Ghadiri, A. M., Etessamifar, F., Jaberizadeh, A. H., & Shakeri, A. (2020). Biosynthesis of copper oxide nanoparticles with potential biomedical applications. *International Journal of Nanomedicine*, 3983-3999.

[348] Turan, N., Buldurun, K., Çolak, N., & Özdemir, İ. (2019). Preparation and spectroscopic studies of Fe (II), Ru (II), Pd (II) and Zn (II) complexes of Schiff base containing terephthalaldehyde and their transfer hydrogenation and Suzuki-Miyaura coupling reaction. *Open Chemistry*, *17*(1), 571-580.
[349] Wu, G., & Jacobi von Wangelin, A. (2018). Iron-catalysed Suzuki biaryl couplings. *Nature Catalysis*, *1*(6), 377-378.
[350] Reckling, A. M., Martin, D., Dawe, L. N., Decken, A., & Kozak, C. M. (2011). Structure and C–C cross-coupling reactivity of iron (III) complexes of halogenated amine-bis (phenolate) ligands. *Journal of Organometallic Chemistry*, *696*(3), 787-794.
[351] Dong, D., Li, Z., Liu, D., Yu, N., Zhao, H., Chen, H., ... & Liu, D. (2018). Postsynthetic modification of single Pd sites into uncoordinated polypyridine groups of a MOF as the highly efficient catalyst for Heck and Suzuki reactions. *New Journal of Chemistry*, *42*(11), 9317-9323.
[352] Ding, S. Y., Gao, J., Wang, Q., Zhang, Y., Song, W. G., Su, C. Y., & Wang, W. (2011). Construction of covalent organic framework for catalysis: Pd/COF-LZU1 in Suzuki–Miyaura coupling reaction. *Journal of the American Chemical Society*, *133*(49), 19816-19822.
[353] Rabiee, N., Bagherzadeh, M., Kiani, M., Ghadiri, A. M., Zhang, K., Jin, Z., ... & Shokouhimehr, M. (2020). High gravity-assisted green synthesis of ZnO nanoparticles via Allium ursinum: Conjoining nanochemistry to neuroscience. *Nano Express*, *1*(2), 020025.
[354] Rabiee, N., Bagherzadeh, M., Ghadiri, A. M., Kiani, M., Fatahi, Y., Tavakolizadeh, M., ... & Varma, R. S. (2021). Multifunctional 3D hierarchical bioactive green carbon-based nanocomposites. *ACS Sustainable Chemistry & Engineering*, *9*(26), 8706-8720.
[355] Afshari, R., Hooshmand, S. E., Atharnezhad, M., & Shaabani, A. (2020). An insight into the novel covalent functionalization of multi-wall carbon nanotubes with pseudopeptide backbones for palladium nanoparticles immobilization: A versatile catalyst towards diverse cross-coupling reactions in bio-based solvents. *Polyhedron*, *175*, 114238.
[356] Rabiee, N., Bagherzadeh, M., Heidarian Haris, M., Ghadiri, A. M., Matloubi Moghaddam, F., Fatahi, Y., ... & Shokouhimehr, M. (2021). Polymer-coated NH2-UiO-66 for the codelivery of DOX/pCRISPR. *ACS Applied Materials & Interfaces*, *13*(9), 10796-10811.

[357] D'Alterio, M. C., Casals-Cruañas, È., Tzouras, N. V., Talarico, G., Nolan, S. P., & Poater, A. (2021). Mechanistic aspects of the palladium-catalyzed Suzuki-Miyaura cross-coupling reaction. *Chemistry–A European Journal*, *27*(54), 13481-13493.
[358] Franzén, R., & Xu, Y. (2005). Review on green chemistry Suzuki cross coupling in aqueous media. *Canadian journal of chemistry*, *83*(3), 266-272.
[359] Sherwood, J., Clark, J. H., Fairlamb, I. J., & Slattery, J. M. (2019). Solvent effects in palladium catalysed cross-coupling reactions. *Green Chemistry*, *21*(9), 2164-2213.
[3600] Hailes, H. C. (2007). Reaction solvent selection: the potential of water as a solvent for organic transformations. *Organic process research & development*, *11*(1), 114-120.
[361] Katara, P. (2016). Review paper on catalytic converter for automobile exhaust emission. *Int. J. Sci. Res*, *5*, 30-33.
[362] Taylor, K. C. (1987). Automobile catalytic converters. In *Studies in Surface Science and Catalysis* (Vol. 30, pp. 97-116). Elsevier.
[363] O'Dell, J. W. (1993). Method 410.4, revision 2.0: the determination of chemical oxygen demand by semi-automated colorimetry. *US Environmental Protection Agency, Office of Research and Development, Environmental Monitoring Systems Laboratory: Cincinnati, Ohio, USA) Available at [verified 2 July 2019]*.
[364] Yazici Guvenc, S., & Varank, G. (2021). Degradation of refractory organics in concentrated leachate by the Fenton process: Central composite design for process optimization. *Frontiers of Environmental Science & Engineering*, *15*, 1-16.
[365] Chatterjee, A., & Ward, T. R. (2016). Recent advances in the palladium catalyzed Suzuki–Miyaura cross-coupling reaction in water. *Catalysis Letters*, *146*, 820-840
[366] Hanhan, M. E., & Senemoglu, Y. (2012). Microwave-assisted aqueous Suzuki coupling reactions catalyzed by ionic palladium (II) complexes. *Transition Metal Chemistry*, *37*, 109-116
[367] Khan, D., & Parveen, I. (2021). Chroman-4-one-Based Amino Bidentate Ligand: An Efficient Ligand for Suzuki-Miyaura and Mizoroki-Heck Coupling Reactions in Aqueous Medium. *European Journal of Organic Chemistry*, *2021*(35), 4946-4957.
[368] Lamola, J. L., Moshapo, P. T., Holzapfel, C. W., & Maumela, M. C. (2024). Application of Biaryl Phosphacycles in Palladium-Catalysed Suzuki-Miyaura

Cross-Coupling Reactions of Aryl Chlorides. *European Journal of Inorganic Chemistry*, e202400068.
[369] Mercadante, A., Campisciano, V., Morena, A., Valentino, L., La Parola, V., Aprile, C., ... & Giacalone, F. (2022). Catechol-Functionalized Carbon Nanotubes as Support for Pd Nanoparticles: a Recyclable System for the Heck Reaction. *European Journal of Organic Chemistry*, *2022*(38), e202200497
[370] Sharma, S., Kumar, M., & Bhalla, V. (2023). Pyrazine derivative as supramolecular host for immobilization of palladium nanoparticles for efficient suzuki coupling. *European Journal of Organic Chemistry*, *26*(31), e202300594.
[371] Zhou, F., Simon, M. O., & Li, C. J. (2013). Transition-Metal-Free One-Pot Synthesis of Biaryls from Grignard Reagents and Substituted Cyclohexanones. *Chemistry–A European Journal*, *19*(22), 7151-7155
[372] Zhou, W. J., Wang, K. H., Wang, J. X., & Huang, D. F. (2010). Reusable, Polystyrene-Resin-Supported, Palladium-Catalyzed, Atom-Efficient Cross-Coupling Reaction of Aryl Halides with Triarylbismuths.
[373] Iyer, K. S., Nelson, C., & Lipshutz, B. H. (2023). Facile, green, and functional group-tolerant reductions of carboxylic acids… in, or with, water. *Green Chemistry*, *25*(7), 2663-2671.
[374] Zhang, G., Luo, X., Guan, C., Cui, Y., & Ding, C. (2023). Pd/Ni Co-catalyzed Selective Cross-Coupling of Aryl Bromides and Aryl Fluorosulfonates at Room Temperature. *European Journal of Organic Chemistry*, *26*(17), e202300114
[375] Ambre, R., Yang, H., Chen, W. C., Yap, G. P., Jurca, T., & Ong, T. G. (2019). Nickel Carbodicarbene Catalyzes Kumada Cross-Coupling of Aryl Ethers with Grignard Reagents through C–O Bond Activation. *European Journal of Inorganic Chemistry*, *2019*(30), 3511-3517.
[376] Bárta, O., Císařová, I., & Štěpnička, P. (2017). Synthesis, palladium (II) complexes, and catalytic use of a phosphanylferrocene ligand bearing a guanidinium pendant. *European Journal of Inorganic Chemistry*, *2017*(2), 489-495.
[377] Lu, H. K., Liu, T., Shi, Z., Yan, H., Li, Z., & Ye, K. Y. (2023). Electrochemical Bromination of Substituted Thiophenes in Batch and Continuous Flow. *European Journal of Organic Chemistry*, *26*(7), e202200963.
[378] Zhang, J., Li, T., Li, X., Zhang, G., Fang, S., Yan, W., ... & Szostak, M. (2022). An air-stable, well-defined palladium–BIAN–NHC chloro dimer: a fast-activating, highly efficient catalyst for cross-coupling. *Chemical Communications*, *58*(53), 7404-7407

[379] Fricke, C., Sherborne, G. J., Funes-Ardoiz, I., Senol, E., Guven, S., & Schoenebeck, F. (2019). Orthogonal nanoparticle catalysis with organogermanes. *Angewandte Chemie International Edition*, *58*(49), 17788-17795.
[380] Tang, J., Biafora, A., & Goossen, L. J. (2015). Catalytic Decarboxylative Cross-Coupling of Aryl Chlorides and Benzoates without Activating ortho Substituents. *Angewandte Chemie International Edition*, *54*(44), 13130-13133.
[381] Bao, Z., Zou, J., Mou, C., Jin, Z., Ren, S. C., & Chi, Y. R. (2022). Direct reaction of nitroarenes and thiols via photodriven oxygen atom transfer for access to sulfonamides. *Organic Letters*, *24*(48), 8907-8913.
[382] Rao, M. L., & Dhanorkar, R. J. (2014). Triarylbismuthanes as Threefold Aryl-Transfer Reagents in Regioselective Cross-Coupling Reactions with Bromopyridines and Quinolines. *European Journal of Organic Chemistry*, *2014*(24), 5214-5228.
[383] Jullien, H., Quiclet-Sire, B., Tetart, T., & Zard, S. Z. (2014). Flexible routes to thiophenes. *Organic Letters*, *16*(1), 302-305.
[384] Zhang, L., Hu, W., Li, H., Shi, J., & Yuan, B. (2023). TXPhos: a highly stable and efficient ligand designed for ppm level Pd-catalyzed Suzuki–Miyaura coupling in water. *Green Chemistry*, *25*(17), 6635-6641.
[385] Groll, K., Bluemke, T. D., Unsinn, A., Haas, D., & Knochel, P. (2012). Direct Pd-Catalyzed Cross-Coupling of Functionalized Organoaluminum Reagents. *Angewandte Chemie International Edition*, *51*(44), 11157-11161
[386] Sinha, N., Heijnen, D., Feringa, B. L., & Organ, M. G. (2019). Murahashi Cross-Coupling at− 78° C: A One-Pot Procedure for Sequential C− C/C− C, C− C/C− N, and C− C/C− S Cross-Coupling of Bromo-Chloro-Arenes. *Chemistry–A European Journal*, *25*(39), 9180-9184.
[387] Qi, X., Li, C. L., & Wu, X. F. (2016). A convenient palladium-catalyzed reductive carbonylation of aryl iodides with dual role of formic acid. *Chemistry–A European Journal*, *22*(17), 5835-5838.
[388] Valentini, F., Di Erasmo, B., Ciani, M., Chen, S., Gu, Y., & Vaccaro, L. (2024). Microwave assisted batch and continuous flow Suzuki–Miyaura reactions in GVL using a Pd/PiNe biowaste-derived heterogeneous catalyst. *Green Chemistry*, *26*(8), 4871-4879.
[389] Wei, X. J., Xue, B., Handelmann, J., Hu, Z., Darmandeh, H., Gessner, V. H., & Gooßen, L. J. (2022). Ylide-Functionalized Diisopropyl Phosphine (prYPhos): A Ligand for Selective Suzuki-Miyaura Couplings of Aryl Chlorides. *Advanced Synthesis & Catalysis*, *364*(19), 3336-3341.

[390] Tsuchiya, N., Nojiri, T., & Nishikata, T. (2024). Oxazaborolidinones: Steric Coverage Effect of Lewis Acidic Boron Center in Suzuki–Miyaura Coupling Reactions. *Chemistry–A European Journal*, *30*(9), e202303271.
[391] Liu, Q. X., Zhang, W., Zhao, X. J., Zhao, Z. X., Shi, M. C., & Wang, X. G. (2013). NHC PdII Complex Bearing 1, 6-Hexylene Linker: Synthesis and Catalytic Activity in the Suzuki–Miyaura and Heck–Mizoroki Reactions. *European Journal of Organic Chemistry*, *2013*(7), 1253-1261.

Appendix 1

Table 8 BAT-associated emission levels (BAT-AELs) for direct discharges to a receiving water body [107]

Substance/Parameter		BAT-AEL (1)	Waste treatment process to which the BAT-AEL applies
Total organic carbon (TOC) (2)		10-60 mg/L	All waste treatments except treatment of water-based liquid waste
		10-100 mg/L (3)(4)	Treatment of water-based liquid waste
Chemical oxygen demand (COD) (2)		30-180 mg/L	All waste treatments except treatment of water-based liquid waste
		30-300 mg/L (3)(4)	Treatment of water-based liquid waste
Total suspended solids (TSS)		5-60 mg/L	All waste treatments
Hydrocarbon oil index (HOI)		0,5-10 mg/L	- Mechanical treatment in shredders of metal waste - Treatment of WEEE containing VFCs and/or VHCs - Re-refining of waste oil - Physico-chemical treatment of waste with calorific value - Water washing of excavated contaminated soil - Treatment of water-based liquid waste
Total nitrogen (Total N)		1-25 g/L (5)(6)	- Biological treatment of waste - Re-refining of waste oil
		10-60 g/L (5)(6)(7)	Treatment of water-based liquid waste
Total phosphorus (Total P)		0,3-2 mg/L	Biological treatment of waste
		1-3 mg/L (4)	Treatment of water-based liquid waste
Phenol index		0,05-0,2 mg/L	- Re-refining of waste oil - Physico-chemical treatment of waste with calorific value
		0,05-0,3 mg/L	Treatment of water-based liquid waste
Free cyanide (CN^-) (8)		0,02-0,1 mg/L	Treatment of water-based liquid waste
Adsorbable organically bound halogens (AOX) (8)		0,2-1 mg/L	Treatment of water-based liquid waste
Metals and metalloids (8)	Arsenic (expressed as As)	0,01-0,05 mg/L	- Mechanical treatment in shredders of metal waste - Treatment of WEEE containing VFCs and/or VHCs - Mechanical biological treatment of waste - Re-refining of waste oil - Physico-chemical treatment of waste with calorific value - Physico-chemical treatment of solid and/or pasty waste - Regeneration of spent solvents - Water washing of excavated contaminated soil
	Cadmium (expressed as Cd)	0,01-0,05 mg/L	
	Chromium (expressed as Cr)	0,01-0,15 mg/L	
	Copper (expressed as Cu)	0,05-0,5 mg/L	
	Lead (expressed as Pb)	0,05-0,1 mg/L (9)	
	Nickel (expressed as Ni)	0,05-0,5 mg/L	

	Mercury (expressed as Hg)	0,5-5 µg/L	
	Zinc (expressed as Zn)	0,1-1 mg/L (10)	
	Arsenic (expressed as As)	0,01-0,1 mg/L	Treatment of water-based liquid waste
	Cadmium (expressed as Cd)	0,01-0,1 mg/L	
	Chromium (expressed as Cr)	0,01-0,3 mg/L	
	Hexavalent chromium (expressed as Cr(VI))	0,01-0,1 mg/L	
	Copper (expressed as Cu)	0,05-0,5 mg/L	
	Lead (expressed as Pb)	0,05-0,3 mg/L	
	Nickel (expressed as Ni)	0,05-1 mg/L	
	Mercury (expressed as Hg)	1-10 µg/L	
	Zinc (expressed as Zn)	0,1-2 mg/L	

(1) The averaging periods are defined in the General considerations.

(2) Either the BAT-AEL for COD or the BAT-AEL for TOC applies. TOC monitoring is the preferred option because it does not rely on the use of very toxic compounds.

(3) The upper end of the range may not apply:

— when the abatement efficiency is ≥ 95 % as a rolling yearly average and the waste input shows the following characteristics: TOC > 2 g/l (or COD > 6 g/l) as a daily average and a high proportion of refractory organic compounds (i.e. which are difficult to biodegrade); or

— in the case of high chloride concentrations (e.g. above 5 g/l in the waste input).

(4) The BAT-AEL may not apply to plants treating drilling muds/cuttings.

(5) The BAT-AEL may not apply when the temperature of the waste water is low (e.g. below 12 °C).

(6) The BAT-AEL may not apply in the case of high chloride concentrations (e.g. above 10 g/l in the waste input).

(7) The BAT-AEL only applies when biological treatment of waste water is used.

(8) The BAT-AELs only apply when the substance concerned is identified as relevant in the waste water inventory mentioned in BAT 3.

(9) The upper end of the range is 0,3 mg/l for mechanical treatment in shredders of metal waste.

(10) The upper end of the range is 2 mg/l for mechanical treatment in shredders of metal waste.

Table 9 BAT-associated emission levels (BAT-AELs) for indirect discharges to a receiving water body [107]

Substance/Parameter		BAT-AEL (1)(2)	Waste treatment process to which the BAT-AEL applies
Hydrocarbon oil index (HOI)		0,5-10 mg/L	- Mechanical treatment in shredders of metal waste - Treatment of WEEE containing VFCs and/or VHCs - Re-refining of waste oil - Physico-chemical treatment of waste with calorific value - Water washing of excavated contaminated soil - Treatment of water-based liquid waste
Free cyanide (CN^-) (8)		0,02-0,1 mg/L	Treatment of water-based liquid waste
Adsorbable organically bound halogens (AOX) (8)		0,2-1 mg/L	Treatment of water-based liquid waste
	Arsenic (expressed as As)		- Mechanical treatment in shredders of metal

Metals and metalloids (8)		0,01-0,05 mg/L	waste - Treatment of WEEE containing VFCs and/or VHCs - Mechanical biological treatment of waste - Re-refining of waste oil - Physico-chemical treatment of waste with calorific value - Physico-chemical treatment of solid and/or pasty waste - Regeneration of spent solvents - Water washing of excavated contaminated soil
	Cadmium (expressed as Cd)	0,01-0,05 mg/L	
	Chromium (expressed as Cr)	0,01-0,15 mg/L	
	Copper (expressed as Cu)	0,05-0,5 mg/L	
	Lead (expressed as Pb)	0,05-0,1 mg/L (4)	
	Nickel (expressed as Ni)	0,05-0,5 mg/L	
	Mercury (expressed as Hg)	0,5-5 µg/L	
	Zinc (expressed as Zn)	0,1-1 mg/L (5)	
	Arsenic (expressed as As)	0,01-0,1 mg/L	Treatment of water-based liquid waste
	Cadmium (expressed as Cd)	0,01-0,1 mg/L	
	Chromium (expressed as Cr)	0,01-0,3 mg/L	
	Hexavalent chromium (expressed as Cr(VI))	0,01-0,1 mg/L	
	Copper (expressed as Cu)	0,05-0,5 mg/L	
	Lead (expressed as Pb)	0,05-0,3 mg/L	
	Nickel (expressed as Ni)	0,05-1 mg/L	
	Mercury (expressed as Hg)	1-10 µg/L	
	Zinc (expressed as Zn)	0,1-2 mg/L	

(1) The averaging periods are defined in the General considerations.

(2) The BAT-AELs may not apply if the downstream waste water treatment plant abates the pollutants concerned, provided this does not lead to a higher level of pollution in the environment.

(3) The BAT-AELs only apply when the substance concerned is identified as relevant in the waste water inventory mentioned in BAT 3.

(4) The upper end of the range is 0,3 mg/l for mechanical treatment in shredders of metal waste.

(5) The upper end of the range is 2 mg/l for mechanical treatment in shredders of metal waste.

Table 10 Water emission monitoring according to EN and ISO standards [107]

Substance/ parameter	Standard(s)	Waste treatment process	Minimum monitoring frequency (1)(2)	Monitoring associated with

Adsorbable organically bound halogens (AOX) (3)(4)	EN ISO 9562	Treatment of water-based liquid waste	Once every day	BAT 20
Benzene, toluene, ethylbenzene, xylene (BTEX)(3)(4)	EN ISO 15680	Treatment of water-based liquid waste	Once every month	
Chemical oxygen demand (COD)(5)(6)	No EN standard available	All waste treatments except treatment of water-based liquid waste	Once every month	
		Treatment of water-based liquid waste	Once every day	
Free cyanide (CN^-)(3)(4)	Various EN standards available (i.e. EN ISO 14403-1 and -2)	Treatment of water-based liquid waste	Once every day	
Hydrocarbon oil index (HOI)(4)	EN ISO 9377-2	Mechanical treatment in shredders of metal waste	Once every month	
		Treatment of WEEE containing VFCs and/or VHCs		
		Re-refining of waste oil		
		Physico-chemical treatment of waste with calorific value		
		Water washing of excavated con-taminated soil		
		Treatment of water-based liquid waste	Once every day	
Arsenic (As), Cadmium (Cd), Chromium (Cr), Copper (Cu), Nickel (Ni), Lead (Pb), Zinc (Zn) (3)(4)	Various EN standards available (e.g. EN ISO 11885, EN ISO 17294-2, EN ISO 15586)	Mechanical treatment in shredders of metal waste	Once every month	
		Treatment of WEEE containing VFCs and/or VHCs		
		Mechanical biological treatment of waste		
		Re-refining of waste oil		
		Physico-chemical treatment of waste with calorific value		
		Physico-chemical treatment of solid and/or pasty waste		
		Regeneration of spent solvents		
		Water washing of taminated soil		
		Treatment of water-based liquid waste	Once every day	

Manganese (Mn) (3)(4)		Treatment of water-based liquid waste	Once every day	
Hexavalent chromium (Cr(VI))(3)(4)	Various EN standards available (i.e. EN ISO 10304-3, EN ISO 23913)	Treatment of water-based liquid waste	Once every day	
Mercury (Hg) (3)(4)	Various EN standards available (i.e. EN ISO 17852, EN ISO 12846)	Mechanical treatment in shredders of metal waste	Once every month	
		Treatment of WEEE containing VFCs and/or VHCs		
		Mechanical biological treatment of waste		
		Re-refining of waste oil		
		Physico-chemical treatment of waste with calorific value		
		Physico-chemical treatment of solid and/or pasty waste		
		Regeneration of spent solvents		
		Water washing taminated soil		
		Treatment of water-based liquid waste	Once every day	
PFOA (3)	No EN standard available	All waste treatments	Once every six months	
PFOS (3)				
Phenol index (6)	EN ISO 14402	Re-refining of waste oil	Once every month	
		Physico-chemical treatment of waste with calorific value		
		Treatment of water-based liquid waste	Once every day	
Total nitrogen (Total N) (6)	EN 12260, EN ISO 11905-1	Biological treatment of waste	Once every month	
		Re-refining of waste oil		
		Treatment of water-based liquid waste	Once every day	
Total organic carbon (TOC) (5)(6)	EN 1484	All waste treatments except treatment of water-based liquid waste	Once every month	
		Treatment of water-based liquid waste	Once every day	
	Various EN standards available (i.e. EN ISO	Biological treatment of waste	Once every month	

Total phosphorus (Total P) (6)	15681-1 and -2, EN ISO 6878, EN ISO 11885)	Treatment of water-based liquid waste	Once every day	
Total suspended solids (TSS) (6)	EN 872	All waste treatments except treatment of water-based liquid waste	Once every month	
		Treatment of water-based liquid waste	Once every day	

(1) Monitoring frequencies may be reduced if the emission levels are proven to be sufficiently stable.

(2) In the case of batch discharge less frequent than the minimum monitoring frequency, monitoring is carried out once per batch.

(3) The monitoring only applies when the substance concerned is identified as relevant in the waste water inventory mentioned in BAT 3.

(4) In the case of an indirect discharge to a receiving water body, the monitoring frequency may be reduced if the downstream waste water treatment plant abates the pollutants concerned.

(5) Either TOC or COD is monitored. TOC is the preferred option, because its monitoring does not rely on the use of very toxic compounds.

(6) The monitoring applies only in the case of a direct discharge to a receiving water body.

Table 11 Techniques used to limit water emissions [107]

Technique (1)	Typical pollutants targeted	Applicability	
Preliminary and primary treatment, e.g.			
a.	Equalisation	All pollutants	Generally applicable.
b.	Neutralisation	Acids, alkalis	
c.	Physical separation, e.g. screens, sieves, grit separators, grease separators, oil-water separation or pri- mary settlement tanks	Gross solids, suspended solids, oil/grease	
Physico-chemical treatment, e.g.			
d.	Adsorption	Adsorbable dissolved non-biodegradable or inhibitory pollutants, e.g. hydrocarbons, mercury, AOX	Generally applicable.
e.	Distillation/ rectification	Dissolved non-biodegradable or inhibitory pollutants that can be distilled, e.g. some solvents	
f.	Precipitation	Precipitable dissolved non-biodegradable or inhibitory pollutants, e.g. metals, phos- phorus	
g.	Chemical oxidation	Oxidisable dissolved non-biodegradable or inhibitory pollutants, e.g. nitrite, cyanide	
h.	Chemical reduction	Reducible dissolved non-biodegradable or inhibitory pollutants, e.g. hexavalent chro- mium (Cr(VI))	

i.	Evaporation	Soluble contaminants	
j.	Ion exchange	Ionic dissolved non-biodegradable or inhib-itory pollutants, e.g. metals	
k.	Stripping	Purgeable pollutants, e.g. hydrogensulphide (H_2S), ammonia (NH_3), some adsorbable organically bound halogens (AOX), hydro- carbons	
Biological treatment, e.g.			
l.	Activated sludge process	Biodegradable organic compounds	Generally applicable
m.	Membrane bioreactor		
Nitrogen removal			
n.	Nitrification/denitrification when the treatment includes a biological treatment	Total nitrogen, ammonia	Nitrification may not be ap-plicable in the case of high chloride concentrations (e.g. above 10 g/l) and when the reduction of the chloride concentration prior to nitri-fication would not be justi- fied by the environmental benefits. Nitrification is not applicable when the tem- perature of the wastewater is low (e.g. below 12 °C).
Solids removal, e.g.			
o.	Coagulation and floccula- tion	Suspended solids and particulate-bound metals	Generally applicable.
p.	Sedimentation		
q.	Filtration (e.g. sand filtra-tion, microfiltration, ultra-filtration)		
r.	Flotation		

(1) The descriptions of the techniques are given in Section 6.3.

List of Publications

1) Sini, V., Carluccio, A., Marangi, M., Ragni, R., D'Onghia, G., & Cotugno, P. (2022, October). Green production of biofuels from fish discards using supercritical Carbon Dioxide as the extraction solvent. In *2022 IEEE International Workshop on Metrology for the Sea; Learning to Measure Sea Health Parameters (MetroSea)* (pp. 91-95). IEEE.

2) Exploring end-of-life automotive SCRAP catalytic converters as catalyst in Suzuki-Miyaura cross-coupling reaction. (In preparation for the submission to the journal ChemsusChem)

3) Eco-friendly reduction of the Chemical Oxygen Demand for landfill leachate by means of Scrap Automotive catalytic converter waste. (In preparation for the submission to the journal ACS Sustainable Chemistry & Engineering)

Green production of biofuels from fish discards using supercritical Carbon Dioxide as the extraction solvent

1st Valeria Sini
Department of Biology University of Bari "Aldo Moro" Italy
valeria.sini@uniba.it

2nd Angela Carluccio
Department of Biological and Environmental Sciences and Technologies University of Salento Lecce, Italy
angela.carluccio@uniba.it

3rd Mariella Marangi
Department of Chemistry University of Bari Aldo Moro" Italy
mariella.marangi@uniba.it

4th Roberta Ragni
Department of Chemistry University of Bari Aldo Moro" Italy
roberta.ragni@uniba.it

5th Gianfranco D'Onghia
Department of Biology University of Bari Aldo Moro" Italy
gianfranco.donghia@uniba.it

6th Pietro Cotugno*
Department of Chemistry University of Bari Aldo Moro" Italy
pietro.cotugno@uniba.it

Abstract

Fishing discards and wastes have great potential as renewable energy sources of biofuel, biogas and bioactive molecules for a variety of applications. Fish oils have features resembling those of petroleum fuels, being a promising and eco-friendly alternative to fossil derivatives. Here we report a preliminary investigation of a green method of biofuel production from fishing discards, obtained by two trawl hauls in the South-Western Adriatic Sea. The method is based on the use of supercritical carbon dioxide (sc-CO_2) as a green solvent for lipid oils extraction and subsequent conversion into fatty acid methyl esters (FAMEs) suitable as biodiesel.
Experiments were carried out to optimize yields of lipid extracted oil by tuning sc-CO_2 pressure, flow rates and temperature, with the best result of 10% (w/w) of fish oil extract recorded at 30 MPa, 50°C and 1 l/min sc-CO_2 flow rate.

Keywords—Fishing discards, Fishing wastes, Supercritical carbon dioxide extraction, Biofuel, Biodiesel

I. INTRODUCTION

The annual catches from world fisheries are around 90 million tons (mts). The greatest fraction of about 90% is due to marine species and the remaining comes from inland fisheries. In recent times, the production of marine animals from aquaculture has been almost comparable to that of fisheries [1]. An average of about 10% of fisheries catches is discarded annually [2,3]. The discarded catch is the portion of the catch thrown away at sea and its composition depends on several variables, among which the season, the gear utilized, the fishing grounds exploited, the depth, the occurrence of juveniles, the duration of hauls and the space on board to keep caught fish of low commercial value [4]. At global level, almost 60% of total annual fishery discard is due to combined trawl fisheries. Bottom otter trawl fisheries provide the greatest discard contribution, corresponding to about 2.4 million tons (mts) on average, that is over a quarter of global discards. Crustacean fisheries have the highest discard rate of about 32.4% on average and tuna fisheries the lowest (5.4%) on average. Fisheries targeting demersal fishes show the highest discard levels, contributing over one third of global discards, while fisheries targeting mollusks (excluding cephalopods) had the lowest, contributing only for 2% of global levels [2,3]. In the Mediterranean Sea, fishing discard reaches annual values around 230.000 tons, over 18% of the total annual capture [5,6]. Several studies in this basin evidenced that the discarded portion of catch is generally due to unwanted species (without commercial value), by-catch species (of low commercial value) and undersized specimens of species with higher commercial value [7-9]. In addition to the portions of fishing catch thrown away at sea ("fishing discards"), there are the fractions of fishing catch (as well as of aquaculture production) made of animal tissues, such as fins, heads, bones, skin, gills and viscera, which are discarded as they are considered "wastes". Discards and wastes from the world's fisheries, estimated to be approximately 20 million tons (mts) each year, are a great potential for their use as raw materials [10-12]. With this regard, the expansion of fish processing has caused increasing amounts of by-products, which may represent up to 70% of processed fish. In the past, fish by-products were often thrown away as waste while, more recently, fish by-products have been envisaged to be suitable for a wide variety of applications, such as production of food like fish sausages, snacks, jelly, soups, sauces and other products for human consumption [1]. By-products are also used as feed for aquaculture, mostly in the form of fish meal and fish oil, livestock, pet or fur animal food and fertilizers. Fish, more in general marine organisms and their associated by-products are also used as sources for extraction of biologically active molecules, such as enzymes, peptides, biopolymers for pharmaceutical application [13-18], or other products of interest for industrial processes [19-21], like natural pigments for cosmetics, nanostructured materials for nanotechnology [22-28], and biofuel or biogas for energy production [29-33]. Among the various fields of application of fishing discards and wastes, the production of biofuel acquires significant importance especially for the historical period, low availability of fossil fuels and environmental issues. Indeed, the production of biofuel and biogas from fishing discards and wastes could alleviate the environmental problem of soil and water consumption related to cultivation of biofuel vegetable sources [29, 34], over and above reducing waste disposal issues by promoting principles central to the circular economy. Fishing discards

and wastes provide significant amounts of fish oil which is a natural source of triacyl glycerides (TAGs) that can be easily converted into polyunsaturated fatty acids (PUFAs) suitable for production of methyl ester derivatives as biofuels [30]. Indeed, fish oil has similar properties to petroleum-derived fuel oils as calorific/heating value and combustion efficiency [31-33]. Additionally, biofuels have higher biodegradation rates, low toxicity and no sulphur content [31, 32, 35]. Various processes have been reported to extract oil from fish wastes, mainly based on hexane extraction, Soxhlet extraction, modified fishmeal (MFM) and supercritical carbon dioxide extraction [36-41]. The latter has been mainly studied to extract fish oils from wastes, showing promising extraction yields versus alternative less eco-friendly methods [42]. Extraction yields depend on operational chemical-physical parameters (temperature, pressure and CO_2 mass flow rate) as well as on fish species used. Nevertheless, supercritical carbon dioxide extraction has only been used as a method of extracting oil from fish wastes and not from fishing discards to produce biofuel. Therefore, in this work, sc-CO_2 has been used for the first time as a valid green method for the oil extraction from fishing discards. Sc-CO_2 represents an eco-friendly alternative since high temperatures and toxic solvents are not required. In addition, the use of carbon dioxide as a solvent is advantageous as it is not a limiting resource, it is not flammable and toxic. Carbon dioxide does not require additional disposal costs and does not alter the original sample that is directly employed for applications such as animal feed. Extracted oils may be directly used as low-quality fuels or they can be subjected to transesterification processes to obtain higher quality fuels such as biodiesel (FAME - Fatty Acid Methyl Esters).

Here we report our preliminary results on the potential of fishing discards as sources for eco-friendly production of biofuels. Discards are a promising source with respect to wastes, in terms of biomass weight and abundance of fish, crustaceans and cephalopods collected during hauls without additional costs, having low commercial value. Hence, the extraction of fish oil based on supercritical carbon dioxide as the green solvent and subsequent transesterification reaction provide a promising method of recovery of biofuel from discards, being in accordance with the principles of circular economy.

Sc-CO_2 extraction was carried out at 30 MPa, CO_2 mass flow rate of 1 l/min. A series of experiments at 40°C, 50°C and 60°C were carried out to evaluate the effect of temperature on extraction yields. Moreover, the oil extracted in higher yield was subjected to a transesterification reaction to evaluate the nature and abundance of fatty acid methyl esters in the final mixture.

II. EXPERIMENTAL PROCEDURES

A. Materials

Fishing discards were collected in April 2022, during two trawl hauls in the South-Western Adriatic Sea. A total of 39 species (9 crustaceans, 1 cephalopod, 1 cartilagineous fish and 28 teleost fishes) were identified, according to Table 1. The discard's composition reveals the presence of unwanted species without commercial value, by-catch species of low commercial value and undersized or crushed or ruined specimens of species with higher commercial value (target species) (Table 1).

Table 1 - Discard species collected during two hauls of trawl fishing carried out on the continental shelf in the South-Western Adriatic Sea (** target species; *species with low commercial value).

	Species	***Number***	***Weight (g)***
Crustaceans	*Chlorotocus crassicornis**	11	14.6
	Liocarcinus depurator	2	10.5
	Macropipus tuberculatus	2	6.5
	Munida iris	126	282.8
	*Nephrops norvegicus***	104	434.6
	*Parapenaeus longirostris***	20	115.8
	*Plesionika heterocarpus**	16	24.5
	*Solenocera membranacea**	4	14.3
	*Squilla mantis**	1	2.2
Cephalopods	*Illex coindetii**	6	65.1
Chondrichthyes	*Raja asterias*	1	9.5
Osteichthyes	*Alosa alosa**	2	350.8
	Argentina sphyraena	16	213.1
	Arnoglossus rueppelii	49	313.7
	*Boops boops**	2	110.2
	*Cepola macrophthalma**	3	8.9
	*Chelidonichthys cuculus**	1	12.5
	Chlorophthalmus agassizi	3	19.1
	Citharus linguatula	1	20.4
	*Conger conger**	4	306.3
	*Engraulis encrasicolus**	23	380
	*Eutrigla gurnardus**	7	124.5
	Gadiculus argenteus	6	22.4
	Gaidropsarus biscayensis	3	17.1
	Gnathophis mystax	4	123.2
	*Helicolenus dactylopterus**	15	136.5
	Lepidotrigla cavillone	8	74.9
	*Lophius budegassa**	31	1239.5
	*Merluccius merluccius***	98	1125.3
	*Micromesistius poutassou**	71	2191
	*Mullus barbatus***	9	128.3
	Peristedion cataphractum	1	31.2
	*Sardina pilchardus**	1	14.8
	Serranus hepatus	5	51.5
	*Spicara flexuosa**	66	1417.7
	Synchiropus phaeton	1	2.1
	*Trachurus trachurus**	32	951.3
	*Trigla lyra**	2	68.2
	*Trisopterus capelanus**	3	48.1
TOTAL		**760**	**10483**

B. *Sample preparation and Supercritical Carbon Dioxide (sc-CO_2) Extraction*

Samples were freeze-dried at −20°C for 4 days until the dry fish weight was constant. Then, the dried samples were ground by a dry mixer and kept at 3°C. In each experiment, approximately 5 g of ground sample (dry weight) were placed in a 10-ml extraction vessel. The extraction experiment were performed using at 1 ml/min CO_2 continuous flow for 3 h, working at 30 MPa pressure and 40 °C, 50 °C and 60 °C, respectively. The total oil yield was evaluated as percentage ratio of extracted oil biomass versus the total sample weight, as reported in (1):

$$\text{Yield (\%)} = \frac{Grams\ oil\ extracted}{Grams\ of\ sample} \text{ x } 100 \qquad (1)$$

C. *Transesterification and FAME analysis*

A sample (150 mg) of oil extracted by sc-CO_2 at 50 °C was subjected to the transesterification reaction. The oil was reacted with a solution of sodium hydroxide in methanol (30 ml, 0.1 M) stirring at 50°C for 1.5 h. Then, the solvent was removed at reduced pressure and the product was extracted three times with heptane (3x50 ml) in the presence of water (3x50 ml) inside a separatory funnel. The collected organic phase was dried with anhydrous sodium sulphate, filtered and analysed via Gas Chromatography-Mass Spectrometry (GC-MS) to identify FAME derivatives. The final oil product was isolated by distillation of the solvent at reduced pressure.

III. Results and Discussion

Sc-CO_2 extraction yields are reported in Table 2, with maximum value (10%, *i.e.* 10 g of oil *vs* 100 g of dry fish waste) observed at 50 °C.

The transesterification reaction performed on the oil extracted at 50°C led to a final product mixture (21 mg *vs* 150 mg of initial oil) that, GC-MS analysis confirmed to be composed of both saturated and unsaturated FAMEs with C_{14}-C_{25} carbon atoms, as shown in Figure 1, 2 and Table 3. Individual FAME, corresponding to each peak, has been detected via NIST MS Search 2.0 library. The degree of saturated and unsaturated fatty acids methyl esters determines oil specific properties [36]. In particular, saturated fatty acids own better combustion qualities although they are characterized by poor flow properties due to the higher viscosity than the unsaturated counterpart [43].

The prevailing FAMEs are represented by methyl hexadecanoate, (Z,Z)-methyloctadeca-9,12-dienoate *trans*-methyl-13-octadecenoate suitable as biodiesel oils [44-46].

Table 2 – Comparison of extraction yields for different operating parameters.

		SC-CO_2 EXTRACTION	
	Extraction 1	**Extraction 2**	**Extraction 3**
Temperature (°C)	40	50	60
Pressure (MPa)	30	30	30
Flow rate (l/min)	1	1	1
Yield (%)	6.9	10	8.5

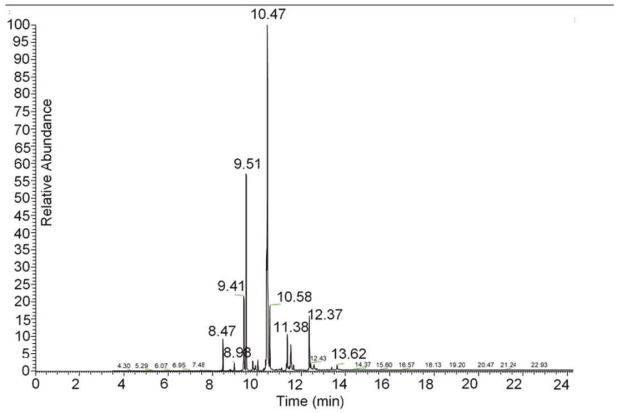

Figure 1 – Complete chromatogram of Fatty Acid Methyl Esters (FAME) obtained by transesterification of fishing discards oils extracted by sc-CO_2.

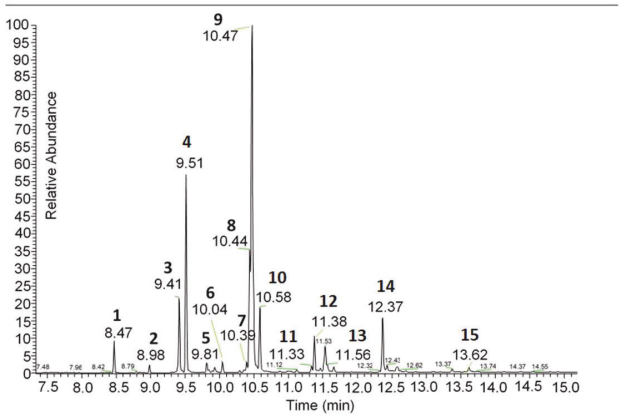

Figure 2 – Detail of the chromatogram of Fatty Acid Methyl Esters (FAME) obtained by transesterification of fishing discards oils extracted by sc-CO_2.

Table 3 – Fatty Acid Methyl Esters (FAME) profile obtained by transesterification of fishing discards oils extracted by sc-CO_2.

Peak number	***Fatty Acids Methyl Esters (FAME)***
1	Methyl tetradecanoate
2	Pentadecanoic acid, methyl ester
3	Methyl hexadec-9-enoate
4	Hexadecanoic acid, methyl ester
5	6-Hexadecenoic acid, 7-methyl,methyl ester (Z)
6	Heptadecanoic acid, methyl ester
7	Methyl stearidonate
8	9,12-Octadecadienoic acid (Z,Z)-, methyl ester
9	Trans-13-Octadecenoic acid, methyl ester
10	Octadecanoic acid, methyl ester
11	5,8,11,14-Eicosatetraenoic acid, methyl ester, (all-Z)-
12	5,8,11,14,17-Eicosapentaenoic acid, methyl ester, (all-Z)-
13	Cyclopropanebutanoic acid, 2-[[2-[[2-[(2-pentylcyclopropyl)methyl]cyclopropyl] methyl]cyclopropyl]methyl]-, methyl ester
14	4,7,10,13,16,19-Docosahexaenoic acid, methyl ester, (all-Z)-
15	15-Tetracosenoic acid, methyl ester, (Z)-

IV. Conclusion

In summary, fishing discards are promising eco-friendly sources of biofuels by using supercritical carbon dioxide based extraction. In particular, a preliminary study of effects of temperature on extraction yields has been performed, leading the best yield (10%) at 50°C. Definitely, sc-CO_2 and subsequent green transesterification reaction have provided a promising method of recovery of biofuel from discards, with significant potential due to their huge amounts (in Mediterranean about 230000 tons per year), in accordance with the principles of circular economy.

Acknowledgment

This work was financially supported by Horizon Europe Seeds: RESources of TARanto seas: L'utilizzo delle risorse del mare per il risanamento degli ecosistemi marini e lo sviluppo di bio-economia circolare (RESTART) financed from Next Generation EU – Horizon Europe Seeds – fondi MUR, D.M. 737/2021 – Prog. S66 – CUP H99J21017520006.

References

[1] FAO. 2020a. The State of World Fisheries and Aquaculture 2020. Sustainability in action. Rome. https://doi.org/10.4060/ca9229en

[2] M. Perez Roda, E. Gilman, T. Huntington, S. Kennelly, P. Suuronen, M. Chaloupka & P. Medley, "A Third Assessment of Global Marine Fisheries Discards". FAO fisheries and aquaculture technical paper 633. ISBN 978-92-5-131226-1, 2019. (Food and Aquaculture Organization of the United Nations, Rome, 2019).

[3] E. Gilman, A. Perez Roda, T. Huntington, S. J. Kennelly, P. Suuronen, M. Chaloupka, P.A.H Medley, "Benchmarking global fisheries discards". Scientific Reports, 10(1), 2020, pp. 1-8.

[4] D.L. Alverson, M.H. Freeberg, S.S. Muraski, J.G. Pope, "A global assessment of fisheries bycatch and discards". FAO Fisheries and aquaculture technical paper, vol. 339, 1994, pp. 233-339.

[5] K. Tsagarakis, A. Palialexis, V. Vassilopoulou, "Mediterranean fishery discards: Review of the existing knowledge". ICES Journal of marine science, 71(5), 2014, pp. 1219-1234.

[6] FAO. 2020b. The State of Mediterranean and Black Sea Fisheries 2020. General Fisheries Commission for the Mediterranean. Rome. https://doi.org/10.4060/cb2429en

[7] A. Carbonell, P. Martin, S. De Ranieri, WEDIS team, "Discards of the Western Mediterranean trawl fleet". Rapport commission international Mer Méditerranée, 1998, pp. 392-393.

[8] A. Machias, V. Vassilopoulou, D. Vatsos, P. Bekas, A. Kallianotis, C. Papaconstantinou, N. Tsimenides, "Bottom trawl discards in the northeastern Mediterranean Sea". Fisheries research, 53(2), 2001, pp. 181-195.

[9] G. D'Onghia, R. Carlucci, P. Maiorano, M. Panza, "Discards from deep-water bottom trawling in the Eastern-Central Mediterranean Sea and effects of mesh size changes". Journal of Northwest Atlantic fishery science, vol. 31, 2003, pp. 245-261.

[10] T. Rustad, "Utilization of marine by-product". Electronic journal of environmental, agricultural and food chemistry, 2003, pp. 458–463.

[11] S.K. Kim, E. Mendis, "Bioactive compounds from marine processing byproducts - A review". Food research international, 39(4), 2006, pp. 383–393.

[12] G. Caruso, "Fishery wastes and by-products: a resource to be valorized". Journal of fisheries science, 10(1), 2016, pp. 080-083.

[13] A.P. Bimbo, "Current and future sources of raw materials for the long-chain omega-3 fatty acid market". Lipid technology, 19(8), 2007, pp. 176–179.

[14] H. Malve, "Exploring the ocean for new drug developments: marine pharmacology". Journal of pharmacy & bioallied sciences, 8(2), 2016, pp. 83–91.

[15] F. Al Khawli, M. Pateiro, R. Dom.nguez, J.M. Lorenzo, P. Gull.n,, K. Kousoulaki, E. Ferrer, H. Berrada & F.J. Barba, "Innovative green technologies of intensification for valorization of seafood and their by-products". Marine drugs, 17(12), 2019, pp. 689.

[16] D. Vona, G. Leone, R. Ragni, F. Palumbo, A. Evidente, M. Vurro, G. M. Farinola & S. R. Cicco, "Diatoms Biosilica as Efficient Drug-Delivery System", Materials Research Society MRS Advances, 3(4), 2015, pp. 3825-3830.

[17] G. Di Bari, E. Gentile, T. Latronico, G. Corriero, A. Fasano, C.N. Marzano, G. M. Liuzzi, "Comparative analysis of protein profiles of aqueous extracts from marine sponges and assessment of cytotoxicity on different mammalian cell types", Environmental Toxicology Pharmacology, 38(3), 2014, pp.1007-1015.

[18] G. Di Bari, E. Gentile, T. Latronico, G. Corriero, A. Fasano, C. Nonnis Marzano, G. M. Liuzzi, "Inhibitory Effect of Aqueous Extracts from Marine Sponges on the Activity and Expression of Gelatinases A (MMP-2) and B (MMP-9) in Rat Astrocyte Cultures", PLoS One, 10(6), 2015.

[19] G. Difonzo, A. Aresta, P. Cotugno, R. Ragni, G. Squeo, C. Summo, F. Massari, Antonella Pasqualone, M. Faccia, C. Zambonin and F. Caponio, "Supercritical CO_2 Extraction of Phytocompounds from Olive Pomace Subjected to Different Drying Methods". Molecules, 26(3), 2021, pp. 598.

[20] A. Aresta, P. Cotugno, N. De Vietro, F. Massari & C. Zambonin, "Determination of Polyphenols and Vitamins in Wine-Making by-Products by Supercritical Fluid Extraction (SFE)", Analytical Letters, 53(16), 2020, pp. 2585.

[21] A. Aresta, P. Cotugno & C. Zambonin, "Determination of Ciprofloxacin, Enrofloxacin, and Marbofloxacin in Bovine Urine, Serum, and Milk by Microextraction by a Packed Sorbent Coupled to Ultra-High Performance Liquid Chromatography", Analytical Letters, 52(5), 2019, pp. 790.

[22] D. Vona, R. Ragni, E. Altamura, P. Albanese, M. M. Giangregorio, S. R. Cicco, G.M. Farinola "Light emitting biosilica by in vivo functionalization of Phaeodactylum tricornutum diatom microalgae with organometallic complexes", Applied Sciences, 11 (82), 2021, pp. 3327.

[23] R. Ragni, F. Scotognella, D. Vona, L. Moretti, E. Altamura, G. Ceccone, D. Mehn, S. R. Cicco, F. Palumbo, G. Lanzani, G.M. Farinola, "Hybrid Photonic Nanostructures by In Vivo Incorporation of an Organic Fluorophore into Diatom Algae", Advanced Functional Materials, 28(24), 2018, 1706214.

[24] D. Vona, S. R. Cicco, R. Ragni, G. Leone, M. Lo Presti, G. M. Farinola, "Biosilica/polydopamine/silver nanoparticles composites: new hybrid multifunctional heterostructures obtained by chemical modification of Thalassiosira weissflogii silica shells", MRS Commuications, 8(3), 2018, pp. 911−917.

[25] M.L. Presti, R. Ragni, D. Vona, G. Leone, S. Cicco & G. M. Farinola. "In vivo doped biosilica from living Thalassiosira weissflogii diatoms with a triethoxysilyl functionalized red emitting fluorophore", Materials Research Society MRS Advances, 2018, 3(27), pp. 1509-1517.

[26] S. R. Cicco, D. Vona, G. Leone, E. De Giglio, M. R. Bonifacio, S. Cometa, S. Fiore, F. Palumbo, R. Ragni, G.M. Farinola, " In vivo functionalization of diatom biosilica with sodium alendronate as osteoactive material", Materials Science Engineering C, 104, 2019, 109897.

[27] G. Della Rosa, D. Vona, A. Aloisi, R. Ragni, R. Di Corato, M. Lo Presti, S. R. Cicco, E. Altamura, A. M. TaurinoCatalano, G. M. Farinola, "Luminescent silica based nanostructures from in vivo Iridium-doped diatoms microalgae", ACS Sustainable Chemistry Engineering, 7(2), 2019, pp. 2207-2215.

[28] G. Leone, G. De la Cruz Valbuena, S. R. Cicco, D. Vona, E. Altamura, R. Ragni, E. Molotokaite, M. Cecchin, S. Cazzaniga, M. Ballottari, C. D'Andrea, G. Lanzani "Incorporating a molecular antenna in diatom microalgae cells enhances photosynthesis", Scientific Reports, 11(1), 2021, pp. 5209.

[29] J.R. Kiniry, L. Lynd, N. Greene, M.-V. V. Johnson, M. Casler, M.S. Laser, "Biofuel and water use: comparison of maize and switchgrass and general perspectives". In: J. H. Wright and D.

A. Evans (ed), New Research on Biofuels, Nova science publishers, Inc, 2008, pp. 17-30.
[30] P. Jayasinghe & K. Hawboldt, "A review of bio-oils from waste biomass: Focus on fish processing waste". Renewable and sustainable energy reviews, 16(1), 2012, pp. 798-821.
[31] I. A. Adeoti, K. Hawboldt, "A review of lipid extraction from fish processing by-product for use as a biofuel". Biomass & bioenergy, 63, 2014, pp. 330–340.
[32] S. Kalligeros, F. Zannikos, S. Stournas, E. Lois, G. Anastopoulos, C. Teas, et al., "An investigation of using biodiesel/marine diesel blends on the performance of a stationary diesel engine". Biomass & bioenergy, 24(2), 2003, pp. 141–149.
[33] F. Preto, F. Zhang, J. Wang, "A study on using fish oil as an alternative fuel for conventional combustors". Fuel, 87(10-11), 2008, pp. 2258–2268.
[34] FAO, 2008. The State of Food and Agriculture. Part I: Biofuels: Prospects, Risks and Opportunities. Rome. http://www.fao.org/catalog/inter-e.htm
[35] CK. Westbrook, "Biofuels combustion". Annual review of physical chemistry, 2013, pp. 201–219.
[36] I. A. Adeoti & K. Hawboldt, 2015. "Comparison of biofuel quality of waste derived oils as a function of oil extraction methods". Fuel, pp. 158, 183-190.
[37] S. Ferdosh, Z. I. Sarker, N. Norulaini, A. Oliveira, K. Yunus, A. J. Chowdury ... & M. Omar, "Quality of tuna fish oils extracted from processing the by-products of three species of neritic tuna using supercritical carbon dioxide". Journal of food processing and preservation, 39(4), 2015, pp. 432-441.
[38] N. Rubio-Rodríguez, M. Sara, S. Beltrán, I. Jaime, M. T. Sanz & J. Rovira, "Supercritical fluid extraction of the omega-3 rich oil contained in hake (*Merluccius capensis–Merluccius paradoxus*) by-products: study of the influence of process parameters on the extraction yield and oil quality". The journal of supercritical fluids, 47(2), 2008, pp. 215-226.
[39] N. Rubio-Rodríguez, M. Sara, S. Beltrán, I. Jaime, M. T. Sanz & J. Rovira, "Supercritical fluid extraction of fish oil from fish by-products: A comparison with other extraction methods". Journal of food engineering, 109(2), 2012, pp. 238-248.
[40] F. Sahena, I. S. M. Zaidul, S. Jinap, A. M. Yazid, A. Khatib & N. A. N. Norulaini, "Fatty acid compositions of fish oil extracted from different parts of Indian mackerel (*Rastrelliger kanagurta*) using various techniques of supercritical CO_2 extraction". Food chemistry, 120(3), 2010, pp. 879-885.
[41] M. Z. I. Sarker, J. Selamat, A. S. M. Habib, S. Ferdosh, M. J. H. Akanda & J. M. Jaffri, "Optimization of supercritical CO_2 extraction of fish oil from viscera of African catfish (*Clarias gariepinus*). "International journal of molecular sciences, 13(9), 2012, pp. 11312-11322.
[42] K. Ivanovs & D. Blumberga, "Extraction of fish oil using green extraction methods: A short review". Energy Procedia, 2017, pp. 477-483.
[43] SS. Sidibé, J. Blin, G. Vaitilingom, Y. Azoumah, "Use of crude filtered vegetable oil as a fuel in diesel engines state of the art: literature review". Renewable and sustainable energy reviews, 14(9), 2010, pp. 2748–2759.
[44] S. Rasoul-Amini, P. Mousavi, N. Montazeri-Najafabady, M. A. Mobasher, S. B. Mousavi, F. Vosough, ... & Y. Ghasemi, "Biodiesel properties of native strain of *Dunaliella salina"*. International journal of renewable energy research (IJRER), 4(1), 2014, pp. 39-41.
[45] Y. X. Li & B. X. Dong, "Optimization of lipase-catalyzed transesterification of cotton seed oil for biodiesel production using response surface methodology". Brazilian archives of biology and technology, 2016, pp. 59.
[46] S. M. Dangoggo, I. Dhikrah, N. A. Sani, A. S. Baki & B. U. Bagudo, "Preparation and Characterization of Biodiesel Produced from Jatropha Seed Oil Using Sulphated Zirconia as Catalyst". Industrial chemistry, 4(126), 2018, pp. 2.

Ringraziamenti

Dedico questo piccolo spazio alle persone che, con il loro supporto, mi hanno accompagnato in questo meraviglioso percorso. La vita mi ha insegnato che per realizzare i propri sogni, è necessario affrontare le difficoltà con coraggio e perseveranza, rimanendo fedeli alle proprie scelte nonostante ogni ostacolo. Ed è grazie a chi mi è stato vicino, oggi posso guardare con orgoglio il traguardo raggiunto.

Un sentito ringraziamento va all'Ing. Cangialosi e all'Ing. Intini dell'azienda Tecnologia e Ambiente, per aver creduto in me e per aver finanziato il mio dottorato. La loro guida e i loro consigli sono stati preziosi durante ogni fase delle mie attività di ricerca, così come il loro sostegno costante. Ringrazio di cuore anche la Professoressa Roberta Ragni e il Professor Petro Cotugno, per avermi aiutato a crescere professionalmente, credendo nelle mie capacità e guidandomi con pazienza e attenzione lungo questo percorso.

A tutti i miei colleghi del gruppo Farinola, grazie per il vostro straordinario senso di comunità, la gioia e il sostegno reciproco dimostrati dentro e fuori dal laboratorio. Grazie, Carola, Annarita, Cesar, Abraham, Davide M., Alessandro, Matteo, Ambra, Danilo, Davide B., Enrico, Vincenzo, Riccardo, Dario, Rossella, Gianfranco, Giorgio, Gianluigi. Insieme a voi ho scoperto cosa significa lavorare in un ambiente di grande unione e amicizia, e questo ha reso unico ogni giorno.

Un ringraziamento speciale va a Valeria Sini, la mia "little b.", con cui ho condiviso momenti di gioia, ansia, follia e qualche lacrima. Sei molto più di una collega: sei un’amica con un cuore prezioso, di cui non potrei mai fare a meno. Ringrazio anche Giulia, Angelica, Roberta e Danilo O., che sono stati sempre al mio fianco in questi tre anni, credendo in me e sostenendomi ogni volta che ne avevo bisogno.

Infine, ma non per importanza, ringrazio il mio tutto, la mia famiglia. Mi avete supportato in ogni scelta e siete stati al mio fianco in ogni piccolo traguardo. Spero di avervi reso orgogliosi di me, vi amo incondizionatamente. Un grazie va anche a tutte le persone "speciali" della mia vita, i miei cugini e gli amici, per esserci stati in questo periodo intenso. Non serve elencare i loro nomi: loro sanno già quanto sono importanti per me.

Grazie anche a te, amore mio Andrea. Tu che mi hai supportato e sopportato dall'inizio di questo percorso, senza mai farmi mancare il tuo appoggio.

Infine, questa tesi è dedicata anche a te, piccola Aries, mia stellina, anche se ci hai lasciati ad agosto, rimarrai sempre parte del mio cuore e proprio come il giorno della mia laurea, sarai con me, anche in questo traguardo.